The biorhythm of human juvenile skeletal growth

Rosie Pitfield

Skeletal Biology Research Centre

School of Anthropology and Conservation

University of Kent

A thesis submitted for the degree of

Doctor of Philosophy in Anthropology

May 2019

Abstract

Biorhythms are cyclic changes in an organism's growth or functioning that can be driven by an internal biological clock and synchronised through environmental cues. Evidence of two biorhythms is retained in human tooth enamel in the form of incremental growth lines. The first biorhythm corresponds with a daily, circadian, rhythm that has been linked to the secretory activity of ameloblasts. The second biorhythm is a longer period infradian biorhythm that is marked by Retzius lines and can be quantified in days as Retzius periodicity (RP). There is some evidence to suggest that body size, basal metabolic rate, life history traits, and RP might be linked by a centrally coordinated autonomic biorhythm that is related to growth and development. Earlier studies have demonstrated links in adult humans between RP and body size, and between RP and aspects of cortical bone microstructure. If the biorhythm is related to the growth and development of the body, there should also be indications of this biorhythm retained in the juvenile skeleton. This thesis examines these links, for the first time, in skeletal samples of human children from one population.

The aim of this thesis is to use 2D static histomorphometry to explore how, or if, evidence of an infradian biorhythm retained in tooth enamel as Retzius line periodicity is linked to the growth of human bone growth during ontogeny. In addition to the potential effect of a biorhythm on skeletal growth, many other factors may potentially affect bone microstructure. This thesis examines some of these influences prior to investigating the biorhythm. Variation in histomorphometric measures of cortical bone microstructure is sought between children of different regions in England (Canterbury, York, Newcastle), and between high- and low-status children from Canterbury. Additionally, bone microstructure varies between the bones in a single skeleton, so the intra-skeletal microstructural variation between eight bones from ten young adults was explored and compared to their RP. Finally, the potential for a relationship between RP and rib cortical bone microstructure is investigated.

This thesis begins with a background review of the underlying biology of bone growth, enamel secretion, and biorhythms. The introductory sections are followed by a detailed materials and methods chapter. The investigative parts of the thesis are presented as three data chapters that have been designed as manuscripts that are suitable for publication. Each has a focus on a specific aim and has individual introduction, aims, methods, results, and discussion sections. Together, the three data chapters contain histomorphometric variables that were measured from the skeletal remains of 188 juvenile and young adults from four archaeological sites from medieval England. The RP of a permanent tooth from each skeleton was calculated and combined with measures of bone modelling – indicated by bone size variables – and remodelling – indicated by osteon population density, osteocyte lacunae density, and osteon size and shape. This thesis ends with a discussion of the main findings of each data chapter and how they contribute to the overall aim of the thesis, which is to assess evidence of the biorhythm in tooth enamel against aspects of growth in the juvenile skeleton.

The results support the idea that an infradian biorhythm coordinates aspects of human hard tissue growth, particularly relative amounts of lamellar formation during modelling and remodelling. The biorhythm was related to the proportion of interstitial and osteonal lamellar bone, and to body size. These results imply that a child with a fast biorhythm tends to have a high proportion of lamellar bone and small Haversian canals in their osteons and a high proportion of bone in their ribs compared to the medullary cavities. Whereas, a child with a slow biorhythm tends to have a low proportion of lamellar bone and large Haversian canals in their osteons and a low proportion of bone in their ribs compared to the medullary cavities. The biorhythm did not relate to any measure of bone turnover, including osteon population density, intact osteon density, fragmentary osteon density, or osteocyte density. This biorhythm could be one of the many factors that affect macroscopic bone growth and microscopic bone modelling and remodelling during childhood growth in medieval Canterbury.

Acknowledgements

This PhD was supported by funding from the Dora Harvey Memorial Research Scholarship (University of Kent), for which I am very grateful. Additional funding to support this research was provided by the Skeletal Biology Research Centre (School of Anthropology and Conservation, University of Kent).

I would first like to thank my supervisors, Patrick Mahoney and Chris Deter, for their invaluable advice and unwavering support throughout my research. I have learnt so much from them. I am thankful to Patrick for teaching me the technical skills for histology. I am also thankful to Justyna Miszkiewicz for introducing me to bone histology and giving me guidance on bone histomorphometric technique whenever I've needed it.

I would also like to thank everyone who enabled my research by allowing me to access skeletal and dental samples. This research would not have been possible otherwise. Pia Nystrom and Petra Verlinden from the Department of Archaeology at the University of Sheffield, Tina Jakob and Beth Upex from the Department of Archaeology at Durham University, and James Harris from the Corinium Museum.

My lab colleagues and friends deserve a special acknowledgement for always being there with helpful discussions, ideas, and constant support. I would particularly like to thank Jeremy, Jessica, Josh, Simon, Alice, Ana, and Simone. I look forward to working with you in the future!

Finally, to my family: thank you for supporting me and letting me always ask "but why?".

Published PhD Thesis Chapters

Appendix C Preliminary Study: Does linear enamel hypoplasia affect the appearance of incremental markings?

This study was published in modified form as part of a larger research project entitled "Enamel biorhythms of humans and great apes: the Havers-Halberg Oscillation hypothesis reconsidered" which was published by the *Journal of Anatomy* on 22nd August 2016; 230:272-281.

Chapter 3 Bone histomorphometric measures of physical activity in children from Medieval England.

This manuscript was published in the *American Journal of Physical Anthropology* on 14th May 2019; 169: 730-746.

Chapter 4 Intraskeletal variation in bone remodelling and how it relates to a biorhythm.

This manuscript is being prepared for submission for peer review.

Chapter 5 Microscopic markers of an infradian biorhythm in human juvenile ribs.

This manuscript was published in the journal *BONE* on 29th November 2018; 120:403-410.

Table of Contents

List of Figures

List of Tables

List of Abbreviations

Abbreviations of bone histology variables have been taken from Dempster *et al.*, (2013).

BMR	Basal metabolic rate
BMU	Basic multicellular unit
DSR	Daily secretion rate
Ct.Ar	Cortical area
Ct.Wi	Cortical width
H.Ca.Ar	Haversian canal area
H.Ca.Dm	Haversian canal diameter
LEH	Linear enamel hypoplasia
N.On	Intact osteon density
N.On.Fg	Fragmentary osteon density
On.Ar	Osteon area
On.Cr	Osteon circularity
On.Dm	Osteon diameter
On.Pm	Osteon perimeter
OPD	Osteon population density
Ot.Dn	Osteocyte density
Pr.Ca.Dn	Primary vascular canal density
Re.Ct.Ar	Relative cortical area
Re.On.Ar	Relative osteon area
Tt.Ar	Total area
RP	Retzius periodicity

Chapter 1

Background Review

1.1 | INTRODUCTION

Many extrinsic, external to the body, and intrinsic, internal to the body, factors can influence the physiological processes that lead to adult body size and stature. Lately it has been suggested modern humans may have a hypothesised biological rhythm, or biorhythm, that influences their growth trajectory and eventual adult body size (Bromage *et al.*, 2009; Mahoney *et al.*, 2018). A marker of the hypothesised biorhythm is preserved in tooth enamel as Retzius lines. The underlying mechanism behind Retzius line formation is still poorly understood, but it is believed to be a long-period biorhythm that affects the growth of multiple tissues (Bromage *et al.*, 2009, 2012). The Retzius line periodicity (RP) is quantified using histomorphometry, as are aspects of microstructural bone growth. This thesis will use histomorphometry to explore the idea that a biorhythm influences ontogenetic skeletal growth in a large sample of medieval English juvenile skeletons. The results may reveal how this relatively unknown biorhythm relates to juvenile skeletal growth and eventual adult body size.

To date, most research on this biorhythm has focussed on final adult body size, either through comparisons between species or within species (Bromage *et al.*, 2009, 2012, 2016; Hogg *et al.*, 2015; Mahoney *et al.*, 2018). Retzius periodicity scales positively with body size across mammalian species (Smith *et al.*, 2003; Smith, 2008; Bromage *et al.*, 2009, 2012). It has also been proposed that RP relates to basal metabolic rate (BMR) and many life history traits that are also linked to body mass (Bromage *et al.*, 2012). However, the opposite relationship has been found specifically within humans,

where RP scales negatively with adult body size (Bromage *et al.*, 2016; Mahoney *et al.*, 2018). These results suggest that, for humans, RP is related to development because the time available to attain adult size is constrained within a species (Mahoney *et al.*, 2018). The developmental rate must vary to achieve different adult body sizes within the same length of growth period (Bromage *et al.*, 2009). So, a person on a growth trajectory to attain a smaller adult body size will have a slower developmental rate and a higher RP, and a person on a growth trajectory to attain a larger adult body size will have a faster developmental rate and a lower RP.

While an understanding has been gained into the relationship between RP and final adult body size and stature, it is unclear how this relationship manifests during ontogenetic growth and it is important to understand if and how this biorhythm relates to childhood growth. However, other factors may influence bone biology during ontogeny, for example biomechanics, diet, and disease. So, before the biorhythms influence on bone microstructure can be understood, the other factors that affect cortical bone microstructure must be explored. Here these will include age, activity, and socioeconomic status, as well as how bone microstructure varies across the skeleton.

1.2 | BONE GROWTH

The skeleton can reveal much about human life and growth in the past. Bones develop, grow, and are maintained through a complex mechanism that optimises each individual bone for its function and environment. Bone development refers to the increase in functional ability (Cameron, 2012) whereas bone growth refers to the particular changes in size and shape that occur during the development of an individual (Cunningham, Scheuer and Black, 2016). Bone tissue is named according to its origin, structure, and function. Bone is first divided into either trabecular bone or cortical bone (White, Black

and Folkens, 2011). Trabecular bone, sometimes known as cancellous bone or spongey bone, is a particularly porous bone type made up of individual plates called trabeculae (Martin *et al.*, 1998). The trabeculae are arranged as struts to optimise mechanical strength (Wolff, 1892; Martin *et al.*, 1998). Trabeculae are found inside flat bones, such as those of the cranial vault, and irregular bones, such as the vertebrae, as well as inside the long bone articular ends, or epiphyses.

Cortical bone, sometimes known as compact bone, is a dense bone that makes up the shafts of long bones and covers the trabecular bone of flat bones and irregular bones, as well as the epiphyses of long bones (Martin *et al.*, 1998). Cortical bone may be woven or lamellar. Woven bone is rapidly deposited and poorly organised with randomly arranged collagen fibres and hydroxyapatite crystals (Caccia *et al.*, 2016). Lamellar bone is formed more slowly in a well organised structure and it is usually divided into primary bone and secondary bone depending on the formation process (Caccia *et al.*, 2016). Primary bone is bone that is formed where there was no pre-existing bone, whereas secondary bone is bone that is formed where it replaces pre-existing bone. A single lamella is approximately 5-6 μm thick and has two 2-3 μm layers, each with a different collagen orientation (Johnson, 1964; Ascenzi, Benvenuti and Bonucci, 1982; Reid, 1986; Martin *et al.*, 1998). They are formed by the calcification of an osteoid seam that is usually 15 μm thick (Johnson, 1964; Martin *et al.*, 1998). Hence one osteoid seam will become mineralised as three lamellae, each comprising of two layers. Lamellar bone is the main structural material of cortical bone.

Cortical bone macrostructure and microstructure of the humerus and ribs will be examined in this thesis in relation to a potential biorhythm that influences bone growth. It is important to understand the development, growth, anatomy, and biomechanical environment of both bones, to understand the underlying bone biology, before

interpreting the results of the histology in the data chapters. By studying the humerus and rib bones in combination, it may reveal how bone microstructure varies between people according to variations in biomechanical loading (the humerus) or metabolic needs (the humerus and the rib) (Eleazer and Jankauskas, 2016).

1.2.1 | Biology, Anatomy, and Development of the Humerus

The humerus is the largest bone in the arm and links the shoulder to the forearm (**Figure 1.1**) (White, Black and Folkens, 2011). The proximal humerus, closest to the axial skeleton, is part of the shoulder joint. The humerus head articulates with the glenoid fossa of the scapula, and the rotator cuff muscles (Supraspinatus, infraspinatus, teres minor, and subscapularis) attach between the greater and lesser tubercles of the proximal humerus and the scapula to hold and stabilise the shoulder joint (White, Black and Folkens, 2011). These muscles also aid in the abduction, internal rotation, and external rotation of the shoulder (Stone and Stone, 2003).

The shaft of the humerus is rounded proximally in cross-section, but more triangular distally (White, Black and Folkens, 2011). Several major muscles have insertion points on the shaft. The pectoralis major and the latissimus dorsi insert on the crests of the greater and lesser tubercles respectively and originate from the sternum and clavicle and the spine respectively (White, Black and Folkens, 2011). The teres major inserts medially to the tubercle crests and originates from the scapula. Together these muscles have a key role in adducting and internally rotating the humerus (Stone and Stone, 2003). The deltoideus, the major abductor of the humerus, inserts on the deltoid tuberosity on the anterolateral humeral mid-shaft and originates from the clavicle and scapula (White, Black and Folkens, 2011). The coracobrachialis inserts medially on the humeral mid-shaft from an origin on the scapula and acts to flex and adduct the humerus

and stabilise the glenohumeral joint. On the distal end of the shaft the brachialis originates on the anterior side and the triceps brachii originates on the posterior side (White, Black and Folkens, 2011). Both muscles have insertion sites on the proximal ulna and are the major flexor and extensor of the elbow joint respectively (Stone and Stone, 2003).

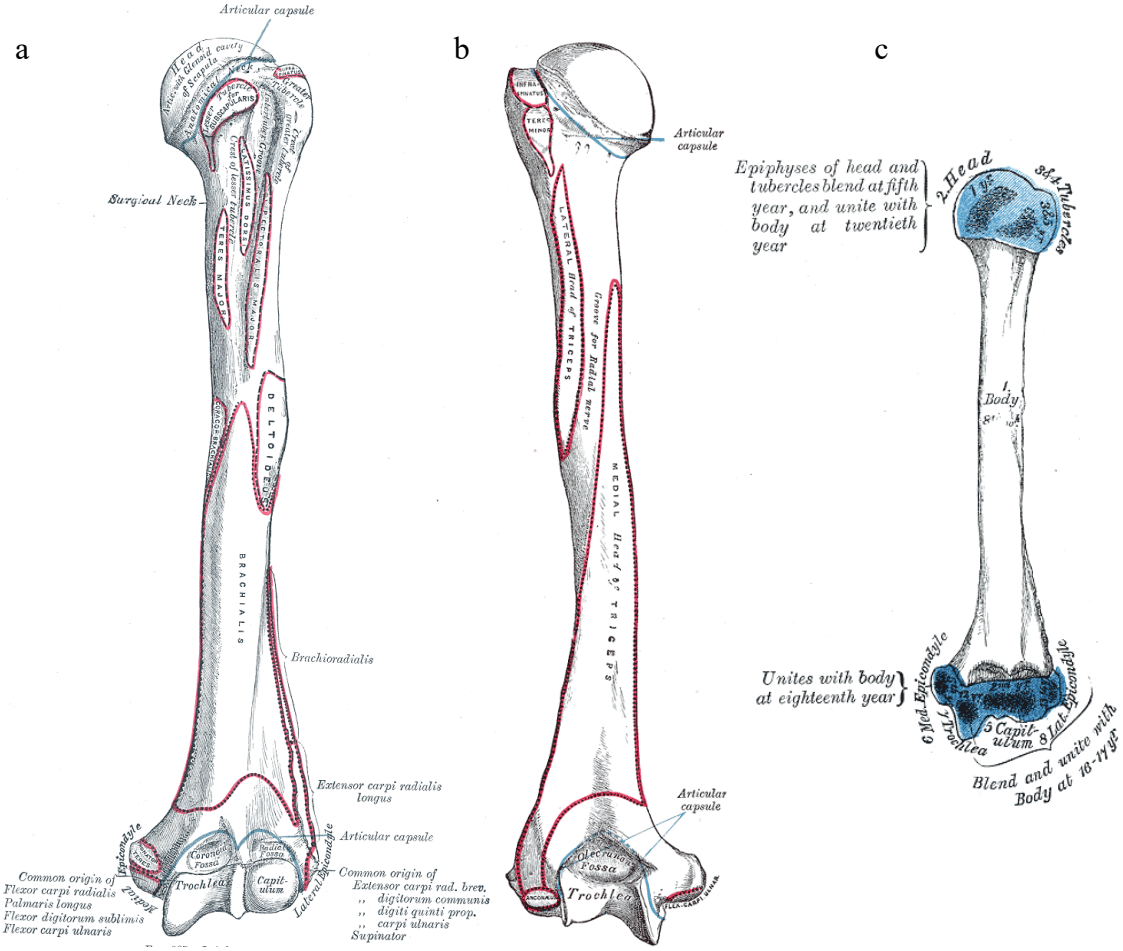

Figure 1.1 *The left humerus. a – anterior view. b – posterior view. c – epiphyseal fusion. From Gray (1918) Anatomy of the Human Body, plate 207, plate 208, and plate 210*

The distal humerus, furthest from the axial skeleton, is part of the elbow joint. At the distal end of the humerus the capitulum, on the lateral side, articulates with the radial head and the trochlea, on the medial side, articulates with the olecranon of the ulna (White, Black and Folkens, 2011). The medial and lateral epicondyles are on either side of the distal articular facets and are the point of origin for several muscles and tendons

involved in the flexion, extension, pronation and supination of the forearm, wrist, and hand (Stone and Stone, 2003).

The humeri begin to develop *in utero*. A primary ossification centre appears for each diaphysis between the eighth and ninth week of gestation (Noback and Robertson, 1951). Three secondary ossification centres appear at the proximal end of each humeri and coalesce between five and seven years, and four secondary ossification centres appear at the distal end of each humeri and coalesce between ten and 12 years (Cunningham, Scheuer and Black, 2016). Bone modelling thickens the cortices and modelling drift moves the humerus diaphysis postero-medially during childhood (Maggiano *et al.*, 2015) (modelling is discussed further in section 1.2.4 on page 18). The distal epiphyses typically fuse around 11-18 years with the medial epicondyle fusing separately at approximately 13-18 years, followed by the proximal epiphyses at around 14-21 years (Cunningham, Scheuer and Black, 2016).

The anatomy of the shoulder joint, coupled with complex musculature, allows for a particularly broad range of movement of the arm in humans and other great apes. The arm is capable of flexion, extension, circumduction, and pronation and supination of the forearm, as well as fine motor control of the hand. This vast range of movements causes a complicated pattern of loading that influences not only the morphology of the humerus but also its micro-anatomy.

1.2.2 | Biology, Anatomy, and Development of the Ribs

There are twelve ribs on each side of the skeleton. Each rib attaches at its proximal end, closest to the axial skeleton, posteriorly to the thoracic vertebra (**Figure 1.2b**) (White, Black and Folkens, 2011). Ribs one to seven are sternal ribs and are sometimes referred to as "true ribs" because their distal ends, furthest from the axial skeleton, articulate

directly with the sternum anteriorly. Ribs eight to ten are known as "false ribs" because they only articulate with the sternum via a common cartilage bridge. Ribs 11 and 12 are known as "floating ribs" because they do not articulate at their distal end.

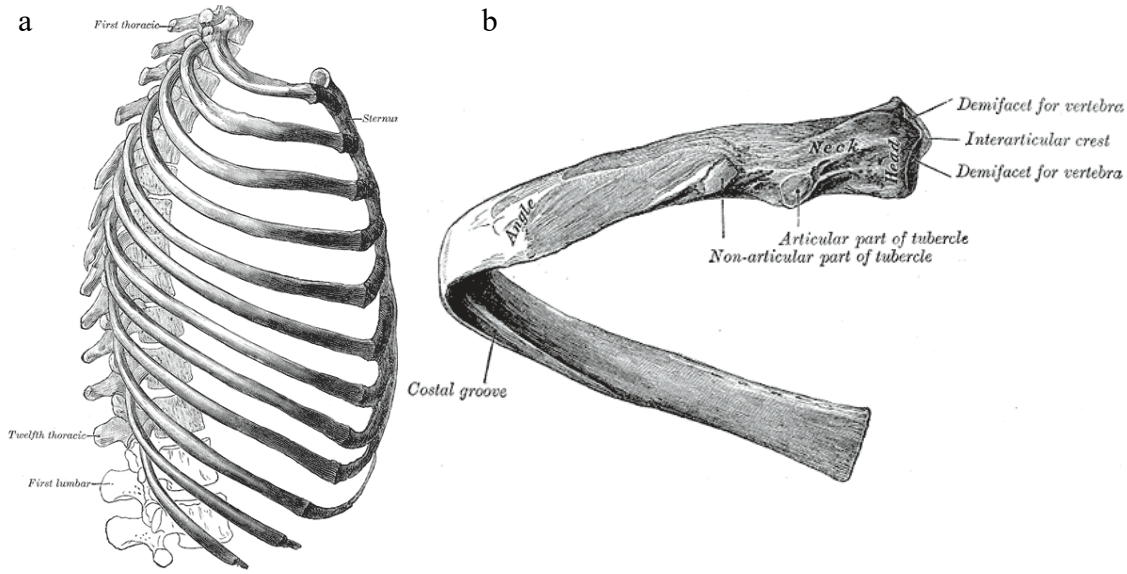

Figure 1.2 *The ribs. a – the thorax from the right. b – posterior view of a left rib. From Gray (1918) Anatomy of the Human Body, plate 114 and plate 123*

The head of each rib has two articulations, divided horizontally, with the superior facet for the vertebral body above and inferior facet for the vertebral body below. Ribs one, and ten to 12 do not have these demi-facets. There is a narrowing at the neck of the ribs between the head and the tubercle. The tubercle is on the most postero-inferior point on the rib and is the point of articulation between the rib and the transverse process of the lower vertebrae as well as the attachment point for ligaments (White, Black and Folkens, 2011). Lateral to the tubercle is the costal angle where the rib shaft curves sharply. On the external surface of the angle is a bony line that is the attachment site of the deep back muscles (White, Black and Folkens, 2011). On the medial inferior edge of the shaft there is a costal groove for the intercostal arteries, veins, and nerves that is most prominent on

ribs five to seven.

The sternal end of each rib, except the floating ribs, is a rough oval shaped surface where the costal cartilage attaches to the bone (White, Black and Folkens, 2011). Ribs 11 and 12 taper at their distal ends. The scaleni muscles, the external intercostal muscles, and the diaphragm (attached to the xiphoid process, the lower four ribs, and the bodies and arches of lumbar vertebrae 1-2) elevate the ribs during respiration and the internal intercostal muscles depress the ribs during forceful exhalation (Stone and Stone, 2003; White, Black and Folkens, 2011).

Ribs begin to develop *in utero* through chondrofication followed by ossification. Primary ossification centres appear at the posterior angle between the 8^{th}-12^{th} week of gestation (Noback and Robertson, 1951). Bone modelling thickens the cortices and modelling drift ensures the medullary cavity remains in the centre of the diaphysis while the ribs move ventrally during childhood as the thorax expands (Streeter, 2010) (modelling is discussed further in section 1.2.4 on page 18). Rib growth is complete between 15-24 years of age (Cunningham, Scheuer and Black, 2016).

The ribs form a protective cage around the heart and lungs and are only involved in respiration related movement, with a rhythmic expansion and contraction of the rib cage (**Figure 1.2a**) (White, Black and Folkens, 2011). Since movement of the rib is more dependent on cyclical breathing than on activity, the loading pattern varies little between people (Dominguez and Agnew, 2016).

1.2.3 | Bone Cells

Mature bone cells are named osteoblasts, bone lining cells, osteocytes, and osteoclasts. These are the cells responsible for bone formation, maintenance, and breakdown and they are all descended from mesenchymal stem cells or haematopoietic stem cells (Aubin,

2001). Mesenchymal stem cells are capable of differentiating into multiple cell types, including osteoblasts, chondroblasts, myoblasts, and adipocytes (**Figure 1.3**) (Aubin and Liu, 1996). Mesenchymal cells differentiate into progenitor cells that are committed to a particular lineage that leads the final cell type (Kousteni and Bilezikian, 2008). Osteoprogenitors are committed to the osteoblast lineage and future bone formation (Kousteni and Bilezikian, 2008). Osteoprogenitor cells differentiate to become preosteoblasts and then osteoblasts that form bone tissue (Martin *et al.*, 1998).

Osteoblasts secrete the organic component of bone, osteoid, but also induce the deposition of inorganic crystals, calcium and phosphate, that mineralise the osteoid (Martin *et al.*, 1998). Some osteoblasts differentiate into bone lining cells that stay on the bone surface as the osteogenic layer of the periosteum and endosteum. In the future these bone lining cells can de-differentiate into osteoblasts (Robling, Castillo and Turner, 2006). Most osteoblasts differentiate into osteocytes that become entombed in cavities, called lacunae, between the layers of lamellar bone. Osteocytes are mechanosensing cells that do not secrete osteoid (Martin and Burr, 1989). They sense the surrounding bone tissue with their tentacle like projections called canaliculi and communicate with one another via gap junctions on the canaliculi. At the end of their lifespan osteocytes either undergo apoptosis or are removed by osteoclasts during remodelling (Parfitt, 2002a). Osteoclasts are large cells that resorb bone at the ruffled border on the base of the cell (Martin and Burr, 1989). The mineralised bone matrix is dissolved by acidification and the organic matrix is digested by enzymes (Vaananen *et al.*, 2000). Unlike the other bone cells, osteoclasts are not derived from osteoprogenitors, but from the fusion of macrophages that arise from haematopoietic stem cells (Ash, Loutit and Townsend, 1980).

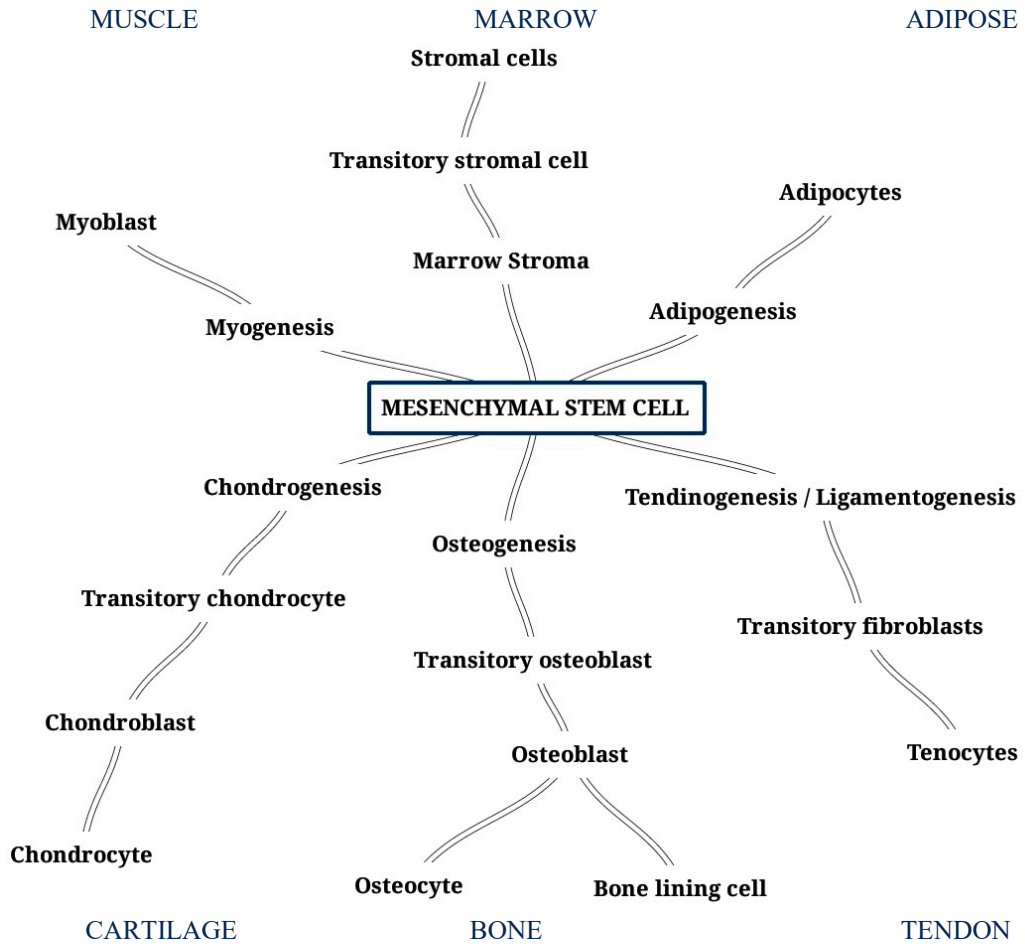

Figure 1.3 *Schematic illustration of mesenchymal stem cell differentiation*

1.2.4 | Growth, Modelling, and Morphology

Growth is a general term that encompasses the change in size and morphology of tissues during ontogeny (Cunningham, Scheuer and Black, 2016). It relates to an increase in size and an increase in maturity, but the processes are not necessarily coupled. So, it is possible for each child to attain different developmental stages while being at the same chronological age. Bones grow in length by bone formation at the epiphyseal plates and change morphology by bone modelling of the diaphysis, appositional growth, cortical drift, and lamellar compaction (Maggiano, 2012a). Together these processes are responsible for achieving the adult size, shape, and position of each bone.

The bone formation process of endochondral ossification involves the replacement of a hyaline cartilage model with bone tissue. It is the mechanism of longitudinal bone growth in the skeleton, which is regulated by systemic hormones including growth hormone, insulin-like growth factor-1, thyroid hormone, glucocorticoids, and, during adolescence, the sex steroids, testosterone and oestrogen (van der Eerden, Karperien and Wit, 2003; Gosman, 2012). Endochondral ossification can be divided into the five broad phases described below (**Figure 1.4**) (Cunningham, Scheuer and Black, 2016).

1. Cartilage models of the future bones form *in utero* (**Figure 1.4 - 1**). Mesenchymal stem cells condense at the sites of the future bones and differentiate into chondrocytes (Berendsen and Olsen, 2015). The cells on the periphery of the blastema condense, forming the perichondrium. This is a bilaminar membrane that surrounds the cartilage model and will in time become the periosteal membrane surrounding the bones. Chondroblasts line the internal layer of the perichondrium, where they hypertrophy and produce a calcified cartilaginous extracellular matrix and angiogenic stimulators (Dai and Rabie, 2007). In the humerus chondrofication starts at the shaft, proceeding to the head and epicondyles, and then the neck, tubercles, and condyles last (Scheuer and Black, 2000). In the rib chondrofication starts at the shaft, and then the head and the articular and non-articular parts of the tubercle (Cunningham, Scheuer and Black, 2016).

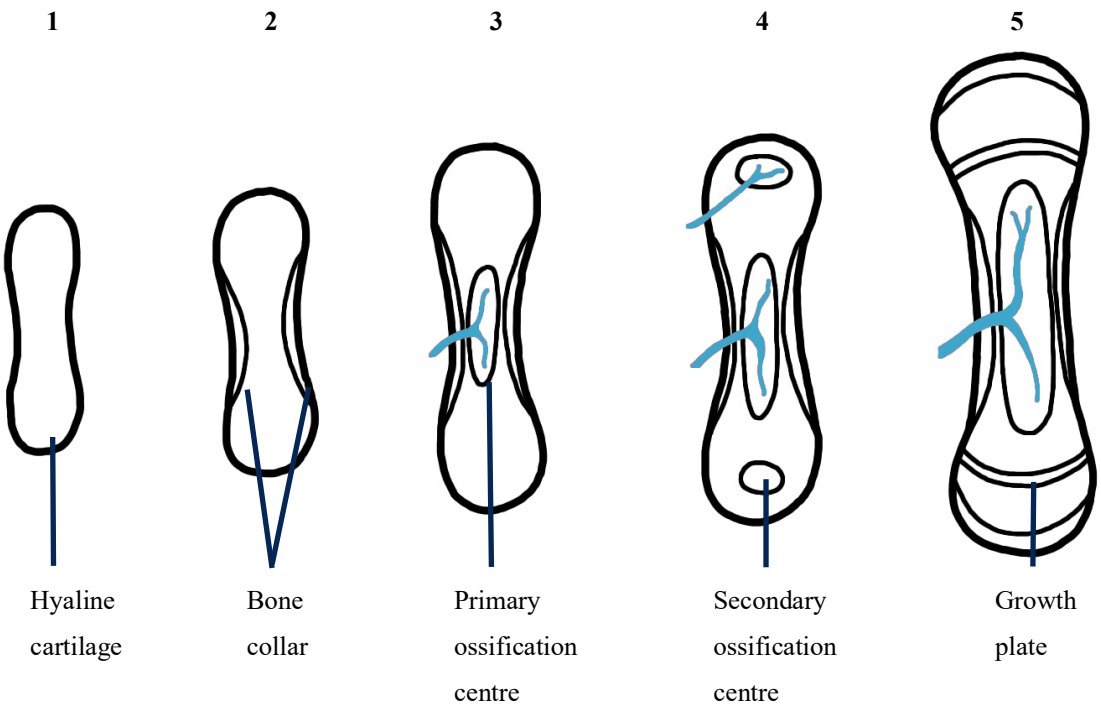

Figure 1.4 *Endochondral ossification divided into five sequential phases*

2. The perichondrium develops into the periosteum (**Figure 1.4 - 2**). The periosteum covers all external bone surface that is not covered by articular cartilage (White, Black and Folkens, 2011). Its purpose is to aid in bone growth and to provide nourishment to bone via its vascular supply (Cunningham, Scheuer and Black, 2016). Osteoblasts line the inside of the periosteum throughout life (Shopfner, 1966). The osteoblasts surrounding the cartilage diaphysis secrete osteoid that develops into a bony collar around the shaft. Osteoid is an organic matrix containing type 1 collagen and ground substance, and it is mineralised by inorganic hydroxyapatite crystals (Marks and Odgren, 2002; Zhu, Robey and Boskey, 2009).

3. The cartilage model is avascular, but bone tissue needs a constant blood supply to support its normal function (**Figure 1.4 - 3**). Angiogenic stimulators act as a target

for capillary invasion and angiogenesis (Alini *et al.*, 1996; Dai and Rabie, 2007). A nutrient foramen appears and perforates the diaphysis to transport blood vessels into the interior of the cartilage model so that the osteoblasts can receive nutrients (Trueta, 1963). At the primary ossification centre, the osteoblasts begin to form trabecular bone. This is a spongey web of bone that houses red bone marrow for haematopoiesis (Bruder and Caplan, 1989) that in mature bone is usually located in the epiphyses.

4. The trabecular bone in the diaphysis is resorbed by osteoclasts and the red bone marrow is replaced with yellow bone marrow (Martin *et al.*, 1998) (**Figure 1.4 - 4**). This leaves a central medullary cavity housing the yellow bone marrow, that is useful as a fat reserve for the body. By this phase, the woven bone collar around the diaphysis has been replaced by dense cortical bone. The interface between the medullary cavity and the cortical bone diaphysis is lined with a vascular membrane called the endosteum (White, Black and Folkens, 2011). Like the periosteum, the endosteum is lined with a layer of osteoblasts for future bone formation. There are more osteoblasts lining the periosteum in sub-adults than adults because of the rapid bone growth that occurs during childhood, but the potential for osteogenesis remains throughout life (Scheuer and Black, 2000).

During this fourth phase the secondary ossification centres appear (Cunningham, Scheuer and Black, 2016). The humerus has secondary ossification centres proximally for the head, and greater and lesser tubercles, and distally for the capitulum, trochlea, and medial and lateral epicondyles. At either end of the humerus the secondary ossification centres will merge together to produce compound epiphyses that will fuse to the diaphysis. The medial epicondyle will

fuse to the diaphysis separately from the distal compound epiphysis. (Scheuer and Black, 2000). The ribs have secondary ossification centres for the head and the articular and non-articular parts of the tubercle (White, Black and Folkens, 2011). The two ossification centres for the tubercle will merge to form a compound epiphysis before fusing to the rib shaft.

5. Growth plates form between the diaphysis and each epiphysis (Cunningham, Scheuer and Black, 2016) (**Figure 1.4 - 5**). As the amount of cortical bone in the diaphysis grows and the shaft increases in length, the space between the primary and secondary ossification centres diminishes, leaving a band of cartilage between them (Rang, 1969). On the epiphyseal side of the cartilage there is a terminal plate forming a barrier between the two ossification centres. The terminal plate is formed from fused trabeculae, which also keeps the red and yellow bone marrow separate throughout life (Cunningham, Scheuer and Black, 2016). The cartilage band beneath the terminal plate has four distinct layers: the germinal zone, the proliferating zone, the degenerating zone, and the ossification zone (Cunningham, Scheuer and Black, 2016). The germinal zone is closest to the terminal plate and has quiescent chondrocytes. Some blood vessels penetrate through the terminal plate to supply blood to the germinal zone. The proliferating zone is the next zone where the chondrocytes accumulate and grow (Mackie *et al.*, 2008). They become arranged into pillars of up to half of the height of the whole growth plate (Mackie, Tatarczuch and Mirams, 2011). In the degenerating zone, the chondrocytes start to hypertrophy and release matrix vesicles. The vesicles contain proteins that are thought to provide the nucleation site for mineralisation of the matrix by hydroxyapatite crystals (Kirsch *et al.*, 1997; Mackie *et al.*, 2008). The ossification

zone is closest to the diaphysis and is where osteoblasts secrete bone tissue onto the mineralised cartilage (Mackie *et al.*, 2008). Osteoclasts act in this zone to rearrange the originally deposited bone to give it a more organised structure. Eventually the rate of osteogenesis will overtake the rate of chondrogenesis, and the cartilage band of the growth plate will get smaller. This causes the fusion of the epiphyses to the diaphysis (Cunningham, Scheuer and Black, 2016). Once epiphyseal fusion is complete the bones cannot increase in length.

Bone modelling happens during growth and development to alter the size and shape of a bone to its adult morphology (Cambra-Moo *et al.*, 2014). It occurs by the independent action osteoblasts and osteoclasts at the periosteal and endosteal membranes (Maggiano, 2012b). Primary lamellar bone is deposited by osteoblasts without the removal of any existing bone at that particular site. At the same time, existing bone can be removed by osteoclasts elsewhere, but no new bone will be deposited by osteoblasts at that site. In general, bone is removed at the endosteum and deposited at the periosteum for bone to grow in size diametrically in a process known as periosteal apposition (Martin *et al.*, 1998; Maggiano, 2012b). Circumferential lamellae are deposited in layers beneath the periosteum and primary vascular canals are formed when blood vessels are trapped between the layers (Parfitt, 1983; Currey, 2013). Primary vascular canals contain few or no lamellae and do not have a boundary cement line (Currey, 2013). Lamellae can also be deposited at the endosteum, although this is more limited than at the periosteum and longitudinal vessel entrapment is rare (Maggiano, 2012b). All of the primary lamellar bone in the cortex can also be known as interstitial lamellar bone (Pinto and Pace, 2015). In addition to the normal periosteal apposition during ontogeny, bone formation at the periosteum can be induced by biomechanical loading of the bone (Mosley *et al.*, 1997;

Mosley and Lanyon, 1998, 2002; Robling *et al.*, 2001). Peak cross-sectional area is usually achieved during adolescence.

Other changes in the shape of the growing bones occur by the sculpting achieved by the uncoupled action of the osteoblasts and osteoclasts (Maggiano, 2012b). Modelling is responsible for the resorption of the metaphysis during longitudinal growth, known as metaphyseal reduction, and also the infilling of existing voids with primary lamellar bone, known as lamellar compaction (Enlow, 1962). Additionally, modelling drift keeps the medullary cavity in the centre of the diaphysis during growth and morphological change by the independent action of osteoclasts and osteoblasts on opposing sides of the diaphysis (Rubin, 1964; Epker and Frost, 1965; Parfitt *et al.*, 2000). Endosteal resorption and periosteal apposition occur on one side of the diaphysis as endosteal apposition and periosteal resorption occur on the other side of the diaphysis during modelling drift (Maggiano *et al.*, 2011). The result is that the whole bone diaphysis moves laterally, and the medullary cavity remains in the centre of the diaphysis.

1.2.5 | Remodelling

Remodelling is a distinct process from modelling because remodelling removes pre-existing bone and replaces it with new bone, but modelling does not remove bone prior to bone deposition (Maggiano, 2012b). Since remodelling removes old bone it is involved in both mineral homeostasis and the repair of microscopic damage (Burr, 2002). It is the mechanism of bone turnover. During remodelling, osteoblasts and osteoclasts are coupled in a basic multicellular unit (BMU) that produces a basic structural unit (BSU) of bone (Martin *et al.*, 1998). The BSUs are also known as Haversian systems or secondary osteons in cortical bone, and as hemi-osteons in trabecular bone (Martin *et al.*, 1998) (**Figure 1.5**).

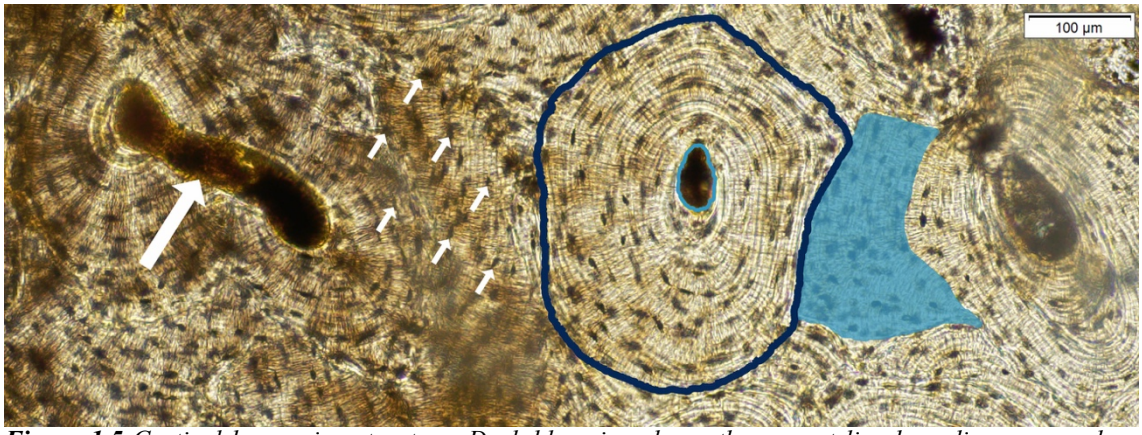

Figure 1.5 *Cortical bone microstructure. Dark blue ring shows the cement line bounding a secondary osteon. Light blue ring shows the Haversian canal. Blue highlighted area shows a secondary osteon fragment. Small white arrows point to osteocytes. Large white arrow points to a Volkmann's canal*

Secondary osteons track longitudinally through bone along the course that the BMU took and they can reach over 1cm in length in human cortical bone (Maggiano *et al.*, 2016). Recent 3D imaging of osteonal bone has shown that secondary osteons have a more complex network of branching and interconnectedness within cortical bone than was previously thought (Arhatari *et al.*, 2011; Cooper *et al.*, 2011; Maggiano *et al.*, 2016). Secondary osteons can divide into separate systems by lateral branching, resulting in unequal sized osteons, or by dichotomous branching, resulting in equal sized osteons (Maggiano *et al.*, 2016). Volkmann's canals are the branches that join the Haversian canals of neighbouring osteons together, and they are visualised as horizontal canals in 2D histomorphometry, (Maggiano *et al.*, 2016). It is also possible for new secondary osteons to grow within existing osteons (Arhatari *et al.*, 2011) and for some osteons to be sealed (Congiu and Pazzaglia, 2011; Maggiano *et al.*, 2016; Skedros *et al.*, 2018). While the full extent of the secondary osteon network can only be visualised by 3D imaging, 2D histomorphometry can give information on secondary osteon structure at particular cross sections.

In cross-section, secondary osteons appear as concentric rings of lamellae surrounding a central Haversian canal and bounded by a cement line (**Figure 1.5**) (LaCroix, 1971), but secondary osteons can have several morphological forms, including type I, type II, double zonal, or drifting. Lamellar forms can vary within the osteons and the lamellae are not always arranged in concentric rings, but can be spiral lamellae, which overlap themselves, or crescent lamellae, which do not form a ring (Pazzaglia *et al.*, 2012). Type I osteons are most common (**Figure 1.6a,b**). Type II, or embedded, osteons appear as a small secondary osteon that has an intact cement line and is embedded within another, larger, secondary osteon that also has an intact cement line (**Figure 1.6c**) (Ericksen, 1991). Type II osteons can form when new BMUs follow the path of existing osteons, resulting in a new osteon that is nested within a pre-existing osteon (Maggiano *et al.*, 2016). Double zonal osteons are similar in appearance to type II osteons, but they are a single osteon with a hypercalcified ring that resembles a cement line (**Figure 1.6e**) (LaCroix, 1971). The hypercalcified ring is thought to be a sign of arrested growth. Drifting osteons appear to move laterally through the cortex because of uneven lamellar formation on either side of the osteon that results in a 'tail' of lamellae that shows the drift of the BMU (**Figure 1.6d**) (Robling and Stout, 1999). Drifting osteons are more commonly found in juvenile bone than in adult bone (LaCroix, 1971; Burton, Nyssen-Behets and Dhem, 1989; Streeter, 2010).

Figure 1.6 *Secondary osteon morphology. a – type 1. b – type I. c – type II. d – drifting. e – double zonal*

The remodelling process follows a defined sequence: Activation – Resorption - Formation (ARF). The activation phase is prompted by the disruption of an inhibitory signal from local osteocytes (Burger and Klein-Nulend, 1999). Osteoclasts respond to that and accumulate at the site via the local blood supply (Pettit *et al.*, 2008).

1. During the resorption phase, the osteoclasts secrete proteases and acids that demineralise the existing bone and dissolve the collagen (Roodman, 1996; Vaananen *et al.*, 2000) leaving a histologically observable resorptive bay or cutting cone (Parfitt, 2002b). The action of the osteoclasts determines the diameter of the cutting cone and future secondary osteon, which is usually between 150 μm and 350 μm (van Oers, Ruimerman, Tanck, *et al.*, 2008). The edges of the cutting cone have scallops known as Howship's lacunae. The BMUs have been reported to advance through bone at a rate of 20 μm per day (Martin *et al.*, 1998). A capillary grows immediately behind the advancing BMU to supply nutrients and additional osteoclast precursor cells.

2. There is a brief reversal phase between bone resorption and bone deposition, lasting nine days (Ott, 2002), when the boundary of the secondary osteon is defined. Bone lining cells line the cutting cone and smooth the edges of the Howship's lacunae (Everts *et al.*, 2002). Next, a layer of sulphur-rich matrix is deposited that will form the reversal line, or cement line, that separates an osteon from the surrounding bone (Robling, Castillo and Turner, 2006). The bone lining cells release a growth factor (TGF-β1) that attracts mesenchymal stem cells to the BMU (Tang *et al.*, 2009), which then differentiate into osteoblasts over two to three days (Martin *et al.*, 1998).

In the formation phase the osteoblasts secrete osteoid which is composed of type 1 collagen, noncollagenous proteins, proteoglycans, and water (Marks and Odgren, 2002). Next, the osteoblasts secrete calcium phosphate crystals that mineralise the osteoid, although, there is a delay of around 10 days between secretion and mineralisation (Martin *et al.*, 1998). The site of mineralisation is known as the mineralisation front and this is the point at which in vivo labels are incorporated into bone (Stout and Crowder, 2012). Mineralisation is regulated by fluctuating levels of inorganic pyrophosphate. The level of pyrophosphate is increased by nucleotide pyrophosphatase pyrophodiesterase 1 (NPP1) and ankylosis protein (ANK) and decreased by tissue nonspecific alkaline phosphatase (TNAP) (Orimo, 2010). Osteopontin (OPN) may also regulate bone mineralisation by affecting the ability of NPP1 and ANK to regulate mineralisation (Johnson *et al.*, 2003). The mineralised bone forms in concentric lamellae that fill in the cutting cone. A Haversian canal is left in the centre of the osteon to house the bones vascular and nerve supply.

All osteoclasts undergo apoptosis when bone resorption is complete, but after bone deposition, the osteoblasts can undergo apoptosis or differentiate into either bone lining cells or osteocytes (Burger and Klein-Nulend, 1999; Everts *et al.*, 2002). The osteoblasts that are trapped in the matrix differentiate into osteocytes that become entombed in lacunae between the layers of mineralised bone. Each osteocyte has many cytoplasmic processes extending in canaliculi into the surrounding bone (Knothe Tate *et al.*, 2004). Gap junctions form where the canaliculi of neighbouring osteocytes meet so they form a network of osteocytes throughout the bone. Their primary role is as mechanosensing cells (Burger and Klein-Nulend, 1999). Osteocytes emit a continuous

signal that inhibits BMU activation, but the signal can be disrupted by strain induced microcracks or osteocyte apoptosis. A new ARF sequence begins when the signal is disrupted, and the damaged bone is remodelled (Burger and Klein-Nulend, 1999).

1.2.6 | Factors Affecting Remodelling

The factors that influence remodelling in cortical bone are commonly split into two groups according to whether they have a systemic effect on the skeleton or a local effect on particular bones or parts of bones. The systemic factors usually originate within the body: (1) age, (2) sex, (3) genetics, (4) metabolism (including diet and disease). While, the local factors can have an external source: (5) biomechanics. Still, bone biology is complex and there may be other factors affecting bone turnover that are currently unknown.

1. ***Age*** – secondary osteons accrue with age (Gocha, Robling and Stout, 2018) and many studies have reported a positive relationship between age and OPD (Stout and Lueck, 1995; Mulhern and Van Gerven, 1997; Mulhern, 2000; Keough, L'Abbé and Steyn, 2009; Cho and Stout, 2011; Botha *et al.*, 2018). Asymptote is reached around the sixth decade of life, when new secondary osteons remove all traces of previously existing osteons (Cho *et al.*, 2002). Subsequently, OPD will not increase. The exact chronological age that asymptote is reached varies according to osteon size, remodelling rate, and cortical area (Andronowski and Crowder, 2018).

   Osteon size and shape also show an age-related change (Pfeiffer *et al.*, 2016). Numerus studies have reported that secondary osteons become smaller and/or more circular with advancing age (Currey, 1964; Takahashi, Epker and Frost,

1965; Jowsey, 1966; Landeros and Frost, 1966; Evans, 1976; Yoshino *et al.*, 1994; Han *et al.*, 2009; Cho and Stout, 2011; Dominguez and Agnew, 2016; Goliath, Stewart and Stout, 2016). Although, other studies that have not reported this relationship between osteon size and age (Pfeiffer *et al.*, 2006). Smaller and more circular osteons may be more efficient at reducing the spread of microcracks that accumulate in cortical bone (Skedros, Knight, *et al.*, 2013). Alternatively, it has been suggested that the previously observed relationship between osteon size and age may be a consequence of the statistical likelihood that larger osteons will be remodelled over time (Cho and Stout, 2011). Thus, the larger osteons would only appear as fragmentary osteons and would not contribute to the assessment of osteon size. However, recent 3D imaging supports the findings that secondary osteons do become smaller and/or more circular with advancing age (Hennig *et al.*, 2015). Haversian canal size does not appear to change with age (Keough, L'Abbé and Steyn, 2009; Botha *et al.*, 2018).

2. ***Sex*** – There are conflicting findings relating to sex differences in osteon geometry. Sex differences have been noted in the rib but not in the femur of the same individuals (Cho and Stout, 2011), but also conversely in the femur and not in the rib (Mulhern, 2000). Some studies have reported that males had smaller femoral osteons than females (Burr, Ruff and Thompson, 1990; Mulhern and Van Gerven, 1997), but another reported that females had smaller femoral osteons than males (Britz *et al.*, 2009). Other studies have reported no sex differences in bone microstructure (Stout and Paine, 1992; Stout and Lueck, 1995; Stout, Porro and Perotti, 1996; Mulhern, 2000; Dominguez and Agnew, 2016; Botha *et al.*, 2018). Generally, any sex differences in cortical bone microstructure could be related to

sexual dimorphism, or endocrine or metabolic differences (Andronowski and Crowder, 2018), or to biomechanical differences (Dominguez and Agnew, 2016).

It is possible that the sex related pattern in osteon size can change according to age. Younger females had larger femoral osteons than males, but this pattern is reversed in older adults (Dominguez and Crowder, 2015). Similarly, sex differences have been reported for aging bone, with females having a greater reduction in rib osteon area with advancing age than males (Cho and Stout, 2011; Beresheim *et al.*, 2018). The sex and age-related difference could be linked to fatigue prevention given that menopause related bone loss will increase strain, but smaller osteons are associated with reduced strains (van Oers, Ruimerman, van Rietbergen, *et al.*, 2008).

3. ***Genetics*** – It has been suggested that genetic factors can affect bone microstructure and maintenance (Cho, Stout and Bishop, 2006). An experimental animal study demonstrated that genetic factors can affect the total area and cortical area of the mouse femur (Wallace *et al.*, 2012). Another study showed that, after accounting for age and sex, significant genetic effects were evident for the proportion of osteonal bone in the cortex, the secondary osteon area, and the secondary osteon wall thickness in the baboon femur (Havill *et al.*, 2013).

4. ***Metabolism*** – Non-targeted remodelling is a continuously occurring process involved in mineral homeostasis (Burr, 2002; Kousteni and Bilezikian, 2008). Non-targeted remodelling and targeted remodelling – in response to local biomechanical strains – are balanced across the skeleton to preserve strength (Eleazer and Jankauskas, 2016). Some dietary factors that affect metabolism have

been found to also affect bone microstructure (Richman, Ortner and Schulter-Ellis, 1979; Alexy *et al.*, 2005; Paine and Brenton, 2006). Some diseases can affect bone microstructure, for instance osteoporosis and its treatment can influence bone turnover (Storm *et al.*, 1993).

5. ***Biomechanics*** – Mechanical loading during growth encourages increased subperiosteal bone modelling that increases the cortical thickness (Ruff, Holt and Trinkaus, 2006). The larger cross-sectional area reduces compressive stress and increases resistance to bending and twisting (Lieberman, Devlin and Pearson, 2001). Strain-induced micro-cracks accumulate over time, but targeted remodelling replaces the damaged bone with new lamellar bone in the form of secondary osteons (Burr *et al.*, 1985).

   Animal studies have indicated that bone remodelling can be mechanically induced since higher osteon counts have been consistently noted in regions of bone that are subjected to increased loading (Lanyon *et al.*, 1982; Lanyon and Rubin, 1984; Raab *et al.*, 1991; Yamada, Tadano and Fujisaki, 2011; Wojda *et al.*, 2013). Animal studies have also linked osteocyte density to the loading of cortical bone (Nicolella *et al.*, 2006; Totland *et al.*, 2011; Sugawara *et al.*, 2013). As such both osteon density and osteocyte density have been used to infer behaviour in past human populations (Pfeiffer *et al.*, 2006; Miszkiewicz and Mahoney, 2016).

1.2.7 | Bone Histomorphometry

Quantifying the features of bone remodelling is possible with 2D static histomorphometry. Histomorphometry is the quantitative approach to measuring

microstructure (Stout and Crowder, 2012). Most of the existing bone histomorphometric studies can be grouped into one of three areas: age estimation; intraskeletal variation and other methodological advances; the factors affecting remodelling. Earlier histomorphometric studies focused on adults, particularly age estimation techniques, and across all types of histological studies there has traditionally been a focus on the ribs, femur, and tibia. The first age estimation techniques were based on the femur, tibia, and fibula (Kerley, 1965; Kerley and Ubelaker, 1978), and then on the rib and clavicle (Stout and Paine, 1992). These studies all report an age-related increase in the number of secondary osteons and secondary osteon fragments.

More recently there has been a focus on intra-section and intra-bone variability and the distribution of tissue types. Patterns of intra-skeletal microstructural variation have most commonly been described between the rib and femur (Cho and Stout, 2011; Goliath, Stewart and Stout, 2016), or rib, femur, and humerus (Eleazer and Jankauskas, 2016), but also from the femur, fibula, humerus, radius, tibia, and ulna for the purpose of investigating the effect of unloading on the skeleton (Schlecht *et al.*, 2012). Not only does microstructure vary between bones, it also varies within individual bones. Inter-section microstructurally variation along the long bone shaft has been studied primarily for the shaft of the femur (Chan, Crowder and Rogers, 2007), and tibia (Ural and Vashishth, 2006). The potential variation between bones in a similar loading environment has also been studied, for instance, the intra-costal variation between ribs three to eight (Crowder and Rosella, 2007). This body of research suggests that cortical bone microstructure is highly variable throughout the skeleton.

Further studies have investigated the factors affecting bone biology, including: age (Stout and Paine, 1992; Goliath, Stewart and Stout, 2016; Pfeiffer *et al.*, 2016), sex (Seeman, 2002; Tommasini, Nasser and Jepsen, 2007; Jepsen, Bigelow and Schlecht,

2015), and genetics (Cho, Stout and Bishop, 2006; Wallace *et al.*, 2012; Havill *et al.*, 2013), as well as metabolism (Burr, 2002; Eleazer and Jankauskas, 2016), diet (Richman, Ortner and Schulter-Ellis, 1979; Alexy *et al.*, 2005; Paine and Brenton, 2006), health (Martin and Armelagos, 1979; Storm *et al.*, 1993), and biomechanics (Young *et al.*, 1986; Frost, 1997; Pearson and Lieberman, 2004; Britz *et al.*, 2009). Biomechanics and metabolism are the most influential of all of the factors affecting bone remodelling (Botha, Bhagwandin, Lynnerup, & Steyn, 2018; Cho & Stout, 2011; Keough, L'Abbé, & Steyn, 2009; Mulhern, 2000; Mulhern & Van Gerven, 1997; Stout & Lueck, 1995), since biomechanical strain causes micro-damage that is replaced by targeted remodelling and systemic bone remodelling is related to mineral homeostasis and metabolism (Burr, 2002). It has been recognised that population specific variation in activity, socioeconomic status, diet, and disease, through their links to biomechanics and metabolism, can result in bone microstructure that shows population specific patterns. Consequently, population specific regression equations for estimating age-at-death from cortical bone histology have been developed (Cho *et al.*, 2002) and these population-based studies have branched out to inferring behaviour from bone microstructure by applying bone remodelling principles (Miszkiewicz and Mahoney, 2016).

Despite the proliferation of histological studies of adult bone, juvenile bone microstructure has been less well explored. The existing ontogenetic studies have characterised the tissue type distributions across the cortex (Cambra-Moo *et al.*, 2012, 2014; Maggiano *et al.*, 2015; Maggiano *et al.*, 2016), the cross-sectional geometry (Goldman *et al.*, 2009; Gosman *et al.*, 2013), or provided histomorphological descriptions of the microstructure (Streeter, 2005). Juvenile humerus histomorphometric studies have shown that the cortex becomes more mineralised (Cambra-Moo *et al.*, 2014) and secondary osteons accrue with age (Pitfield, Miszkiewicz and Mahoney, 2017), while the

entire cortex drifts postero-medially during ontogeny (Maggiano *et al.*, 2016). Juvenile rib histomorphometric studies have also described the accrual of secondary bone during ontogeny (Streeter, 2010) and demonstrated that the total area and cortical area increase with age (Takahashi and Frost, 1966). However, there have been few studies of juvenile microstructure to use the histomorphometric methods that are commonly used on adult cortical bone. Juvenile bone tissue has a different structure to mature bone but remodelling, shown by the presence of secondary osteons, can begin as early as two to three months old (Schnitzler and Mesquita, 2013). Thus, it is possible to apply static histomorphometric measurements of secondary osteon density and geometry to juvenile bone and interpret the results within the framework of bone biology.

1.3 | ENAMEL FORMATION

1.3.1 | Biology, Anatomy, and Development

Each person has two sets of teeth during their lifetime. Deciduous teeth begin developing prenatally and erupt into the mouth during early childhood, but they are later shed and replaced by the permanent dentition. Permanent teeth are larger and have thicker enamel than deciduous teeth (Grine, 2005; Mahoney, 2010), so they are also formed more slowly than deciduous teeth (Moorrees, Fanning and Hunt, 1963a, 1963b). Most of the permanent teeth initiate after birth, although the first permanent molar can begin to develop prenatally (Christensen and Kraus, 1965). The permanent teeth erupt in sequence from six years of age to around 20 years. This eruption sequence has long been used as a method of age estimation for juvenile skeletal remains (Moorrees, Fanning and Hunt, 1963a; Haavikko, 1970; Gustafson and Koch, 1974; Smith, 1991; Al Qahtani, Hector and Liversidge, 2010).

Each tooth is made up of four tissue types: enamel, dentine, pulp, and cementum.

The crown has a central pulp chamber covered in dentine and enamel. Mature enamel contains 95% hydroxyapatite crystals, 4% water, and 1% enamelin protein (Berkovitz, Holland and Moxham, 1992). Dentine is softer than enamel because it contains only 70% hydroxyapatite crystals, as well as 20% collagen fibres, 10% water, and traces of protein (Reiche, Vignaud and Menu, 2002). The connection between dentine and the enamel and cement layers are termed the enamel-dentine junction and the cement-dentine junction respectively. The central pulp chamber contains pulp, which is a connective tissue with blood vessels and nerves. The pulp chamber typically has conical hollows in its roof and an opening into a root canal. The dentine of the root is covered in a layer of cementum (Nanci, 2017). Cementum is a hard tissue that protects the root and is the attachment site for the periodontal ligament fibres. Once the teeth have erupted into the oral cavity they are anchored to the bone via the periodontal ligaments.

The first permanent molar is the first permanent tooth to form, often initiating prenatally, and is the first permanent tooth to erupt (Christensen and Kraus, 1965). The upper molars have four major cusps: mesio-lingual, mesio-buccal, disto-buccal, and disto-lingual (**Figure 1.7**) (van Beek, 1983). The disto-lingual cusp is usually the smallest, so the other three cusps leave a triangularly shaped central fossa (Hillson, 1996). The lingual side of the crown is more rounded and bulging than the buccal side. The pulp chamber is located in the cervical part of the crown and has four diverticles, one underneath each of the cusps (Hillson, 1996). The diverticles beneath the buccal cusps are the largest because those are the largest cusps. The base of the pulp chamber opens out into three root canals, corresponding to the three roots. The upper molars have a large lingual root and two smaller buccal roots.

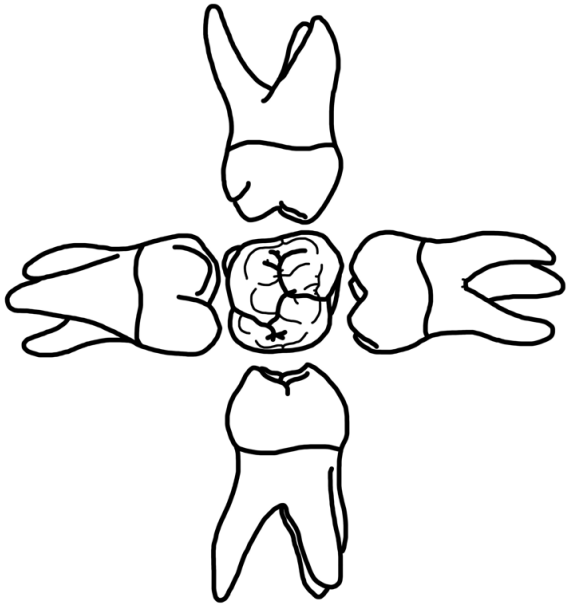

Figure 1.7 *Right maxillary first molar, lingual side left and distal side lower. (Redrawn from van Beek, 1983)*

Lower first molars have five cusps, with one at each corner of the crown and a fifth cusp that is located on the distal part of the occlusal surface (**Figure 1.8**) (van Beek, 1983). Lower second molars have four main cusps that are located at each corner of the crown and a central fossa (Hillson, 1996). Unlike the upper molars, the four main cusps of the lower molars are all approximately equal sized (van Beek, 1983). The lower third molar may have four or five cusps (van Beek, 1983). The additional cusps are smaller than the four main cusps. In each of the lower molars, the pulp chamber is inside the cervical part of the crown and the number of diverticles corresponds to the number of cusps on each individual molar (Hillson, 1996). The base of the pulp chamber has two root canals because lower molars only have two roots. There is a larger, mesial root, and a smaller, distal root.

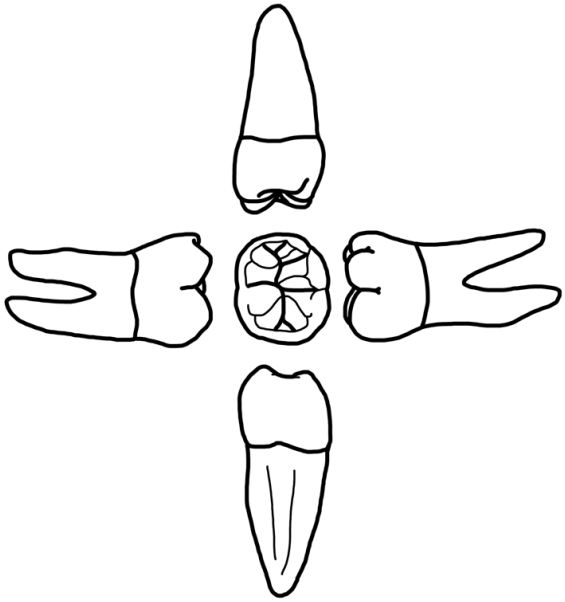

Figure 1.8 *Right mandibular first molar, lingual side left and mesial side down. (Redrawn from van Beek, 1983)*

Deciduous tooth development begins *in utero*, approximately six weeks after fertilisation (Nanci, 2017). Odontogenesis, the process of tooth formation, is a continuous process but it is often divided into four phases; (1) initiation, (2) the bud stage, (3) the cap stage, and (4) the bell stage.

1. ***The initiation stage*** – The surfaces of the developing mouth have of a layer of epithelium lying over a layer of mesenchymal tissue (Hillson, 1996; Jernvall and Thesleff, 2012). The mesenchyme condenses into an arch shape that extends along the jaws and the epithelial layer grows into this to make the primary epithelial band (Nanci, 2017). The primary epithelial band divides into two lobes that are known as the vestibular laminar and the dental lamina (Nanci, 2017).

2. ***The bud stage*** – By the tenth week of gestation the dental lamina has ten swellings, or epithelial buds, on each jaw that correspond to the 20 future deciduous teeth (Nanci, 2017). The swellings are the enamel organs that will

eventually form the enamel of the tooth crowns. The first of the enamel organs for the permanent dentition form after the sixteenth week of gestation and the last form after birth (Hillson, 1996).

3. ***The cap stage*** – A hollow filled with mesenchyme develops on one side of the enamel organ. This is termed the dental papilla (Nanci, 2017). Concurrently, the remaining mesenchyme assumes a bag-like formation that is called the dental follicle (Hillson, 1996). The developing tooth is anchored to the dental lamina by an outgrowth called the lateral lamina (Nanci, 2017). Together the enamel organ, the dental papilla, and the dental follicle are known as the tooth germ. Eventually, the enamel organ will form the enamel, the dental papilla will form the dentine and pulp, and the dental follicle will form the cement (Nanci, 2017). At the end of the cap stage, part of the enamel organ differentiates into the internal enamel epithelium which will produce the enamel matrix.

4. ***The bell stage*** – The primary enamel knot develops that will determine the future crown shape by inducing the formation of secondary enamel knots at the future cusp tips (Jernvall and Thesleff, 2000). In teeth with multiple cusps, some groups of cells in the internal enamel epithelium cease cell division, while other groups continue with normal cell division (Hillson, 2014). This causes a buckling of the internal enamel epithelium that results in the folding of the cusps. At the folds, odontoblasts differentiate from the outer mesenchymal cells of the dental papilla (Arana-Chavez and Massa, 2004). Odontoblasts are responsible for dentine formation in teeth and they secrete organic matrix that is subsequently mineralised (Arana-Chavez and Massa, 2004). Immediately after this, internal enamel

epithelium cells differentiate into pre-ameloblasts and then ameloblasts (Åberg, Wozney and Thesleff, 1997). Ameloblasts are enamel forming cells that are only present during tooth development (Hillson, 1996). The ameloblasts secrete enamel matrix onto the existing layer of predentine. This will be the position of the enamel dentine junction.

Enamel is deposited by ameloblasts in layers to form the crown (Risnes, 1986). The first layers are those within the folds of the enamel organ that will make up the cores of the future cusps. Successive layers are deposited on top, gradually increasing the size of the cusp (Beynon and Dean, 1988). The additional layers splay out to form the sides of the cusps (Beynon and Reid, 1987). Any ridges in the crown are formed by further folding of the enamel organ (Jernvall and Jung, 2000). As enamel layers are deposited on the sides of the ridges, the ridges grow towards one another until they coalesce (Hillson, 1996). In molars, the cusps first coalesce into a ring, and the centre of the occlusal surface is left open until the cusp bases become large enough to meet and form the fissures of the crown (Beynon *et al.*, 1998). After the occlusal surface has come together, the sides of the crown are formed by successive overlapping layers of enamel, which become narrower towards the cervix. The enamel deposition ceases at the cervix.

Pre-dentine is deposited on the inner side of the enamel organ slightly in advance of the initial enamel layer (Nanci, 2017). Subsequent layers of pre-dentine are secreted by odontoblasts, which build up in the same way as the enamel layers. The pre-dentine layers are more sharply angled than the enamel layers, so they project out below the enamel in a growing crown. The layers of pre-dentine will eventually splay out to form the diverticles, roof, and then sides of the pulp chamber. Pre-dentine secretion continues after crown completion until the roots are complete at the apex (Hillson, 1996). The

predentine matrix is mineralised by noncollagenous matrix proteins secreted by fully differentiated odontoblasts and odontoblast leaves a dentine tubule that is similar to the prism paths in enamel (Arana-Chavez and Massa, 2004).

The completion of the enamel crown is more variable than the initiation of the crown. The first molar crowns are completed at around three years after birth, but this can vary between two and a half to three years (Hillson, 1996). Once the crowns are completed the roots begin to grow (Li, Parada and Chai, 2017). The tooth crowns are encased in bone crypts inside the mandible and maxilla while they develop. The tissue remodels to form an epithelial canal that can accommodate the emerging tooth (Hillson, 2014). The overlying bone is resorbed to allow the tooth to erupt through the gums and into the mouth. The periodontal ligament and alveolar bone remodel to anchor the root into the jaw as the roots reach completion (Hillson, 1996). Root completion is even more variable than crown completion, taking between two and four years in most teeth. The permanent first molars and the incisors complete their roots first, between nine and 12 years. Females have been found to sometimes be in advance of boys by approximately 3% throughout the sequence of crown initiation, crown completion, and root formation (Garn *et al.*, 1958).

1.3.2 | Enamel Secretion and Structure

Enamel is an acellular material, but its formation is cellular and involves the internal enamel epithelium. This is a layer composed of cells called ameloblasts which secrete enamel matrix. Enamel formation, or amelogenesis, occurs in two stages (Hillson, 1996):

1. ***The matrix secretion stage*** – Ameloblast cells become more columnar in shape and the nucleus migrates to the proximal end and a Tomes' process develops at

the secretory end of the cell. Tomes' process are a cytoplasmic process on the distal end of each ameloblast (Risnes, 1998). Enamel matrix is 90% amelogenin, but it also includes enamelin, tuftelin, and ameloblastin (Robinson *et al.*, 1998), as well as the protease metalloproteinase-20 (Sierant and Bartlett, 2012). Matrix destined for the enamel prisms is secreted by one side of the Tomes' process and matrix destined for the interprismatic enamel is secreted by the other side (Warshawsky *et al.*, 1981; Nanci and Warshawsky, 1984). The matrix is mineralised by apatite crystallites that are seeded into the matrix by the ameloblast Tomes' processes. Completion of the matrix secretion stage results in partially mineralised enamel.

2. ***The maturation stage*** – After the ameloblasts have finished secreting matrix between the EDJ and the cusp surface, they lose their Tomes' process, reduce in size, and proceed to break down the organic part of the matrix (Robinson, Kirkham and Hallsworth, 1988). Ameloblasts secrete calcium, phosphate, and bicarbonate and remove water from the organic material as part of the mineralisation process (Robinson *et al.*, 1998). As this is happening, the apatite crystallites increase in size to between 50 and 100 nm in diameter (Hillson, 1996). This results in mature enamel that is almost entirely mineral.

When a tooth crown is developing both stages of amelogenesis can be observed in the crown at the same time. A zone of unmineralised enamel matrix can be seen at the edge of the crown where the tooth is forming. Further up the crown, towards older enamel, there is a transitional zone that is characterised by a loss of the organic matrix, and then a maturation zone that contains maturing and fully mature, mineralised enamel (Robinson

et al., 1998).

Mature enamel retains the discontinuities that were created by every Tomes' process during the first stage of enamel formation. The discontinuities are known as prisms. One ameloblast forms one prism from the EDJ to the enamel surface (Skobe, 2006). The prisms appear using scanning electron microscopy arranged in one of three patterns (Boyde and Jones, 2017). Pattern 1 enamel contains individual prisms that are arranged in a honeycomb-shaped mesh of enamel with inter-prismatic enamel sheets between them. The centres of the prisms are approximately 5.5 μm apart (Boyde and Jones, 2017). This structure is observed if it is sectioned transversely, but in longitudinal sections they appear as alternating wide and narrow bands. Pattern 2 enamel has prisms that are stacked above each other in columns. The prisms approximately 4.5 μm apart and they are separated by sheets of inter-prismatic enamel (Boyde and Jones, 2017). When this pattern is section transversely alternative rows of prisms and inter-prismatic sheets can be seen, but when they are sectioned longitudinally an irregular pattern is seen. Pattern 3 enamel has prisms that have a projection of inter-prismatic enamel that connects to the two prisms in the layer below. The prism centres are located approximately 6 μm apart (Boyde and Jones, 2017). When they are sectioned transversely the regular shape of these prisms creates a keyhole-like pattern, but if they are sectioned longitudinally there is a series of regular lines (Meckel, Griebstein and Neal, 1965).

All of these patterns have been found in human enamel, although the most common pattern is pattern 3 enamel. Irregularities in the pattern are common and so it has been suggested that two types of pattern 3 enamel exist in humans (Gantt, 1982). However, it is more likely that these variations are an artefact of a variation in the plane of sectioning (Vrba and Grine, 1978). A single tooth may have more than one type of enamel pattern. Most people have a thin layer of aprismatic enamel that makes up the

crown surface. Underneath this is usually a layer of pattern 1 enamel, and underneath that is pattern 3 enamel, which makes up most of the enamel thickness (Boyde and Martin, 1984; Martin and Boyde, 1984; Martin, 1985, 1986; Martin, Boyde and Grine, 1988). The orientation of the apatite crystallites can be observed by using polarised light microscopy. The different orientations of the head and tail of a prism can be seen as alternating bands of light and dark when viewed under polarised light. Generally, the angle of orientation increases from the crown tip down towards the cervical margin.

Prisms track the path that the ameloblasts took from the enamel dentine junction to the crown surface during amelogenesis. The paths are only perpendicular to the crown surface at the cusp tips and at the cervix and between these regions the prism paths approach the crown surface at an oblique angle. The prism paths are not completely straight through the enamel. Scanning electron microscopy (SEM) has shown that the prism paths have undulations (Osborn, 1970). Each prism path has slightly different undulations to its neighbours, and this produces a cycle of variation that is known as decussation (Boyde, 1989; Nanci, 2017). The decussation appears as alternating bands of light and dark under polarised light because of the different orientations of the prisms that are at different points in the undulation. This phenomenon is known as Hunter-Schreger bands (Osborn, 1990).

1.4 | BIORHYTHMS

Biorhythms are internally controlled fluctuations in biochemistry that influence a body's ontogenetic growth, life history traits, or daily functions (Hastings, 1997). They often respond to environmental stimuli that trigger an internal biochemical reaction. They can manifest as so-called hour-glass mechanisms for singly occurring life events, for example the onset of menarche or menopause, or as oscillating rhythms for recurring

cycles, for example the sleep wake cycle or oestrous cycle. Each oscillating biorhythm within a body can have a different periodicity. These are grouped into three categories according to the length of the oscillation. Circadian rhythms are 24 hours long. Infradian rhythms have an oscillation longer than 24 hours and intradian rhythms have an oscillation shorter than 24 hours. Markers of all three lengths of oscillating biorhythm are retained in enamel microstructure (Boyde, 1976, 1989).

1.4.1 | Cross Striations – A Circadian Biorhythm in Human Enamel

A series of cross striations along the prisms can be visualised under the microscope as swellings and constrictions approximately 2-5 μm apart in modern human enamel (Hillson, 1996). The variation appears as alternating dark and light bands via transmitted light microscopy. The exact distance between adjacent cross striations varies throughout the crown, they are spaced closer together near to the EDJ than at the crown surface, and closer together at the cervix than at the occlusal surface. The striations are believed to be caused by a cyclical variation in the enamel matrix secretion rate (Boyde, 1976), with the bulges of the prism head representing faster enamel secretion and the constrictions representing slower enamel secretion. The interval between the cross striations matches the reported enamel matrix secretion rate of 4-4.5 μm per day (Schour and Poncher, 1937; Schour and Hoffman, 1939; Massler and Schour, 1946). When tested experimentally using periodic marker injections, the number of cross striations also corresponded to the number of days between injections (Mimura, 1939; Bromage, 1991; Smith, 2006). The periodicity of cross striations has also been confirmed in known age human teeth (Antoine, Hillson and Dean, 2009). This indicates that the cross striations are formed by a systemic pause in the secretory activity of the enamel-forming cells in a 24-hour cycle, or circadian rhythm (Boyde, 1989; Hillson, 1996) (**Figure 1.9**).

Cross striations occur at regular time increments, so they can be used to calculate the timing of other incremental markings. Cross striations can be divided by fine lines that split them into two segments (Smith, 2006). Since cross striations have a circadian rhythm, these fine lines must have a sub-daily, or intradian, rhythm, of approximately 12 hours (Smith, 2006) (**Figure 1.9**).

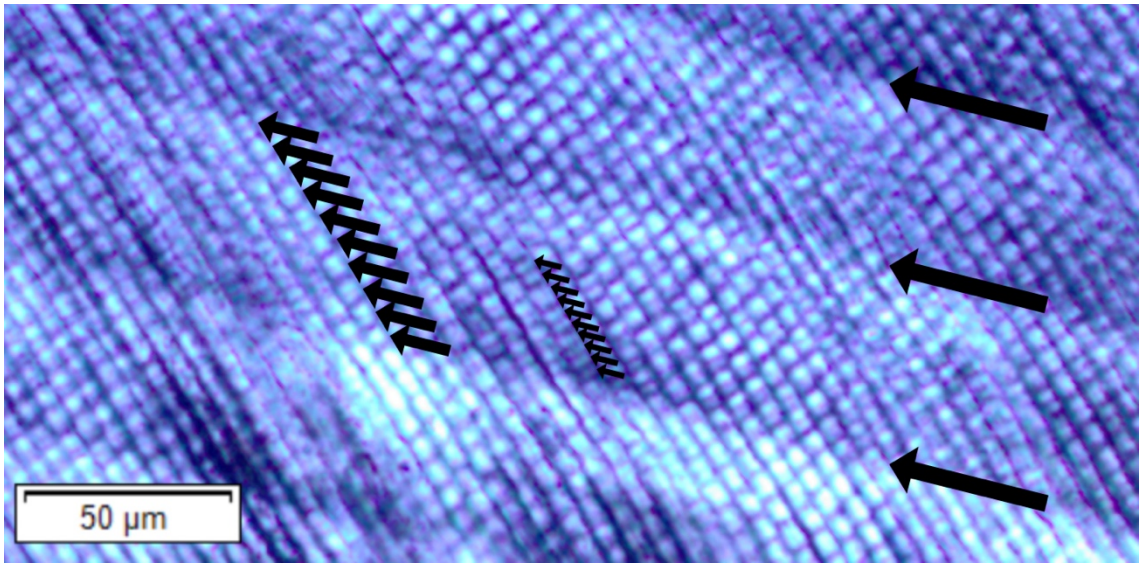

Figure 1.9 *Incremental markings in enamel under polarised light. Medium black arrows – cross striations. Small black arrows – intradian lines. Large black arrows – Retzius lines*

1.4.2 | Retzius Lines– An Infradian Biorhythm in Human Enamel

In addition to the daily and sub-daily incremental markings there are longer period growth markings in enamel that are called striae of Retzius or Retzius lines (Risnes, 1998) that are named after Anders Retzius who first described them in 1837 (Retzius, 1837). Light microscopy of thin-sections of teeth reveals a series of markings that radiate from the enamel dentine junction to the crown surface. Similar to cross striations, they are believed to be a result of a systemic pause in amelogenesis (Dean, 1987). As such they form a record of the position of all of the ameloblasts at certain points in time, or the enamel forming front (Beynon and Wood, 1986). The pause, and resultant Retzius line, has a

periodicity of approximately a week in humans. Multiple cross striations are grouped between Retzius lines, so by counting the number of cross striations between pairs of Retzius lines, a Retzius periodicity can be calculated in days (Mahoney, 2008). For human permanent dentition RPs between six and 12 days have been observed, with modal periodicities of seven, eight, or nine days reported (Gysi, 1939; Fukuhara, 1959; Newman and Poole, 1974; Beynon and Reid, 1987; Bullion, 1987; Dean, 1989; Beynon, 1992; FitzGerald, 1998; Reid, Beynon and Ramirez Rozzi, 1998; Risnes, 1998; Schwartz, Reid and Dean, 2001; Reid and Dean, 2006, 2006; Reid and Ferrell, 2006; Smith *et al.*, 2007; Mahoney, 2008; Smith, 2008; McFarlane, Littleton and Floyd, 2014; Tan, Sim and Hsu, 2017; Mahoney *et al.*, 2018; Nava, Frayer and Bondioli, 2019) (**Figure 1.9**).

Retzius lines are difficult to see in the deeper layers of enamel and are poorly defined in the cervical region but are often well defined closer to the crown surface in the lateral enamel (Weber and Ashrafi, 1979). When they are visible under transmitted light, they vary in colour from pale brown to very dark brown and appear as stripes within the enamel that extend to the enamel surface (Wilson and Shroff, 1970). They are typically spaced between 30 and 40 μm apart in the occlusal part of the crown which decreases to between 15 and 20 μm apart in the cervical part (Hillson, 1996). Although the appearance of Retzius lines varies throughout the crown, in antimeres (matched left and right pairs of teeth) there is an identical pattern of lines because they formed at the same time (Gustafson, 1955). Any enamel that is forming a particular time will have the same Retzius line pattern. In teeth that have overlapping crown development they will have the same pattern of Retzius lines for the period of growth that they share, but the location of the pattern will be in different places within the crown, reflecting the different stages of development. This phenomenon can be used to match isolated teeth to a particular individual (Fujita, 1939; Gustafson, 1955; Gustafson and Gustafson, 1967).

A singly occurring enamel mark called the neonatal line is an accentuated line that forms at the time of birth. It was first described as 'a prominent line in the enamel of deciduous teeth and permanent first molars marking, in each tooth, the expected state of development at birth' (Rushton, 1933; Schour, 1936). Enamel that is formed prenatally rarely contains Retzius lines, and so it is normally the first accentuated line to develop. It is possible that the thickness of the neonatal line relates to the circumstances that surround the birth (Schour, 1936).

1.4.3 | Causes of Retzius Periodicity

The origin of the biorhythm is unknown, but it is likely that it has an endogenous origin, especially since RP can change between deciduous and permanent dentition and in response to some instances of non-specific stress (Mahoney *et al.*, 2017). Multiple biological pathways have been suggested, including control by the autonomic nervous system (Appenzeller *et al.*, 2005), or the suprachiasmatic nucleus of the hypothalamus (Bromage *et al.*, 2009, 2012), or a manifestation of overlapping endogenous and exogenous biorhythms (Newman and Poole, 1993).

The Havers-Halberg Oscillation (HHO) hypothesis proposes that RP represents a centrally coordinated autonomic biorhythm that influences cell proliferation and adult body size (Bromage *et al.*, 2009, 2012). It is likely that the biorhythm controlling RP is driven by an oscillating rhythm (Bromage *et al.*, 2012). It has been suggested that the biorhythm originates in the hypothalamus because of the links between RP, body size, BMR, and life history traits (Bromage *et al.*, 2009, 2012, 2016). Body size, BMR, and life history traits are all regulated by the hypothalamic-pituitary axis and the anterior pituitary secretions that regulate growth, development, and metabolism (Bromage *et al.*, 2012). According to the hypothesised scenario, the hypothalamus signals via the

suprachiasmatic nucleus to the anterior pituitary gland. Which, in turn, stimulates a sympathetic response that controls the body mass linked life history traits and is expressed in enamel as Retzius lines (Bromage *et al.*, 2012).

Since the hypothalamic-pituitary axis has a role in somatic growth, puberty, metabolism, and the timing of other life history traits (Bogin, 2015), it is possible that hypothalamic-pituitary axis is also involved in the infradian biorhythm that manifests as Retzius lines in enamel. In this scenario the hypothalamus signals to the anterior pituitary gland, which then secretes hormones that interact with the thyroid gland, the adrenal gland, and the gonads, to influence growth, development, and metabolism (Bromage *et al.*, 2009, 2012; Norman and Litwack, 2014). Anterior pituitary secretions regulate many aspects of growth and development, including growth hormone which stimulates skeletal growth, thyroid-stimulating hormone which affects metabolism, growth, and development, and follicle-stimulating hormone and luteinising hormone which affect reproductive functions (Norman and Litwack, 2014). There is a reasonable circumstantial case for the involvement of the hypothalamic-pituitary axis in the biorhythm, but concrete evidence of these biological pathways generating or sustaining an infradian biorhythm linked to RP is currently lacking. It is plausible that the endocrine system is involved because of the demonstrable link between endocrinology and somatic growth. However, this is currently speculative.

1.4.4 | Retzius Periodicity and Body Size

Retzius periodicity has been linked to body size across several mammal species (Smith *et al.*, 2003; Smith, 2008; Bromage *et al.*, 2009; Hogg *et al.*, 2015). Retzius periodicity is reported to vary between one and 14 days in mammals (Dean and Shellis, 1998; FitzGerald, 1998; Shellis, 1998), and between two and 11 days in non-human primates

specifically (Bromage and Janal, 2014). Small bodied mammalian species have lower periodicities than large bodied mammalian species (Bromage *et al.*, 2009). Also, small bodied mammals usually have faster growth trajectories and life history phases than large bodied mammals. Life history phases are key events in lives of mammals, such as age at weaning, age at menarche and first reproduction in females, gestational length, inter-birth interval, and lifespan (Promislow and Harvey, 1990; Charnov and Berrigan, 1993). The timing of these events is linked to the allocation of metabolic energy to growth, reproduction, and maintenance of life (Stearns, 1989). The inter-species relationships between RP and body size, and between body size and life history, indicate that an increase in body size from one species to the next is associated with a slower developmental rate over a longer duration of time (Bromage *et al.*, 2009). Though there are some exceptions, such as lemurs, which have much lower than expected RPs given their body size (Schwartz *et al.*, 2005; Hogg *et al.*, 2015). In addition to overall body size, the same relationship exists between RP and individual organ masses, whereby mammalian species with higher RPs also have larger organs (Bromage and Janal, 2014). These results suggest that the biorhythm that causes Retzius lines to appear may also influence cell proliferation rates throughout the body.

Retzius periodicity has also been linked to several life history traits in mammals via its association with adult body size, including age at sexual maturity and first reproduction in females, gestational length, birth weight, neonatal brain size, lactation length, inter-birth interval, endocranial volume in adults, and lifespan (Bromage *et al.*, 2012; Bromage and Janal, 2014). Each life history trait was positively associated with RP, indicating that species with a slower biorhythm had extended life history periods. As such Retzius periodicity may be an important consideration when reconstructing the life history traits of fossil hominins. It is hoped that by understanding RP and its underlying

biorhythm more questions about our own evolutionary history and life history traits can be answered.

Life history, body size, and BMR are all linked (Harvey and Clutton-Brock, 1985; Bromage and Janal, 2014). Body mass is positively associated with BMR and negatively associated with daily energy expenditure across vertebrates (Speakman, 2005). This means that larger animals expend more energy overall but at a slower rate over a longer lifespan (Speakman, 2005). Additionally, slower cellular metabolic rates are associated with slower cell proliferation rates (Savage *et al.*, 2007). Thus, small animals with low BMRs and low RPs have fast growth and shortened life histories when compared to large animals with high BMRs and high RPs that have slow growth and extended life histories (Bromage *et al.*, 2012). The high daily energy expenditure of fast-growing small animals may not be sustainable over a longer life history. So, the reduced daily energy expenditures and slower cell proliferation and growth in large animals may be more energy efficient across their extended lives.

Curiously, the opposite trend is observed within humans specifically, in that smaller bodied adults have higher RPs than larger bodied adults do (Bromage *et al.*, 2009, 2016; Mahoney *et al.*, 2018). In modern human adults RP negatively correlates with stature (Bromage *et al.*, 2016; Mahoney *et al.*, 2018) and also with body mass (Bromage *et al.*, 2016). This apparent anomaly likely occurs because the time available to attain adult body size is constrained within a species and the developmental rate varies to achieve different adult body sizes within the same length of growth period (Bromage *et al.*, 2009). So, it is hypothesised that a person on a growth trajectory to attain a smaller adult body size will have a slower developmental rate and a higher RP. Higher RPs have more days between each 'beat' of the biorhythm (Mahoney *et al.*, 2018). Modern humans have limited variation in the length of their ontogenetic period, but a wide variation in

adult body size. The cell proliferation rate during growth, and RP if they are linked, must be quite variable to result in the amount of variation seen in adult body size (Bromage *et al.*, 2016).

1.4.5 | Retzius Periodicity and Bone Formation

Since RP is linked to adult body size is it plausible that the biorhythm underlying RP is linked to bone growth. There is preliminary evidence that bone may be an incremental structure, in a way that is generally similar to the formation of tooth enamel. The potential for periodic rhythmic lamellae formation was first noted in small mammals (rat, chipmunk, rabbit, and dog) that were vitally labelled with lead salts and each lamella was shown to form in a 24-hour period (Shinoda and Okada, 1988). The number of lamellae between the lead lines corresponded to the number of days between the labelling injections (Shinoda and Okada, 1988). In another study of mammalian samples (rat, macaque, patas monkey, and sheep) that were vitally labelled with tetracycline, one bone lamella formed in the same number of days as the species-specific RP (Bromage *et al.*, 2009). There is additional circumstantial evidence for the same phenomenon in humans. In one vitally labelled adult human female, each single lamella formed in the same time as the human modal RP of eight days, in both the interstitial lamellar bone and in the osteonal lamellar bone (Bromage *et al.*, 2009). Thus, one lamella formed in the same number of days as one Retzius 'layer'. This evidence of a relationship between RP and bone lamella formation lends some support for the existence of a biorhythm coordinating hard tissue formation and adult body size (Mahoney, Miszkiewicz, *et al.*, 2016). However, this assumes that this one individual had the modal human RP, and that bone and enamel are responding to the same biorhythm, for which there is no unequivocal evidence.

Osteocyte density is used as a proxy for inferring bone proliferation, for example growth and remodelling rates, and it has been reported to scale inversely with body mass across a range of mammal taxa (Mullender *et al.*, 1996; Bromage *et al.*, 2009). However, some studies have not reported a relationship between osteocyte density and body mass in mammalian, reptilian, and amphibian taxa (Hobdell and Howe, 1971; Marotti *et al.*, 1990; Remaggi *et al.*, 1998; Ferretti *et al.*, 1999). Within a sample of 11 modern humans, a positive correlation was found between osteocyte density of the femur and adult stature, but that there was no relationship between osteocyte density and body mass (Bromage *et al.*, 2016). As part of the same study four teeth were sectioned; the two teeth from the tallest two people both had an RP of 7 days and the two teeth from the shortest two people both had an RP of 8 days. This indicates that a person with a faster biorhythm (7 days) can attain a greater adult stature than a person with a slower biorhythm (8 days). That study found a positive correlation between osteocyte density in the femur and stature, and a negative correlation between stature and RP, but the relationship between osteocyte density and RP was not tested. Consequently, the hypothesised regulation of osteocyte cell proliferation (signified by osteocyte density) by the infradian biorhythm (signified by RP) remains unsupported. Yet no link was found when another study did test the relationship between RP and osteocyte density of the posterior femoral midshaft (Mahoney *et al.*, 2018). Thus, there is only circumstantial evidence supporting a relationship between osteocyte cell proliferation and the biorhythm. While adult stature is related to both osteocyte density and to RP (Bromage *et al.*, 2016), it has been indicated that osteocyte density and RP are not linked (Mahoney *et al.*, 2018). Further testing of the potential link is needed with larger sample sizes and a consideration of the variability of osteocyte density throughout the body (Hunter and Agnew, 2016).

Currently, there is evidence for a common link between RP and bone formation in adult humans (Mahoney *et al.*, 2018). But it remains unclear how the biorhythm affects skeletal growth during ontogeny. One study discovered lower than previously observed RPs in human deciduous teeth of four and five days and reported increased primary bone deposition at the site of vascular canals in the humerus was associated with thicker enamel and higher RPs (Mahoney, Miszkiewicz, *et al.*, 2016). The low RPs of the deciduous teeth and the unexpected relationship with primary bone formation in the sample of two-year olds could suggest that RP and the biorhythm could change with age.

1.5 | THESIS STRUCTURE

The primary aim of this thesis is to explore the potential link between RP in enamel, as a hypothesised biorhythm that coordinates and influences hard tissue growth, and cortical bone microstructure. A marker of this hypothesised infradian biorhythm manifests as Retzius lines within human tooth enamel (Retzius, 1837; Bromage *et al.*, 2009). To achieve this aim, RP will be collected from permanent teeth alongside microscopic bone growth variables from a sample of medieval English juvenile and young adult skeletons. The three data chapters in this thesis (Chapters 3, 4 and 5) each focus on a specific aim that will contribute to answering the primary research question of this thesis: *Is evidence of a biorhythm retained in tooth enamel as Retzius line periodicity related to bone growth during ontogeny?* The aims of each data chapter are:

Chapter 3. To describe population level variation in juvenile bone microstructural growth that may relate to activity and/or social status differences.

Chapter 4. To explore how cortical bone microstructure varies intra-skeletally and how Retzius periodicity relates to this microstructural variation.

Chapter 5. To investigate how Retzius periodicity relates to microstructural bone growth in the juvenile rib.

To satisfy these aims, this thesis is divided into six chapters. Chapter 1 has described the underlying biology of bone growth, enamel secretion, and biorhythms, and reviewed the current literature on these topics. Chapter 2 describes the materials and methodology that are used in the subsequent data chapters. It also contains brief archaeological and historical backgrounds to contextualise the skeletal samples.

Chapters 3-5 are data chapters, each with individual introduction, aims, methods, results, and discussion sections. In Chapter 3, the bone microstructure of the humerus and ribs will be compared between juveniles, aged three to 18 years of age, from a high-status group and a low-status group from Canterbury, and then from three medieval English sites (Canterbury, York, and Newcastle) to explore population level variation in juvenile bone growth. The literature review in Section 1.2.6 revealed that cortical bone microstructure can vary according to metabolism and biomechanical loading (Richman, Ortner and Schulter-Ellis, 1979; Lanyon *et al.*, 1982; Lanyon and Rubin, 1984; Raab *et al.*, 1991; Burr, 2002; Alexy *et al.*, 2005; Paine and Brenton, 2006; Eleazer and Jankauskas, 2016). According to textual and archaeological evidence the lifestyle factors that affect both metabolism (diet and health) and biomechanics (physical activity and manual labour) varied between populations and social status groups in medieval England (Ben-Amos, 1994; Lomas, 1996; Lyle, 2002; Bennike *et al.*, 2005; Woolgar, Serjeantson

and Waldron, 2006; Nicholas, 2014; Palliser, 2014; Miszkiewicz, 2015). The potential for inter-population variation in bone microstructure will need to be accounted for when examining the potential link between bone and RP. **Therefore, the aim in Chapter 3 is to describe population level variation in juvenile bone microstructural growth that may relate to activity and/or social status differences, which will be answered with the following research questions:**

1. **Is there a difference in remodelling in the humerus compared to the rib?**

2. **Are there age-related differences in remodelling of the humerus, or the rib?**

3. **Does the histomorphometry of the humeri and rib vary between children of different social status in Medieval England?**

4. **Does the histomorphometry of the humeri and rib vary between children from different locations in Medieval England?**

In Chapter 4, thin-sections from eight bones will be examined from ten age-matched young adult skeletons from medieval Canterbury to examine how RP relates to intra-skeletal variation in cortical bone microstructure. The literature review in section 1.2.6 revealed that cortical bone microstructure can vary between bones across the skeleton according to local biomechanical loading (Ural and Vashishth, 2006; Chan, Crowder and Rogers, 2007; Crowder and Rosella, 2007; Cho and Stout, 2011; Schlecht *et al.*, 2012; Goliath, Stewart and Stout, 2016). The potential for intraskeletal variation in bone microstructure will need to be accounted for when examining the potential link

between bone and RP. **Therefore, the aim in Chapter 4 is to explore how cortical bone microstructure varies intra-skeletally and then Retzius periodicity relates to this microstructural variation, which will be answered with the following research questions:**

1. **How does bone microstructure, specifically osteon density and morphology, and osteocyte density vary across the skeleton?**

2. **Is there a consistent pattern of relationship between Retzius periodicity and bone microstructure across the skeleton?**

Chapter 5 will investigate how RP relates to the cortical bone microstructure of the ribs in a sample of juveniles, aged three to 12 years of age, from medieval Canterbury. The literature review in sections 1.4.4 and 1.4.5 suggest that body size, BMR, life history traits, and RP are all linked by a centrally coordinated autonomic biorhythm that is related to growth and development and regulated by the hypothalamus (Bromage *et al.*, 2009, 2012, 2016; Bromage and Janal, 2014). If this is correct, then there should be evidence of this retained in the juvenile skeleton. By examining the macroscopic and microscopic features of the cortical bone of medieval human children and comparing it to their RP, further information about the biorhythms influence on growth and adult body size attainment should be made apparent. **The aim of Chapter 5 is to investigate how Retzius periodicity relates to microstructural bone growth in the juvenile rib, which will be answered with the following research questions:**

1. **Is bone remodelling linked to Retzius periodicity?**

2. **Is osteon morphology linked to Retzius periodicity?**

3. **Is bone modelling linked to Retzius periodicity?**

Chapter 6 is a discussion of the findings of the preceding data chapters and how they contribute to the overall thesis aim of exploring evidence of how a biorhythm, retained in tooth enamel as Retzius line periodicity, relates to bone growth during ontogeny, as well as suggestions of future directions for this topic and the conclusion of this thesis.

Chapter 2

Materials and Methods

The materials and methodology that were used in the subsequent data chapters are explained in this chapter. It will begin with a brief discussion of the archaeological and historical contexts of the samples, followed by an explanation of the sampling criteria, and will then cover the methodology in detail. The methodology section will include parts describing the age-at-death estimation, histological procedures, and microscopic measurements.

2.1 | HISTORICAL BACKGROUND

The historical background of the skeletal sample – including living conditions, social status, physical activity and manual labour, diet, and health – can aid in the interpretation of the histomorphometric results, because bone microstructure is affected by biomechanical loading from physical activity, and metabolism, that involves diet and health status (Burr, 2002; Eleazer and Jankauskas, 2016). Some of the influences on bone development, modelling, and remodelling can be accounted for by understanding more about the way that these people lived. This contextualisation is especially important since the skeletal samples studied here are undocumented.

The four skeletal assemblages that are studied all date to the Christian medieval period, which is eighth century AD to the early sixteenth century AD. This time period spanned a period of change in the lifestyles of many people in Britain. The introduction of Christianity in the eighth century AD represented a new dominant religion that changed social behaviour and the Norman Invasion of 1066 AD brought further social, cultural,

and economic changes (Dyer, 2000). There was a period of growth in both the towns and the countryside in the following centuries, with archaeological evidence for widespread urbanisation at several places after 1180 AD (Schofield and Vince, 2003). Subsequently, the first half of the fourteenth century AD was a particularly harsh period for many people living in England. It was a time of significant political turmoil and economic hardship. Crop failures and disease epidemics affecting farm animals led to widespread famine in the years between 1315-1325 AD (DeWitte and Slavin, 2013) and wars with Scotland and France were funded through increased taxation, leading to rising levels of poverty (Schofield and Vince, 2003). The Black Death of 1348 AD, a bubonic plague, decimated the population and was a turning point in socioeconomics of the medieval period (Britnell, 1994; Schofield and Vince, 2003). After 1350 AD there was a shortage of peasant labourers, and increasing numbers of women began employment, particularly in towns (Goldberg, 1992). By the end of the medieval period in the early sixteenth century AD the social structure of the population had changed, and large urban centres were growing.

In 1086 AD the population density of Kent was particularly high while the population density of the Newcastle area was particularly low, with the population density of York falling between the two (Astill and Grant, 1988). The modern city of Newcastle did not exist in the early medieval period when the Black Gate cemetery was in use (Nolan, Harbottle and Vaughan, 2010). The area surrounding the Black Gate cemetery would have been part of the rural north-east of England. The suburbs of both Canterbury and York expanded rapidly during the eleventh and twelfth centuries AD as the urban population grew (Lyle, 2002; Schofield and Vince, 2003). By 1377 AD the population of Yorkshire had swelled by seven times and evidence from poll tax returns shows that Yorkshire and Kent now had similarly high population densities (Baker, 1976; Astill and Grant, 1988). York and Canterbury were both major medieval cities, but each had a

different character. The Fishergate area of York was a centre of industry and manufacturing in the medieval period, with a particular emphasis on textiles (Nicholas, 2014; Palliser, 2014). The Northgate area of Canterbury, where St Gregory's Priory was situated, was a relatively poor area of the city, but the local people could be employed by the wealthy religious houses in domestic jobs or construction (Lyle, 2002) (**Figure 2.1**).

Figure 2.1 *Map displaying the locations of the archaeological sites in England. St Gregory's Priory and Cemetery, Canterbury is south-east. The Black Gate cemetery, Newcastle is north. Fishergate House and Fishergate Barbican, both York are central*

2.1.1 | Activity

The medieval feudal system dictated most aspects of peoples day to day lives, including their activity and occupation (Rigby, 1995). The wealthiest people were the royalty, nobility, knights, and clergy. The nobility generally had the most comfortable lives (Dyer,

2002) and were occupied with running their estates and political matters (Holt, 1972), as well as leisure activities including dancing, feasting, and hunting (Dyer, 2000). The clergy led religious services and could be involved in tending small gardens growing fruit and vegetables for their own consumption (Dyer, 2006a). The clergy also ministered to the sick who could not afford other medical care (Clegg and Reed, 1994). Both the nobility and the clergy were likely to have had some form of formal education.

Most people in medieval England were low-status peasants involved in manual labour (Dyer, 2000). Rural dwelling peasants were involved in farming, which was often on the estates of the nobility or gentry. They would plough fields to sow and harvest crops, as well as engage in animal husbandry. The rural farmers were increasingly responsible for feeding the urban dwellers and nobility as the urban populations grew (Sykes, 2006). Urban dwelling peasants were employed in a wider range of occupations, including as domestic servants, crafters, carpenters, smiths, and millers (Dyer, 2002). They could also be involved in heavier industries including building, mining, and weaving (Dyer, 2000). Generally, low-status people had little time for leisure activities. A new middle class of people was emerging towards the end of the Medieval period (Dyer, 1989). They could have profited from skilled production and lucrative trading opportunities in urban settlements. Adult men would work as agricultural labourers or have a trade such as tanning, milling, carpentry or butchery, while women would work in more domestic environments, such as cooking, brewing, spinning cloth, and domestic service. Though there was not a strict sexual division of labour (Hanawalt, 1977).

Medieval children spent more time with their working parents from the age of four and were given greater independence from between the ages of eight and 12 years (Hanawalt, 1977; Fleming, 2001). In rural areas, boys of this age from families of lower-status commonly worked as shepherds, mill hands, reapers or servants, and girls worked

gathering wood, childminding, or in the fields at harvest time (Hanawalt, 1977). This was also the age at which the children of crafting, mercantile, or landed families would begin to learn the necessary skills to carry on the family trade (Fleming, 2001). Although, some adolescents would migrate to nearby towns and cities for employment, particularly after the Black Death (Goldberg, 1986).

In urban areas, high-status boys would attend school (Hanawalt, 1977) or go into apprenticeships as grocers, mercers, or merchant tailors (Ben-Amos, 1994). Some high-status children, mostly males, were taken on as servants, pages, or grooms in noble houses to advance their social standing (Du Boulay, 1970; Fleming, 2001). Lower-status children, whose family could afford the fee, could be apprenticed to craftsmen as weavers, carpenters, builders, farriers, and smiths (Ben-Amos, 1994). The more prestigious apprenticeships were longer lasting and more expensive (Fleming, 2001). Many low-status adolescents, whose families could not afford an apprenticeship, would gain work and lodgings as a household servant on yearly contracts (Fleming, 2001). Female household servants were usually employed as unskilled domestic servants rather than in a craft or trade (Goldberg, 1992). There is skeletal evidence from spinal and joint disease suggesting that urban adolescents undertook more strenuous activity than their rural counterparts (Lewis, 2016).

2.1.2 | Diet

Social status not only dictated where a person lived and their activity but was also one of the most important determinants of a medieval person's diet (Woolgar, 2006). The wealthy, high-status, people had access to a much broader range of food than the poor, low-status, people did. However, grains were the basis of everyone's diet and formed up to 80% of a peasant's calories, 75% of a soldier's calories, and 65% of the calories

consumed by a person of high-status, such as a nobleman. (Murphy, 1998). They were eaten in the form of bread and ale, and pottage for the poor (Stone, 2006). Pottage was a simple type of stew made from oats, beans, and peas (Stone, 2006). High-status people, the royalty, the nobility, and the religious houses, could keep gardens to grow fruit and vegetables (Dyer, 2006a). Although, this was still only a small part of the diet and any surplus produce was sold in markets. High-status people ate more pork, fish, and game than low-status people (Serjeantson and Woolgar, 2006; Sykes, 2006) and were the only group to eat venison (Birrel, 2006). People of all social statuses consumed poultry, but the variety of game birds that were consumed was a sign of high-status (Serjeantson, 2006). If low-status people did eat pork it was as preserved bacon or ham (Albarella and Woolgar, 2006).

Urban dwellers had access to a wider range of food than rural dwellers. The markets in towns brought in crops and meat from the surrounding rural farms as well as preserved fish and other goods from further afield (Lyle, 2002). Even within towns, the growing middle class could afford a better standard of food than the urban poor. Rural dwelling people consumed more mutton than urban dwelling people and it is possible that they were selling beef in the urban markets (Sykes, 2006). It is estimated that up to 80% of the meat consumed in Fishergate York was beef (O'Connor, 1994).

The normal diet was very similar for children from different regions of England, and for those of different socioeconomic statuses, up to a certain age. Historical records report that weaning began between seven to nine months of age (Fildes, 1986). Mixed-feeding practice was used where an infant's diet was spilt between breastmilk and supplementary foods such as panada (bread soaked in broth) or pap (flour, milk, and egg yolk) with an increasing proportion of supplementary food until the infant is weaned (Fildes, 1986; Humphrey, 2014). Numerus isotopic studies have shown that medieval

children were completely weaned by two years old (Mays, Richards and Fuller, 2002; Richards, Mays and Fuller, 2002; Fuller, Richards and Mays, 2003; Burt, 2013; Haydock *et al.*, 2013), and that children who died in infancy did not have a different diet to the children who survived longer (Fuller, Richards and Mays, 2003). Dental macroscopic wear and microscopic wear analyses suggest that the dietary hardness for children up to approximately eight to ten years old was alike between different geographic locations and social statuses (Dawson and Brown, 2013; Mahoney, Schmidt, *et al.*, 2016).

Despite these findings for children, social status differences in the quality, variety, and type of adult diet have been reported (Powell, Serjeantson and Smith, 2001; Dyer, 2006b; Serjeantson, 2006; Woolgar, 2006). Various studies using different methodologies have indicated a change in childhood diet occurred at approximately seven to ten years old, after which time an adult diet was consumed (Richards, Mays and Fuller, 2002; Macpherson, 2005; Mahoney, Schmidt, *et al.*, 2016). A tougher diet was introduced at around four to six years of age and a harder diet at around six to eight years of age in children from medieval Canterbury, indicating a more adult-like diet (Mahoney, Schmidt, *et al.*, 2016). Children over the age of eight years old had a diet that was higher in animal protein than children between the ages of four and eight years did (Richards, Mays and Fuller, 2002). From nine years old children at Black Gate, Newcastle had the same diet as adults, where the primary protein source was from terrestrial mammals (Macpherson, 2005) and grains and legumes were a significant part of the diet (Stone, 2006). These studies show that between the ages of seven to ten years old children began to be treated like adults and consume an adult diet that was dependent on their social status.

2.1.3 | Health

Childhood growth profiles for stature were broadly similar in rural and urban medieval locations, as were incidences of skeletal manifestations of stress, such as hypoplastic enamel defects, maxillary sinusitis, cribra orbitalia, and non-specific indicators of stress (Lewis, 2002). Though there is evidence that maternal stress was more common in urban areas (Lewis, 2002). Degenerative joint disease and Schmorl's node prevalence were significantly higher in urban adolescents compared to rural adolescents, which could indicate that these people engaged in more strenuous physical activity and manual labour than their rural counterparts (Lewis, 2016).

In addition to regional differences, social status could influence childhood growth and disease (Bennike *et al.*, 2005). There is dental evidence that non-specific stress during childhood and adolescence could vary according to social status. High-status people in medieval Canterbury had significantly fewer enamel indicators of non-specific stress than low-status people (Miszkiewicz, 2015b). This indicates that, while children of both high- and low-status experienced physiological stress during growth, the higher social status of some children provided a buffer against some of the insults. The high-status children were more likely to have better health than low-status children due to more sanitary and better living conditions and diets.

2.2 | ARCHAEOLOGICAL BACKGROUND

Further information about the skeletal samples can be gained from the archaeological contexts of the sites. In particular, the burial context – including grave location, coffin presence and material, and grave goods – can provide an indication of a person's social and economic status during life. Also, the preservation and condition of the skeletons can impact the preservation and visualisation of the cortical bone microstructure.

2.2.1 | St Gregory's Priory, Canterbury

Canterbury Archaeological Trust excavated the site of St Gregory's Priory, Canterbury (**Figure 2.1**) between 1988 and 1991 (Hicks and Hicks, 2001). During this time, 1342 articulated skeletons were retrieved and are curated in the Skeletal Biology Research Centre at the University of Kent. Of these, 135 skeletons were examined for this thesis. On the basis of textual and archaeological evidence, the earliest burials date to 1084 AD, with the cemetery in constant use until the latest burials in 1537AD when the Priory was dissolved.

In 1084AD a church was commissioned by the Archbishop Lanfranc on a site lying adjacent to the city walls on the eastern edge of Canterbury. The original building was a simple, modest sized church, based on a Norman style (Clover and Gibson, 1974). St Gregory's church was built to serve the adjacent St John's Hospital, to tend to the religious needs of the patients, and to provide an appropriate burial site (Tatton-Brown, 1995). It was also designated as the burial place for the people of the parish of St Mary Northgate (Tatton-Brown, 1995). In 1133AD the church became an Augustinian Priory, and the church building was extended, but the building was badly damaged in a fire shortly after the work had finished. Archbishop Theobald subsequently commissioned the construction of a grander Priory complex at the site, completed in 1225AD (Hicks and Hicks, 2001). Small-scale expansion and modification continued throughout the next 300 years until St Gregory's Priory was dissolved in 1537AD on the orders of King Henry VIII, and the buildings were destroyed (Hicks and Hicks, 2001).

The preservation of the skeletons from St Gregory's Priory is good, with many skeletons complete and showing little taphonomic damage, despite 90% of the burials showing no evidence for the presence of a coffin (Anderson and Andrews, 2001). It is likely that most people were buried wrapped in shrouds (Knowles, 1951). Chemical

erosion of the bones was minimal because the soil at this site was predominantly clay with a low acidity level (Hicks and Hicks, 2001). Later burials intercut several graves and parts of those skeletons were destroyed, but, 40% of the individuals had at least three-quarters of their skeleton present, and only 20% were classed as fragmentary (Anderson and Andrews, 2001). The juvenile remains were as well preserved overall as the adult remains. Approximately 25% of the total collection were juveniles, with nearly half of those juveniles aged between birth and six years old at the time of their death. When the site is split between high-status burials from inside the Priory buildings and low-status burials from the surrounding cemetery, juvenile burials account for only 8% inside the Priory, but 40% of the burials within the cemetery (Anderson and Andrews, 2001). The rate of juvenile mortality at St Gregory's Priory is comparable to that found at other medieval sites, such as St. Andrew, Fishergate (Stroud and Kemp, 1993), and the Church of the Franciscans Hartlepool (Birkett and Daniels, 1986).

2.2.2 | Fishergate House, York

Field Archaeology Specialists Ltd excavated the site of Fishergate House, York (**Figure 2.1**) between 2000 and 2002 (Spall and Toop, 2005). There were 244 articulated skeletons were retrieved at this time and are curated in the Fenwick Human Osteology Laboratory at Durham University. Twenty juvenile skeletons were examined for this thesis. Archaeological evidence shows that the earliest burials date to the late tenth century AD, with the site in constant use until the latest burials in the sixteenth century AD.

Little is known about the site, but it has been suggested based on documentary evidence that the cemetery would have belonged to St Helen's Church. St Helen's Church and Hospital was founded in Fishergate in 1399AD, but its exact location is unknown (Holst, 2005). While St Helen's may be the source of the burials, it remains uncertain,

and there has been no archaeological evidence of a church found at the Fishergate House site (Holst, 2005).

All of the burials were traditional Christian burials with the graves oriented on an east-west axis and the bodies in an extended supine position (Holst, 2005). More than half of the skeletons from Fishergate House had good or excellent preservation although most were buried without coffins and some were affected by root growth or intercutting graves (Holst, 2005). The preservation of the juvenile skeletons was particularly good, with 53% of the one to 12 year olds and 74% of the 13-17 year olds having good or excellent preservation and 68% of juveniles were more than 50% complete (Holst, 2005). Approximately 45% of the total skeletal collection were juveniles, with just over half of those juveniles having died between birth and six years old.

2.2.3 | All Saints' Church, York

The site of All Saints' Church, York (**Figure 2.1**), more commonly known as Fishergate Barbican, was excavated by York Archaeological Trust between 2007 and 2008 (McIntyre and Bruce, 2010). During this time, 667 articulated skeletons were retrieved and are curated in the Department of Archaeology at the University of Sheffield. Thirteen medieval juvenile skeletons were examined for this thesis. On the bases of documentary and archaeological evidence the medieval burials date to between the eleventh and fourteenth centuries AD. Seven skeletons were dated to the Roman period, and 113 skeletons were dated to the post-medieval seventeenth century AD.

Little is known about All Saint's Church. The first documentary evidence for a church at the site dated to 1091 and 1095 AD when it was given over to Whitby Abbey (McIntyre and Bruce, 2010). The church did not survive long after 1539 AD, and its location was lost as the parish was merged with the parish of St. Lawrence in 1586 AD.

2.2.4 | Black Gate Cemetery, Newcastle

Newcastle Archaeology Unit excavated the Black Gate cemetery site between 1973 and 1992 (**Figure 2.1**). There were 663 articulated skeletons were excavated from 660 burials between 1977 and 1992, representing the largest group of Christian Anglo-Saxon burials excavated in Northeast England (Nolan, Harbottle and Vaughan, 2010; Swales, 2013). The skeletons are curated in the Department of Archaeology at the University of Sheffield. Seventeen juvenile skeletons from the Black Gate cemetery were examined as part of this thesis, and these were excavated during the 1978, 1979, 1980, 1982, and 1992 seasons. These 17 skeletons date to the eighth to twelfth centuries AD.

There is some limited evidence for the presence of people in the area before the Roman period, including some flint tool and a Neolithic axe head, as well as plough-marks beneath the Roman layer which may indicate Iron Age agriculture at the site (Snape and Bidwell, 2002; Nolan, Harbottle and Vaughan, 2010). A Roman fort, named Pons Aelius, was constructed on the site during the second century AD and was later abandoned at the end of the fourth century AD or beginning of the fifth century AD (Snape and Bidwell, 2002). Much of the stone from the structure was removed from the site and may have been reused elsewhere, but it is not known where this might have been (Nolan, Harbottle and Vaughan, 2010), and it is unclear if the site was still in use over the following 400 years. Radiocarbon dating of burials indicates that the cemetery was established around 700 AD (Nolan, Harbottle and Vaughan, 2010; Swales, 2013). However, there is no documented settlement at the site at this time, but some dateable archaeological finds, such as coins, indicate that people were in the area in the eighth and ninth centuries AD. It is possible that the cemetery was linked to an unrecorded seventh century AD monastic settlement (Nolan, Harbottle and Vaughan, 2010). The cemetery was well established by the tenth century AD and was most likely serving a local lay

population. It is possible that a church had been built by around 1000 AD (Nolan, Harbottle and Vaughan, 2010). The foundations of a building were found within the cemetery, and it is possible that this could have been a church or chapel. All of the burials are most likely Christian, based on the east-west burial orientation, and the lack of grave goods (Nolan, Harbottle and Vaughan, 2010).

The earliest date of definite settlement at the site since the Roman period of occupation is 1080 AD. In 1080AD an earthwork castle was built, with the castle ditch and ramparts cutting through the cemetery in places. Some burials post-date this time and could be the graves of the castle garrison rather than a local population (Nolan, Harbottle and Vaughan, 2010). The cemetery was disturbed further when the castle was rebuilt in stone between 1168 AD and 1178 AD on the orders of King Henry II, and when the castle was refortified at the time of the Civil War (Nolan, Harbottle and Vaughan, 2010). The latest burials at the site post-date the building of the stone Keep in 1178 AD. The construction of a public house with an extensive cellar, a railway line, and new roads in the eighteenth and nineteenth centuries AD removed many of the burials from across the cemetery.

The individuals who were buried here were most likely from a small settlement or some locally dispersed smaller groups (Nolan, Harbottle and Vaughan, 2010). Estimates of the living population size yield a possible living generation size of 53 people, although, this figure may be an underestimation as a result of the disturbed graves and the unknown extent of the cemetery (Halsall, 1995; Nolan, Harbottle and Vaughan, 2010). The lack of archaeological and documentary evidence for a settlement concurrent with the cemetery use is problematic. However, it can be surmised that this was not an urban centre like York or Canterbury during the eighth to twelfth centuries AD. Osteological evidence can provide a more explicit depiction of the lives of these people.

2.3 | SAMPLING CRITERIA

The primary skeletal sample for this thesis was selected from the extensive skeletal collection excavated from St Gregory's Priory and cemetery. These skeletons date to the medieval period from Canterbury in south east England (Hicks and Hicks, 2001). This collection was selected on the basis that it includes a large cohort of complete juvenile skeletons. The preservation of the skeletal remains is good. Accordingly, age-at-death estimations could be obtained from 125 juvenile skeletons and ten young adult skeletons, that also had a permanent tooth and suitable bone available for sampling.

Three comparative skeletal collections from medieval England were selected to investigate the potential for geographic variation in juvenile growth and hard tissue microstructure. These were the Black Gate Cemetery from Newcastle (Nolan, Harbottle and Vaughan, 2010), and two skeletal collections from York: Fishergate House (Spall and Toop, 2005), and Fishergate Barbican (McIntyre and Bruce, 2010). The total sample examined in this thesis is in **Table 2.1**, split by geographic location, archaeological site, and age-at-death group. An in-depth list of each skeleton sampled can be found in **Appendix A, Table A.A.1**. Each data chapter draws its sample from this total sample based on the specific aims and research questions of each data chapter.

Table 2.1 *Total sample size, split by location, archaeological site, and age group*

Location	Site	Site code	Younger child	Older child	Adole-scent	Young adult	**Total**
Canterbury	St Gregory's Priory		55	33	37	10	**135**
	- High-status	*NGB89*	*8*	*5*	*6*	*0*	***19***
	- Low-status	*NGA88*	*47*	*28*	*31*	*10*	***116***
York	Fishergate House	YFH00	7	8	5	0	**20**
	All Saint's Church	YFB02	2	6	5	0	**13**
Newcastle	Black Gate	BGN92	7	5	5	0	**17**
Total			**71**	**52**	**52**	**10**	**185**

All skeletons had to satisfy a particular set of criteria to be included in this study. Firstly, all the skeletons had to be those of juveniles who died between the ages of three and 18 years old. The age of three was set as the lower limit because this is often the earliest age at which a permanent tooth crown is fully formed (Moorrees, Fanning and Hunt, 1963; Reid and Dean, 2006) and enamel may not be mineralised well enough for histological analysis before crown completion. Eighteen years of age at the time of death was chosen as the upper limit because the long bone growth is usually complete around this time, with the epiphyseal plates of most long bones typically fused by 18 years of age. Once epiphyseal fusion is complete, the bones cannot grow longitudinally and individuals have typically achieved their adult length (Scheuer and Black, 2000; Zoetis *et al.*, 2003). The ten young adult skeletons included in Chapter 4 were between the ages of 20 and 35 years old at death. The ability to confidently reconstruct age-at-death was important because age is an important factor affecting bone microstructure and growth during ontogeny (e.g. Cambra-Moo et al., 2014; Pitfield, Miszkiewicz, & Mahoney, 2017; Streeter, 2005). Unfortunately, the chronological age of the skeletons is unknown since they are undocumented medieval skeletons. However, age estimation techniques based on hard tissue development are quite reliable for juveniles, particularly where multiple methods are used in combination.

Secondly, a permanent tooth had to be available for sampling. Retzius periodicity has been reported to be stable between permanent tooth types within individuals (FitzGerald, 1998; Reid, Beynon and Ramirez Rozzi, 1998) and enamel formation is affected by fewer external stimuli than bone tissue growth (Lewis and Garn, 1960; Smith, 1991), but there is some evidence that RP can change within an individual between deciduous and permanent teeth (Mahoney *et al.*, 2017). On this basis, only permanent teeth were examined here. A permanent first molar was preferentially chosen because of

their early crown completion times. Either a permanent central incisor or a permanent second molar was selected when no first molar was available.

Thirdly, either a humerus or a third to eighth rib must have been available for sampling to investigate the effect of local biomechanical factors or systemic factors on bone microstructure. Any systemic influences on bone microstructure will be seen within both bones (Eleazer and Jankauskas, 2016), but local biomechanical strains will be seen within the humerus since activity levels and use of the arm will vary between people. The rib is subjected to the constant biomedical influence of respiration (Agnew and Stout, 2012) so any inter-personal differences seen in the rib are more likely to show systemic influences on bone microstructure than biomechanical ones (Robling and Stout, 2003; Agnew and Stout, 2012). Using this 'combined bone' approach may lead to a better understanding of the factors that affect juvenile bone growth, and the microstructural variability of this sample (Eleazer and Jankauskas, 2016).

Fourthly, skeletons with signs of hard tissue pathology were excluded. Some chronic illnesses cause physiological stress that can reduce the rate of bone growth in children (Vercellotti *et al.*, 2011; Watts, 2015). Evidence of bone infections and metabolic disease were searched for on each skeleton to limit the impact of this potentially confounding factor. Metabolic diseases affect the normal metabolism of the skeleton, for example osteoporosis, anaemia, or rickets (Waldron, 2009). However, for many infections or diseases to have a bony response they must be chronic conditions (Cunningham, Scheuer and Black, 2016), so some of the individuals included here could have suffered from acute infections or diseases which would not have left a bony response (Wood *et al.*, 1992). Although in these cases of rapid death, it is not likely to have affected the bone microstructure. Further, any humerus or rib with evidence of a healed fracture was not sampled because the fracture healing process can show abnormal microstructure.

For dental pathology, any tooth that had a linear enamel hypoplastic defect was not sampled. A recent study has shown that RP can sometimes change after a LEH and recommended that such teeth be avoided in studies investigating RP (Mahoney et al., 2017; see **Appendix C** for additional detail).

2.4 | AGE-AT-DEATH ESTIMATION

Multiple standard methods of age estimation were used together to reconstruct age-at-death for every skeleton in this project. The methods are all based on dental or skeletal development and growth. Two dental age estimation methods were used, one based on tooth formation times (Moorrees, Fanning and Hunt, 1963), and the other based on dental eruption timing and sequence (Al Qahtani, Hector and Liversidge, 2010). Additionally, two skeletal age estimation methods were used, one based on epiphyseal union timing (Coqueugniot and Weaver, 2007; Cunningham, Scheuer and Black, 2016), and the other based on long bone longitudinal growth (Hoppa, 1992). Dental development and eruption are more closely tied to chronological age than skeletal development and growth are (Lewis and Garn, 1960; Smith, 1991; Cardoso, 2007; Conceição and Cardoso, 2011). Age estimation methods that are based on long bone growth are the least accurate because of the high level of skeletal variability (Saunders and Hoppa, 1993). As such, if the age estimations diverged between the different methods, a higher weighting was given to the dental methods.

Once the age-at-death for each skeleton was estimated, they were assigned to one of three age groups that corresponded to the phases of juvenile growth. These were young childhood (three to seven years at death), middle, or older, childhood (eight to 12 years at death), and adolescence (13 to 18 years at death). The juvenile period has two main growth phases, which occur during young childhood and then again during adolescence

(Cameron and Bogin, 2012). Between these periods the growth rate slows down in the middle childhood developmental phase (DelGiudice, 2018).

Chapter 4 includes ten young adult skeletons, aged 20-35 years of age. The age-at-death of these skeletons was recreated from the age-related changes to the pubic symphysis and the auricular surface of the pelvis (Lovejoy *et al.*, 1985; Meindl *et al.*, 1985). Only young adults, between 20-35 years old at the time of death, were selected because osteon density and size are linked to advancing age (Britz *et al.*, 2009).

No attempt was made to estimate sex for the juvenile skeletons as it is not possible to accurately reconstruct sex for juvenile skeletons. More than half of the sample were pre-pubescent, and so the secondary sexual characteristics that are used to estimate sex in adult skeletal remains would not yet have developed in this sample. For the ten young adult skeletons included in Chapter 4, biological sex was assessed from the standard morphological characteristics on the pelvis including the greater sciatic notch (Buikstra and Ubelaker, 1994) and the Phenice characteristics: the ventral arc; the subpubic concavity; the medial aspect of the ischiopubic ramus (Phenice, 1969). Biological sex was also assessed from the standard morphological characteristics on the cranium, including the mastoid process, supraorbital margin, mental eminence, and nuchal crest (Buikstra and Ubelaker, 1994).

2.5 | HISTOLOGICAL PREPARATION

The method of creating the thin-sections for this project is based on previously published histological techniques (Reid, Beynon and Ramirez Rozzi, 1998; Mahoney, 2008, 2010; Miszkiewicz and Mahoney, 2016; Pitfield, Miszkiewicz and Mahoney, 2017). A thin-section can be produced in three days by following this methodology. **The same basic stages are used for both tooth histology and bone histology.** However, a few essential

methodological differences must be considered. Below is the method for creating un-decalcified hard tissue thin-sections.

1. ***Sampling*.** Select the tooth that will be sectioned. Ideally, the tooth should have minimal macro-wear and no dental caries or taphonomic damage to the enamel. If possible, the tooth should have an antimere that can remain *in situ* for future osteological studies. The tooth should be recorded before sectioning, either with high-resolution photographs or with resin casts. Clean the enamel surface with ethanol and mark the tooth with a marker pen as a guide to where the section will be taken. It can be difficult to accurately gauge where the cusp tips are after the tooth is embedded in resin without the markings. Here, the mesial cusps of the molars will be sectioned, so the teeth are marked with permanent ink at the tips of the two mesial cusps and the cementoenamel junction in line with the cusps (**Figure 2.2**). The chance of cutting through the tips of the dentine horns is higher when the tooth is marked. This orientation provides the best visibility of the incremental lines within the enamel.

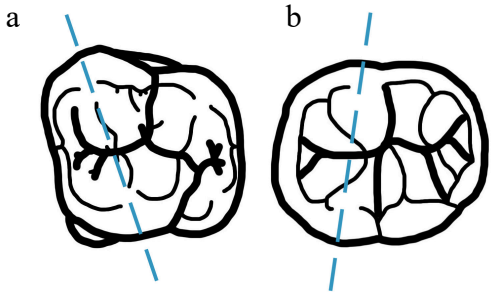

Figure 2.2 Plane of sectioning through the mesial cusps of the (a) maxillary and (b) mandibular first molars. (Redrawn from van Beek, 1983)

Select the bone that will be sectioned. Ideally, the bone should have no evidence of pathology and minimal taphonomic damage to the cortex. If possible, the bone should have an antimere that can remain intact in situ. The bone should be photographed before a thick-section is removed for embedding. The precise sampling location should be identified and marked with a pencil. Either the anterior mid-shaft of the humerus or the complete cross-section of the 3rd-8th rib was sampled for this project. The location of the humerus sections were standardized by finding the mid-shaft at 50% of the maximum length – or diaphyseal length where epiphyses were not united with the shaft – of the complete humerus (Pitfield, Miszkiewicz and Mahoney, 2017). When the humerus was fragmented, the midshaft was located by comparing it to the complete antimere. The location of the rib sections were standardized by finding the mid-shaft at 50% of the length between the tubercle and the sternal end (Agnew and Stout, 2012). The bone should be held in a vice while the thick-section (approx. 5 mm ± 2 mm) is removed with a Dremel rotary tool with a diamond blade.

2. ***Embedding***. The samples should be embedded in resin to stabilise them and reduce the risk of fracturing during sectioning (Li and Risnes, 2004; Mahoney, 2008). To do this prepare a plastic specimen cup (30 mm SamplKup™, Buehler) by coating the inside with release agent (Buehler) to ensure that the embedded sample can be removed from the cup easily once the resin has set. Use the smallest specimen cup that is available to minimise the amount of resin that will have to be cut off later. Place the tooth into the specimen cup in the correct orientation and so that the marked cusps are towards the edge of the specimen cup. The

markings will be visible and make it easier to cut the correct part of the cusps when the tooth is sectioned. The bone section should also be placed into a prepared specimen cup in the correct orientation.

Next, measure four parts epoxy resin (EpoxiCure™ Resin, Buehler) to one-part epoxy hardener (EpoxiCure™ Hardener, Buehler) in a small glass vial. Here, 20 ml disposable glass scintillation vials are used. Mix the resin and hardener with a spatula for two minutes, until the mixture has turned clear with no streaks. It should be mixed gently with a lifting and stirring motion that avoids violent stirring that will introduce air bubbles into the mixture. If the ratio is wrong, or it is insufficiently mixed, it will be either too sticky to cut or too hard and will fracture when cut. When the epoxy resin is thoroughly mixed, pour it slowly onto the section in the cup, taking care not to move the sample. Pour in enough to cover the sample. While the epoxy resin has a low viscosity, air can become trapped inside incomplete roots and trabecular bone and cause the sample to float and alter the sample orientation. The sample should be gently agitated immediately after the resin is poured on it to release any trapped air. Leave the resin to cure for between 18 and 24 hours at room temperature.

3. ***Cutting***. The samples, within the resin block, must be cut open so that a section can be affixed to a microscope slide. Once the resin is completely hardened, the block containing the sample can be removed from the sample cup. The resin block is held in a saddle chuck (Buehler) to stabilise it during the cutting process. Excess resin is removed from the block using a diamond blade mounted on a Buehler IsoMet 1000 precision saw. The embedded tooth is cut along the earlier markings. Between 100 rpm and 300 rpm should be used as higher revolutions risk damaging

the enamel (Silva, Moreira and Alves, 2011). Bucco-lingual sections will be taken through the molars to reveal the mesial dentine horns. The bone samples are cut transversely at a 90° orientation to the long axis of the shaft.

4. ***Mounting***. The cut face of the section is mounted on a glass slide. To begin, grind the section briefly with two fingers against silicon carbide paper with a grit of P 600 followed by a finer grit (e.g. P 1200). The abrasion will smooth any protuberances from the cut face and allow the section to lie completely flat against the slide (Wighton, Jones and Bell, 2012). Rinse the ground surface with water to remove any loose particles and allow it to air dry. Prepare a glass slide by cleaning it with 100% ethanol on a cotton swab and allow it to air dry. The ethanol will remove any particles that are on the slide that could obscure the histological features. The section will be affixed to the slide with more epoxy resin. Mix a small amount of epoxy resin and hardener using a plastic spatula. Evostik is a quick drying epoxy that will start to harden 30 seconds after it is mixed. Apply the resin to the ground side of the section and use two fingers to press the section down on to the slide firmly, with a depressed circular motion, until the resin has spread underneath the section evenly. The resin will have cured within an hour. The embedded section should now be attached to the slide.

5. ***Second cutting***. The samples, now affixed to the slides, must be cut a second time to reduce the excess thickness and minimise the amount of grinding that must be done later to further reduce the section. The slides were held in a slide chuck (Buehler).

6. ***Grinding***. The samples need to be thin enough for light to pass through them. The final thickness of the section can vary but will be less than 100 μm (Silva, Moreira and Alves, 2011). This can be achieved by grinding the section down using a Buehler EcoMet 300 grinder-polisher with a metal magnetic plated mounted with silicon carbide paper. The grit size used here is in a series that ranges from P 400 to P 1200 for permanent molars and bone. The abrasive paper should be kept wet throughout to prevent a friction build-up that could damage the section. Additionally, the surface beneath the abrasive paper must be completely smooth as any surface defects could ruin the section (Maat, Van Den Bos and Aarents, 2001). The section will be held in place with a histolic precision grinding fixture to prevent over grinding. Even so, the section should be visually checked with a light microscope regularly to prevent it from being ground too thin.

7. ***Polishing***. Once the section has been reduced enough to reveal the incremental lines within the enamel or the lamellar structure with the bone it should be polished. Polishing will remove any surface scratches that were caused by the grinding process that could confuse the identification of some incremental lines. Here a 0.3 μm aluminium oxide (Al_2O_3) polish (Micropolish II, Buehler) is used with a polishing cloth mounted on a Buehler EcoMet 300 grinder-polisher. Polish the section for two minutes, or until all the surface scratches have been removed. Rinse any remaining polish off with water.

8. ***Covering***. Once the section has been reduced to the correct thickness and polished, it should be protected with a coverslip. A coverslip protects the section from contamination and protects it for future storage and use (de Boer, Aarents and

Maat, 2012; Maggiano, 2012a). Before the coverslip is applied, the exposed surface of the section must be clean. Place the mounted section into a glass beaker that is one quarter filled with water, with the section above the waterline, and place the beaker into a half-filled ultrasonic water bath. Set the water bath to vibrate for two minutes. No heating is required. Spray ionised water onto the section at 30-second intervals. The water, combined with the vibration, will remove any particles that are on the surface of the section.

Let the section completely air dry, then place it into a beaker of 95% ethanol for two minutes. Let the section completely air dry again, and then place the section into a beaker of 100% ethanol for two further minutes. The ethanol will dehydrate the section by extracting lipids and water along with any soluble molecules (Hillman, 2000). The section should be left to air dry again before it is briefly dipped into a beaker of Histoclear (Fisher brand) twice. The clearing solution removes the traces of ethanol (Hillman, 2000). The section will then be left to air dry for the final time. Prepare a glass coverslip by cleaning it with 100% ethanol on a cotton swab and allow it to air dry. Apply DPX mounting medium to the exposed sample face with a cotton swab when both the section and the coverslip are dry. It should cover an area that is the same length as the coverslip. Lay the coverslip gently on to the slide and allow the DPX to spread, sealing the edges of the coverslip. Once this is completely dry the slide is ready for microscopic examination.

2.6 | MICROSCOPY

2.6.1 | Bone Histomorphometry

The thin-sections were imaged with an Olympus BX51 microscope mounted with an Olympus DP25 camera. Images of the thin-sections were obtained for particular regions of interest (ROIs) using Olympus CellD software. For the bone thin-sections in Chapter 4, five ROIs were positioned sub-periostealy in the cortex and a minimum of 11.20 mm^2 of bone was examined. For the humerus thin-sections in Chapter 3, five ROIs were positioned sub-periostealy in the cortex, and a minimum of 11.20 mm^2 of bone was examined. These were located lateral (1), antero-lateral (2), anterior (3), antero-medial (4), and medial (5) (**Figure 2.3**). The ROIs were positioned sub-periostealy to avoid the endocortical primary bone in the antero-lateral region of the humerus that is known as the endosteal lamellar pocket and marks the direction of cortical drift (Maggiano *et al.*, 2016). These regions of interest were selected to be an unbiased method of choosing ROIs. Each ROI can be moved fractionally to avoid local areas of taphonomic damage but will remain in comparable areas of bone (Miszkiewicz and Mahoney, 2016). The measurements were repeated in 10 % of samples (n=19) for intra-observer error testing and in 5 % of samples (n=10) inter-observer error testing with paired parametric correlations and paired samples t tests (**Appendix B, Table A.B.1 and Table A.B.2**). For the rib bone thin-sections in Chapters 3 and 5, the entire cortex was imaged and split into pleural and cutaneous ROIs.

The bone thin-sections were imaged at 4x magnification with a 10x oculus to measure the cortical bone size and to act as a reference image. All histomorphometric measurements are defined in **Table 2.2**. Bone size was quantified by cortical width for the anterior humerus sections and by cortical area and relative cortical area for the rib cross-sections. The anterior humerus cortical width (Ct.Wi, mm) was measured as the straight-line distance between the endosteum and the periosteum at the most anterior part

of the cortex. The total rib subperiosteal area (Tt.Ar, mm^2) and endosteal area (Es.Ar, mm^2) were measured, and the cortical area was calculated (Ct.Ar, mm^2 = Tt.Ar – Es.Ar). Relative cortical area was calculated as a percentage (Re.Ct.Ar, % = (Ct.Ar / Tt.Ar) * 100) to control for allometry (Dominguez and Agnew, 2016).

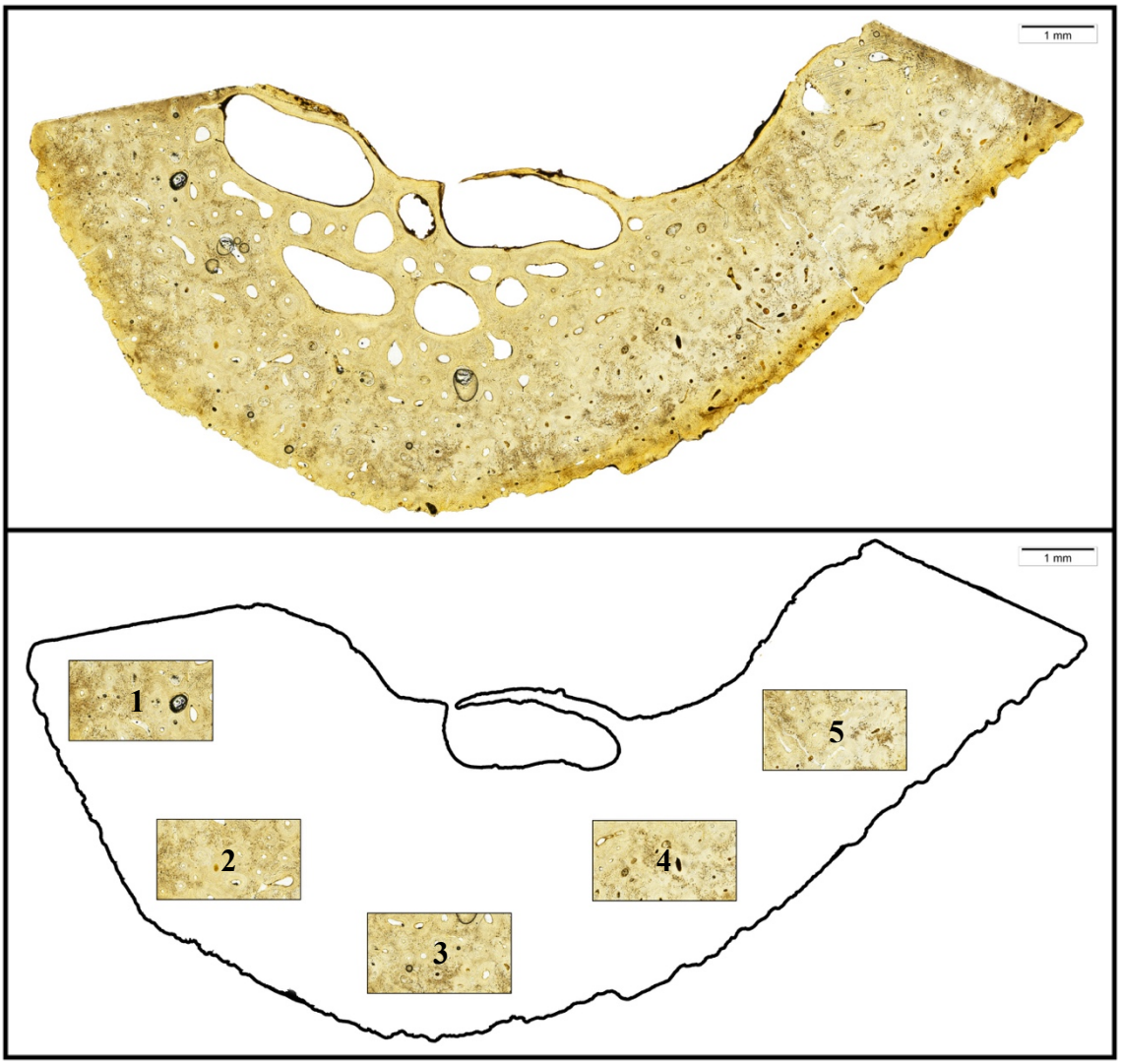

Figure 2.3 Anterior humerus ROI selection [lateral (1), antero-lateral (2), anterior (3), antero-medial (4), and medial (5)].

Each bone ROI was imaged at 10x magnification with a 10x oculus. The numbers of intact and fragmentary osteons are counted from the digital image and confirmed on the virtual microscope image. Osteons were included if they were within or touching the ROI boundary (Britz *et al.*, 2009). Primary vascular canals were identified by the presence

of a vascular canal with no associated cement line (Currey, 2013). Primary vascular canal density (Pr.Ca.Dn) was calculated by dividing the number of primary vascular canals by the area of the ROI. Secondary osteons were identified by the presence of a complete cement line and intact Haversian canals, and fragments were identified as partial secondary osteons (Currey, 2013). These osteon counts formed the osteon population density (OPD), which was calculated from dividing the intact osteon density (N.On) and the fragmentary osteon density (N.On.Fg) together by the area of the ROI. These measurements show the number of osteons (N.On), the number of osteon fragments (N.On.Fg), and the combined number of osteons and osteon fragments (OPD) per mm^2.

Each ROI is subsequently imaged at 20x magnification with a 10x oculus. The osteon size and shape measurements are taken at this higher magnification. The size of osteons was measured as osteon area (On.Ar, μm^2) and diameter (On.Dm, μm) and Haversian canal area (H.Ar, μm^2) and diameter (H.Dm, μm). Osteon lamellar area (On.Lm.Ar, μm^2) was determined (On.Lm.Ar = On.Ar – H.Ar) to calculate relative osteon area as a percentage (Re.On.Ar, % = (On.Lm.Ar / On.Ar) * 100). This gives a measure of the proportion of lamellar bone in an osteon within the cement line, irrespective of overall secondary osteon size. Higher percentages relate to higher proportions of lamellar bone area to total osteon area, and is based on a previously described ratio of H.Ar: On.Ar (Miszkiewicz and Mahoney, 2018). Osteon shape was quantified by calculating the circularity (On.Cr) from the area and perimeter measurements using the equation $4 * \pi * (On.Ar)/(On.Pm^2)$ (Goliath, 2010; Dominguez and Crowder, 2012). Values closer to 1 indicate more circular osteons, and values closer to 0 indicate more elliptical osteons. For the adult bone in Chapter 4 additional images were obtained at 40x magnification with a 10x oculus to count osteocyte lacunae. Osteocyte lacunae density (Ot.Dn) was calculated from the number of

lacunae divided by the area of the ROI.

2.6.2 | Enamel Histomorphometry

The thin-sections were imaged with an Olympus BX51 microscope mounted with an Olympus DP25 camera. Images of the tooth thin-sections in Chapters 4 and 5 were obtained for the entire enamel area using Olympus CellD software, and an ROI was positioned in the outer lateral enamel of the crown. The teeth were examined at 20x and 40x magnification with a 10x oculus.

The Retzius periodicity (RP) was calculated by counting the number of cross striations along an enamel prism between two Retzius lines (Mahoney, 2008). Daily secretion rates (DSR) were also calculated for the enamel area adjacent to the Retzius lines. The DSR was calculated by measuring between six cross striations, which corresponds to five days of enamel formation, and dividing the measurement by five to get a daily mean secretion rate. This process was repeated six times in each third so that a grand mean local DSR could be calculated (Mahoney, 2008). Subsequently, the distance between four Retzius lines, which corresponds to three repeat intervals, was measured along the prism path and divided by three to give the average distance between Retzius lines. The average distance between Retzius lines was then divided by the local DSR grand mean to give an estimate of the number of days between the Retzius lines (Mahoney, 2008).

2.7 | ANALYSES

All analyses are performed in IBM SPSS 24. The level of significance was set at 0.05 for all tests.

Table 2.2 *Bone histomorphometric variables with their abbreviations (taken from Dempster* et al.*, 2013) and definitions*

Variable	Abbrev.	Definition	Reference
Cortical width	Ct.Wi	The straight-line distance between the endosteum and the periosteum in mm.	(Agnew *et al.*, 2013)
Total area	Tt.Ar	Total cross-sectional area within the periosteum in mm^2.	(Dominguez and Agnew, 2016)
Endosteal area	Es.Ar	Total medullary area within the endosteum in mm^2.	(Dominguez and Agnew, 2016)
Cortical area	Ct.Ar	Total cortical bone area between the periosteal and endosteal margins. Tt.Ar – Es.Ar.	(Dominguez and Agnew, 2016)
Relative cortical area	Re.Ct.Ar	The amount of cortical bone relative to the total cross-sectional area as a percentage. (Ct.Ar/Tt.Ar)*100	(Dominguez and Agnew, 2016)
Primary vascular canal density	Pr.Ca.Dn	Total number of primary vascular canals per section area.	
Osteon density	N.On	Total number of osteons with intact cement lines and complete Haversian canals per section area.	(Stout and Crowder, 2012)
Osteon fragment density	N.On.Fg	Total number of fragmentary osteons that showed Haversian canals and/or osteon surfaces indicative of 10 % or more resorption per section area.	(Stout and Crowder, 2012)
Osteon population density	OPD	The density of intact and fragmentary secondary osteons. N.On + N.On.Fg.	(Stout and Crowder, 2012)
Osteon area	On.Ar	Total area within the cement line in μm^2.	(Skedros, Knight, *et al.*, 2013)
Osteon perimeter	On.Pm	Total length of the cement line in µm.	
Osteon circularity	On.Cr	The circularity of the osteon. 4*pi*area/square root of perimeter.	(Britz *et al.*, 2009)
Osteon diameter	On.Dm	Minimum diameter taken at a midpoint in µm. Accounts for elongated osteons and those that might have been obliquely sectioned.	(Britz *et al.*, 2009)
Haversian canal area	H.Ca.Ar	Total area within the complete Haversian canal in μm^2.	(Skedros, Knight, *et al.*, 2013)
Haversian canal diameter	H.Ca.Dm	Minimum diameter taken at a midpoint in µm. Accounts for elongated canals and those that might have been obliquely sectioned.	(Miszkiewicz, 2016)
Osteon lamellar area	On.Lm.Ar	Total lamellar bone area between the cement line and Haversian canal. On.Ar – H.Ar.	
Relative osteon area	Re.On.Ar	The amount of lamellar bone relative to the total osteon area as a percentage. On.Lm.Ar/On.Ar*100%	(Miszkiewicz and Mahoney, 2018)
Osteocyte density	Ot.Dn	Total number of osteocyte lacunae per section area.	(Skedros, Sybrowsky, *et al.*, 2003)

Chapter 3

Bone Histomorphometric Measures of Physical Activity in Children from Medieval England

3.1 | ABSTRACT

Histomorphometric studies show consistent links between physical activity patterns and the microstructure underlying the size and shape of bone. Here a 'combined bone' approach is used to explore variation in microstructure of ribs and humeri related to physical activity and historical records of manual labour in skeletal samples of children (*n*=175) from medieval England. The humerus reflects greater biomechanically induced microstructural variation than the rib which is used here as a control. Variation in microstructure is sought between regions in England (Canterbury, York, Newcastle), and between high- and low-status children from Canterbury. Thin-sections were prepared from the humerus or rib and features of bone remodelling were recorded using high-resolution microscopy and image analysis software. The density and size of secondary osteons in the humerus differed significantly in children from Canterbury when compared to those from York and Newcastle. Amongst the older children, secondary osteon circularity and diameter differed significantly between higher and lower-status children. By applying bone remodelling principles to the histomorphometric data we infer that medieval children in Canterbury engaged in less physically demanding activities than children from York or Newcastle. Within Canterbury, high-status and low-status children experienced similar biomechanical loading until around seven years of age. After this age low-status children performed activities that resulted in more habitual loading on their arm bones than the high-status children. This inferred change in physical activity is

consistent with historical textual evidence that describes children entering the work force at this age.

3.2 | INTRODUCTION

The primary goal of this thesis is to determine if a long period biorhythm is related to cortical bone microstructure. But the literature review in section 1.2.6 revealed that cortical bone microstructure can vary according to metabolism and biomechanical loading (Richman, Ortner and Schulter-Ellis, 1979; Lanyon *et al.*, 1982; Lanyon and Rubin, 1984; Raab *et al.*, 1991; Burr, 2002; Alexy *et al.*, 2005; Paine and Brenton, 2006; Eleazer and Jankauskas, 2016). According to textual and archaeological evidence the lifestyle factors that affect both metabolism (diet and health) and biomechanics (physical activity and manual labour) varied between populations and social status groups in medieval England (Ben-Amos, 1994; Lomas, 1996; Lyle, 2002; Bennike *et al.*, 2005; Woolgar, Serjeantson and Waldron, 2006; Nicholas, 2014; Palliser, 2014; Miszkiewicz, 2015). **Therefore, the aim in this data chapter is to describe population level variation in juvenile bone microstructural growth that may relate to activity and/or social status differences, which will be answered with the following research questions:**

1. **Is there a difference in remodelling in the humerus compared to the rib?**
2. **Are there age-related differences in remodelling of the humerus, or the rib?**
3. **Does the histomorphometry of the humeri and rib vary between children of different social status in Medieval England?**
4. **Does the histomorphometry of the humeri and rib vary between children from different locations in Medieval England?**

Studies of bioarchaeology in recent years have inferred aspects of childhood behaviour and physical activity from skeletal remains (Shapland, Lewis and Watts, 2015; Lewis, 2016; Mays *et al.*, 2017). However, juvenile skeletons are often poorly preserved and fragmented when recovered from the archaeological record. Previous histomorphometric studies have inferred behaviour and patterns of physical activity from fragments of human skeletons (Miszkiewicz, 2016; Miszkiewicz and Mahoney, 2016), within the context of evidence that has linked physical activity to bone microstructure (Skedros, Hunt, *et al.*, 2003; Skedros, Sybrowsky, *et al.*, 2003; Hedgecock *et al.*, 2007; Skedros, Keenan, *et al.*, 2013). Several studies have described age-related changes in the juvenile rib or humerus (Streeter, 2010; Maggiano *et al.*, 2016; Pitfield, Miszkiewicz and Mahoney, 2017) or used a 'combined bone' approach that incorporated the rib, humerus, and femur, to investigate the effect of biomechanics and metabolism on bone microstructure during ontogeny (Eleazer and Jankauskas, 2016). Here histomorphometric measures of bone microstructure are calculated for the humerus and rib from skeletal samples of children that date to the English medieval period. Variation in their microstructure is related to textual evidence that describes behaviour and manual labour for children from this period.

3.2.1 | Childhood Lifestyles in Medieval England

Several aspects of medieval lifestyles could potentially influence the bone microstructure of growing children, including social status and environment, diet, and behaviour (e.g. Specker and Vukovich, 2007; Eleazer and Jankauskas, 2016; Miszkiewicz and Mahoney, 2016). Medieval England had a hierarchical socioeconomic structure that dictated medieval lifestyles, with a particular influence over diet, occupation and physical activity, and disease risk (Dyer, 2000) (see section 2.1 for a more detailed historical background).

Childhood growth profiles were similar in rural and urban medieval places, as were incidences of skeletal manifestations of stress, such as hypoplastic enamel defects, maxillary sinusitis, cribra orbitalia, and non-specific indicators of stress (Lewis, 2002) (see section 2.1.3 for a more detailed account of medieval health). However, there is evidence that maternal stress was more common in urban areas than in rural areas (Lewis, 2002). The prevalence of non-specific infection and specific infection, including treponemal disease, leprosy, and tuberculosis were similar in urban and rural populations of older children and adolescents (Lewis, 2016). However, spinal and joint disease was more common for urban adolescents, which could indicate that these people engaged in more strenuous physical activity and manual labour than their rural counterparts (Lewis, 2016).

In addition to regional differences, social status could influence childhood growth and disease (Bennike *et al.*, 2005). There is dental evidence that non-specific stress during childhood and adolescence could vary according to social status. High-status people in medieval Canterbury had significantly fewer enamel indicators of non-specific stress than low-status people (Miszkiewicz, 2015b). This indicates that, while children of both high- and low-status experienced physiological stress during growth, the higher social status of some children provided a buffer against some of these stressors. The high-status children were more likely to have better health than low-status children due to better living conditions and diets.

The everyday life and diet were broadly similar for younger children from different regions of England, but it could vary greatly with socioeconomic status for older children (see section 2.1.2 for a more detailed account of medieval diet). Historical records report that weaning began between seven to nine months of age (Fildes, 1986) and isotopic studies have shown that medieval children were entirely weaned by two

years old (Mays, Richards and Fuller, 2002; Burt, 2013; Haydock *et al.*, 2013). Dental macroscopic and microscopic wear analyses suggest that the physical properties of diet for children up to approximately eight to ten years old was similar when compared between different geographic locations and between children of different social status (Dawson and Brown, 2013; Mahoney, Schmidt, *et al.*, 2016). Despite this similarity in one aspect of childhood diet, social status determined the quality, variety, and type of adult diet (Woolgar, Serjeantson and Waldron, 2006). Various studies using different methodologies have indicated a change in diet occurred at approximately seven to ten years old, after which time a more adult-like diet was consumed (Macpherson, 2005; Mahoney, Schmidt, *et al.*, 2016). The textual and archaeological evidence shows that after weaning at two years old, there was a transitional period of several years before children were consuming an adult diet at approximately seven to ten years of age. At this time, children began to be treated like adults and consume an adult diet that was dependent on their social status.

Medieval children spent more time with their parents until the age of 4 and were given greater independence between the ages of eight to 12 years (Hanawalt, 1977) (see section 2.1.1 for a more detailed account of medieval physical activity and manual labour). In rural areas, boys of this age from lower-status families commonly worked as farm labourers, and girls worked gathering, childminding, or in the fields at harvest time (Hanawalt, 1977). This was also the age at which the children of higher-status families would begin to learn the necessary skills to carry on the family trade (Fleming, 2001). In urban areas, the high-status boys would attend school (Hanawalt, 1977), or go into apprenticeships (Ben-Amos, 1994), while the low-status adolescents, whose families could not afford an apprenticeship, would gain work and lodgings as a household servant (Fleming, 2001). Female household servants were usually employed as unskilled

domestic servants rather than in a craft or trade (Goldberg, 1992). The occupations of low-status people usually involved more physically demanding manual labour than the occupations of high-status people.

Few historical textual records of childhood physical activity exist, and it is unknown if physical activity varied between children from different geographic locations. However, historical records show that adult occupation varied across regions of England. The area surrounding Newcastle was a politically unstable border area between Scotland and England in the tenth and eleventh centuries AD (Rollason, 2003). The population were subjected to ongoing scorched earth and siege campaigns, whilst also undertaking intensive farming to provide for themselves and the occupying armies (Lomas, 1996). York and Canterbury were both major medieval cities, but each had a different character. The Fishergate area of York was a center of industry and manufacturing in the medieval period, with a particular emphasis on textiles (Nicholas, 2014; Palliser, 2014). The Northgate area of Canterbury was a relatively poor area of the city, but the local people could be employed by the wealthy religious houses in domestic jobs or construction (Lyle, 2002). A medieval English person's experience of manual labour could vary according to age, social status, and geographic area. If the regional differences in occupation caused sufficiently different patterns of loading on the skeleton, it is possible that this may be reflected in bone microstructure, during later childhood after the children had taken on their more adult-like roles.

3.2.2 | The Archaeological Sites

St Gregory's Priory (1084-1537 AD). Canterbury Archaeological Trust excavated the site of St Gregory's Priory, Canterbury, between 1988 and 1991 (Hicks and Hicks, 2001). During this time, 1342 articulated skeletons were retrieved (Anderson and Andrews,

2001). St Gregory's Priory was located just outside the city walls of Canterbury, Kent and it was in use as a burial ground between 1084 AD and 1537 AD. High status lay people could pay for burial within the Priory, alongside the members of the clergy. Juvenile skeletons excavated from graves within the foundations of the Priory were likely members of high-status families and juvenile skeletons buried in the surrounding cemetery were members of the lower-status lay community. Given that this archaeological site has two socioeconomic groups, it is an ideal population to study whether bone microstructure varies according to social status in children.

Fishergate House (1399-1539 AD) and All Saint's Church (1091-1539 AD). Fishergate House, York, was excavated between 2000 and 2002 (Spall and Toop, 2005). During this time, 244 articulated skeletons were retrieved. It has been suggested based on documentary evidence that the cemetery would have belonged to St Helen's Church. St Helen's Church and Hospital was founded in Fishergate in 1399 AD, but its exact location is unknown (Holst, 2005). While St Helen's may be the source of the burials, it remains uncertain, and there has been no archaeological evidence of a church found at the Fishergate House site (Holst, 2005).

All Saints' Church, York, more commonly known as Fishergate Barbican, was excavated between 2007 and 2008 (McIntyre and Bruce, 2010). During this time, 667 articulated skeletons were retrieved. The first documentary evidence for a church at the site dated to 1091 and 1095 AD. The church did not survive long after 1539 AD, and its location was lost as the parish was merged with the parish of St. Lawrence in 1586 AD. The shroud burials and lack of grave goods indicate that the population of Fishergate were low-status.

Black Gate cemetery (c. 800-1168 AD). The Black Gate cemetery, Newcastle, was excavated between 1973 and 1992. There were 663 articulated skeletons excavated

from 660 burials between 1977 and 1992, representing the largest group of Christian Anglo-Saxon burials excavated in Northeast England (Nolan, Harbottle and Vaughan, 2010; Swales, 2013). Radiocarbon dating of burials indicates that the cemetery was established around 800 AD (Nolan, Harbottle and Vaughan, 2010; Swales, 2013). However, there was no documented settlement at the site at that time, but some dateable archaeological finds, such as coins, indicate that people were in the area in the eighth and ninth centuries AD (Nolan, Harbottle and Vaughan, 2010). By the tenth century AD, the cemetery was well established and was most likely serving a local lay population. All of the burials are most likely Christian, based on the east-west burial orientation, and the lack of grave goods (Nolan, Harbottle and Vaughan, 2010).

3.2.3 | Bone Biology

Ontogeny of Humeri. The humeri begin to develop *in utero* (see section 1.2.1 for a more detailed description of humerus development). Primary ossification centres appear for the diaphyses between the eighth to ninth week of gestation (Noback and Robertson, 1951). Three secondary ossification centres appear at the proximal end and coalesce between five to seven years, and four secondary ossification centres appear at the distal end and coalesce between ten to 12 years (Cunningham, Scheuer and Black, 2016). Bone modelling thickens the cortices and modelling drift moves the humerus diaphysis postero-medially during childhood (Maggiano *et al.*, 2015). The distal epiphyses typically fuse around 11-18 years with the medial epicondyle fusing separately at approximately 13-18 years, followed by the proximal epiphyses at around 14-21 years (Cunningham, Scheuer and Black, 2016).

Ontogeny of Ribs. Ribs begin to develop *in utero* through chondrofication followed by ossification (see section 1.2.2 for a more detailed description of rib

development). Primary ossification centres appear at the posterior angle between the eighth to 12th week of gestation (Noback and Robertson, 1951). Bone modelling thickens the cortices and modelling drift ensures the endosteal area remains in the centre of the diaphysis while the ribs move ventrally during childhood as the thorax expands (Streeter, 2010). Rib growth is complete between 15-24 years of age (Cunningham, Scheuer and Black, 2016).

Microstructure. Primary vascular canals are formed when blood vessels are incorporated into the periosteal cortex during bone modelling (Parfitt, 1983). They contain few or no lamellae and do not have a boundary cement line (Currey, 2013). Remodelling differs to modelling because existing bone is removed prior to the deposition of new bone only in remodelling (see section 1.2.4 for a detailed description of bone modelling and section 1.2.5 for a detailed description of bone remodelling). During remodelling, osteoblasts and osteoclasts are coupled in a basic multicellular unit (BMU) that produces a basic structural unit of bone, also known as a secondary osteon (Martin, Burr, Sharkey, & Fyhrie, 1998). Each BMU follows a defined sequence: Activation – Resorption – Formation. The activation phase is prompted by the disruption of an inhibitory signal from local osteocytes (Burger and Klein-Nulend, 1999). Osteoclasts within a cutting cone remove a core of existing bone during the resorption phase (Vaananen *et al.*, 2000). This results in a resorption cavity that is bounded by a cement line separating the osteon from the surrounding bone. The action of the osteoclasts determines the diameter of the cutting cone and of the future secondary osteon, which is usually between 150 μm and 350 μm (van Oers, Ruimerman, Tanck, *et al.*, 2008). The resorption cavity will subsequently by infilled with concentric rings of lamellae during the formation phase. Osteoblasts, lining a closing cone, deposit osteoid and calcium phosphate crystals at the cement line and deposition proceeds towards the central

Haversian canal (Martin *et al.*, 1998).

As remodelling occurs, existing osteons are intercut by new osteons and fragments of the osteons accumulate in the bone and cause an age-related increase in OPD (Stout and Paine, 1992). Targeted remodelling replaces areas of strain induced micro-cracks and cause higher OPDs in those regions (Burr, 2002). The number of intact and fragmentary osteons can be combined as osteon population density (OPD) to give an indication of bone turnover rate since secondary osteons are the product of bone remodelling. OPD is linked to age (Stout and Paine, 1992; Goliath, Stewart and Stout, 2016; Pfeiffer *et al.*, 2016), and biomechanics (Young *et al.*, 1986; Britz *et al.*, 2009), as well as diet (Richman, Ortner and Schulter-Ellis, 1979), and health (Martin and Armelagos, 1979). Osteon density and osteon morphology are closely linked, and high OPDs are often associated with smaller osteons (Miszkiewicz, 2016). Osteon size and shape are quantified as osteon area, diameter, and circularity (On.Ar, On.Dm, On.Cr). Generally, On.Ar, On.Dm, Haversian canal area (H.Ca.Ar), and Haversian canal diameter (H.Ca.Dm) are inversely related to biomechanical strain magnitude (van Oers, Ruimerman, van Rietbergen, *et al.*, 2008). Osteon morphology can provide an indication of the type of loading on a bone which may be used to infer aspects of behaviour (Miszkiewicz and Mahoney, 2016).

Cortical bone microstructure is influenced by a) age, b) metabolism, and c) biomechanics (Specker and Vukovich, 2007; Goldman *et al.*, 2009; Eleazer and Jankauskas, 2016) (see section 1.2.6 for a detailed review). A ‘combined bone’ approach can be used to infer population level differences in factors affecting systemic remodelling and biomechanical loading induced local remodelling (Eleazer and Jankauskas, 2016). When age is accounted for, the biomechanical forces that affect the ribs do not vary substantially between individuals because the ribs are non-weight bearing and the

biomechanical effect of breathing is consistent between people (Tommerup *et al.*, 1993). Accordingly, due to the limited inter-personal variation in biomechanical forces affecting the ribs, they reflect systemic bone remodelling (Agnew and Stout, 2012). Whereas the biomechanical forces that affect the humerus can vary between people to a greater extent, since physical activity and behaviour can vary between people. The humerus reflects both systemic bone remodelling and greater biomechanically induced microstructural variation (Eleazer and Jankauskas, 2016). Here the cortical bone microstructure of the humerus and rib is studied within the context of the behaviour and manual labour practices described in textual evidence.

3.2.4 | Research Questions and Predictions

1. **Is there a difference in remodelling in the humerus compared to the rib?** – Since the ribs are reported to have a higher remodelling rate than the long bones (Frost, 1969) the rib is expected to show evidence of greater remodelling as an increased OPD, intact osteon density (N.On), and osteon fragment density (N.On.Fg).

2. **Are there age-related differences in remodelling of the humerus, or the rib?** – Osteons accumulate with advancing age (Stout and Paine, 1992; Goliath, Stewart and Stout, 2016; Pfeiffer *et al.*, 2016). Given this, an increase in OPD, N.On, and N.On.Fg is expected in older children compared to younger children. Osteon size decreases with advancing age (Britz *et al.*, 2009; Dominguez and Agnew, 2016) and a reduction in On.Ar, On.Dm, H.Ca.Ar, and H.Ca.Dm is expected in older children compared to younger children. The same age-related pattern in both bones is expected since age has a systemic effect on the skeleton.

3. **Does the histomorphometry of the humeri and rib vary between children of different social status in Medieval England?** – Textual and archaeological evidence indicates that children could transition to a different and sometimes more active lifestyle at around seven to eight years of age, when they engaged in occupations determined by social status. Low-status children could sometimes undertake more physically strenuous work than high-status children (Ben-Amos, 1994). It is hypothesised that older children and adolescents from the low-status group will show more strain induced remodelling in the humerus, as smaller and more dense osteons, than the older children and adolescents from the high-status group. Differences in rib microstructure when compared between groups of different social status are not expected. However, there could be differences in the rib microstructure if the health and nutritional status of the low-status children was poor enough that the energetic demands of normal bone remodelling could not be met.

4. **Does the histomorphometry of the humeri and rib vary between children from different locations in Medieval England?** – It is possible that there will be a change in the microstructure of the humerus when compared between the samples of older children, if there are regional differences in the type of occupation and physical activity undertaken. There is historical textual and archaeological evidence for regional variation in adult occupation in medieval England (Lomas, 1996; Lyle, 2002; Nicholas, 2014; Palliser, 2014). If children from different regions follow a similar trend, then those that are more physically active might have higher habitual loading on the humerus and show more strain induced remodelling than juveniles from a less active region. This would manifest

as smaller and more dense secondary osteons. No significant differences in the rib microstructure are expected between regional groups, unless the health and nutritional status of a population was poor enough that the energetic demands of normal bone remodelling could not be met.

3.3 | MATERIALS AND METHODS

3.3.1 | Study Sample

This study included 175 medieval juvenile skeletons excavated from three locations in England (**Figure 2.1**). St Gregory's Priory and Cemetery, Canterbury *n* = 125 (high-status *n* = 19 and low-status *n* = 116), York *n* = 33 (Fishergate House *n*= 20 and All Saint's Church *n* = 13), and The Black Gate Cemetery, Newcastle *n* = 17. No permits are required for the present study as these skeletal samples pre-date the Human Tissue Act, and all of the sampling followed the appropriate codes of ethics for research conducted on human skeletons (Mays *et al.*, 2013).

3.3.2 | Age-at-death Estimation

The age estimation methods are explained in further detail in section 2.4. These methods were the assessment of tooth formation times (Moorrees, Fanning and Hunt, 1963), the timing of dental eruption (Al Qahtani, Hector and Liversidge, 2010), and epiphyseal union timing (Scheuer and Black, 2000). Each skeleton was assigned to one of the following age groups; younger child (3–7 years, *n* = 71), older child (8–12 years, *n* = 52), or adolescent (13–18 years, *n* = 52).

3.3.3 | Histomorphometric Methods

The rib was selected as it is less influenced by physical activity patterns, it is a non-weight bearing bone and as such has limited inter-skeletal variation in respiration induced loading (Tommerup *et al.*, 1993). Accordingly, ribs reflect systemic bone remodelling (Agnew and Stout, 2012), whereas the humerus reflects both systemic bone remodelling and greater biomechanically induced microstructural variation (Eleazer and Jankauskas, 2016). Here, the rib is used as a control for inferring physical activity related changes in the cortical microstructure of the humerus. A single bone section was removed from each skeleton, from either the humeri (n=102) or the rib (n=73). The right humerus was preferentially chosen (n=70), but the left humerus was sampled when the right was damaged, pathological, or absent (n=32). The rib samples were taken from un-sided 3rd-8th ribs.

The histological methods are explained in further detail in section 2.5. Transverse sections of a 90° orientation to the long axis of the shaft were removed from either the anterior mid-shaft region of the humerus or complete sections of the mid-shaft rib using a Dremel Rotary Tool®. The location of the humerus sections were standardised by finding the mid-shaft at 50% of the maximum length – or diaphyseal length where epiphyses were not united with the shaft – of the complete humerus (Pitfield, Miszkiewicz and Mahoney, 2017). When the humerus was fragmented, the midshaft was located by comparing it to the complete antimere. The location of the rib sections were standardised by finding the mid-shaft at 50% of the length between the tubercle and the sternal end (Agnew and Stout, 2012). Each section was approximately 0.7±0.2 cm thick. Thick-sections were embedded in epoxy resin (Buehler EpoxiCure®), reduced to 0.3 ±0.1 cm thickness using a Buehler Isomet 1000 precision saw and fixed to glass microscope slides (Evo Stick® resin). Each section was ground to a final thickness of 50-100 μm (Buehler

EcoMet 300), polished with a 0.3 μm Al_2O_3 powder (Buehler® Micro-Polish II), cleaned in an ultrasonic bath, dehydrated in 95% and 100% ethanol, cleared (Histoclear®), and mounted with a coverslip using a xylene-based mounting medium (DPX®).

3.3.4 | Microscopy

The histomorphometric methods are explained in further detail in section 2.6.1 An Olympus BX51 microscope and an Olympus DP25 camera were used to collect images from five regions of interest (ROIs) from each humerus thin-section. The histological variables, with their abbreviations and definitions, appear in **Table 2.2**. The anterior humerus cortical width (Ct.Wi, mm) was measured from the endosteum to the periosteum at the most anterior part of the humeri. The rib thin-sections had much smaller cortical areas, so the entire cortex was imaged and stitched together into a montage. The total rib subperiosteal area (Tt.Ar, mm^2) and endosteal area (Es.Ar, mm^2) were measured, and the cortical area was calculated (Ct.Ar, mm^2 = Tt.Ar – Es.Ar). Each ROI within the humerus was positioned sub-periostealy in the cortex to exclude the endosteal and periosteal surfaces. The rib thin-sections were divided into two ROIs, one for the pleural cortex and one for the cutaneous cortex. Histomorphometry was performed using CELL® Live Biology Imaging software.

The number of primary vascular canals, secondary osteons, and secondary osteon fragments were counted in each ROI. Primary vascular canals were identified by the presence of a vascular canal with no associated cement line (Currey, 2013). Primary vascular canal density (Pr.Ca.Dn) was calculated by dividing the number of primary vascular canals by the area of the ROI (Humerus = 2.24 mm^2. Rib = pleural cortical area or cutaneous cortical area). Secondary osteons were identified by the presence of a complete cement line and intact Haversian canals, and fragments were identified as partial

secondary osteons (Currey, 2013). Osteons were included if they were within or touching the ROI boundary (Britz *et al.*, 2009). These osteon counts formed the osteon population density (OPD), which was calculated by dividing the number of osteons and fragments by the area of the ROI (Humerus = 2.24 mm^2. Rib = pleural cortical area or cutaneous cortical area).

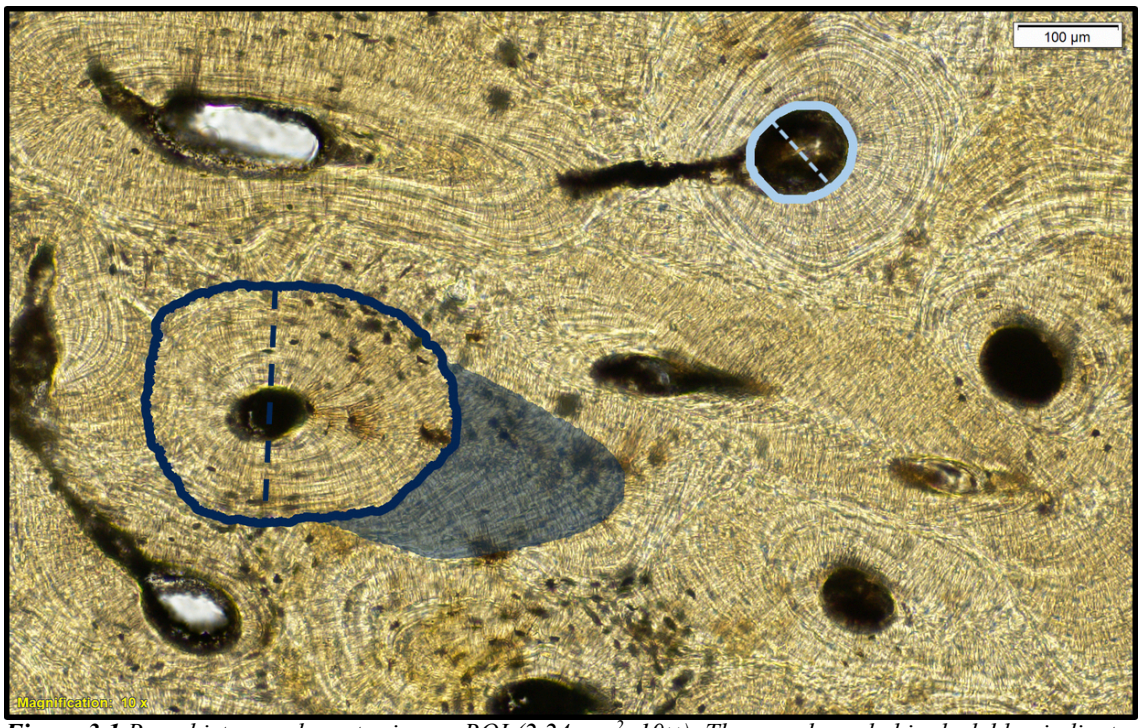

Figure 3.1 *Bone histomorphometry in one ROI (2.24 mm^2, 10×). The area bounded in dark blue indicates an intact osteon and area highlighted in blue indicates a fragmentary secondary osteon (N.On, N.On.Fg, and OPD). The area bounded in light blue indicates a Haversian canal. Measurements of osteon structure (20×) – the circles indicate the secondary osteons (dark blue) and Haversian canals (light blue) measured (On.Ar, On.Pm, and H.Ca.Ar). The dashed lines indicate the diameters of secondary osteons (dark blue) and Haversian canals (light blue) (On.Dm, H.Ca.Dm)*

In both the humerus and rib, secondary osteon structure was quantified in each ROI (**Figure 3.1**) by measuring the osteon area (On.Ar, μm^2), diameter (On.Dm, µm), and perimeter (On.Pm, µm), and the Haversian canal area (H.Ca.Ar, μm^2), and diameter (H.Ca.Dm, µm). Osteon circularity (On.Cr) was calculated from the area and perimeter

measurements using the equation $4 * \pi * (On.Ar)/(On.Pm^2)$ (Dominguez and Crowder, 2012). Values closer to 1 indicate more circular osteons, and values closer to 0 indicate more elliptical osteons.

3.3.5 | Analyses

All statistical analyses were performed in IBM SPSS® 24 with the Type 1 error alpha value set at $p < 0.05$ for all tests. Differences between the left and right humeri were tested with Mann-Whitney *U* tests. The normality of each variable was assessed with Kolmogorov-Smirnov tests, and any not normally distributed variables were transformed by square root for the count variables (Pr.Ca.Dn, OPD, N.On, N.On.Fg) or log10 for the measurement variables (Ct.Wi, Ct.Ar, On.Ar, On.Cr, On.Dm, H.Ca.Ar, H.Ca.Dm). Mann-Whitney *U* tests were used to test for differences in microstructure between the rib and humerus and between high-status and low-status children because of the unequal sample sizes. Non-parametric Kruskal Wallis tests, combined with Dunn-Bonferroni post-hoc analyses, were used to test for interpopulation differences in the microstructure of each bone. Finally, a discriminant function analysis (DFA) was performed to classify the juveniles to a population (either Canterbury, York, or Newcastle) based on their bone microstructural properties.

3.4 | RESULTS

There were no significant differences between right and left humeri (**Appendix D, Table A.D.1**), so the sample of humeri were pooled for all further analyses. Kolmogorov-Smirnov tests indicated that the transformed variables met the normality assumption (**Appendix D, Table A.D.2**).

3.4.1 | Variation in Microstructure Between the Rib and Humerus

Descriptive statistics for the histomorphometric variables of each bone are shown in **Table 3.1**, alongside Mann-Whitney *U* results comparing the histological variables between the humeri and ribs. Each variable, except Pr.Ca.Dn, On.Ar, and On.Cr differed between the rib and the humerus, when all ages were pooled. Osteon density was higher in the ribs than in the humeri (OPD, N.On, and N.On.Fg) and osteons were larger in the ribs than in the humeri (On.Ar and On.Dm). However, Haversian canals (H.Ca.Ar) were smaller in the ribs compared to the humeri.

Table 3.1 *Descriptive statistics (non-transformed) of the histological variables from the humeri and ribs of all ages pooled, and the younger children (3-7 yrs), older children (8-12 yrs), and adolescents (13-18 yrs). All populations are pooled. With Mann-Whitney U results comparing histological variables between the humeri and ribs*

		Humerus			Rib			
Age	Variable	N	Mean	SD	N	Mean	SD	*p*
All ages	Ct.Wi (mm)	102	2.89	0.88				
	Ct.Ar (mm^2)				54	19.75	7.82	
	Pr.Ca.Dn	102	2.65	1.87	73	2.68	3.26	0.15
	OPD	102	4.78	3.48	73	6.51	3.64	<0.01**
	N.On	102	3.22	2.64	73	4.31	2.51	0.02*
	N.On.Fg	102	0.59	0.77	73	1.69	1.66	<0.01**
	On.Ar (μm^2)	93	35344.93	9948.68	70	38464.62	9740.23	0.06
	On.Cr	93	0.86	0.03	70	0.87	0.03	0.32
	On.Dm (μm)	93	145.40	34.77	70	185.20	23.70	<0.01**
	H.Ca.Ar (μm^2)	93	1797.52	536.36	70	1534.11	512.98	<0.01**
	H.Ca.Dm (μm)	93	28.67	8.85	70	34.78	5.67	<0.01**
3-7 yrs	Ct.Wi (mm)	44	2.24	0.59				
	Ct.Ar (mm^2)				23	14.26	3.98	
	Pr.Ca.Dn	44	3.88	1.39	27	5.36	3.73	0.19
	OPD	44	2.10	2.61	27	3.48	2.64	0.01**
	N.On	44	1.29	1.70	27	2.15	1.77	0.04*
	N.On.Fg	44	0.18	0.47	27	0.71	1.44	0.13
	On.Ar (μm^2)	35	32462.70	10650.67	24	35136.84	7888.39	0.22
	On.Cr	35	0.87	0.03	24	0.86	0.02	0.71
	On.Dm (μm)	35	143.52	30.81	24	178.79	24.01	<0.01**
	H.Ca.Ar (μm^2)	35	1818.95	666.64	24	1656.25	485.07	0.70
	H.Ca.Dm (μm)	35	29.76	9.13	24	36.47	5.72	<0.01**
8-12 yrs	Ct.Wi (mm)	32	3.05	0.57				
	Ct.Ar (mm^2)				17	19.05	3.54	
	Pr.Ca.Dn	32	2.49	1.42	20	2.06	1.64	0.30
	OPD	32	5.31	1.84	20	6.15	1.84	0.10
	N.On	32	4.00	1.36	20	4.77	1.44	0.08
	N.On.Fg	32	0.60	0.50	20	1.48	0.91	<0.01**
	On.Ar (μm^2)	32	35681.79	8087.01	20	40400.89	10772.81	0.17
	On.Cr	32	0.86	0.04	20	0.87	0.03	0.44
	On.Dm (μm)	32	144.40	35.94	20	189.54	27.92	<0.01**
	H.Ca.Ar (μm^2)	32	1808.57	415.02	20	1592.33	691.93	<0.04*
	H.Ca.Dm (μm)	32	28.86	7.52	20	35.55	6.09	<0.01**
13-18 yrs	Ct.Wi (mm)	26	3.79	0.71				
	Ct.Ar (mm^2)				14	29.64	6.90	
	Pr.Ca.Dn	26	0.78	1.39	26	0.43	0.84	0.26
	OPD	26	8.66	2.07	26	9.95	2.46	0.15
	N.On	26	6.45	1.78	26	6.76	1.75	0.81
	N.On.Fg	26	1.48	0.84	26	3.31	1.45	<0.01**
	On.Ar (μm^2)	26	38810.27	10227.35	26	40046.97	10008.17	0.55
	On.Cr	26	0.86	0.02	26	0.87	0.02	0.17
	On.Dm (μm)	26	149.09	39.06	26	187.77	19.13	<0.01**
	H.Ca.Ar (μm^2)	26	1755.09	487.90	26	1376.57	321.10	<0.01**
	H.Ca.Dm (μm)	26	27.02	10.01	26	32.63	4.72	0.03*

† Statistical significance value: *$p < 0.05$, **$p < 0.01$.

3.4.2 | Age-related Variation in Microstructure

Descriptive statistics for the histomorphometric variables are split by age category and bone type and are shown in **Table 3.1**. Kruskal Wallis (**Table 3.2**) revealed that there are significant differences in the microstructure of the humerus, when compared between the age groups. The Dunn-Bonferroni post-hoc tests show significant changes between the age groups. The variables Ct.Wi (all $p < 0.05$) and OPD (all $p < 0.01$) increased from the younger children, aged three to seven years, to the older children, aged eight to 12 years, and to the adolescents, aged 13 to 18 years, and also from the older children to the adolescents. Whilst the variable Pr.Ca.Dn (all $p < 0.01$), decreased between each age group (from young children to older children, from young children compared to adolescent, and from older child to adolescent). The variables N.On (both $p < 0.01$), and N.On.Fg (both $p < 0.01$) also increased from the younger children to the older children aged eight to 12 years, and to the adolescents aged 13 to 18 years. The On.Ar of the humerus was significantly larger in the adolescents compared to the younger children ($p < 0.05$).

Kruskal Wallis (**Table 3.2**) showed additional significant differences in the rib microstructure when compared between the age groups. The Dunn-Bonferroni post-hoc tests show significant increases between every age group (from young children to older children, from young children compared to adolescent, and from older child to adolescent) in Ct.Ar (all $p < 0.05$) and OPD (all $p < 0.05$), and decreases between every age group in Pr.Ca.Dn (all $p < 0.01$). The variable N.On (both $p < 0.01$) increased from the younger children to the older children, and from the younger children to the adolescents. The variable N.On.Fg also increased between the younger children and the adolescents and between the older children and the adolescents (both $p < 0.05$).

Table 3.2 *The Kruskal Wallis results comparing histological variables in the humeri and ribs between the age groups, younger children (3-7 yrs), older children (8-12 yrs), and adolescents (13-18 yrs). All populations are pooled*

	Humerus				Rib			
Variable	N	df	χ^2	*p*	N	df	χ^2	*p*
lgCt.Wi (mm)	102	2	55.85	<0.01**				
lgCt.Ar (mm^2)					54	2	33.46	<0.01**
sqrtPr.Ca.Dn	102	2	47.19	<0.01**	73	2	42.74	<0.01**
sqrtOPD	102	2	59.53	<0.01**	73	2	44.06	<0.01**
sqrtN.On	102	2	43.79	<0.01**	73	2	25.60	<0.01**
sqrtN.On.Fg	102	2	37.62	<0.01**	73	2	20.46	<0.01**
lgOn.Ar (μm^2)	93	2	6.66	0.04*	70	2	4.64	0.10
lgOn.Cr	93	2	2.92	0.23	70	2	0.14	0.93
lgOn.Dm (μm)	93	2	0.24	0.89	70	2	4.16	0.13
lgH.Ca.Ar (μm^2)	93	2	1.03	0.60	70	2	6.13	0.05*
lgH.Ca.Dm (μm)	93	2	1.25	0.54	70	2	8.27	0.02*

† Statistical significance value: *$p < 0.05$, **$p < 0.01$.

3.4.3 | Social Status and Microstructure of the Humerus and Rib

Descriptive statistics are shown for the humerus microstructure of a high-status group and a low-status group from medieval Canterbury in **Table 3.3**, alongside Mann-Whitney *U* results comparing the histological variables between the two social status groups. Individuals from the adolescent group were not tested because of the low sample number in the high-status group. None of the histomorphometric variables from the humeri differed significantly between the high-status and low-status children when the young children and older children were pooled, or when just the young children were considered. Osteons were significantly more circular ($p < 0.05$) with larger diameters ($p < 0.05$) in the humeri of high-status compared to low-status older children between the ages of 8-12 years, though sample sizes were very small.

There were no significant differences in histomorphometric variables from the ribs when sub-divided by age-group and compared between high-status and low-status children in Canterbury (**Appendix D, Table A.D.3**).

Table 3.3 *Descriptive statistics (non-transformed) of the humerus histological variables from high-status and low-status children from Canterbury, with Mann-Whitney U results comparing humerus histological variables from high-status and low-status children (3-12 yrs), younger children (3-7 yrs) and older children (8-12 yrs) from Canterbury*

		High-status			Low-status			
Age group	Variable	N	Mean	SD	N	Mean	SD	*p*
3-12 yrs	Ct.Wi (mm)	10	2.65	0.74	46	2.45	0.69	0.36
	Pr.Ca.Dn	10	2.95	0.92	46	3.75	1.45	0.10
	OPD	10	1.79	2.43	46	2.82	2.45	0.32
	N.On	10	1.47	1.81	46	2.48	2.08	0.16
	N.On.Fg	10	0.31	0.70	46	0.34	0.48	0.40
	On.Ar (μm^2)	8	34372.78	11202.01	39	32387.63	10976.17	0.59
	On.Cr	8	0.88	0.04	39	0.86	0.04	0.10
	On.Dm (μm)	8	138.65	17.67	39	124.78	24.99	0.07
	H.Ca.Ar (μm^2)	8	2267.83	646.23	39	1830.08	612.42	0.06
	H.Ca.Dm (μm)	8	30.03	10.57	39	25.03	6.78	0.19
3-7 yrs	Ct.Wi (mm)	6	2.16	0.50	29	2.15	0.55	0.98
	Pr.Ca.Dn	6	3.20	1.03	29	4.11	1.34	0.17
	OPD	6	0.30	0.23	29	1.71	2.24	0.24
	N.On	6	0.30	0.23	29	1.49	1.81	0.08
	N.On.Fg	6	0.00	0.00	29	0.22	0.51	0.45
	On.Ar (μm^2)	4	26176.28	6199.86	22	31861.56	12415.02	0.52
	On.Cr	4	0.86	0.02	22	0.87	0.04	0.81
	On.Dm (μm)	4	132.98	19.77	22	130.11	25.74	0.50
	H.Ca.Ar (μm^2)	4	2331.40	828.56	22	1807.06	735.76	0.11
	H.Ca.Dm (μm)	4	33.88	13.56	22	25.91	8.09	0.23
8-12 yrs	Ct.Wi (mm)	4	3.37	0.26	17	2.96	0.60	0.07
	Pr.Ca.Dn	4	2.57	0.67	17	3.13	1.46	0.57
	OPD	4	4.02	2.55	17	4.73	1.41	0.52
	N.On	4	3.24	1.69	17	4.18	1.27	0.36
	N.On.Fg	4	0.78	0.99	17	0.55	0.34	0.90
	On.Ar (μm^2)	4	42569.29	8672.14	17	33068.42	9108.17	0.08
	On.Cr	4	0.91	0.04	17	0.85	0.03	0.02*
	On.Dm (μm)	4	144.32	15.87	17	118.19	23.08	0.02*
	H.Ca.Ar (μm^2)	4	2222.27	529.10	17	1859.88	422.60	0.24
	H.Ca.Dm (μm)	4	26.19	6.10	17	23.93	4.70	0.57

† Statistical significance value: *$p < 0.05$, **$p < 0.01$.

3.4.4 | Bone Microstructure Compared Between the Regions

Descriptive statistics are shown for the microstructure of the humerus of each population in **Table 3.4**, alongside Kruskal Wallis tests that revealed significant differences in the microstructure of the humerus, but not the ribs, when compared between the regions

(Humeri: OPD $p < 0.01$; On.Dm, $p < 0.01$; H.Ca.Dm $p < 0.01$). Dunn-Bonferroni post-hoc tests show that OPD of the humerus is significantly lower in juveniles from Canterbury than from York ($p < 0.01$) or Newcastle ($p < 0.01$). The On.Dm of the humerus is significantly lower in juveniles from Canterbury than from York ($p < 0.01$) or Newcastle ($p < 0.01$). The H.Ca.Dm of the humerus was significantly lower in juveniles from Canterbury than from York ($p < 0.01$) or Newcastle ($p < 0.01$). This result was consistent within each age group, except there was no significant difference in OPD among the adolescents from different regions.

A DFA was performed with the regional group as the dependent variable and OPD, On.Dm, and H.Ca.Dm as the predictor variables based on the significant results of the Kruskal Wallis tests. The analysis produced two discriminant functions, but the first function, which was composed of the variable H.Ca.Dm, was the most successful at discriminating between the dependent variables (**Table 3.5**). The DFA assigned 83.7% of cases to the correct regional group. The Eigen value of 3.11 and the U (canonical correlation) value of 0.87, together with the visual representation for the result in **Figure 3.2a**, confirms the good separation between the groups. When the analysis was repeated, and the sample was split by age group, the DFA successfully classified 82.4% of younger children (**Figure 3.2b**), 87.5% of older children (**Figure 3.2c**), and 88.5% of adolescents (**Figure 3.2d**).

A second DFA was performed with the regional group as the dependent variable, but with Canterbury split according to social status, and OPD, On.Dm, and H.Ca.Dm as the predictor variables. The analysis produced three discriminant functions. The DFA classified 72.8% of cases to the correct regional group (**Table 3.6**). The Eigen value of 3.21 and the U (canonical correlation) value of 0.87, together with the visual representation for the result in **Figure 3.3a**, confirms the good separation between the

groups. When the sample was split by age group, the discriminant function successfully classified 79.4% of younger children (**Figure 3.3b**), 75.0% of older children (**Figure 3.3c**), and 76.9% of adolescents (**Figure 3.3d**).

Table 3.4 *Descriptive statistics (non-transformed) of the humerus histological variables from children from Canterbury, York, or Newcastle, with the Kruskal Wallis results comparing histological variables from the humeri of children from Canterbury, York, or Newcastle when all ages are pooled within each population*

Site	Variable	N	Mean	SD	*p*
Canterbury	Ct.Wi (mm)	72	8.51	4.41	0.17
	Pr.Ca.Dn	72	3.06	1.77	0.06
	OPD	72	3.81	3.24	<0.01**
	On.Ar (μm^2)	63	34179.51	11130.28	0.12
	On.Cr	63	0.86	0.03	0.57
	On.Dm (μm)	62	126.4050	24.28	<0.01**
	H.Ca.Ar (μm^2)	63	1873.55	608.96	0.29
	H.Ca.Dm (μm)	62	24.27	7.26	<0.01**
York	Ct.Wi (mm)	13	11.50	3.55	
	Pr.Ca.Dn	13	1.11	1.01	
	OPD	13	7.10	2.62	
	On.Ar (μm^2)	13	37548.56	3818.17	
	On.Cr	13	0.86	0.01	
	On.Dm (μm)	13	187.45	9.89	
	H.Ca.Ar (μm^2)	13	1598.23	185.79	
	H.Ca.Dm (μm)	13	38.23	1.94	
Newcastle	Ct.Wi (mm)	17	10.21	4.30	
	Pr.Ca.Dn	17	2.10	2.08	
	OPD	17	7.11	3.18	
	On.Ar (μm^2)	17	37978.72	7840.19	
	On.Cr	17	0.87	0.02	
	On.Dm (μm)	17	182.53	15.96	
	H.Ca.Ar (μm^2)	17	1668.16	344.28	
	H.Ca.Dm (μm)	17	37.43	3.20	

† Statistical significance value: *$p < 0.05$, **$p < 0.01$.

Table 3.5 *Discriminant function analysis result (DV = Canterbury vs. Newcastle vs. York) for all ages pooled, and the younger children (3-7 yrs), older children (8-12 yrs), and adolescents (13-18 yrs)*

Age Group	Predictors	N	Function χ^2	df	*P*	Function 1 loading matrix	Function 2 loading matrix	Classify %
All	H.Dm	92	124.44	6	<0.001	0.588*	0.209	83.7
	On.Dm					0.657	-0.752*	
	OPD					0.240	0.365*	
3-7 yrs.	On.Dm	34	29.32	6	<0.001	0.705*	-0.682	82.4
	H.Dm					0.466*	-0.256	
	OPD					0.433	0.829*	
8-12 yrs.	H.Dm	32	55.13	6	<0.001	0.556*	-0.391	87.5
	OPD					0.265	0.914*	
	On.Dm					0.534	-0.598*	
13-18 yrs.	H.Dm	26	70.63	6	<0.001	0.643*	-0.586	88.5
	OPD					0.106	0.842*	
	On.Dm					0.290	0.445*	

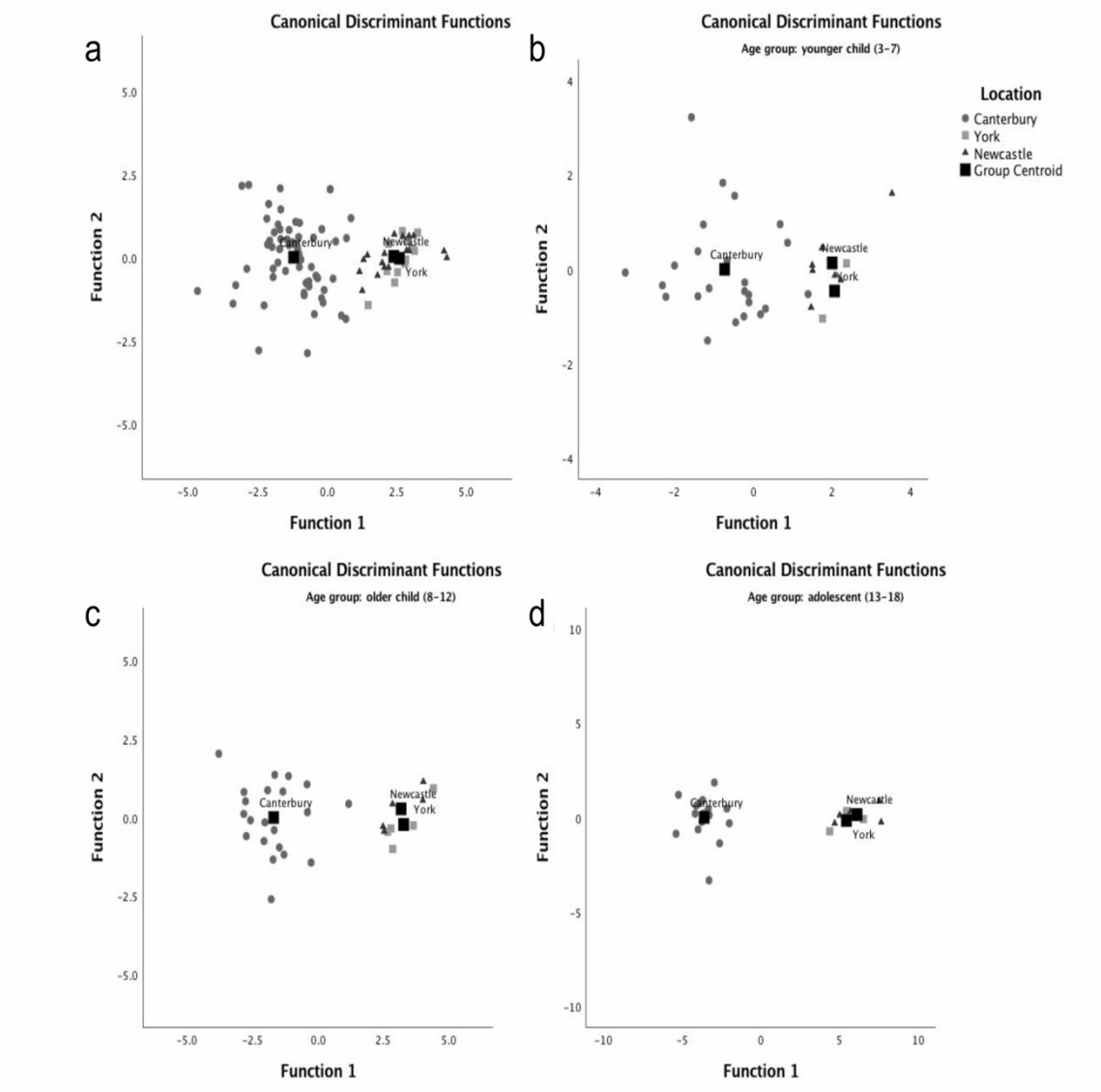

Figure 3.2 *Discriminant function analysis demonstrated how well the calculated functions discriminated (separation is shown by the group centroids) between the populations (Canterbury, York, and Newcastle). a – all ages, E (Eigen value) = 3.11, U (canonical correlation) = 0.87, b – 3-7 year olds, E = 1.61, U = 0.79, c – 8-12 year olds, E = 6.00, U = 0.93, d – 13-18 year olds, E = 23.53, U = 0.98*

Table 3.6 *Discriminant function analysis result (DV = Canterbury high-status vs. Canterbury low-status Newcastle vs. York)* for all ages pooled, and the younger children (3-7 yrs), older children (8-12 yrs), and adolescents (13-18 yrs)

Age Group	Predictors	N	Function χ^2	df	*P*	Function 1 loading matrix	Function 2 loading matrix	Function 3 loading matrix	Classify %
All	OPD	92	130.31	9	<0.001	0.230	0.973*	-0.010	72.8
	H.Dm					0.604	-0.614*	0.508	
	On.Dm					0.663	-0.306	-0.684*	
3-7 yrs.	On.Dm	34	33.95	9	<0.001	0.698*	0.322	-0.640	79.4
	H.Dm					0.468	0.794*	0.388	
	OPD					0.477	-0.777*	0.411	
8-12 yrs.	OPD	32	60.81	9	<0.001	0.244	0.754*	0.611	75.0
	On.Dm					0.584	-0.709*	0.396	
	H.Dm					0.541	-0.043	-0.840*	
13-18 yrs.	H.Dm	26	70.25	9	<0.001	0.651*	-0.611	0.450	76.9
	OPD					0.105	0.882*	-0.459	
	On.Dm					0.286	0.371	0.883*	

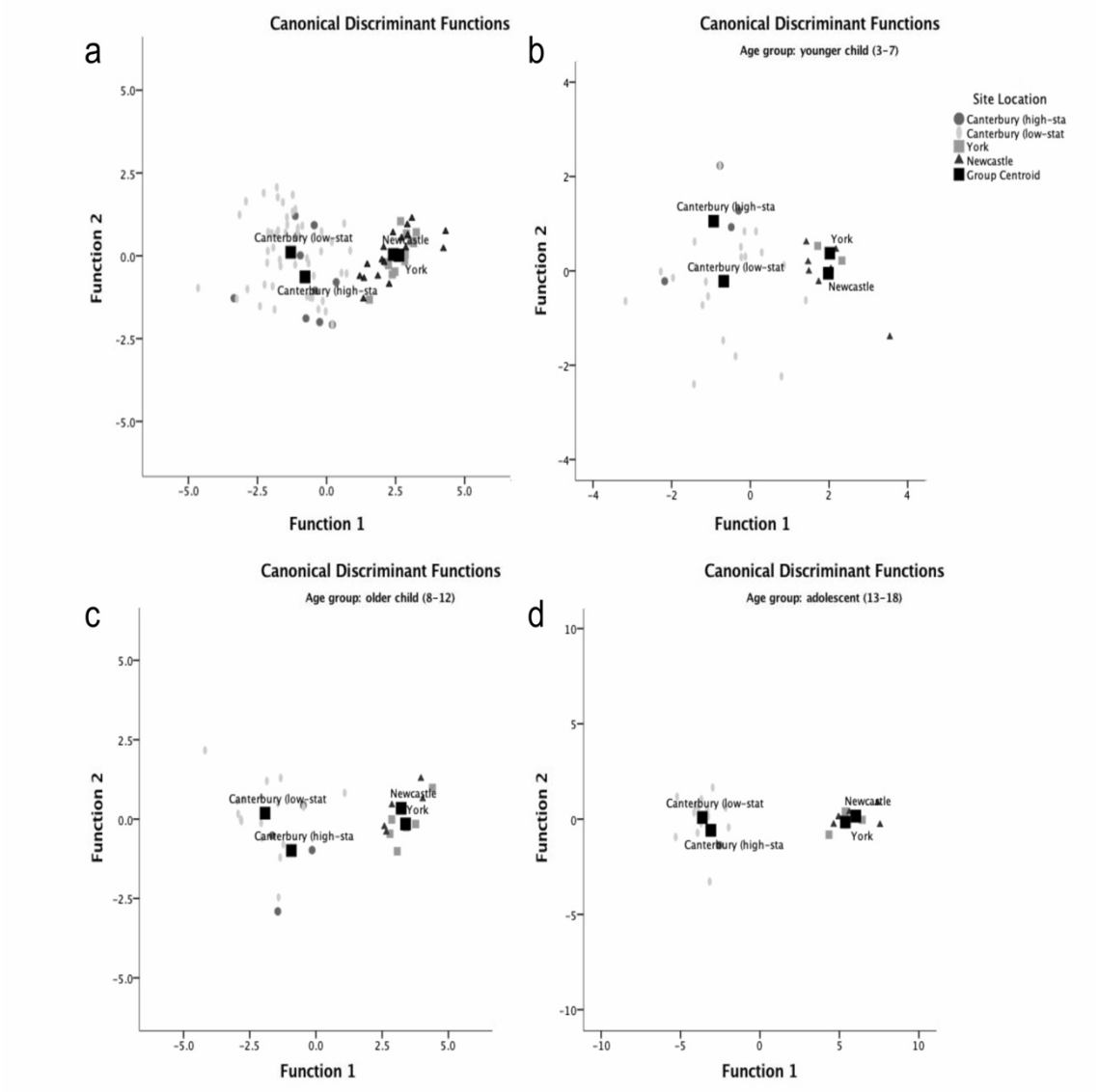

Figure 3.3 *Discriminant function analysis demonstrated how well the calculated functions discriminated (separation is shown by the group centroids) between the populations (Canterbury high-status, Canterbury low-status, York, and Newcastle). a – all ages, E = 3.21, U = 0.87, b – 3-7 year olds, E = 1.63, U = 0.79, c – 8-12 year olds, E = 6.67, U = 0.93, d – 13-18 year olds, E = 24.07, U = 0.98*

3.5 | DISCUSSION

3.5.1 | Variation in Bone Microstructure Between the Humerus and Rib

For all age groups combined, and when each age group was considered separately, osteons were larger in the ribs than in the humeri (On.Ar and On.Dm) but the Haversian canals were smaller (H.Ca.Ar) though they had larger diameters. This means that the osteons of the rib were larger, and more bone was deposited during infilling resulting in smaller canals, than the osteons in the humerus. The small Haversian canal area but large Haversian canal diameters could suggest that the canals in the rib are less circular than the canals in the humerus. This morphological variation could be due to a difference in the levels of strain that affected the ribs compared to the humerus. Smaller osteons are associated with larger strains (van Oers, Ruimerman, van Rietbergen, *et al.*, 2008). When applied to the findings here, this suggests that the humerus experiences larger habitual strain than the ribs even though the ribs are in constant motion during respiration throughout life. Secondary osteon appearance can also relate to targeted remodelling that repairs microdamage and maintains bone structural integrity (Burr, 2002). Thus, osteon size may vary intra-skeletally according to differences in the habitual loading environment of each bone. Studying the microstructure of the humerus and rib together may therefore provide a way of accessing information about physical activity. The humerus is relatively more liable to be affected by physical activity patterns than the rib.

3.5.2 | Age-related Variation in Microstructure

Primary vascular canal density decreased between the younger children and older children and then decreased again between the older children and the adolescents in both the humerus and the ribs of the children from all populations pooled together. Secondary osteons and secondary osteon fragments accumulated with advancing age in the humerus

and the ribs of the children from Canterbury, York and Newcastle, when pooled together. All of the secondary osteon count variables (OPD, N.On, N.On.Fg) in both bones increased significantly from younger children to the older children and again to the adolescents. This age-related feature of bone remodelling has been well described previously for adults (Stout and Paine, 1992; Cho *et al.*, 2002; Pfeiffer *et al.*, 2016) and children (Goldman *et al.*, 2009; Streeter, 2010; Pitfield, Miszkiewicz and Mahoney, 2017). Osteons accumulate in bones because of targeted remodelling to repair microdamage and nontargeted remodelling for mineral homeostasis (Burr, 2002) and the primary vascular canals are removed by this remodelling. The mean age for the birth of adult compacta in the rib is 12.5 years, which could explain some of the differences observed in the rib histology between the children and the adolescents (Frost and Wu, 1967).

Osteon area was significantly larger in the adolescent humeri than in the humeri of the younger children. Yet, in adults, osteon area is negatively correlated with age (Britz *et al.*, 2009; Dominguez and Agnew, 2016). The opposite relationship seen in the juveniles of this study could be accounted for by changes to bone size. The anterior humerus cortical width also increased significantly between the younger children and the adolescents, and the larger osteons of adolescents were associated with these thicker cortices. A similar scaling pattern has been noted in the adult tibia (Goldman *et al.*, 2014) and adult rib (Dominguez and Agnew, 2016). There may be a site-specific balance between limiting the spread of microdamage and maintaining a low porosity for optimum bone stiffness (Goldman *et al.*, 2014) and minimal skeletal weight (Martin, 2003), and a thicker cortex may support the formation of larger osteons (Dominguez and Agnew, 2016). The complicated relationship between bone dimensional structure and bone

functional adaptation needs further exploration, especially in relation to the interplay between modelling and remodelling during ontogeny.

3.5.3 | Social Status and Microstructure

Humerus microstructure was not related to social status amongst the younger children from Canterbury. Amongst the older children age eight to twelve years, osteon circularity and diameter differed significantly between those of higher and lower-status from Canterbury. The low-status older children had smaller (On.Ar, On.Dm) and less circular osteons (On.Cr) than the high-status older children. Smaller osteons are linked to higher strains (van Oers, Ruimerman, van Rietbergen, *et al.*, 2008), indicating a response to greater habitual loading. These results indicate that high-status and low-status children did activities that led to broadly similar levels of strain in their upper limbs in early childhood, but physical activity patterns differed after seven years of age. Historical records report that from around the age of seven onward children became more independent and could begin work, or apprenticeships outside of their family homes (Hanawalt, 1977). The bone microstructural data support this change in habitual physical activity for older children. The microstructural data also indicate that this was around the age that differences in social status began to have a noticeable influence on the lives and activities of medieval children in Canterbury. There were higher levels of biomechanical loading for the low-status children, which is compatible with the idea that they had started to become involved in more physical forms of manual labour from around the age of seven or eight years of age onwards. The low-status people in medieval Canterbury were probably employed in relatively more strenuous manual labour including domestic jobs, construction, trading, or farming (Lyle, 2002). Whilst the high-status children were likely to be involved in relatively less strenuous occupations (Ben-Amos, 1994), which in

medieval Canterbury would have meant learning the skills needed to become members of the clergy, land holders, or business owners (Lyle, 2002).

3.5.4 | Regional Variation in Bone Microstructure

The humerus cortical bone microstructure of the children varied between Canterbury, York, and Newcastle. Children from Canterbury had lower OPDs and smaller osteon and Haversian canal diameters in their humeri than children from York or Newcastle. However, rib cortical bone microstructure did not vary between these regions. This pattern was consistent for the whole sample, and when each of the three age groups when tested separately to account for age-related variation.

The results imply that there was regional variation in the factors that affect localised bone remodelling in the humerus. Differences in the microstructure of the humeri only, and none in the rib, supports the idea that the children of all ages from Canterbury engaged in less strenuous behaviour or physical activity than children from York or Newcastle. Differences in the intensity or type of physical activity result in differences in habitual loading, which in turn cause differences in the habitual strain magnitude and mode that affects the humerus. Increased OPD is linked to increased strain magnitudes (van Oers, Ruimerman, Tanck, *et al.*, 2008; van Oers, Ruimerman, van Rietbergen, *et al.*, 2008) and larger osteon diameters are linked to strain mode. On this basis, we can infer that humeri of children from medieval Canterbury experienced lower habitual strain magnitudes than the humeri of children from medieval York or Newcastle. This suggests that children from Canterbury engaged in activities that were less physically demanding on their upper arms, compared to children from medieval York or Newcastle.

Microstructural variation increases with age when compared between regions. This indicates that the habitual loading and the behavioural differences causing the

loading became larger, or else changed, as the children became older. If this can be attributed to the start of manual or skilled labour in the older children and adolescents (Hanawalt, 1977), it would imply that people in York and Newcastle undertook more physically demanding occupations than people in Canterbury. This idea is be supported by the historical records that show a general north-south divide in lifestyles in medieval England (Jewell, 1991, 1994). The population of the region surrounding modern day Newcastle were living in a politically unstable area and had to undertake physically demanding intensive farming to provide for themselves and the occupying armies (Lomas, 1996). The population of Fishergate York would have been involved in heavy industry and manufacturing, with a particular emphasis on textiles (Nicholas, 2014; Palliser, 2014). These occupations would have involved relatively more physically demanding manual labour than the common occupations for the people of Northgate Canterbury, which included religious orders, land holding, or business owning for the high-status people, and domestic jobs, construction, trading, or low-intensity farming for the low-status people (Lyle, 2002).

While OPD was found to increase with age, this study found no significant relationship between age and On.Dm or H.Ca.Dm, indicating that the findings are not attributable to aging. Additionally, when the social status of the children from Canterbury was taken into account, it showed that the difference between high-status and low-status children from Canterbury was less than the difference between either status children from Canterbury (with their status pooled) when compared to the children from York and Newcastle. This indicates that while low-status children in Canterbury were more physically active and undertook more intense manual labour tasks than their high-status contemporaries, all children from Canterbury, regardless of status, were less physically active than the children from York or Newcastle, who, according to historical records,

may have undertaken more intense manual labour (Lomas, 1996; Lyle, 2002; Nicholas, 2014; Palliser, 2014). This implies that social status had less influence on bone microstructure than where a child lived in medieval England.

Recent studies have related bone microstructural properties to bone gross morphology (Goldman *et al.*, 2009; Dominguez and Agnew, 2016; Miszkiewicz and Mahoney, 2018). Robusticity and cortical width have been linked to larger secondary osteons in the adult human tibia (Goldman *et al.*, 2009) and rib (Dominguez and Agnew, 2016) but to smaller secondary osteons and Haversian canals in the human femur (Miszkiewicz and Mahoney, 2018). Scaling analysis has shown negative allometry between humerus On.Ar and adult body size and humerus H.Ca.Ar and adult body size (Felder *et al.*, 2017). These relationships between microstructure and macrostructure cannot explain the difference found in the current study because the children from York and Newcastle did not have thicker cortices than the children from Canterbury. The population-level difference in microstructure seen here was not attributable to a difference in the dimensional bone adaptation, but it can be attributed to bone functional adaptation.

3.6 | CONCLUSION

This study applied histomorphometric methods to bone thin-sections from medieval English children. Results were interpreted though principles of bone remodelling within the context of historical textual records that describe behaviour and manual labour. Population specific variation in microstructure was detected in the humeri of the children, but not their ribs. Children from Canterbury had a lower osteon population density and smaller osteon diameters than children from York and Newcastle. It was inferred that these differences in microstructure related to different loading environments caused by

different physical activity levels and manual labour practices during life. Both high-status and low-status children from Canterbury had a lower level of habitual loading and were likely to have been less physically active with their upper limbs than children from York and Newcastle. The textual evidence supports the histological findings, since children from Canterbury could have undertaken less strenuous forms of manual labour than the children from York or Newcastle. High-status and low-status children from Canterbury experienced similar biomechanical loading until around seven years of age. After this age low-status children performed activities that resulted in more habitual loading on their bones than the high-status children. The textual evidence describes children taking on more adult-like occupations after eight years of age. Taken together, the findings imply that social status and habitual physical activity from manual labour influenced the bone microstructure of children who lived and worked in medieval England.

Chapter 4

Intraskeletal Variation in Bone Remodelling and How it Relates to a Biorhythm

4.1 | ABSTRACT

Recent studies have indicated that there is a potential link between tooth enamel Retzius periodicity (RP) and the time taken to form one bone lamella for some mammalian species. It has been hypothesised that this link in hard tissue formation is influenced by a biorhythm. So far, this has been explored in single bones only. However, bone formation and the resultant microstructure can vary intra-skeletally, from one bone to the next within a skeleton. Here the hypothesis is tested in a sample of ten adult human skeletons (*n*=5 male; *n*=5 female). Using histological methods, the measures of bone remodelling, indicated by osteon population density, osteocyte lacunae density, and osteon size and shape were compared between eight different bones from each skeleton. This intra-skeletal variation was then compared to the RP of a permanent molar from each skeleton. RP was related to Haversian canal size most consistently throughout the skeleton. If RP is related to skeletal growth via an infradian biorhythm, it appears that the biorhythm has more to do with an overall growth trajectory than specific bone turnover rates. The results support the existence of a biorhythm that links aspects of microstructural bone growth, but not bone turnover, to RP.

4.2 | INTRODUCTION

The primary goal of this thesis is to determine if a long period biorhythm is related to cortical bone microstructure. But the literature review in section 1.2.6 revealed that cortical bone microstructure can vary between bones across the skeleton according to local biomechanical loading (Ural and Vashishth, 2006; Chan, Crowder and Rogers, 2007; Crowder and Rosella, 2007; Cho and Stout, 2011; Schlecht *et al.*, 2012; Goliath, Stewart and Stout, 2016). Therefore, the aim in this data chapter is to explore how cortical bone microstructure varies intra-skeletally and then Retzius periodicity relates to this microstructural variation, which will be answered with the following research questions:

1. **How does bone microstructure, specifically osteon density and morphology, and osteocyte density vary across the skeleton?**
2. **Is there a consistent pattern of relationship between Retzius periodicity and bone microstructure across the skeleton?**

Recent studies have linked the Retzius periodicity (RP), as evidence of an underlying biorhythm, to aspects of macroscopic and microscopic bone (Bromage *et al.*, 2009, 2012; Bromage and Janal, 2014; Mahoney, Miszkiewicz, *et al.*, 2016; Mahoney *et al.*, 2017, 2018). Much of this research was conducted on single bones but there can be considerable intra-skeletal variation in bone microstructure (Stewart *et al.*, 2015). It remains unclear if and how this variation links to Retzius periodicity as a marker of the biorhythm. This study seeks to explore intra-skeletal variation in bone remodelling and then assess this variation against the RP of the same skeleton.

4.2.1 | Bone Biology of Adult Humans

Intra-skeletal bone microstructural variation occurs naturally within the body (see section 1.2.5 for a more detailed explanation of bone remodelling). Different bones experience different loading patterns, including differing modes and durations of strain. Patterns of intra-skeletal microstructural variation have most commonly been described between the rib and femur (Cho and Stout, 2011; Goliath, Stewart and Stout, 2016). One of these studies found that the rib has a higher OPD than the femur, but that osteon size was comparable between the two bones (Cho and Stout, 2011). The other study found that the rib has smaller osteons than the femur, but the two bones have similar OPDs (Goliath, Stewart and Stout, 2016). This variation could be linked to the higher mean age-at-death of the sample used by Goliath, Stewart, and Stout (2016). Intra-skeletal variation in bone microstructure has been described for the femora, fibula, humerus, radius, tibia, and ulna for the purpose of investigating the effect of disuse on the skeleton (Schlecht *et al.*, 2012). The humerus and femur were reported to have the highest bone turnover rates. To date most investigation into the intra-skeletal variation in bone remodelling has been in the context of age-related bone loss and limited to assessing two to three bones per individual.

Not only does microstructure vary between bones, it also varies within individual bones. This is likely the result of localised differences in the loading environment of a bone (Chan, Crowder and Rogers, 2007). Within-bone microstructural adaptions withstand differing strain magnitudes and directional forces. Inter-section microstructurally variation along the long bone shaft has been studied primarily for the shaft of the femur (Chan, Crowder and Rogers, 2007), and tibia (Ural and Vashishth, 2006). Significant intra-sectional variation has been reported for the femora. Along the femoral shaft the posterior regions were most variable and the anterior regions least variable at all points, although distal samples were more variable than proximal samples

(Chan, Crowder and Rogers, 2007). Similar results have been found in the tibia (Ural and Vashishth, 2006). The potential variation between bones in a similar loading environment has also been studied. For instance, the intra-costal variation in OPD was not significant when compared between ribs three to eight, although OPD was highest in the sixth rib and most variable in the eighth rib (Crowder and Rosella, 2007). This body of research suggests that cortical bone microstructure is highly variable throughout the skeleton.

4.2.2 | Biorhythms

Biorhythms are internally controlled fluctuations or cycles of biochemistry, resulting in changes to ontogenetic growth, life history traits, or daily functions (see section 1.4 for a more detailed explanation of biorhythms). Markers of a circadian biorhythm appear in enamel as cross striations when the enamel-forming ameloblasts pause every 24-hours (Risnes, 1998; Antoine, Hillson and Dean, 2009). The periodicity of cross striations has been confirmed by the analyses of vitally labelled mammalian teeth (Mimura, 1939; Bromage, 1991; Smith, 2006) and in known age human teeth (Antoine, Hillson and Dean, 2009). Since cross striations occur at regular time increments, they can be used to calculate the timing of Retzius lines, which is expressed as RP - the number of days between adjacent Retzius lines - and gives RP in increments of whole days (Mahoney, 2008). It has been suggested that the Retzius lines are a manifestation of an underlying infradian biorhythm (Newman and Poole, 1993; Appenzeller *et al.*, 2005; Bromage *et al.*, 2009). In humans the RP of permanent teeth has been observed to vary between six and twelve days, with modal periodicities of seven, eight, or nine days reported (Gysi, 1939; Fukuhara, 1959; Newman and Poole, 1974; Beynon and Reid, 1987; Bullion, 1987; Dean, 1989; Beynon, 1992; FitzGerald, 1998; Reid, Beynon and Ramirez Rozzi, 1998; Risnes, 1998; Schwartz, Reid and Dean, 2001; Reid and Dean, 2006, 2006; Reid and Ferrell,

2006; Smith *et al.*, 2007; Mahoney, 2008; Smith, 2008; McFarlane, Littleton and Floyd, 2014; Tan, Sim and Hsu, 2017; Mahoney *et al.*, 2018; Nava, Frayer and Bondioli, 2019).

Retzius periodicity has been provisionally linked to aspects of bone microstructure. The potential for periodic rhythmic lamellae formation was first noted in vitally labelled small mammals (rat, chipmunk, rabbit, and dog) where each lamella formed in a 24-hour period (Shinoda and Okada, 1988). One lamella has been shown to form in a time period that corresponds to the species-specific RP in rat, macaque, patas monkey, and sheep (Bromage *et al.*, 2009). In the femoral midshaft of one adult human female one bone lamella formed in the same number of days as the modal human RP, in both the interstitial lamellar bone and in the osteonal lamellar bone (Bromage *et al.*, 2009). Another study has found that osteocyte density in the femur positively, but not significantly, correlates with stature, but that there was no relationship between osteocyte density and body mass (Bromage *et al.*, 2016). However, femoral osteocyte lacunae density was inconsistently related to RP in a sample of adult humans (Mahoney *et al.*, 2018). The link between osteocyte density and RP in adults remains circumstantial.

These studies have formed the basis for understanding how a biorhythm could be linked to bone formation. Though previous histomorphometric bone studies have shown that there is much intra-skeletal variation in bone turnover, and to date, no study has examined the potential relationships of RP and intra-skeletal variation in bone remodelling. The present study seeks to explore the variation in cortical bone microstructure in a wider selection of bones from across the skeleton. It will then investigate how the intra-skeletal variation relates to the RP from the same skeleton to assess whether the relationship between the microstructure and a biorhythm represented by RP is stable across the body.

4.2.3 | Research Questions and Predictions

1. **How does bone microstructure, specifically osteon density and size, and osteocyte density vary across the skeleton?** – Based on previous studies (Cho and Stout, 2011) it is hypothesised that the rib and humerus will have faster remodelling rates and the femur will have a slower remodelling rate within the same skeleton.

2. **How does RP relate to bone microstructure variability across the skeleton?** – Previous studies investigating the potential link between RP and osteocyte density have found contradictory results (Bromage *et al.*, 2009; Mahoney *et al.*, 2018). Based on the findings of Mahoney et al (2018) it is hypothesised that there will be no significant relationship between RP and osteocyte density. Based on previous findings lamellar bone formation may be incremental (Shinoda and Okada, 1988; Bromage *et al.*, 2009) it is hypothesised that RP will negatively correlate with relative osteon area. This means that a lower RP, with fewer days between each 'beat' of the biorhythm, will be related to a larger proportion of lamellar bone within the secondary osteons. Relative osteon area shows the proportion of lamellar bone to the Haversian canal area within an osteon. Individuals with a faster biorhythm and lower RP should have a higher proportion of lamellar bone in each osteon if one lamella can form in the same number of days as the RP.

4.3 | MATERIALS AND METHODS

4.3.1 | Age and Sex

The osteological methods are explained in further detail in section 2.4. Ten complete adult human skeletons were selected from the St Gregory's Priory skeletal collection

(Anderson and Andrews, 2001). Biological sex was assessed from the standard morphological characteristics on the pelvis including the Phenice characteristics (Phenice, 1969) and greater sciatic notch (Buikstra and Ubelaker, 1994), and cranium, including the mastoid process, supraorbital margin, mental eminence, and nuchal crest (Buikstra and Ubelaker, 1994). Only young adults, between 20 and 35 years old at the time of death, were selected because osteon density and size is linked to advancing age (Britz *et al.*, 2009). Age-at-death was estimated from the pubic symphysis and the auricular surface of the pelvis (Lovejoy *et al.*, 1985; Meindl *et al.*, 1985).

4.3.2 | Histology

The histological methods are explained in further detail in section 2.5. Standard histological methods were used to create thin-sections from one permanent molar from each skeleton (Mahoney, 2008). All bone thin-sections had been previously produced for Fahy *et al.*, (2017). Transverse bone sections, approximately 0.7 ± 0.2 cm thick, were removed from the anterior mid shaft region of the tibia and humerus, the posterior mid shaft region of the femur, and complete cross-sections were removed from the mid-shaft metacarpal, mid-shaft radius, mid-shaft 5th rib, mid-shaft clavicle, and occipital. All samples were removed using an electronic drill (Dremel Rotary Tool®) with a diamond blade. Bone and tooth samples were embedded in epoxy resin (Buehler EpoxiCure®), further reduced to 0.3 ± 0.1 cm using a Buehler Isomet 4000 precision saw and affixed to glass slides with epoxy resin (Evo Stick® resin). Each section was ground to a final thickness of 50-100 μm using a series of silicon carbide papers (Buehler EcoMet® 300), and polished with a 0.3 μm Al_2O_3 powder (Buehler® Micro-Polish II). The thin-sections were then cleaned in an ultrasonic bath, dehydrated in 95% and 100% ethanol, cleared

(Histo-clear®), and mounted with a coverslip using a xylene-based mounting medium (DPX®).

4.3.3 | Microscopy

The histomorphometric methods for cortical bone are explained in further detail in section 2.6.1. Five regions of interest (ROIs) were selected from each bone using CELL® Live Biology Imaging software (Villa and Lynnerup, 2010; Miszkiewicz and Mahoney, 2016). Each ROI was adjacent to the periosteum within the anterior cortex, with the exception of the femur (sub-periostealy within the posterior cortex), ribs and occipital (sub-periostealy within the external cortex). This method of selecting ROIs allows for fractional movement to avoid the localised areas of diagenesis that are commonly found in ancient bone (Miszkiewicz and Mahoney, 2016).

The total number of intact secondary osteons (N.On) and secondary osteon fragments (N.On.Fg) were counted in each ROI at a magnification of 10x (**Figure 4.1a**). Secondary osteons were identified by the presence of an intact cement line and complete Haversian canal and osteon fragments were identified as partial secondary osteons with >10% of the Haversian canal remodelled (Parfitt, 1983). Any secondary osteon with its Haversian canal within or touching the border of the ROI was included (Britz *et al.*, 2009). Osteon population density (OPD) was calculated by dividing the combined number of osteons and osteon fragments by the area of the ROI (2.24 mm^2). Osteon area (On.Ar, μm^2), and perimeter (On.Pm, μm) were measured for all intact osteons within the ROIs, and these values were used to calculate osteon circularity (On.Cr, unitless) as $4 * \pi * (On.Ar)/\sqrt{(On.Pm)}$ (Britz *et al.*, 2009). Osteon lamellar area (On.Lm.Ar, μm^2) was determined (On.Lm.Ar = On.Ar – H.Ca.Ar) to calculate relative osteon area as a percentage (Re.On.Ar, % = (On.Lm.Ar / On.Ar) * 100). This provides a measure of the

proportion of lamellar bone in an osteon within the cement line irrespective of overall secondary osteon size. Higher percentages relate to higher proportions of lamellar bone area to total osteon area. Osteocyte lacunae were counted in each ROI at 40x, and the osteocyte lacunae density (Ot.Dn) was calculated by dividing the number of osteocyte lacunae by the area of the ROI (**Figure 4.1c**). The Ot.Dn data presented here have been previously reported as part of a study investigating intra-skeletal variation in bone turnover rates (Fahy *et al.*, 2017).

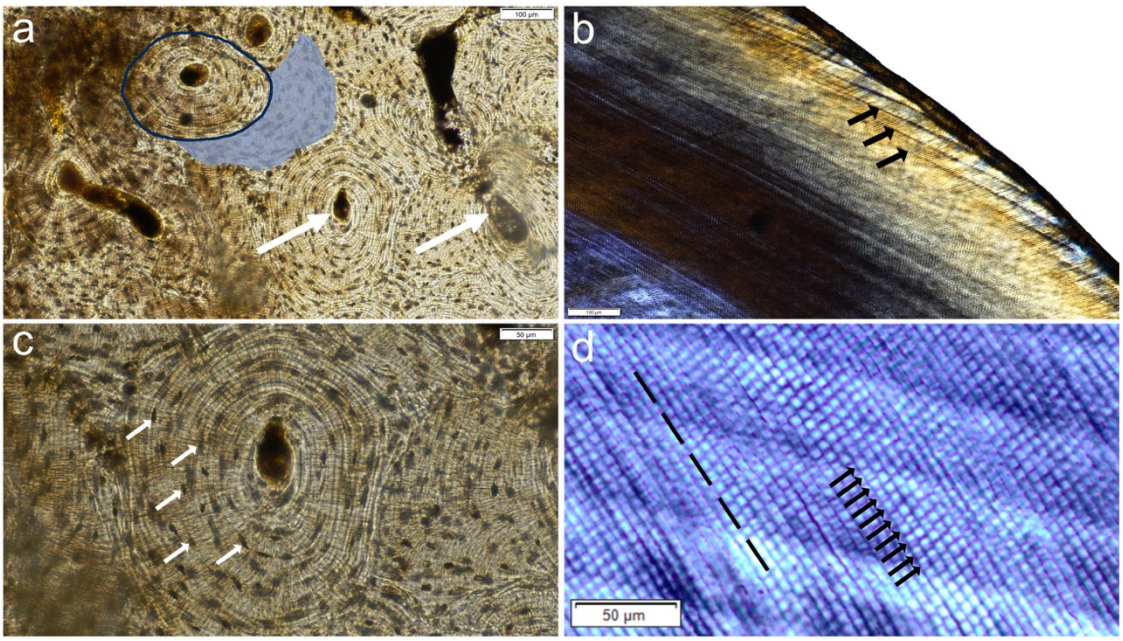

Figure 4.1 *Histological methods. a – An ROI positioned sub-periostealy in cortical bone (10x) with an intact secondary osteon circled in blue and an osteon fragment highlighted in blue. Large white arrows indicate the Haversian canals. b – Lateral enamel (10x), large black arrows indicate Retzius lines. c – Osteocyte lacunae are counted at 40x and are indicated by small white arrows. d – Cross striations (small black arrows) are counted between Retzius lines. Black dashed line indicates the prism path*

The histomorphometric methods for enamel are explained in further detail in section 2.6.2. Images of the entire enamel cap were obtained at 20x magnification and examined in CELL® Live Biology imaging software. Retzius periodicity (RP) was directly calculated by counting the number of cross striations along an enamel prism

between two Retzius lines (**Figure 4.1b**) in the lateral enamel. In cases were the RP could not be obtained directly it was calculated from local daily secretion rates (DSR) of enamel (**Figure 4.1d**) (Mahoney, 2012). DSRs were calculated by measuring between six cross striations, which corresponds to five days of enamel formation, and dividing the measurement by five to get a daily mean enamel secretion rate. This was repeated six times within the local enamel so that a grand mean DSR could be calculated (Mahoney, 2012). Following this, the distance between four Retzius lines was measured, corresponding to three repeat intervals, divided by three and then divided by the grand mean DSR to yield an RP value.

4.3.4 | Statistical Analyses

All statistical analyses were performed in IBM SPSS® 24 with the significance level set at $p < 0.05$ for all tests. The normality of each variable was assessed with Shapiro-Wilk tests. Sex differences were tested using Mann Whitney *U* tests. A repeated measurement General Linear Model (GLM) was used to test for intra-skeletal differences in bone microstructure. Spearman's rank correlations were used to test for relationships within the bone microstructural variables and between RP and the bone microstructural variables.

4.4 | RESULTS

Descriptive statistics are shown in **Table 4.1**. None of the variables were normally distributed so non-parametric tests were performed. Mann-Whitney *U* tests (**Appendix E, Table A.E.1**) showed that there were no significant differences between males and females for any bone microstructure variable, so the samples were pooled for all further analyses.

Table 4.1 *Descriptive statistics (non-transformed) for RP, and the histological variables from the tibia, femora, metacarpals, radii, humeri, ribs, clavicles, and occipitals*

Variable	N	Mean	SD	Variable	N	Mean	SD
RP (days)	10	8.50	1.434				
Tibia				**Humerus**			
N.On	10	6.71	2.01	N.On	10	8.020	3.22
N.On.Fg	10	5.83	3.77	N.On.Fg	10	7.0	1.91
OPD	10	12.54	2.98	OPD	10	14.78	1.52
On.Ar (μm^2)	10	40230.18	8674.75	On.Ar (μm^2)	10	39038.48	5163.21
Re.On.Ar (%)	10	95.57	0.89	Re.On.Ar (%)	10	95.64	0.88
H.Ca.Ar (μm^2)	10	1781.61	551.04	H.Ca.Ar (μm^2)	10	1692.32	372.00
Ot.Dn	10	667.95	112.61	Ot.Dn	10	689.62	59.87
Femur				**Rib**			
N.On	10	7.30	3.12	N.On	10	8.37	2.54
N.On.Fg	10	6.176	3.56	N.On.Fg	10	5.54	3.55
OPD	10	13.47	3.05	OPD	10	13.90	3.69
On.Ar (μm^2)	10	43796.88	7310.23	On.Ar (μm^2)	10	31116.65	4908.20
Re.On.Ar (%)	10	95.12	1.31	Re.On.Ar (%)	10	95.23	0.87
H.Ca.Ar (μm^2)	10	2069.73	436.32	H.Ca.Ar (μm^2)	10	1478.91	300.40
Ot.Dn	10	660.51	116.44	Ot.Dn	9	700.14	72.57
Metacarpal				**Clavicle**			
N.On	10	7.19	2.40	N.On	10	5.82	1.37
N.On.Fg	10	6.88	3.86	N.On.Fg	10	6.01	3.76
OPD	10	14.06	4.21	OPD	10	11.83	3.33
On.Ar (μm^2)	10	36853.79	7016.92	On.Ar (μm^2)	10	48061.72	9727.15
Re.On.Ar (%)	10	95.36	0.96	Re.On.Ar (%)	10	96.40	0.89
H.Ca.Ar (μm^2)	10	1672.11	276.65	H.Ca.Ar (μm^2)	10	1687.07	367.25
Ot.Dn	9	743.30	96.48	Ot.Dn	10	640.38	95.73
Radius				**Occipital**			
N.On	10	6.40	1.81	N.On	10	3.52	0.90
N.On.Fg	10	5.83	2.04	N.On.Fg	10	0.72	0.91
OPD	10	12.23	2.53	OPD	10	4.23	1.13
On.Ar (μm^2)	10	43260.15	8869.48	On.Ar (μm^2)	10	37326.82	11047.07
Re.On.Ar (%)	10	95.06	1.40	Re.On.Ar (%)	10	94.54	1.46
H.Ca.Ar (μm^2)	10	2075.80	603.33	H.Ca.Ar (μm^2)	10	1968.60	566.59
Ot.Dn	10	660.64	108.63	Ot.Dn	8	448.24	91.75

4.4.1 | How Does Bone Microstructure, Specifically Osteon Density and Size, and Osteocyte Density Vary Across the Skeleton?

The repeated measures GLM summary data are shown in **Table 4.2**, box plots are illustrated in **Figure 4.2**, and Bonferroni post-hoc test results are available in **Appendix E, Table A.E.2**. All variables showed significant variation between bones within each skeleton. Bonferroni post-hoc tests revealed that the occipital had significantly fewer markers of remodelling than other skeletal elements. The intact osteon density of the occipital was significantly lower than in the rib, the fragmentary osteon density of the occipital was significantly lower than in the femur, metacarpal, radius, humerus, and clavicle, and the OPD of the occipital was significantly lower than all other bones tested. Additionally, the osteocyte lacunae density of the occipital was significantly lower than in the tibia, metacarpal, humerus, and rib. Further Bonferroni post-hoc tests showed that the OPD of the clavicle was significantly lower than in the humerus, metacarpal, and femur, and the OPD of the radius was significantly lower than in the humerus and femur.

Secondary osteon geometric properties were less variable between skeletal elements than the measures of bone remodelling were. The osteon area of the rib was significantly smaller than in the radius, humerus, and clavicle, and the osteon area of the metacarpal was significantly smaller than in the clavicle. Also, the relative osteon area of the rib was significantly lower than in the clavicle and the Haversian canal area of the rib was significantly lower than in the femur.

Table 4.2 *Repeated measures GLM summary table of the histological variables compared between the tibia, femora, metacarpals, radii, humeri, ribs, clavicles, and occipitals*

Variable	Sum of squares	df	Mean square	*F*-ratio	*p*	ηp²
N.On	161.37	7	23.05	7.82	<0.01**	0.47
Error (N.On)	185.67	63	2.95			
N.On.Fg	282.20	7	40.31	6.41	<0.01**	0.42
Error (N.On.Fg)	396.39	63	6.29			
OPD	783.51	7	111.93	21.52	<0.01**	0.71
Error (OPD)	327.72	63	5.20			
On.Ar (μm²)	1.870E+9	7	267084992	6.53	<0.01**	0.42
Error (On.Ar)	2.577E+9	63	40912400			
Re.On.Ar (%)	20.44	7	2.92	4.02	<0.01**	0.31
Error (Re.On.Ar)	45.75	63	0.73			
H.Ca.Ar (μm²)	3212958.47	7	458994.07	2.74	<0.02*	0.23
Error (H.Ca.Ar)	10563501.6	63	167674.63			
Ot.Dn	348921.50	7	49845.93	6.64	<0.01**	0.53
Error (Ot.Dn)	315260.58	42	7506.20			

† Statistical significance value: *$p < 0.05$, **$p < 0.01$.

‡ ηp² = Partial Eta Squared showing the effect size

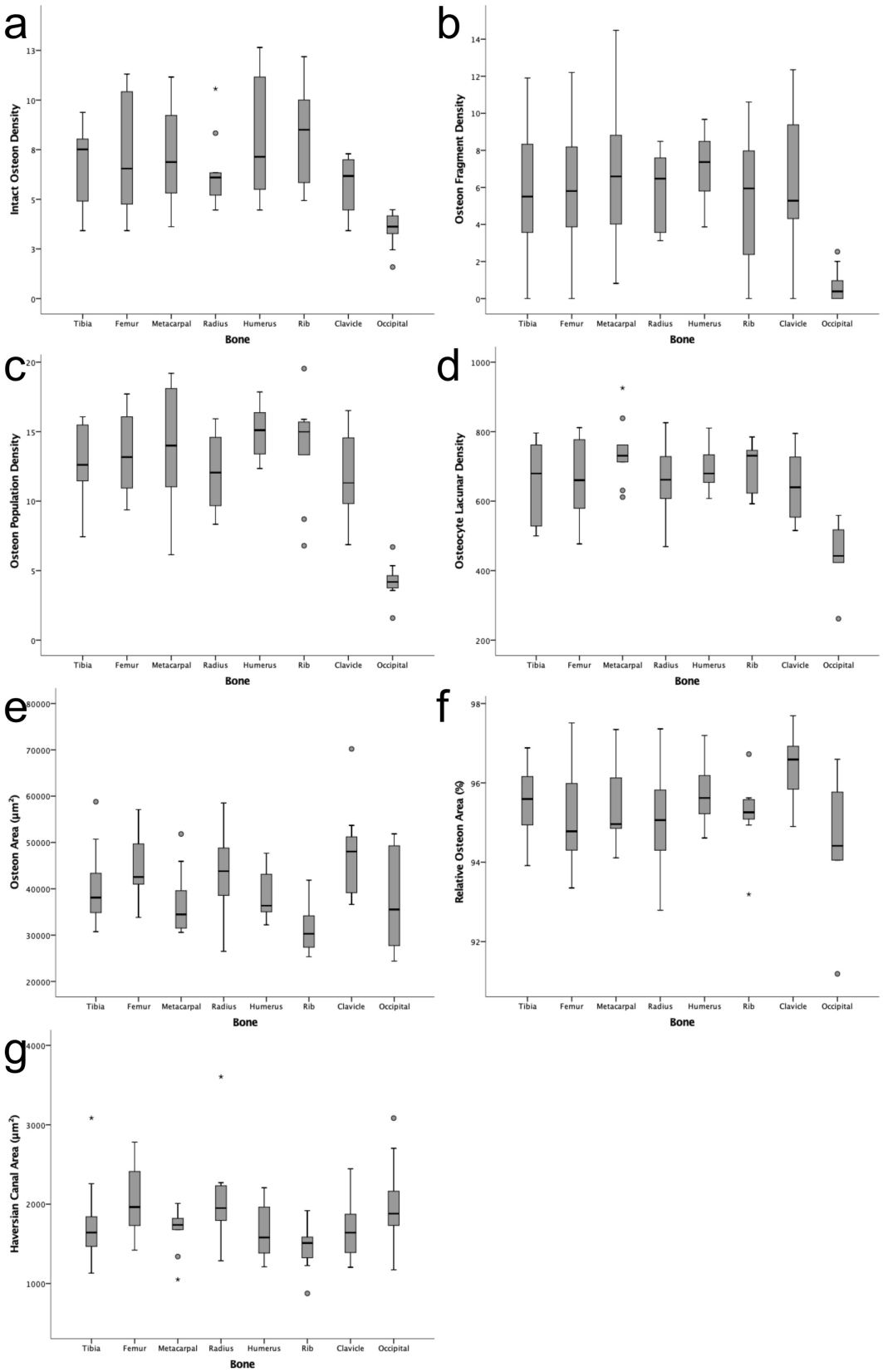

Figure 4.2 *Box plots showing the median, interquartile range, and total range of the histological variables compared between the tibia, femora, metacarpals, radii, humeri, ribs, clavicles, and occipitals. a – N.On. b – N.On.Fg. c – OPD. d – Ot.Dn. e – On.Ar. f – Re.On.Ar. g – H.Ca.Ar*

Within bone microstructural correlations are available in **Table 4.3**. With all bones combined OPD negatively correlated with osteon area ($p < 0.05$) and positively with osteocyte density ($p < 0.01$). Osteon area correlated negatively with osteocyte density ($p < 0.01$). With the bones separated OPD significantly and negatively correlated with osteon area in the tibia ($p < 0.01$) and clavicle ($p < 0.05$) and osteon area correlated significantly and negatively with osteocyte density in the tibia ($p < 0.01$).

Table 4.3 *Spearman's correlations of within bone histological variables from all bones combined and then from the tibia, femora, metacarpals, radii, humeri, ribs, clavicles, and occipitals*

	Bone Variable	OPD	On.Ar (μm²)	Re.On.Ar (%)	H.Ca.Ar (μm²)	Ot.Dn
All bones	OPD		-0.224*	-0.086	-0.082	0.577**
	On.Ar (μm²)	-0.224*		0.418**	0.395*	-0.317**
	Re.On.Ar (%)	-0.086	0.418**		-0.589**	-0.083
	H.Ca.Ar (μm²)	-0.082	0.395*	-0.589**		-0.102
	Ot.Dn	0.577**	-0.317**	-0.083	-0.102	
Tibia	OPD		-0.855**	-0.212	-0.382	0.721*
	On.Ar (μm²)	-0.855**		0.164	0.527	-0.794**
	Re.On.Ar (%)	-0.212	0.164		-0.636*	0.309
	H.Ca.Ar (μm²)	-0.382	0.527	-0.636*		-0.721*
	Ot.Dn	0.721*	-0.794**	0.309	-0.721*	
Femur	OPD		-0.515	-0.467	0.224	0.236
	On.Ar (μm²)	-0.515		0.552	-0.188	-0.176
	Re.On.Ar (%)	-0.467	0.552		-0.806**	0.115
	H.Ca.Ar (μm²)	0.224	-0.188	-0.806**		-0.467
	Ot.Dn	0.236	-0.176	0.115	-0.467	
Metacarpal	OPD		0.164	-0.333	0.212	0.417
	On.Ar (μm²)	0.164		0.624	0.382	-0.550
	Re.On.Ar (%)	-0.333	0.624		-0.297	-0.800**
	H.Ca.Ar (μm²)	0.212	0.382	-0.297		0.383
	Ot.Dn	0.417	-0.550	-0.800**	0.383	
Radius	OPD		-0.122	-0.347	0.109	-0.231
	On.Ar (μm²)	-0.122		0.455	0.261	-0.564
	Re.On.Ar (%)	-0.347	0.455		-0.503	-0.382
	H.Ca.Ar (μm²)	0.109	0.261	-0.503		-0.127
	Ot.Dn	-0.231	-0.564	-0.382	-0.127	
Humerus	OPD		-0.505	-0.462	0.267	0.292
	On.Ar (μm²)	-0.505		0.333	0.224	0.333
	Re.On.Ar (%)	-0.462	0.333		-0.770**	0.030
	H.Ca.Ar (μm²)	0.267	0.224	-0.770**		0.455
	Ot.Dn	0.292	0.333	0.030	0.455	
Rib	OPD		0.164	-0.152	0.079	0.644
	On.Ar (μm²)	0.164		0.676	0.673*	-0.226
	Re.On.Ar (%)	-0.152	0.676		-0.345	-0.218
	H.Ca.Ar (μm²)	0.079	0.673*	-0.345		-0.126
	Ot.Dn	0.644	-0.226	-0.218	-0.126	
Clavicle	OPD		-0.638*	-0.517	0.182	0.602
	On.Ar (μm²)	-0.638*		0.467	0.188	-0.200
	Re.On.Ar (%)	-0.517	0.467		-0.745*	-0.503
	H.Ca.Ar (μm²)	0.182	0.188	-0.745*		0.442
	Ot.Dn	0.602	-0.200	-0.503	0.442	
Occipital	OPD		0.321	0.442	0.091	0.096
	On.Ar (μm²)	0.321		0.406	0.552	0.287
	Re.On.Ar (%)	0.442	0.406		-0.297	-0.144
	H.Ca.Ar (μm²)	0.091	0.552	-0.297		0.659
	Ot.Dn	0.096	0.287	-0.144	0.659	

† Statistical significance value: *$p < 0.05$, **$p < 0.01$.

4.4.2 | How Does Retzius Periodicity Relate to Bone Microstructure Variability Across the Skeleton?

The correlation statistics for bone microstructure and RP are shown in **Table 4.4**. For all bones combined there was a significant positive correlation between Haversian canal area and RP ($p = 0.02$) (**Figure 4.3**). There were no significant relationships between any bone variable and RP when the bones were considered separately.

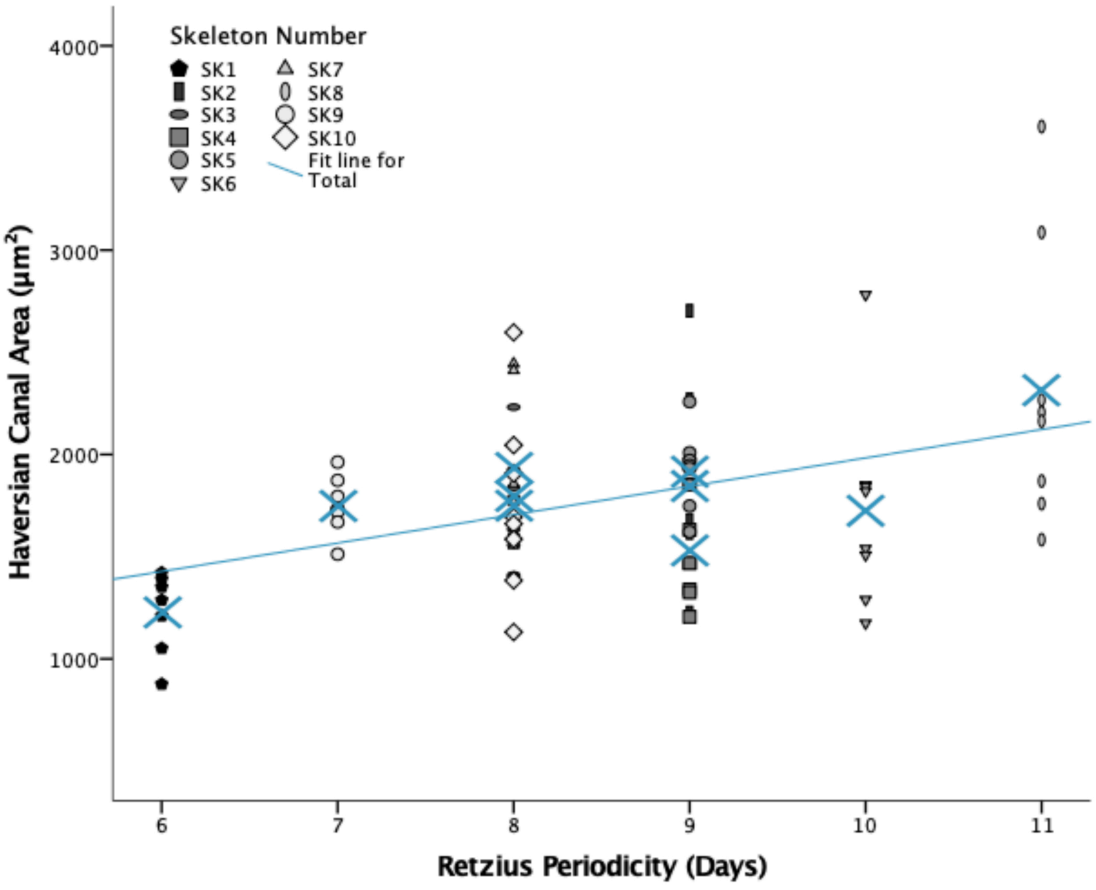

Figure 4.3 *Plot of Retzius periodicity (days) against Haversian canal area (µm²) for all bones combined (n = 80). Blue stars mark the mean Haversian canal area of each skeleton*

Table 4.4 *Spearman's correlations between Retzius periodicity (days) and bone histological variables from all bones combined and then from the tibia, femora, metacarpals, radii, humeri, ribs, clavicles, and occipitals*

Variable	N	*rs*	*p*	Variable	N	*rs*	*p*
All Bones				**All Bones**			
N.On	80	0.312	<0.01**	On.Ar (μm^2)	80	0.051	0.65
N.On.Fg	80	-0.184	0.10	Re.On.Ar (%)	80	-0.143	0.21
OPD	80	0.121	0.29	H.Ca.Ar (μm^2)	80	0.254	0.02*
				Ot.Dn	76	-0.066	0.57
Tibia				**Humerus**			
N.On	10	0.217	0.55	N.On	10	0.598	0.07
N.On.Fg	10	-0.491	0.15	N.On.Fg	10	-0.548	0.10
OPD	10	-0.342	0.33	OPD	10	0.636	<0.05*
On.Ar (μm^2)	10	0.466	0.18	On.Ar (μm^2)	10	-0.081	0.82
Re.On.Ar (%)	10	-0.416	0.23	Re.On.Ar (%)	10	-0.130	0.72
H.Ca.Ar (μm^2)	10	0.628	0.05*	H.Ca.Ar (μm^2)	10	0.267	0.46
Ot.Dn	10	-0.478	0.162	Ot.Dn	10	0.454	0.19
Femur				**Rib**			
N.On	10	0.503	0.14	N.On	10	0.553	0.10
N.On.Fg	10	-0.280	0.43	N.On.Fg	10	-0.491	0.15
OPD	10	0.043	0.91	OPD	10	0.068	0.85
On.Ar (μm^2)	10	-0.081	0.82	On.Ar (μm^2)	10	0.342	0.33
Re.On.Ar (%)	10	-0.217	0.55	Re.On.Ar (%)	10	-0.106	0.77
H.Ca.Ar (μm^2)	10	0.491	0.15	H.Ca.Ar (μm^2)	10	0.143	0.69
Ot.Dn	10	-0.404	0.25	Ot.Dn	9	-0.175	0.65
Metacarpal				**Clavicle**			
N.On	10	0.168	0.64	N.On	10	0.454	0.19
N.On.Fg	10	0.081	0.82	N.On.Fg	10	0.143	0.69
OPD	10	0.267	0.46	OPD	10	0.386	0.27
On.Ar (μm^2)	10	0.217	0.55	On.Ar (μm^2)	10	-0.590	0.07
Re.On.Ar (%)	10	0.143	0.69	Re.On.Ar (%)	10	-0.217	0.55
H.Ca.Ar (μm^2)	10	0.317	0.37	H.Ca.Ar (μm^2)	10	-0.130	0.72
Ot.Dn	10	0.247	0.52	Ot.Dn	10	-0.081	0.82
Radius				**Occipital**			
N.On	10	0.404	0.25	N.On	10	-0.466	0.18
N.On.Fg	10	-0.329	0.35	N.On.Fg	10	0.077	0.83
OPD	10	0.162	0.66	OPD	10	-0.168	0.64
On.Ar (μm^2)	10	0.081	0.82	On.Ar (μm^2)	10	-0.267	0.46
Re.On.Ar (%)	10	-0.516	0.13	Re.On.Ar (%)	10	0.317	0.37
H.Ca.Ar (μm^2)	10	0.603	0.07	H.Ca.Ar (μm^2)	10	-0.143	0.69
Ot.Dn	10	-0.329	0.35	Ot.Dn	8	-0.062	0.89

† Statistical significance value: *$p < 0.05$, **$p < 0.01$.

4.5 | DISCUSSION

The aims of this study were to describe intraskeletal cortical bone microstructural variation in a sample of adult human skeletons and to investigate a potential relationship between RP, as a marker of an infradian biorhythm, and cortical bone microstructure. The microstructure of eight bones from ten individual age matched skeletons was described and compared to RP.

4.5.1 | How Does Bone Microstructure, Specifically Osteon Density and Size, and Osteocyte Density Vary Across the Skeleton?

All of the bone microstructure variables in this study showed significant variation between skeletal elements. The high OPD in the humeri, rib, and metacarpals indicate that these bones have a fast rate of remodelling compared to other bones. The lower OPD of the radius, tibia, and clavicle indicate that these bones have a slower rate of remodelling compared to the humeri, ribs, and metacarpals. The femur showed intermediate values for OPD. The particularly low OPD of the occipital indicates that the skull has the slowest rate of remodelling of the bones that have been investigated. Osteocyte lacunae density displayed a similar intraskeletal pattern, with the osteocyte density of the occipital being significantly lower than in the tibia, metacarpal, humerus, and rib. The ribs are usually considered to have a fast bone turnover rate and the femur a slow turnover rate, especially in isotopic studies (Cox and Sealy, 1997; Lamb *et al.*, 2014). However, in this study neither the OPD or Ot.Dn of the femur were significantly lower than the OPD or Ot.Dn of the rib, which echoes the findings of Goliath, Stewart, and Stout (2016).

In addition to the variability of bone remodelling rate there was intra-skeletal variation in osteon size. Mean osteon area of the femur in this sample was similar to that found in previous studies (Pfeiffer, 1998; Pfeiffer *et al.*, 2006; Britz *et al.*, 2009;

Miszkiewicz and Mahoney, 2016). Here the mean osteon area in the rib was smaller than in all other bones. The osteon area of the rib has previously been found to be smaller than in the femur (Goliath, Stewart and Stout, 2016). However, when osteon area was standardised by the Haversian canal area and the proportion of lamellar bone in the osteon was considered, the relative osteon area in the rib was similar to the metacarpals. The value for the rib was between the smaller relative osteon areas in the femur and radius and larger relative osteon areas in the tibia and humerus. The osteons in the rib are smaller than those in other bones but so too are their canals. Within the skeleton the proportion of lamellar bone in an osteon to its canal size is quite consistent at between 95% and 96% of the total osteon area. Based on the osteon area the clavicles had smaller Haversian canals than expected and the occipitals had larger Haversian canals than expected.

Intra-skeletal variation in relative cortical area was not studied here, but has been described previously for the femur, tibia, fibula, humerus, radius, ulna, and rib (Stewart *et al.*, 2015). They reported that the rib had the lowest relative cortical area compared to the long bones, and the lower limb bones showed less variation than between the upper limb bones. This variation likely has biomechanical implications that affect the intraskeletal variation in remodelling in response to loading (Stewart *et al.*, 2015). The reportedly low relative cortical area of the ribs could indicate that the smaller osteons of the rib found here are linked to a scaling effect with cortical bone size. While this was not examined here, the finding that relative osteon area of the rib was not different to all other bones except the clavicle could support this.

Higher osteon population densities were associated with smaller osteons and higher osteocyte densities across the total sample. This pattern was also significant in the tibia. In the clavicle OPD only significantly related to the osteon area. This indicates that higher rates of remodelling are associated with smaller osteons. Both smaller osteons and

higher remodelling rates have been linked to higher strain and compressive loading. It has also been reported that osteons get smaller and more circular with age (Goliath, 2010; Goliath, Stewart and Stout, 2016). Since the sample in this study was age matched, it is more likely that the link between remodelling and osteon size is attributable to the habitual biomechanical loading environment of each bone than to age.

4.5.2 | How Does RP Relate to Bone Microstructure Variability Across the Skeleton?

None of the variables indicating bone remodelling (N.On, N.On.Fg, OPD, and Ot.Dn) were significantly correlated with RP, for all bones combined or when considered separately. Further, neither of the osteon size variables (On.Ar, Re.On.Ar) were significantly correlated with RP, for all bones combined and separately. It had been hypothesised that RP would negatively correlate with relative osteon area, but this was not supported. However, since this study did not directly test the formation time of lamellae, the results neither support nor refute the studies that have shown that one lamella forms in the same number of days as the RP (Bromage *et al.*, 2009).

Retzius periodicity was positively correlated with Haversian canal size. When all bones were combined, RP and Haversian canal area were significantly and positively related, which implies that a slower biorhythm predicts larger Haversian canals. Final Haversian canal size is dependent upon the amount of infilling by osteoblasts during secondary osteon formation and is related to the size of the blood vessels that they housed during life (Marotti and Zallone, 1980). It is therefore possible that the biorhythm relates to either the duration and/or rate of lamellar deposition during osteon infilling, or to blood vessel size. Unfortunately, assessing lamellar formation and blood vessel size was not possible in the archaeological samples used here.

4.6 | CONCLUSION

The relationship between RP, as an indication of a biorhythm, with intra-skeletal histomorphometric variation was investigated. It was found that RP was related to Haversian canal size most consistently throughout the body, which indicates that the biorhythm is related to osteon infilling and the resultant canal size. If RP is related to bone remodelling in adults via an infradian biorhythm, it appears that the biorhythm has more to do with the proportion of lamellar bone deposited by the BMU, rather than specific bone turnover rates. The results support the existence of a biorhythm that links aspects of secondary osteon geometry, but not bone turnover rate, to RP.

Chapter 5

Microscopic Markers of an Infradian Biorhythm in Human Juvenile Ribs

5.1 | ABSTRACT

Recent studies have indicated that there may be an infradian systemic biorhythm that coordinates aspects of human hard tissue growth and influences adult body size. Here it will be investigated whether evidence of this biorhythm retained in human teeth as the periodicity of Retzius lines (RP) corresponds with the microstructural growth of a non-weight bearing bone, the rib, in a sample of 50 human juvenile skeletons. Using static histomorphometric methods, the RP of one permanent tooth from each skeleton was calculated and combined with measures of bone remodelling in a rib from the same individual. Results provide the first evidence that the infradian biorhythm is linked to bone remodelling in children. Retzius periodicity was negatively related with relative osteon area ($r = -0.563$, $p < 0.01$) and positively related to Haversian canal area ($r = 0.635$, $p < 0.01$) and diameter ($r = 0.671$, $p < 0.01$) in children between the age of eight to 12 years. There was also a negative correlation between RP and the relative cortical area of ribs ($r = -0.500$, $p < 0.05$). Relationships between bone remodelling and the biorhythm were much more variable in younger children. Results imply that as the biorhythm speeds up there is increased bone deposition during remodelling of the rib, leading to the larger osteonal lamellar bone areas and smaller Haversian canals in children between eight and 12 years of age. The results support the idea that there is an infradian biorhythm that coordinates aspects of human hard tissue growth.

5.2 | INTRODUCTION

The primary goal of this thesis is to determine if a long period biorhythm is related to cortical bone microstructure and the aim of this chapter is to investigate how Retzius periodicity relates to microstructural bone growth in the juvenile rib, which will be answered with the following research questions:

1. **Is bone remodelling linked to Retzius periodicity?**
2. **Is osteon morphology linked to Retzius periodicity?**
3. **Is bone modelling linked to Retzius periodicity?**

The rib was selected because the results of Chapter 3 revealed that the cortical bone microstructure of the rib did not vary between high-status and low-status children from medieval Canterbury, or between children from medieval Canterbury, York, or Newcastle. Additionally, the rib is less affected by variations in mechanically induced bone remodelling compared to the limbs (Andriacchi *et al.*, 1974; Tommerup *et al.*, 1993). The results of Chapter 4 indicated that the secondary osteons and their Haversian canals were smaller in the ribs than in any other bone, but the proportion of Haversian canal area to overall osteon area was consistent with the other bones. The results of Chapter 4 also suggested that RP, as a marker of the biorhythm, was related to Haversian canal size and, further, that RP was not related to measures of bone turnover.

5.2.1 | Biorhythms

It is hypothesised that RP, as a measure of an underlying biorhythm, has its origin in the hypothalamus and influences pituitary secretions that act upon the endocrine glands and ultimately bone cell proliferation (Bromage *et al.*, 2012) (see section 1.4 for a more

detailed explanation of biorhythms). The proposed biorhythm has been linked to mammalian body size due to the hypothesised link between the biorhythm, RP, and hormone secretion (Bromage *et al.*, 2012). This hypothesis is consistent with analyses of RP from permanent teeth across mammalian species as smaller bodied mammals tend to have lower RPs than larger bodied mammals (Bromage *et al.*, 2009, 2012), though exceptions have been noted in some animals such as lemurs (Hogg *et al.*, 2015). The lower RP, and thus a biorhythm that occurs over a fewer number of days, suggests that smaller bodied species tend to have a faster developmental rate (Bromage *et al.*, 2009). Life history theory suggests that smaller animals tend to have shorter lifespans and reproduce more frequently and also achieve adult body size quicker when compared to slower maturing animals (Promislow and Harvey, 1990). It is therefore possible that RP, as a marker of a biorhythm, could provide a link between adult body size, developmental rate, and life history traits when compared between some mammalian species (Bromage *et al.*, 2009, 2012).

The role of the infradian biorhythm for human growth and development is poorly understood. Studies of small samples of adult humans indicate that RP is negatively correlated with final attained adult stature (Bromage *et al.*, 2016; Mahoney *et al.*, 2018). This makes sense as the biorhythm is accelerated to achieve greater height within a developmental period that is constrained for humans, relative to inter-specific comparisons of RP (Bromage *et al.*, 2009). Three previous studies have examined the relationship between RP and bone modelling and remodelling. In the femoral midshaft of one adult human female one bone lamella formed in the same number of days as the mean human RP, in both the interstitial lamellar bone and in the osteonal lamellar bone (Bromage *et al.*, 2009). Retzius periodicity was linked to the rate of primary bone deposition in the humeri of seven age-matched children (Mahoney, Miszkiewicz, *et al.*,

2016). Femoral osteocyte lacunae density was inconsistently related to RP in a sample of adult humans (Mahoney *et al.*, 2018). Thus, there is currently some evidence that suggests a relationship between RP and stature in adult humans, and between RP and primary bone growth in a small sample of infants. To date, no study has examined the potential relationships of RP and bone remodelling during ontogeny in humans.

5.2.2 | Human Skeletal Growth

A child's skeletal growth velocity declines from birth until about three years of age and then levels out, followed by a slight increase in velocity around the seventh year, for some but not all children (Tanner, 1951, 1981; Cameron and Bogin, 2012). Skeletal growth in height accelerates with the onset of puberty, that typically commences between eight to 11 years of age for girls, and between nine to 13 years of age for boys in modern populations (Tanner, Whitehouse and Takaishi, 1966; Tanner and Cameron, 1980; Bogin, 2006; Aksglaede *et al.*, 2008). Puberty is often complete between 13-17 years of age for girls, and between 15-18 years of age for boys in modern populations (Hägg and Taranger, 1982). The timing of puberty is affected by an array of variables including body mass, genetics, nutrition, social status (Louis *et al.*, 2008), and in particular, poor health which can delay the onset and completion of puberty (Lewis, Shapland and Watts, 2016). During the recent medieval period in England, which is the period from which the human remains in this study date, puberty commenced at around the same age as contemporary populations but tended to be an extended process that was usually complete between 16-19 years of age (Lewis, Shapland and Watts, 2016). The onset, progress, and completion of puberty is dictated by hormones secreted by the hypothalamus, pituitary glands, adrenal glands, and ovaries or testes. These hormones include leptin, gonadotropin-releasing, and growth hormone (Mantzoros, 1997; Plant and Shahab, 2002), and also the

sex steroids that drive sexual dimorphism (Mauras *et al.*, 1996).

5.2.3 | Bone Histomorphometry

Evidence of previously active bone remodelling is retained in human bones and can be accessed using static histomorphometric techniques (see section 1.2.5 for further details about bone remodelling). As secondary osteons replace primary osteons during skeletal growth secondary osteon density increases during childhood (Streeter, 2010; Cambra-Moo *et al.*, 2012, 2014; Pitfield, Miszkiewicz and Mahoney, 2017). Osteon accumulation continues into adulthood and is closely related with increasing age in younger adults (Stout and Paine, 1992). Secondary osteon population density (OPD) can be used as a proxy for regular bone turnover rates, or changes in bone density that are a result of mechanical, pathological, or dietary alterations (Martin and Armelagos, 1979; Richman, Ortner and Schulter-Ellis, 1979; Young *et al.*, 1986; Britz *et al.*, 2009).

Geometric properties of osteons can be quantified via variables that include osteon area (On.Ar) and osteon diameter (On.Dm). Previous studies have inferred behaviour from On.Ar and On.Dm (Burr, Ruff and Thompson, 1990; Mulhern and Van Gerven, 1997; Mulhern, 2000; Miszkiewicz and Mahoney, 2016) because they can provide an indication of the type of loading on a bone (Skedros, Mason and Bloebaum, 1994; Smit, Burger and Huyghe, 2002; van Oers, Ruimerman, van Rietbergen, *et al.*, 2008). Experimental studies have revealed that osteon size, on average, is inversely related to biomechanical strain (Skedros, Mason and Bloebaum, 2001; Skedros, Sybrowsky, *et al.*, 2003; Skedros, Hunt and Bloebaum, 2004). Osteon diameter is also generally smaller in regions of the cortex that are exposed to larger loads and resulting strains (van Oers, Ruimerman, van Rietbergen, *et al.*, 2008). Other studies have reported that secondary osteons can become smaller and more circular with advancing age in adults (Currey,

1964; Britz *et al.*, 2009; Goliath, Stewart and Stout, 2016). However, secondary osteons have been reported to become larger and less circular during adolescence although the cause remains unknown (Pitfield, Miszkiewicz and Mahoney, 2017). With age, sex, and stature controlled for, human femoral osteon size (area and diameter) has also been reported to be inversely related to body mass, a link that may be mechanical or endocrine in nature (Britz *et al.*, 2009).

The size of the Haversian canal can be quantified as Haversian canal area and diameter (H.Ca.Ar and H.Ca.Dm respectively). Haversian canal size is ultimately related to the infilling of an osteon during BMU activity and can be a reflection of the size of blood vessels residing within bone matrix during life (Marotti and Zallone, 1980). Consequently, it serves as an insight into bone remodelling activity undertaken during the bone resorption and deposition phases (van Oers, Ruimerman, van Rietbergen, *et al.*, 2008). The proportion of lamellar bone area to Haversian canal area in an osteon can be calculated as a percentage of the total On.Ar, as relative osteon area (Re.On.Ar). This measurement shows the proportion of an osteon that is lamellar bone regardless of its overall size and is based on a previously described ratio of H.Ca.Ar: On.Ar (Miszkiewicz and Mahoney, 2018).

5.2.4 | Research Questions and Predictions

The aim in this study is to investigate the relationship between RP in human permanent first molars and past evidence of bone remodelling in ribs from a sample of human juvenile skeletons. The rib was selected because it is less affected by variations in mechanically induced bone remodelling compared to the limbs (Andriacchi *et al.*, 1974; Tommerup *et al.*, 1993). Standard static histomorphometric techniques are applied.

1. **Is bone remodelling linked to RP?** – Taller adults may attain greater height through an increased developmental rate during ontogeny (Bromage *et al.*, 2009, 2012; Mahoney *et al.*, 2018). When this hypothesis is applied to juveniles it suggests that those individuals with a lower RP (and thus fewer number of days of enamel growth between each oscillation of the underlying biorhythm) will be on a faster growth trajectory that would lead to greater adult stature (Mahoney *et al.*, 2018). If this is correct, then a faster growth trajectory, indicated by a lower RP, will be related to higher rates of bone remodelling**.** To account for age-related variation in juvenile bone microstructure (Streeter, 2010; Pitfield, Miszkiewicz and Mahoney, 2017), this hypothesis is tested in younger children who died before the onset of puberty and older children who likely would have commenced puberty.

2. **Is osteon size linked to RP?** – In one adult human female one bone lamellae formed in the same number of days as the mean human RP (Bromage *et al.*, 2009). This finding suggests that larger osteons, with more lamellae, should relate to RP. This idea is tested using relative osteon area as a signifier of the amount of osteonal lamellar bone.

3. **Is bone modelling linked to RP?** – One aspect of bone modelling has previously been linked to RP in children (Mahoney, Miszkiewicz, *et al.*, 2016). Since periosteal bone apposition during childhood contributes to cortical thickness this sign of bone modelling may also be linked to RP. Given the hypothetical premise that juveniles with lower RPs will be on a faster growth trajectory towards a greater stature, it is predicted that RP will be inversely related to bone size in age-

matched children. Cortical area, total area, and relative rib cortical area are used as measures of cross-sectional bone size as proxies for bone modelling.

5.3 | MATERIALS AND METHODS

5.3.1 | Sample

Fifty juvenile skeletons, dating to the recent medieval period in England, and without skeletal lesions indicative of pathology, were selected for the present study (see section 2.3 for further detail on the sampling criteria). One permanent tooth was removed from each skeleton. Permanent first molars were preferentially selected (*n*=47). This molar was unavailable in three skeletons so a central incisor (*n*=2) and second molar (*n*=1) were selected. A 5mm ± 2mm rib thick-section was removed from the middle third of an un-sided 3rd to 8th rib from each skeleton (*n*=50). Given that functional adaption is reflected in bone microstructure, the rib was selected for the analyses as it is a non-weight bearing bone and does not vary greatly inter-skeletally when considering respiration induced loading (Andriacchi *et al.*, 1974; Tommerup *et al.*, 1993). Accordingly, the rib can be considered a skeletal site that reveals systemic bone physiology and remodelling (Agnew and Stout, 2012).

5.3.2 | Age Estimation

The age estimation methods are explained in further detail in section 2.4. The juvenile skeletons were from individuals aged between three and 12 years of age. The age estimations followed standard methods for reconstructing age in juvenile skeletal remains, since the actual chronological age of each skeleton was not known. The sample was split into two age groups as follows; younger child (3–7 years, *n* = 29), and older child (8–12 years, *n* = 21). The younger group includes children who had likely died

before puberty commenced. The older child group includes children who died at an age when puberty can commence. All of the children died prior to the mean age that the adult compacta forms in the rib (Frost and Wu, 1967; Wu *et al.*, 1970).

5.3.3 | Sample Preparation

The histological methods are explained in further detail in section 2.5. Histological thin-sections of teeth were produced using standard methods (Mahoney, 2008). The teeth were embedded in resin (Buehler EpoxiCure®) and sectioned through the tip of the cusp and the dentine horn using a Buehler Isomet 1000 precision saw. The sections were fixed to glass microscope slides (Evo Stick® resin), ground to a final thickness of 50-100 μm with a series of grinding pads (P400, P600, P1200) (Buehler® EcoMet 300), and polished with a 0.3 μm aluminium oxide powder (Buehler® Micro-Polish II). Each section was cleaned in an ultrasonic bath, dehydrated in 95-100% ethanol, cleared (Histoclear®), and mounted with a coverslip using a xylene-based mounting medium (DPX®).

Standard histological methods were used to produce bone thin-sections (Miszkiewicz, 2015a, 2016; Pitfield, Miszkiewicz and Mahoney, 2017). Transverse 5 mm ± 2 mm thick-sections were removed from the middle third of the 3rd-8th ribs using an electronic drill (Dremel Rotary Tool®) (Crowder and Rosella, 2007). The bone was embedded in resin (Buehler EpoxiCure®), further reduced to 0.3 ±0.1 cm using a Buehler Isomet 1000 precision saw and fixed to glass microscope slides (Evo Stick® resin). Each bone thin-section was ground to a final thickness of 50-100 μm, polished, and covered following the same methodology as the tooth thin-sections, above.

5.3.4 | Enamel Histology

The histomorphometric methods for enamel are explained in further detail in section 2.6.2. The teeth were examined using a high-powered microscope (Olympus® BX53) with a mounted camera (Olympus® DP25). Images of the teeth were obtained and examined in CELL® Live Biology imaging software (**Figure 5.1a**). Retzius periodicity (RP) was directly calculated by counting the number of cross striations along an enamel prism between two Retzius lines (**Figure 5.1b,c**) in the lateral enamel at 20x magnification with a 10x oculus. Diagenetic changes, micro-scratches, or blurred lines prevented a direct count being taken for 52% of cases, so RP was calculated from local daily secretion rates (DSR) of enamel (Mahoney, 2012). The DSRs were calculated by measuring between six cross striations, which corresponds to five days of enamel formation, and dividing the measurement by five to get a daily mean enamel secretion rate in microns. This was repeated six times within the local enamel so that a grand mean DSR could be calculated (Mahoney, 2012). Following this, the distance between four Retzius lines was measured, corresponding to three repeat intervals, divided by three and then divided by the grand mean DSR to yield an RP value.

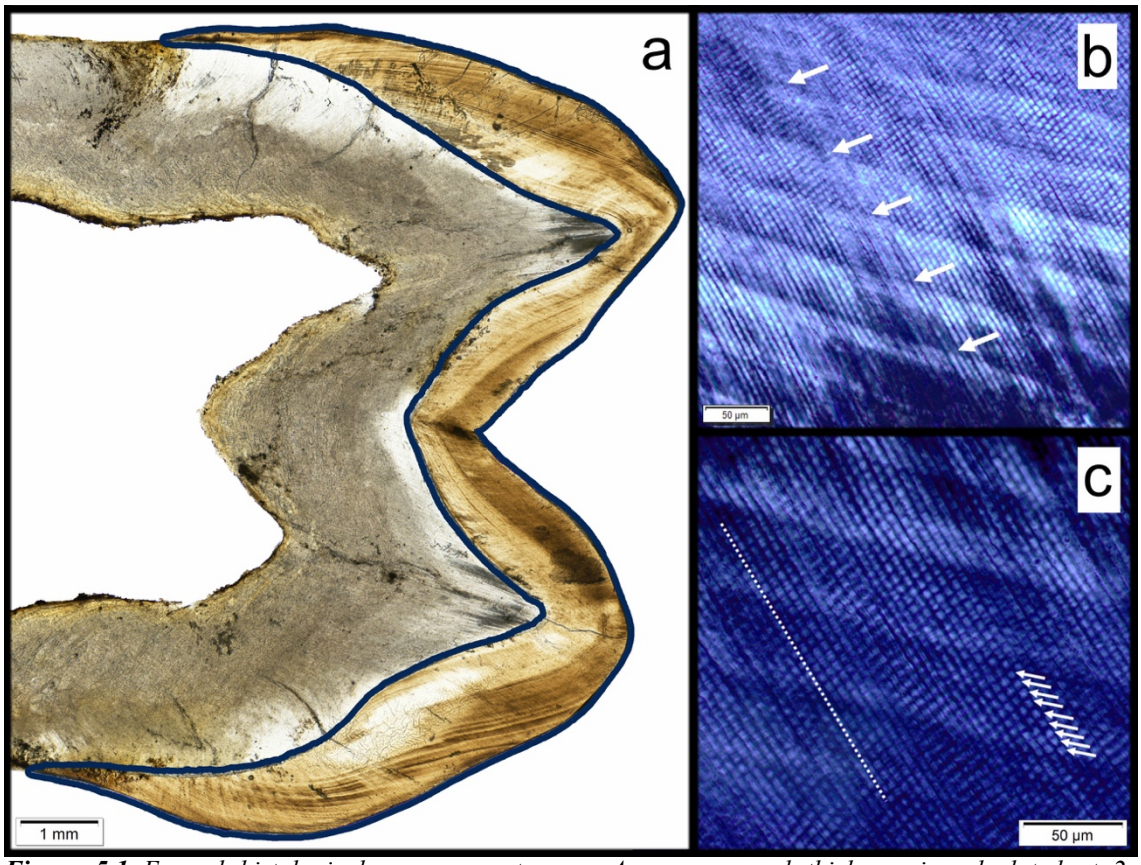

Figure 5.1 *Enamel histological measurements. a – Average enamel thickness is calculated at 2x magnification. Blue line encompasses the enamel area. AET = total enamel area (mm2) / total enamel-dentine junction length (mm). b – Retzius periodicity is measured at 20x-40x (polarised). Large white arrows show Retzius lines. c – Small white arrows show the daily cross striations between two Retzius lines. RP is the number of days between Retzius lines. White dotted line shows the direction of the prism path*

5.3.5 | Bone Histology

The histomorphometric methods for cortical bone are explained in further detail in section 2.6.1. Standard methods were used for imaging undertaken using an Olympus BX51 compound microscope with an Olympus DP25 microscope camera (Villa and Lynnerup, 2010; Miszkiewicz and Mahoney, 2016). For each rib thin-section the entire cortex was imaged at 20x magnification with a 10x oculus and stitched together into a montage using CELL® Live Biology Imaging software (**Figure 5.2a**). The total subperiosteal area (Tt.Ar, mm^2) and medullary cavity area (Es.Ar, mm^2) were measured and cortical area was calculated (Ct.Ar, mm^2 = Tt.Ar – Es.Ar). Relative cortical area was calculated as a

percentage (Re.Ct.Ar, % = (Ct.Ar / Tt.Ar) * 100) to control for allometry (Dominguez and Agnew, 2016). Higher percentages relate to higher proportions of cortical bone in the rib cross-sectional area. The number of secondary osteons and secondary osteon fragments were counted across the entire cross-section. Secondary osteons were identified by the presence of a complete cement line and intact Haversian canals, and secondary osteon fragments were identified as partial secondary osteons (Parfitt, 1983; Stout and Crowder, 2012) (**Figure 5.2b**). These osteon counts formed the osteon population density (OPD), which was calculated by dividing the number of osteons and fragments by the area of the rib cortex. Histomorphometric studies quantify bone turnover as osteon population density by adding the number of intact and fragmentary osteons and dividing the result by the area of the ROI to produce a density score (Stout and Crowder, 2012). The intact osteons are the most recently formed and they intercut the preceding generations of osteons, leaving fragments of the older osteons visible.

Secondary osteon structure was quantified by measuring the osteon area (On.Ar, μm^2) and diameter (On.Dm, μm), and the Haversian canal area (H.Ca.Ar, μm^2), and diameter (H.Ca.Dm, μm) (**Figure 5.2c**). Incomplete Haversian systems, identified by scalloped Haversian canal margins, and drifting osteons were excluded. Drifting osteons have been reported to account for 70% of cortical porosity in children (Schnitzler and Mesquita, 2013). Osteon lamellar area (On.Lm.Ar, μm^2) was determined (On.Lm.Ar = On.Ar – H.Ca.Ar) to calculate relative osteon area as a percentage (Re.On.Ar, % = (On.Lm.Ar / On.Ar) * 100) to provide a measure of the proportion of lamellar bone in an osteon within the cement line irrespective of overall secondary osteon size. Higher percentages relate to higher proportions of lamellar bone area to total osteon area.

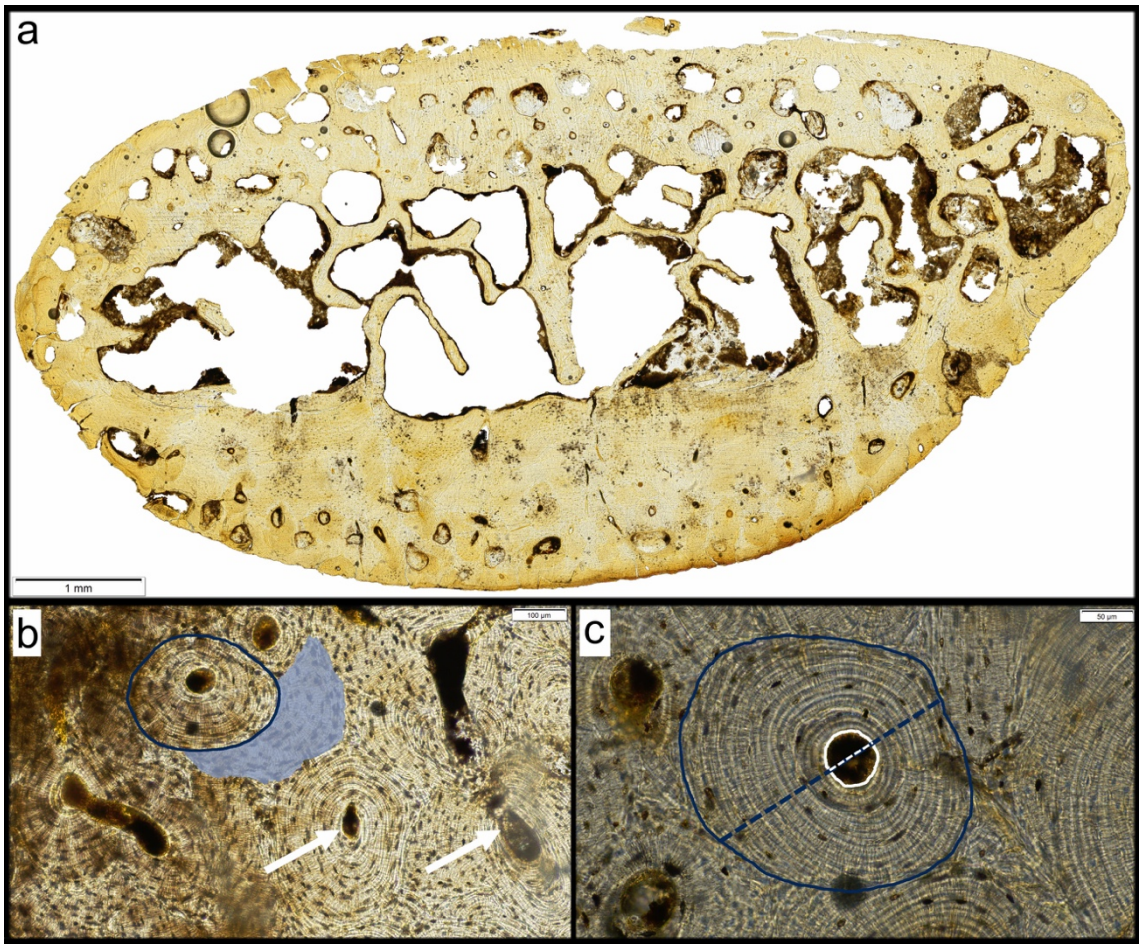

Figure 5.2 *Bone histological measurements. a – Rib cross-section. b – Counting secondary osteons and fragments (10×). White arrows point to Haversian canals. Area bounded in blue indicates an intact osteon and area highlighted in blue indicates a fragmentary secondary osteon (N.On, N.On.Fg, and OPD). c – Measurements of osteon structure (20×). Circles indicate the secondary osteons (blue) and Haversian canals (white) measured (On.Ar, H.Ca.Ar, and H.Ca.Dm). Dashed lines indicate the diameters of secondary osteons (blue) and Haversian canals (white) (On.Dm, H.Ca.Dm)*

5.3.6 | Statistical Analyses

All statistical analyses were performed in IBM SPSS® 24 with the significance level set at $p < 0.05$ for all tests. The normality of each variable was assessed with Kolmogorov-Smirnov tests (**Appendix F, Table A.F.1**). Subsequently, count variables (OPD) were square root transformed and measurement variables (On.Ar, Re.On.Ar, On.Dm, H.Ca.Ar, H.Ca.Dm) were log transformed (Kolmogorov-Smirnov tests of normality on the

transformed data are in **Appendix F, Table A.F.2)**. Independent samples *t*-tests were used to check for differences in microstructure between younger and older children. Linear regression was used to seek relationships between the variables.

5.4 | RESULTS

5.4.1 | Is Bone Remodelling Linked to Retzius Periodicity?

Descriptive statistics and comparisons of the rib microstructure between older and younger children are in **Table 5.1**, whereas descriptive statistics of the transformed data appear in **Appendix F, Table A.F.3**. Osteon density was higher in the older children ($p < 0.01$) and the osteon area and relative osteon area were also larger in the older children (both $p < 0.05$). However, the dimensional measurements just met the threshold of significance. Haversian canal dimensions remained consistent between the two age groups.

Regression statistics for RP and rib microstructure amongst the older children, and younger children, are in **Table 5.2**. Amongst the older children, RP was significantly and negatively related to relative osteon area, ($r = -0.563$, $p < 0.01$), but positively related to Haversian canal area ($r = 0.635$, $p < 0.01$), and Haversian canal diameter ($r = 0.671$, $p < 0.01$) (**Figure 5.3a,b,c**).

Table 5.1 *Descriptive (non-transformed) statistics for the rib microstructure for the younger children (3–7 yrs) and the older children (8–12 yrs), and the results (p value) of a comparison between these groups using an independent samples t-test*

Age group	Variable	N	Min.	Max.	Mean	SD	*p*
3-7 yrs	Tt.Ar (mm^2)	29	15.61	38.14	26.84	7.05	<0.01**
	Ct.Ar (mm^2)	29	8.23	23.42	14.81	3.92	<0.01**
	Re.Ct.Ar (%)	29	37.00	80.00	53.00	9.62	0.61
	OPD	29	0.00	9.33	3.38	2.58	<0.01**
	On.Ar (μm^2)	26	22401.10	53443.69	35073.37	7736.00	<0.05*
	Re.On.Ar (%)	26	92.54	97.07	95.31	1.39	<0.05*
	On.Dm (μm)	26	140.13	257.45	178.54	24.10	0.12
	H.Ca.Ar (μm^2)	26	709.47	2872.17	1616.90	487.13	0.80
	H.Ca.Dm (μm)	26	24.62	48.23	36.09	5.67	0.84
8-12 yrs	Tt.Ar (mm^2)	21	26.37	48.71	37.53	6.31	
	Ct.Ar (mm^2)	21	11.51	25.10	18.87	3.51	
	Re.Ct.Ar (%)	21	39.00	66.00	51.44	8.66	
	OPD	21	1.55	8.79	6.08	1.82	
	On.Ar (μm^2)	21	23383.73	67798.76	40774.59	10638.78	
	Re.On.Ar (%)	21	93.68	97.61	96.06	1.08	
	On.Dm (μm)	21	131.49	265.84	190.58	27.63	
	H.Ca.Ar (μm^2)	21	710.38	4078.07	1606.94	677.73	
	H.Ca.Dm (μm)	21	25.04	52.41	35.77	6.03	

† Statistical significance value: *$p < 0.05$, **$p < 0.01$.

5.4.2 | Is Bone Modelling Linked to Retzius Periodicity?

Descriptive statistics and comparisons of the rib cortical area, and relative cortical area are in **Table 5.1**, whereas descriptive statistics of the transformed data appear in **Appendix F, Table A.F.3**. Total rib cross-sectional area and rib cortical area were significantly larger in the older children than in the younger children (both $p < 0.01$), although relative rib cortical area remained consistent between the age groups.

The regression statistics for RP and rib cortical area and relative rib cortical area are in **Table 5.2**. Within the older child group there was a statistically significant negative correlation between RP and rib relative cortical area ($r = -0.500$, $p < 0.05$) (**Figure 5.3d**).

Table 5.2 *Linear regression analyses of log-RP against log-rib microstructure*

	N	Intercept	Slope	*r*	R^2	*p*	Residual
RP vs Ct.Ar							
3-7 yrs	24	0.788	0.090	0.145	0.021	0.50	98%
8-12 yrs	16	1.112	-0.154	-0.166	0.028	0.51	97%
RP vs Re.Ct.Ar							
3-7 yrs	24	-0.136	-0.164	0.160	0.026	0.46	98%
8-12 yrs	16	0.205	-0.544	0.500	0.250	<0.05*	75%
RP vs OPD							
3-7 yrs	29	1.054	0.280	0.174	0.030	0.37	97%
8-12 yrs	21	7.152	-0.131	0.108	0.012	0.64	99%
RP vs On.Ar							
3-7 yrs	26	4.354	0.196	0.161	0.026	0.43	97%
8-12 yrs	21	4.189	0.449	0.322	0.104	0.15	90%
RP vs Re.On.Ar							
3-7 yrs	26	-0.045	0.026	0.323	0.104	0.11	97%
8-12 yrs	21	0.014	-0.034	0.563	0.317	<0.01**	68%
RP vs On.Dm							
3-7 yrs	26	2.135	0.122	0.171	0.029	0.40	96%
8-12 yrs	21	1.980	0.327	0.413	0.171	0.06	83%
RP vs H.Ca.Ar							
3-7 yrs	26	3.486	-0.322	0.183	0.033	0.37	97%
8-12 yrs	21	2.067	1.226	0.635	0.403	<0.01**	60%
RP vs H.Ca.Dm							
3-7 yrs	26	1.724	-0.187	0.210	0.044	0.30	96%
8-12 yrs	21	0.994	0.611	0.671	0.450	<0.01**	55%

† Statistical significance value: *$p < 0.05$, **$p < 0.01$.

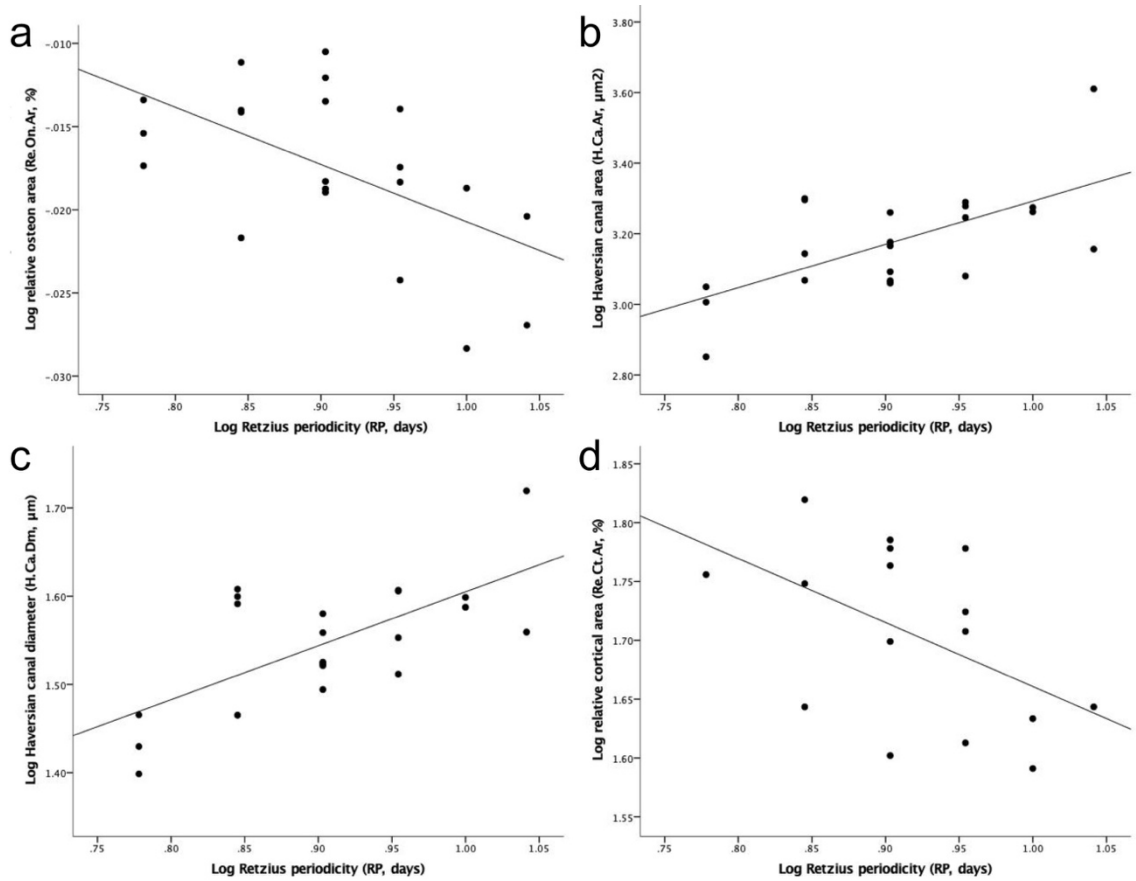

Figure 5.3 *Plots of log-RP against a) log-relative osteon area, b) log-osteon canal area, c) log-osteon canal diameter, and d) log-relative rib cortical area for the older child group*

5.5 | DISCUSSION

This chapter investigated the relationship between RP in human permanent first molars – as a measure of an underlying biorhythm – and past evidence of bone remodelling in ribs from human juvenile skeletons from a single population. There was evidence that the biorhythm was linked to the relative area of osteons, the size of Haversian canals within osteons, and relative cortical area in the ribs of children aged eight to 12 years. There was no evidence that the biorhythm was linked to the frequency of osteons in this sample of children, or to any histomorphometric variable amongst younger children aged three to seven years of age.

5.5.1 | Is Bone Remodelling Linked to Retzius Periodicity?

The results show that osteons with proportionally larger lamellar areas and smaller Haversian canal areas relate negatively to RP amongst the older children. There was no observed relationship between osteon area and RP in either age group. This implies that a faster biorhythm predicts increased bone deposition during remodelling in the rib, leading to larger osteonal lamellar areas relative to their Haversian canal size. However, it does not predict overall osteon size. Prior research in one adult human observed that one lamellae, from both interstitial and osteonal bone, formed in the same number of days as the species specific mean RP in one adult human female (Bromage *et al.*, 2009). Data presented here could be consistent with that observation if the difference in lamellar bone quantity was attributable to a greater number of lamellae. The finding that relative osteon area is related to RP, but not osteon area, could indicate that the biorhythm is related to the number of lamellae in each osteon rather than to the overall osteon size. A faster biorhythm indicated by a lower RP could form more lamellae in the same time period as an individual with a slower biorhythm, indicated by a higher RP. Alternatively, the number of lamellae may not have changed but they may have become thicker, which would also account for the link to RP.

Retzius periodicity and Haversian canal size were positively correlated in the ribs of the older children. This implies that a slower biorhythm predicts larger Haversian canals in the rib. Haversian canal size is related to the size of the blood vessels that were contained within the canal during life (Marotti and Zallone, 1980) suggesting that children with higher RPs could have had larger capillaries within their Haversian canals. Alternatively, the observed link between RP and Haversian canal size could simply be a consequence of the observed relationship between RP and relative osteon area. Since the overall osteon area is consistent between different RPs, the overall amount of bone

removed by the BMU during remodelling will also be constant. But given that the proportion of lamellar bone in the osteon varies according to RP, the amount of bone deposited by the BMU during remodelling will also vary with RP and the resultant Haversian canal area may be a by-product of the increased bone deposition. Thus, the relationship between RP and Haversian canal size observed here may be an incidental relationship to the relationship between RP and osteon infilling by BMUs. A previous study examined Haversian canal to osteon area scaling in multiple mammal species and suggested that the proportion of lamellar bone area to Haversian canal area in osteons may scale with either body size or longevity, but this was not a focus of the study.

Another consideration is the rapid remodelling rate of cortical bone in children that causes increased cortical porosity when compared to adults (Frost, 1969). The link between RP and Haversian canal size could potentially be explained by more rapid bone turnover and increased cortical porosity in children with higher RPs, and *vice versa*, rather than by the amount of osteonal bone deposition. Despite attempting to only include completed Haversian canal in the study, it is possible that some active osteons could have been included. Although, mean Haversian canal area in both the younger children and the older children of this study (1616.90 μm^2 and 1606.94 μm^2 respectively) are similar to the mean Haversian canal area reported for inactive concentric Haversian canals (1544 μm^2) and inactive eccentric Haversian canals (1984 μm) from external iliac cortices of 0-25 year olds (Schnitzler and Mesquita, 2013). This suggests that the canals measured in this study were fully formed.

Retzius periodicity was only related to bone microstructure in the older children. The microstructural data are consistent with expectations for this age group. Both mean OPD and mean On.Ar are greater in the older children compared to the younger children (**Table 5.1**). This is similar to previous findings from the juvenile humerus where OPD

was significantly higher in older children (eight to 12 year olds) than in younger children and infants (Pitfield, Miszkiewicz and Mahoney, 2017). Hence, the bone microstructural data are not unusual or indicative of pathological change, but it does follow the anticipated age-related pattern. The increased osteon density in the older children is also consistent with the increased growth rates that might be expected as puberty commences.

It is hypothesised that a centrally coordinated infradian biorhythm will be accelerated in children that are on a faster growth trajectory (Bromage *et al.*, 2009, 2012; Mahoney *et al.*, 2018). It is thought that this biorhythm stems from the hypothalamus that stimulates pituitary secretions that are linked to puberty, metabolism and body mass (Bromage *et al.*, 2012). The findings show that RP is related to the proportion of lamellar area to overall osteon size in juveniles who were at an age consistent with the onset of puberty, when compared to younger children. If the hypothesised biorhythm is applied to this finding it suggests that amongst the older children, those with a faster biorhythm have more rib osteons with more lamellar bone and smaller Haversian canals, even though overall osteon size remains constant. Thus, RP appears to relate to the infilling of osteons rather than the amount of bone removed by osteoclast during remodelling and the overall osteon size. Since the loading environment of the rib is relatively consistent between individuals (Andriacchi *et al.*, 1974; Tommerup *et al.*, 1993) the rib is considered to reveal systemic influences on bone microstructure and a centrally coordinated biorhythm could be one such systemic influence.

5.5.2 | Is Bone Modelling Linked to Retzius Periodicity?

The results support the hypothesis that RP will be inversely related to bone size in children. Retzius periodicity was inversely related to relative cortical area in the older but not the younger children, although the residual was high, and the relationship was just *p*

= 0.05. There was no relationship between RP and rib cortical area. Relative cortical area was used to standardise the bone area relative to the medullary area and account for variation in overall bone size to assess whether RP could relate to cortical bone area independently of total bone size. A larger relative cortical area means that, as a proportion of overall size, more interstitial lamellar bone was deposited during the process of bone modelling. The findings indicate that an older child with a lower RP, and faster biorhythm, will have a larger cortical bone area proportionally to the total cross-sectional area and vice versa. This relationship between RP and relative cortical area indicates that RP is related to bone modelling.

Potentially, this finding that RP relates to Re.Ct.Ar may support the prediction that individuals possessing a faster biorhythm will attain a greater stature or larger body size. However, the relationships between Re.Ct.Ar and stature and body size was not tested directly. Relative cortical area may not relate to body size, since relative cortical area varies across the skeleton in response to biomechanical demands (Stewart *et al.*, 2015). The data do not address whether these children were on a trajectory towards a large body size, but it does provide a new foundation for future studies to investigate this potential link.

5.5.3 | Limitations

Since the samples in this study were archaeological, formation periods could not be evaluated directly with vital labelling and it was not possible to count lamellae directly, nor measure lamellar thickness due to taphonomy. These measures would help to explain how RP relates to osteonal lamellar area proportion by showing if there was a change in lamellar number or lamellar thickness. Another consideration when using archaeological samples is that fewer factors can be controlled. It was not possible to account for variation

in dietary, sex-specific, or genetic factors potentially contributing to the expression of rib microstructure that did not manifest macroscopically. A sample of fully documented skeletal samples would allow for a more controlled investigation of the research questions. Nevertheless, the clear links between dental and bone microstructure here certainly invite further research into biorhythms of the juvenile skeleton.

5.6 | CONCLUSION

The relationship between RP, as a sign of an underlying infradian biorhythm, and bone microstructure was explored in a sample of 50 human juvenile skeletons from a single population. There was evidence that a fewer number of days between adjacent Retzius lines – indicating a faster biorhythm – was positively related to Haversian canal size, but negatively related to relative osteon area and relative cortical area in the ribs of children aged eight to 12 years old. The results support the idea that an infradian biorhythm coordinates aspects of human hard tissue growth. This biorhythm may be one of the many factors that affect bone growth and remodelling.

Chapter 6

Discussion, Limitations, and Future Directions

6.1 | DISCUSSION OF THE MAIN FINDINGS

6.1.1 | Thesis Summary

The aim of this thesis has been to use histomorphometry to improve the understanding of the link between cortical bone microstructure and Retzius periodicity as evidence of an underlying biorhythm. This discussion will summarise the findings of the preceding data chapters and bring together the strands of information to address the overarching question; **how does a biorhythm influence human hard tissue growth during ontogeny?**

It was important to clarify whether the formation of LEH during enamel secretion could be related to a change in the appearance or timing of incremental markings within the enamel (Mahoney *et al.*, 2017). **Appendix C** is a preliminary study of three teeth that had evidence of linear enamel hypoplasia and the results showed that the presence of LEH can be associated with a change in the the daily rate at which enamel is secreted and the periodicity of Retzius lines. The length of cross striations can be altered in the enamel surrounding the LEH because of a reduction in DSR during the defect and a subsequent increase in DSR after the defect. Additionally, the periodicity of Retzius lines can increase immediately after a LEH when compared to the periodicity of the lines before the defect. These results indicate that RP does not always remain constant within an individual tooth. Consequently, skeletons with evidence of linear enamel hypoplasia on their teeth were excluded from the data chapters.

Many factors can affect cortical bone microstructure and some of these factors can vary between populations, such as physical activity, heath, and nutrition (Keough, L'Abbé and Steyn, 2009). It was important to gain an understanding of some of these factors in the medieval children from Canterbury, York, and Newcastle, before an assessment of Retzius periodicity was undertaken. To achieve this, the microstructure of the humerus and rib was compared between two social status groups from the same population and then between three different populations in Chapter 3. The rib microstructure showed no significant variation, either between social status groups, or between populations. The only significant differences were observed in the humerus microstructure. High-status children tended to have more circular secondary osteons with larger diameters than low-status children. This histomorphometric pattern was seen in the different status groups from eight years of age, which is approximately the age at which children took on more adult-like occupations (Hanawalt, 1977; Fleming, 2001). The high-status children in Canterbury would have undertaken less strenuous occupations than the low-status children in Canterbury (Lyle, 2002). When these findings were compared to contemporary textual evidence it implied that the microstructure of the low-status children undertook more strenuous activity with their upper arms, compared to high-status children.

The comparison of the humeri of children from different geographic regions revealed that children from medieval Canterbury had significantly lower OPDs and significantly smaller secondary osteon and Haversian canal diameters than children from medieval York and Newcastle. The lack of significant differences in the histomorphometry of the rib, compared to the humeri, indicates that there was no significant variation in the factors that affect systemic remodelling within medieval children. But there were differences in the factors that affect localised remodelling in the

humeri. This is most likely attributable to differences in physical activity levels and manual labour practices that had different loading on the arms during life. The textual evidence supports the histological findings, since children from Canterbury could have undertaken less strenuous forms of manual labour than the children from York or Newcastle (Lomas, 1996; Lyle, 2002; Nicholas, 2014; Palliser, 2014). Taken together, the findings imply that social status and habitual physical activity from manual labour influenced the bone microstructure of children who lived and worked in medieval England.

Bone microstructure varies within the skeleton and within individual bones and Chapter 3 has highlighted the variation between the humerus and the ribs that could be attributed to the different loading environments of each bone. To explore the intraskeletal microstructural variation further, the microstructure of eight bones from ten age-matched skeletons was compared to the Retzius periodicity of each skeleton, and the results were reported in Chapter 4. The findings showed that Retzius periodicity was positively related to Haversian canal size most consistently throughout the skeleton, though these links were much weaker when just the individual bones were considered. It is therefore possible that the biorhythm relates to either the duration and/or rate of lamellar deposition during osteon infilling, or to blood vessel size. If RP does relate to skeletal growth, it is likely that the biorhythm has more to do with an overall growth trajectory than specific bone turnover rates. These results support the existence of a biorhythm that links aspects of microstructural bone growth in children, but not bone turnover, to RP and the previously reported final adult body size attainment.

Retzius periodicity has been linked to lamellar formation time and stature in humans (Bromage *et al.*, 2009, 2016) but this has yet to be explored in children. Based on the findings of Chapter 3 that there was no significant inter-population variation in the

rib microstructure of medieval children, Chapter 5 examined how rib microstructural changes through ontogeny related to RP as a marker of a biorhythm. There was evidence that RP was inversely related to relative osteon area and relative cortical area, but positively related to Haversian canal size, in the ribs of children aged eight to 12 years old. This indicates that the biorhythm is related to the proportion of interstitial lamellar bone in a cross-section and to the proportion of osteonal lamellar bone in an osteon. These results also support the idea that an infradian biorhythm exists and coordinates aspects of human hard tissue growth.

This thesis demonstrates the complexity of human juvenile skeletal growth by using a 'combined bone' approach to untangle some of the known factors from the potential influence of a variable infradian biorhythm. Collectively, the studies in this thesis describe a consistent link between an infradian biorhythm, signified by RP, and bone growth. The biorhythm relates to the dimensions of Haversian canals, the proportion of osteonal lamellar bone in each secondary osteon, the amount of interstitial lamellar bone within a cross-section relative to the total bone size, and to overall body size.

Retzius periodicity negatively relates to relative osteon lamellar area and positively relates to Haversian canal area. This means that a child with a low RP is expected to have a high proportion of lamellar bone within their osteons and small Haversian canals. Hence, a faster biorhythm means that more bone is deposited within an osteon in a constrained time. Equally, a child with a high RP is expected to have a low proportion of lamellar bone within their osteons and large Haversian canals. Hence, a slower biorhythm means that less bone is deposited within an osteon in a constrained time.

Retzius periodicity negatively relates to relative cortical area. This means that a person with a low RP is expected to have a high proportion of cortical bone within their

rib cross-section and a small medullary cavity. Hence, a faster biorhythm means that more bone is deposited during cortical bone modelling in a constrained time. Equally, a person with a high RP is expected to have a low proportion of cortical bone within their rib cross-section and a large medullary cavity. Hence, a slower biorhythm means that less bone is deposited during cortical bone modelling in a constrained time.

Retzius periodicity negatively relates to stature. This means that a person with a low RP is expected to be of larger stature and mass. Hence, a faster biorhythm means that a greater body size is attained in a constrained time. Equally, a person with a high RP (slow biorhythm) is expected to be of smaller stature and mass. Hence, a slower biorhythm means that a smaller body size is attained in a constrained time.

6.1.2 | Bone Remodelling

The results of Chapters 4 and 5 show that RP inversely relates to secondary osteon infilling and positively with the resulting Haversian canal size. Individuals with higher RPs have less bone in their osteons and larger Haversian canals regardless of the overall osteon size than people with a lower RP. Since the overall osteon area is consistent between different RPs, the overall amount of bone removed by the BMU during remodelling will also be constant. But given that the proportion of lamellar bone in the osteon varies according to RP, the amount of bone deposited by the BMU during remodelling will vary with RP. The resultant Haversian canal area is determined by the amount of bone deposition during osteon infilling. Whether the relative osteon area variation is because of a change in the rate of bone deposition, in terms of either number of lamellae or thickness of lamellae, or in the length of time of osteon formation was not tested here. A greater proportion of lamellar bone in an osteon could be the result of several mechanisms. There could be a greater number of lamellae deposited in the same

formation period with a faster rate of deposition, or there could be a greater number of lamellae deposited in a longer formation period with a constant rate of deposition. Alternatively, the number of lamellae may not have changed but they may have become thicker which would also account for the link to RP. Thicker lamellae could also be formed in either the same formation period with a faster rate of deposition, or in a longer formation period with a constant rate of deposition. However, lamellar periodicity and individual lamellar thickness were not tested in this thesis.

A previous *in vivo* labelling study found that a single lamella forms in the same time period as RP (Bromage *et al.*, 2009). The potential for periodic rhythmic lamellae formation was first noted in vitally labelled small mammals where each lamella formed in a 24-hour period (Shinoda and Okada, 1988). The number of lamellae between the lead lines corresponded to the number of days between the labelling injections (Shinoda and Okada, 1988). In vitally labelled non-human animal samples (rat, macaque, patas monkey, and sheep), one bone lamella formed in the same number of days as the species-specific RP (Bromage *et al.*, 2009). There is additional circumstantial evidence for the same phenomenon in one human (Bromage *et al.*, 2009). In one vitally labelled adult human female, each lamella formed in the same time as the human modal RP, in both the interstitial lamellar bone and in the osteonal lamellar bone of the femur (Bromage *et al.*, 2009). If it is confirmed that one lamella does form in the same time period as the RP, and this was applied to the results here, it might indicate that the relatively larger areas of lamellar bone in osteons are attributable to a greater number of lamellae. This could be consistent with the finding that RP inversely relates to relative osteon area. If a person with an RP of six can form a single lamella in six days, then twice as many lamellae could form in the same time period as in a person with an RP of 12, who could form a single lamella in twelve days. A faster biorhythm, indicated by a lower RP, can form more

lamellae in the same time period resulting in relatively more lamellae in the osteon than in an individual with a slower biorhythm, indicated by a higher RP.

However, the physical basis of lamellar bone periodicity is uncertain due to difficulty in defining the formation period of a single lamella (Skedros and Doutré, 2019). Lamellae are formed by the calcification of a 15 μm thick osteoid seam (Johnson, 1964; Martin *et al.*, 1998) that results in the formation of three 5-6 μm thick lamellae each comprised of two 2-3 μm layers with different collagen orientations (Johnson, 1964; Ascenzi, Benvenuti and Bonucci, 1982; Reid, 1986; Martin *et al.*, 1998). Thus, it is unclear whether the formation period of lamellar bone refers to the calcification of the 15 μm osteoid seam and the subsequent formation of three lamellae, the formation of a single 5 μm lamella, or to the formation of one 2 μm layer. The proxy measurements of relative osteon area and relative cortical area enable the relationship between RP and lamellar bone formation to be investigated where uncertainty of lamellar bone periodicity exists. By using these measurements, it is apparent that RP does relate to lamellar bone formation, without the need to quantify the lamellar bone periodicity itself.

Another consideration is the rapid remodelling rate of cortical bone in children that causes increased cortical porosity when compared to adults (Frost, 1969). The link between RP and Haversian canal size could potentially be explained by more rapid bone turnover and increased cortical porosity in children with higher RPs, and vice versa, rather than by the amount of osteonal bone deposition. Haversian canal size decreases throughout the remodelling process until osteon infilling is complete and the Haversian canal is a mature size (Cooper *et al.*, 2003). Despite attempting to only include completed Haversian canal in the study, it is possible that some active osteons could have been included. Although, mean Haversian canal area in both the younger children and the older children included in Chapter 5 (1616.90 μm^2 and 1606.94 μm^2 respectively) are similar

to the mean Haversian canal area reported for inactive concentric Haversian canals (1544 μm^2) and inactive eccentric Haversian canals (1984 μm^2) from external iliac cortices of 0–25 year olds (Schnitzler and Mesquita, 2013). This suggests that the Haversian canals measured in this study were fully formed. Additional support for this is shown by the similar results that were found in the young adult sample included in Chapter 4.

6.1.3 | Bone Modelling

The results of Chapter 5 show that RP inversely relates to relative cortical bone area, but not to overall bone cross-sectional area. This means that people with a higher RP have less cortical bone regardless of the overall cross-sectional area than people with a lower RP. A larger relative cortical area means that, as a proportion of overall size, more interstitial lamellar bone was deposited during the process of bone modelling.

An *in vivo* labelling study has found evidence that the lamellae that make up interstitial bone form in the same time as the human modal RP (Bromage *et al.*, 2009). If one interstitial lamella does form in the same time period as the RP, and this was applied to the results here, it would indicate that the relatively larger cortical bone areas in the ribs are attributable to a greater number of interstitial lamellae. This could be consistent with the finding that RP inversely relates to relative cortical area. If it only takes six days to form a single lamella, then more lamellae can form within a constrained time period than if it takes as long as twelve days to form a single lamella. A faster biorhythm, indicated by a lower RP, can form more lamellae in the same time period resulting in relatively more lamellae in the cortex than in an individual with a slower biorhythm, indicated by a higher RP. However, as with osteonal lamellar bone periodicity, the same uncertainties exist when defining the lamellar bone formation period (Skedros and Doutré, 2019).

Modelling at the periosteum can be induced by biomechanical loading (Mosley *et al.*, 1997; Mosley and Lanyon, 1998, 2002; Robling *et al.*, 2001). This increases the cross-sectional area of the bone and increases the bone's resistance to strain (Lieberman, Devlin and Pearson, 2001; Lieberman *et al.*, 2003). The endosteum shows little to no reaction to biomechanical stimuli (Gross *et al.*, 2002; Lee, Maxwell and Lanyon, 2002; Srinivasan *et al.*, 2002). Nevertheless, over 25% of the total cortical thickness is accounted for by modelling at the endosteal membrane (Garn, 1970). Modelling at the endosteum, unlike the periosteum, is not hindered by adjacent soft tissue such as muscle bellies, blood vessels, or entheses (Carpenter and Carter, 2008; Maggiano *et al.*, 2016). The studies in this thesis did not find a link between RP and total cross-sectional area or cortical area. However, there was a link between RP and the amount of cortical bone relative to the total cross-sectional area. It is therefore possible that the biorhythm is linked to bone modelling at the endosteal membrane. This would account for the variation in relative cortical bone area and the consistent total cross-sectional area. The origin of interstitial lamellae was not examined in this thesis, but the endosteal lamellar pocket is detectable histologically (Maggiano, 2012a; Maggiano *et al.*, 2016) so there is potential to examine this phenomenon further.

6.1.4 | Biorhythm

Previous studies have suggested body size, BMR, life history traits, and RP are all linked by a centrally coordinated autonomic biorhythm that is related to growth and development, and regulated by the hypothalamus (Bromage *et al.*, 2009, 2012, 2016; Bromage and Janal, 2014). By studying the juvenile skeleton, it has become apparent that there is an infradian biorhythm that is related to osteon infilling and cortical bone modelling. Each of these is a feature of somatic growth.

The relationship between RP and the proportions of interstitial and osteonal lamellar bone were seen in the older children and the adults but not in the younger children. The older children were in the middle childhood developmental phase at the time of their death, which is a phase marked by cognitive, behavioural, and hormonal changes (DelGiudice, 2018). The duration of the middle childhood phase can affect final body size attainment (Biro *et al.*, 2001; Baer *et al.*, 2006). Each year of pre-pubertal growth can contribute 4-5 cm to the final adult stature, so additional stature can be accrued over a longer pre-pubertal period (Biro *et al.*, 2001). Although juveniles with early onset puberty have greater peak height velocity and attain adult stature early, they attain a smaller final body size than juveniles with late onset puberty with lower peak height velocity and later attainment of adult stature (Biro *et al.*, 2001; Luo *et al.*, 2003; Onland-Moret *et al.*, 2005). Considering that the relationships between RP and bone in this thesis were only noted in the older children and adults it is possible that this middle childhood phase is an important factor relating to the manifestation of the biorhythm.

The origin of the biorhythm is unknown. It is likely that it has an endogenous origin, especially since RP can change between deciduous and permanent dentition and in response to some instances of non-specific stress (Mahoney *et al.*, 2017). Multiple biological pathways have been suggested, including control by the autonomic nervous system (Appenzeller *et al.*, 2005), or the suprachiasmatic nucleus of the hypothalamus (Bromage *et al.*, 2009, 2012), or a manifestation of overlapping endogenous biorhythms (Newman and Poole, 1993). Since the hypothalamic-pituitary axis has a role in somatic growth, puberty, metabolism, and the timing of other life history traits (Bogin, 2015), it is possible that hypothalamic-pituitary axis is also involved in the infradian biorhythm that manifests as Retzius lines in enamel. In this scenario the hypothalamus signals to the anterior pituitary gland, which then secretes hormones that interact with the thyroid gland,

the adrenal gland, and the gonads, to influence growth, development, and metabolism (Bromage *et al.*, 2009, 2012; Norman and Litwack, 2014). Anterior pituitary secretions regulate many aspects of growth and development, including growth hormone which stimulates skeletal growth, thyroid-stimulating hormone which affects metabolism, growth, and development, and follicle-stimulating hormone and luteinising hormone which affect reproductive functions (Norman and Litwack, 2014). There is a reasonable circumstantial case for the involvement of the hypothalamic-pituitary axis in the biorhythm, but concrete evidence of these biological pathways generating or sustaining an infradian biorhythm linked to RP is currently lacking. It is plausible that the endocrine system is involved because of the demonstrable link between endocrinology and somatic growth. However, this is currently speculative because the origin, control, and pathway of the biorhythm that manifests as Retzius lines remain unknown.

6.1.5 | Other Factors

The relationships between RP and bone microstructure are not straightforward. The studies in Chapter 3 and Chapter 4 illustrate that intraskeletal variation and the other factors affecting bone microstructure must be considered when interpreting how the biorhythm relates to cortical bone microstructure. Bone remodelling is closely related to the ageing process (Stout, Porro and Perotti, 1996; Cho *et al.*, 2002; Streeter, 2010; Pfeiffer *et al.*, 2016) and, as expected, secondary osteons accumulated with advancing age in the ribs and humeri of children from Canterbury, York, and Newcastle. This sign of bone turnover was not related to RP in the ribs of children from Canterbury, York, and Newcastle in Chapter 5, contrary to the hypothesis that RP would relate to bone turnover. Additionally, no links between RP and any bone turnover variable (OPD, N.On, N.On.Fg, and Ot.Dn) were found in either Chapter 4 or Chapter 5. It was expected that RP would

have been related to cell proliferation. However, osteocyte lacunae could not be counted in enough juvenile ribs, due to taphonomy, for this measure of cell proliferation to be assessed against RP in Chapter 5.

The results of Chapter 3 provide further evidence that physical activity also has an effect on bone remodelling. Differences in habitual physical activity between children of all ages from the north of England versus the south of England, and for the older children of high-status versus low-status, were apparent in the humerus microstructure. The similarity of the rib microstructure between children from different geographic regions and socioeconomic groups indicates that the factors affecting systemic bone remodelling were also similar between different geographic regions and socioeconomic groups. The localised variation in strain induced remodelling in the humeri may indicate that the localised response to biomechanical strain has a greater influence on bone microstructure at that point than any systemic factor, such as a biorhythm. The variable bone microstructure across the skeletons in Chapter 4 also illustrate the variable effects of biomechanical loading across the skeleton. The size of secondary osteons is linked to habitual strain magnitude (van Oers, Ruimerman, van Rietbergen, *et al.*, 2008) as is the cortical bone size (Mosley *et al.*, 1997; Mosley and Lanyon, 1998, 2002; Robling *et al.*, 2001). Neither of these variables had a relationship to the biorhythm but the relative amounts of lamellar tissue to the overall size of the structure did. This indicates that while biomechanics and a systemic biorhythm both have an effect on bone structure, they affect different aspects of bone biology.

6.1.6 | Limitations

Histomorphometry can be used to explore the potential relationship between a biorhythm and bone growth. Using archaeological samples allows for a much larger sample size and

also more invasive examination than is possible in a longitudinal *in vivo* study. However, taphonomic damage can obscure the microstructure and prevent certain variables, such as Ot.Dn, from being collected. This is a particular problem with juvenile bone.

The unequal sample sizes are a direct consequence of studying medieval juvenile skeletons derived from different burial contexts. Differential burial practices for children in the past and poorer preservation and recovery rates result in fewer than expected juvenile skeletons. Mortality rates during childhood are variable, fewer children die during adolescence than in infancy and early childhood, leading to fewer adolescent skeletons being available for study. Additionally, there were many more low-status children than high-status children in the medieval period. The resultant sample size variability means that care must be taken when interpreting the results.

The archaeological samples were undocumented; therefore, age-at-death was reconstructed using multiple standard osteological methods (Moorrees, Fanning and Hunt, 1963; Scheuer and Black, 2000; Al Qahtani, Hector and Liversidge, 2010). Even though age-at-death estimations for juvenile skeletons are more accurate than those for adults, these estimates may have introduced variation into the analyses of the cortical bone microstructure. This variation was accounted for by splitting the sample into age groups that were based on the ontogenetic growth profile (young child, older child, adolescent, and young adult).

The potential differences between males and females could not be explored because the bony secondary sexual characteristics that are used to estimate biological sex are undeveloped in most of this sample. The timing and duration of puberty is a life history trait that has been related to body size and it is possibly further linked to RP (Bromage *et al.*, 2012). Sex differences in final adult stature are related to the timing of puberty, which usually begins earlier in females than males (Gasser *et al.*, 2000). A longer

growth period for males before the onset of puberty can explain much of the eventual sex difference in adult stature (Hauspie *et al.*, 1985). Sexual dimorphism in body size is likely to be an important consideration when investigating RP because, generally, human males attain a larger adult body size than females do (Eveleth, 1975; Hauspie *et al.*, 1985). A sex-based difference in RP, where males have a lower mean RP than females, has been reported in some studies (Schwartz, Reid and Dean, 2001; Smith *et al.*, 2007), but not in others (Smith *et al.*, 2007; Tan, Sim and Hsu, 2017). If males do have a lower mean RP, it implies that males have a faster biorhythm than females that enables males to achieve a larger adult body size during the relatively constrained growth period. When examining the potential relationship between RP and bone microstructure in Chapter 5, adolescents were not included to limit this potentially confounding factor. Additionally, the population-level approach used here should minimise the effect of the differences in the timing of pubertal growth spurt between males and females.

6.2 | FUTURE DIRECTIONS

6.2.1 | Biorhythms

The source of the biorhythm, and the mechanisms underpinning the biorhythm are currently unknown, so future work should focus on the control of the biorhythm and how it influences hard tissue growth. If the biorhythm is controlled by the hypothalamic-pituitary axis, then the endocrine factors affecting bone growth in ontogeny should be studied within the context of RP and the biorhythm. In particular, the growth factors affecting bone turnover, osteon infilling and angiogenesis in bone, and body size may be of relevance. The biorhythm may influence the secretion of growth factor which then affects tissue growth.

It should be determined if lamellar bone is an incremental structure and, subsequently, the precise definition of lamellar bone periodicity should be established. The results of this thesis provide circumstantial support for lamellar bone as an incremental structure because RP related to secondary osteon infilling and the proportion of lamellar bone to medullary cavity size in the rib. However, lamellar periodicity was not tested here, and neither was lamellar thickness. The observed link between RP and the proportions of lamellar bone could be caused by different numbers of consistently sized lamellae or by consistent numbers of different thicknesses of lamellae. Lamellar formation times cannot be assessed from archaeological bone, so *in vivo* labelling studies would be necessary, especially if they could be matched to the RP of the same individual.

6.2.2 | Methodological Updates

A possible link between the biorhythm and vascularity of cortical bone using 2D static histomorphometry was found in this thesis. However, the vascular network in cortical bone is more complicated than can be visualised using standard 2D methods (Arhatari *et al.*, 2011; Cooper *et al.*, 2011; Maggiano *et al.*, 2016). There is a network of branching, conjoining, and blind vessels that cannot be appreciated using 2D methods. Future studies of the biorhythm and cortical bone vasculature should employ 3D methods to gain a more complete understanding of how the two features relate. Micro-CT scanning is capable of showing the Haversian canal network (Cooper *et al.*, 2003), but synchrotron scanning is capable of showing the entire vascular network, including the osteocyte lacunae, canaliculi, and Volkmann's channels, as well as the lamellar structure of cortical bone. Synchrotron scanning of cortical bone alongside histological analysis of RP could develop the link between the biorhythm and osteon infilling and Haversian canal size.

The analysis of sex differences in the presence of particular peptides in teeth shows promise for determining actual biological sex (Stewart *et al.*, 2017). Knowing the biological sex of the archaeological samples would allow the study of potential sex differences in the biorhythm and explore the potential interrelationships between the biorhythm, growth, and puberty.

6.3 | CONCLUSION

The relationship between RP, as a sign of an underlying biorhythm, and bone microstructure in a sample of medieval English human skeletons was explored in this thesis. The results support the idea that an infradian biorhythm coordinates aspects of human hard tissue growth, specifically, the relative amounts of lamellar formation during modelling and remodelling. The biorhythm was related to the proportion of interstitial and osteonal lamellar bone. A child with a fast biorhythm tends to have a high proportion of lamellar bone and small Haversian canals in their osteons, and a high proportion of bone in their ribs compared to the medullary cavities. Whereas, a child with a slow biorhythm tends to have a low proportion of lamellar bone and large Haversian canals in their osteons, and a low proportion of bone in their ribs compared to the medullary cavities. The biorhythm did not relate to any measure of bone turnover, including osteon population density, intact osteon density, osteon fragment density, or osteocyte lacunar density. This biorhythm could be one systemic factor amongst the many local and systemic factors that are already known to affect macroscopic bone growth and microscopic bone modelling and remodelling. However, the origin, control, and pathway of the biorhythm remain unknown.

References

Åberg, T., Wozney, J. and Thesleff, I. (1997) 'Expression patterns of bone morphogenetic proteins (Bmps) in the developing mouse tooth suggest roles in morphogenesis and cell differentiation', *Developmental Dynamics*, 210(4), pp. 383–396. doi: 10.1002/(SICI)1097-0177(199712)210:4<383::AID-AJA3>3.0.CO;2-C.

Agnew, A. M. *et al.* (2013) 'The response of pediatric ribs to quasi-static loading: mechanical properties and microstructure', *Annals of Biomedical Engineering*, 41(12), pp. 2501–2514. doi: 10.1007/s10439-013-0875-6.

Agnew, A. M. and Stout, S. D. (2012) 'Brief communication: reevaluating osteoporosis in human ribs: the role of intracortical porosity', *American Journal of Physical Anthropology*, 148(3), pp. 462–466. doi: 10.1002/ajpa.22048.

Aksglaede, L. *et al.* (2008) 'Forty years trends in timing of pubertal growth spurt in 157,000 Danish school children', *PLoS ONE*. Edited by L. Wright, 3(7), p. e2728. doi: 10.1371/journal.pone.0002728.

Al Qahtani, S. J., Hector, M. P. and Liversidge, H. M. (2010) 'Brief communication: the London atlas of human tooth development and eruption', *American Journal of Physical Anthropology*, 142(3), pp. 481–490. doi: 10.1002/ajpa.21258.

Albarella, U. and Woolgar, C. M. (2006) 'Pig husbandry and pork consumption in Medieval England', in Woolgar, C. M., Serjeantson, D., and Waldron, T. (eds) *Food in Medieval England: diet and nutrition*. Oxford: Oxford University Press, pp. 72–87.

Alexy, U. *et al.* (2005) 'Long-term protein intake and dietary potential renal acid load are associated with bone modeling and remodeling at the proximal radius in healthy children', *The American Journal of Clinical Nutrition*, 82(5), pp. 1107–1114. doi: 10.1093/ajcn/82.5.1107.

Alini, M. *et al.* (1996) 'A novel angiogenic molecule produced at the time of chondrocyte hypertrophy during endochondral bone formation', *Developmental Biology*, 176(1), pp. 124–132. doi: 10.1006/dbio.1996.9989.

Anderson, T. and Andrews, J. (2001) 'The human remains', in Hicks, M. and Hicks, A. (eds) *St Gregory's Priory, Northgate, Canterbury: excavations 1988-1991*. Canterbury: Canterbury Archaeological Trust Limited.

Andriacchi, T. *et al.* (1974) ‘A model for studies of mechanical interactions between the human spine and rib cage’, *Journal of Biomechanics*, 7(6), pp. 497–507. doi: 10.1016/0021-9290(74)90084-0.

Andronowski, J. M. and Crowder, C. M. (2018) ‘Bone area histomorphometry’, *Journal of Forensic Sciences*. doi: 10.1111/1556-4029.13815.

Antoine, D., Hillson, S. and Dean, M. C. (2009) ‘The developmental clock of dental enamel: a test for the periodicity of prism cross-striations in modern humans and an evaluation of the most likely sources of error in histological studies of this kind’, *Journal of Anatomy*, 214(1), pp. 45–55. doi: 10.1111/j.1469-7580.2008.01010.x.

Appenzeller, O. *et al.* (2005) ‘A hypothesis: autonomic rhythms are reflected in growth lines of teeth in humans and extinct archosaurs’, *Autonomic Neuroscience*, 117(2), pp. 115–119. doi: 10.1016/j.autneu.2004.10.003.

Arana-Chavez, V. E. and Massa, L. F. (2004) ‘Odontoblasts: the cells forming and maintaining dentine’, *The International Journal of Biochemistry & Cell Biology*, 36(8), pp. 1367–1373. doi: 10.1016/j.biocel.2004.01.006.

Arhatari, B. D. *et al.* (2011) ‘Imaging the 3D structure of secondary osteons in human cortical bone using phase-retrieval tomography’, *Physics in Medicine & Biology*, 56(16), p. 5265. doi: 10.1088/0031-9155/56/16/012.

Ascenzi, A., Benvenuti, A. and Bonucci, E. (1982) ‘The tensile properties of single osteonic lamellae: technical problems and preliminary results’, *Journal of Biomechanics*, 15(1), pp. 29–37. doi: 10.1016/0021-9290(82)90032-X.

Ash, P., Loutit, J. F. and Townsend, K. M. S. (1980) ‘Osteoclasts derived from haematopoietic stem cells’, *Nature*, 283(5748), pp. 669–670. doi: 10.1038/283669a0.

Astill, G. and Grant, A. (1988) *The countryside of medieval England*. Oxford: Blackwell.

Aubin, J. E. (2001) ‘Regulation of osteoblast formation and function’, *Reviews in Endocrine and Metabolic Disorders*, 2(1), pp. 81–94. doi: 10.1023/A:101001120.

Aubin, J. E. and Liu, F. (1996) ‘The osteoblast lineage’, in Bilezikian, J. P., Raisz, L. G., and Rodan, G. A. (eds) *Principles of bone biology*. 1st edn. San Diego: Elsevier Academic Press, pp. 51–67.

Baer, H. J. *et al.* (2006) 'Adult height, age at attained height, and incidence of breast cancer in premenopausal women', *International Journal of Cancer*, 119(9), pp. 2231–2235. doi: 10.1002/ijc.22096.

Baker, A. R. H. (1976) 'Changes in the later Middle Ages', in Darby, H. C. (ed.) *A new historical geography of England before 1600*. Cambridge University Press, pp. 186–247.

van Beek, G. C. (1983) *Dental morphology: an illustrated guide*. Second. Wright Elsevier.

Ben-Amos, I. K. (1994) *Adolescence and youth in early modern England*. Yale University Press.

Bennike, P. *et al.* (2005) 'Comparison of child morbidity in two contrasting medieval cemeteries from Denmark', *American Journal of Physical Anthropology*, 128(4), pp. 734–746. doi: 10.1002/ajpa.20233.

Berendsen, A. D. and Olsen, B. R. (2015) 'Bone development', *Bone*, 80, pp. 14–18. doi: 10.1016/j.bone.2015.04.035.

Beresheim, A. C. *et al.* (2018) 'Sex-specific patterns in cortical and trabecular bone microstructure in the Kirsten Skeletal Collection, South Africa', *American Journal of Human Biology*, 30(3), p. e23108. doi: 10.1002/ajhb.23108.

Berkovitz, B. K., Holland, G. R. and Moxham, B. J. (1992) *Color atlas & textbook of oral anatomy, histology, and embryology*. Mosby Inc.

Beynon, A. D. (1992) 'Circaseptan rhythms in enamel development in modern humans and Plio-Pleistocene hominids', in Smith, P. and Tchernov, E. (eds) *Structure, function and evolution of teeth*. London: Freund Publishing House, pp. 295–309.

Beynon, A. D. *et al.* (1998) 'Radiographic and histological methodologies in estimating the chronology of crown development in modern humans and great apes: a review, with some applications for studies on juvenile hominids', *Journal of Human Evolution*, 35(4–5), pp. 351–370. doi: 10.1006/jhev.1998.0234.

Beynon, A. D. and Dean, M. C. (1988) 'Crown-formation time of a fossil hominid premolar tooth', *Archives of Oral Biology*, 32(11), pp. 773–780.

Beynon, A. D. and Reid, D. J. (1987) 'Relationships between perikymata counts and crown formation times in the human permanent dentition', *Journal of Dental Research*, 66, pp. 889–890.

Beynon, A. D. and Wood, B. A. (1986) 'Variations in enamel thickness and structure in East African hominids', *American Journal of Physical Anthropology*, 70(2), pp. 177–193. doi: 10.1002/ajpa.1330700205.

Birkett, D. A. and Daniels, R. (1986) 'The human burials - The excavation of the Church of the Franciscans, Hartlepool, Cleveland', *Archaeological Journal*, 143(1), pp. 260–304. doi: 10.1080/00665983.1986.11021135.

Biro, F. M. *et al.* (2001) 'Impact of timing of pubertal maturation on growth in black and white female adolescents: The National Heart, Lung, and Blood Institute Growth and Health Study', *The Journal of Pediatrics*, 138(5), pp. 636–643. doi: 10.1067/mpd.2001.114476.

Birrel, J. (2006) 'Procuring, preparing, and serving venison in late medieval England', in Woolgar, C. M., Serjeantson, D., and Waldron, T. (eds) *Food in Medieval England: diet and nutrition*. Oxford: Oxford University Press, pp. 11–26.

Blakey, M. L., Leslie, T. E. and Reidy, J. P. (1994) 'Frequency and chronological distribution of dental enamel hypoplasia in enslaved African Americans: a test of the weaning hypothesis', *American Journal of Physical Anthropology*, 95(4), pp. 371–383. doi: 10.1002/ajpa.1330950402.

de Boer, H. H., Aarents, M. J. and Maat, G. J. R. (2012) 'Staining ground sections of natural dry bone tissue for microscopy', *International Journal of Osteoarchaeology*, 22(4), pp. 379–386. doi: 10.1002/oa.1208.

Bogin, B. (2006) 'Modern human life history - The evolution of human childhood and fertility', in Hawkes, K. and Paine, R. R. (eds) *The evolution of human life history*. 1st edn. Santa Fe: School of American Research, pp. 197–230.

Bogin, B. (2015) 'Human growth and development', in Meuhlenbein, M. P. (ed.) *Basics in human evolution*. London: Academic Press, pp. 285–293.

Botha, D. *et al.* (2018) 'The use of stereological methods in the histomorphometric assessment of bone for age-at-death estimation', *Forensic Science International*, 290, pp. 353.e1-353.e7. doi: 10.1016/j.forsciint.2018.06.025.

Boyde, A. (1976) 'Amelogenesis and the structure of enamel', in Cohen, B. and Kramer, I. R. (eds) *Scientific Foundations of Dentistry*. Heinemann Medical, pp. 335–352.

Boyde, A. (1989) ‘Enamel’, in Berkovitz, B. K. B. et al. (eds) *Teeth*. Berlin, Heidelberg: Springer Berlin Heidelberg, pp. 309–473. doi: 10.1007/978-3-642-83496-7_6.

Boyde, A. and Jones, S. J. (2017) ‘Scanning electron microscopic studies’, in Slavkin, H. C. and Bavetta, L. A. (eds) *Developmental aspects of oral biology*. Academic Press, pp. 243–274.

Boyde, A. and Martin, L. B. (1984) ‘A non-destructive survey of prism packing patterns in primate enamels’, in Fearnhead, R. and Suga, S. (eds) *Tooth enamel*. New York: Elsevier, pp. 417–421.

Britnell, R. (1994) ‘The Black Death in English towns’, *Urban History*, 21(02), pp. 195–210. doi: 10.1017/S0963926800011020.

Britz, H. M. *et al.* (2009) ‘The relation of femoral osteon geometry to age, sex, height and weight’, *Bone*, 45(1), pp. 77–83. doi: 10.1016/j.bone.2009.03.654.

Bromage, T. G. (1991) ‘Enamel incremental periodicity in the pig-tailed macaque: a polychrome fluorescent labeling study of dental hard tissues’, *American Journal of Physical Anthropology*, 86(2), pp. 205–214. doi: 10.1002/ajpa.1330860209.

Bromage, T. G. *et al.* (2009) ‘Lamellar bone is an incremental tissue reconciling enamel rhythms, body size, and organismal life history’, *Calcified Tissue International*, 84(5), pp. 388–404. doi: 10.1007/s00223-009-9221-2.

Bromage, T. G. *et al.* (2012) ‘Primate enamel evinces long period biological timing and regulation of life history’, *Journal of Theoretical Biology*, 305, pp. 131–144. doi: 10.1016/j.jtbi.2012.04.007.

Bromage, T. G. *et al.* (2016) ‘The scaling of human osteocyte lacuna density with body size and metabolism’, *Comptes Rendus Palevol*, 15(1–2), pp. 32–39. doi: 10.1016/j.crpv.2015.09.001.

Bromage, T. G. and Janal, M. N. (2014) ‘The Havers-Halberg oscillation regulates primate tissue and organ masses across the life-history continuum’, *Biological Journal of the Linnean Society*, 112(4), pp. 649–656. doi: 10.1111/bij.12269.

Bruder, S. P. and Caplan, A. I. (1989) ‘Cellular and molecular events during embryonic bone development’, *Connective Tissue Research*, 20(1–4), pp. 65–71. doi: 10.3109/03008208909023875.

Buikstra, J. E. and Ubelaker, D. H. (1994) *Standards for data collection from human skeletal remains*. Fayetteville: Arkansas Archaeological Survey.

Bullion, S. K. (1987) *The incremental structure within tooth enamel and their application in archaeology*. PhD Thesis. University of Lancaster.

Burger, E. H. and Klein-Nulend, J. (1999) 'Mechanotransduction in bone – Role of the lacuno-canalicular network', *The FASEB Journal*, 13(9001), pp. S101–S112. doi: 10.1096/fasebj.13.9001.s101.

Burr, D. B. *et al.* (1985) 'Bone remodeling in response to in vivo fatigue microdamage', *Journal of Biomechanics*, 18(3), pp. 189–200. doi: 10.1016/0021-9290(85)90204-0.

Burr, D. B. (2002) 'Targeted and nontargeted remodeling', *Bone*, 30(1), pp. 2–4. doi: 10.1016/S8756-3282(01)00619-6.

Burr, D. B., Ruff, C. B. and Thompson, D. D. (1990) 'Patterns of skeletal histologic change through time: comparison of an archaic native American population with modern populations', *The Anatomical Record*, 226(3), pp. 307–313. doi: 10.1002/ar.1092260306.

Burt, N. M. (2013) 'Stable isotope ratio analysis of breastfeeding and weaning practices of children from medieval Fishergate House York, UK', *American Journal of Physical Anthropology*, 152(3), pp. 407–416. doi: 10.1002/ajpa.22370.

Burton, P., Nyssen-Behets, C. and Dhem, A. (1989) 'Haversian bone remodelling in human fetus', *Cells Tissues Organs*, 135(2), pp. 171–175. doi: 10.1159/000146748.

Caccia, G. *et al.* (2016) 'Histological determination of the human origin from dry bone: a cautionary note for subadults', *International Journal of Legal Medicine*, 130(1), pp. 299–307. doi: 10.1007/s00414-015-1271-6.

Cambra-Moo, O. *et al.* (2012) 'Mapping human long bone compartmentalisation during ontogeny: a new methodological approach', *Journal of Structural Biology*, 178(3), pp. 338–349. doi: 10.1016/j.jsb.2012.04.008.

Cambra-Moo, O. *et al.* (2014) 'An approach to the histomorphological and histochemical variations of the humerus cortical bone through human ontogeny', *Journal of Anatomy*, 224(6), pp. 634–646. doi: 10.1111/joa.12172.

Cameron, N. (2012) 'The human growth curve, canalization and catch-up growth', in Cameron, N. and Bogin, B. (eds) *Human growth and development*. 2nd edn. London: Academic Press, pp. 1–22.

Cameron, N. and Bogin, B. (2012) *Human growth and development*. 2nd edn. New York: Academic Press.

Cardoso, H. F. V. (2007) 'Environmental effects on skeletal versus dental development: using a documented subadult skeletal sample to test a basic assumption in human osteological research', *American Journal of Physical Anthropology*, 132(2), pp. 223–233. doi: 10.1002/ajpa.20482.

Carpenter, R. D. and Carter, D. R. (2008) 'The mechanobiological effects of periosteal surface loads', *Biomechanics and Modeling in Mechanobiology*, 7(3), pp. 227–242. doi: 10.1007/s10237-007-0087-9.

Chan, A. H. W., Crowder, C. M. and Rogers, T. L. (2007) 'Variation in cortical bone histology within the human femur and its impact on estimating age at death', *American Journal of Physical Anthropology*, 132(1), pp. 80–88. doi: doi.org/10.1002/ajpa.20465.

Charnov, E. L. and Berrigan, D. (1993) 'Why do female primates have such long lifespans and so few babies? Or life in the slow lane', *Evolutionary Anthropology: Issues, News, and Reviews*, 1(6), pp. 191–194.

Cho, H. *et al.* (2002) 'Population-specific histological age-estimating method: a model for known African-American and European-American skeletal remains', *Journal of Forensic Sciences*, 47(1), p. 15199J. doi: 10.1520/JFS15199J.

Cho, H. and Stout, S. D. (2011) 'Age-associated bone loss and intraskeletal variability in the Imperial Romans', *Journal of Anthropological Sciences*, (89), pp. 109–125. doi: 10.4436/jass.89007.

Cho, H., Stout, S. D. and Bishop, T. A. (2006) 'Cortical bone remodeling rates in a sample of African American and European American descent groups from the American Midwest: comparisons of age and sex in ribs', *American Journal of Physical Anthropology*, 130(2), pp. 214–226. doi: 10.1002/ajpa.20312.

Christensen, G. J. and Kraus, B. S. (1965) 'Initial calcification of the human permanent first molar', *Journal of Dental Research*, 44(6), pp. 1338–1342. doi: 10.1177/00220345650440063701.

Clegg, N. W. and Reed, C. G. (1994) 'The economic decline of the church in Medieval England', *Explorations in Economic History*, 31(2), pp. 261–280. doi: 10.1006/exeh.1994.1011.

Clover, V. H. and Gibson, M. T. (1974) *The letters of Lanfranc Archbishop of Canterbury*. Oxford: Oxford University Press.

Conceição, E. L. N. and Cardoso, H. F. V. (2011) 'Environmental effects on skeletal versus dental development II: further testing of a basic assumption in human osteological research', *American Journal of Physical Anthropology*, 144(3), pp. 463–470. doi: 10.1002/ajpa.21433.

Congiu, T. and Pazzaglia, U. E. (2011) 'The sealed osteons of cortical diaphyseal bone. Early observations revisited with scanning electron microscopy', *The Anatomical Record*, 294(2), pp. 193–198. doi: 10.1002/ar.21309.

Cooper, D. M. L. *et al.* (2003) 'Quantitative 3D analysis of the canal network in cortical bone by micro-computed tomography', *The Anatomical Record Part B: The New Anatomist*, 274(1), pp. 169–179. doi: 10.1002/ar.b.10024.

Cooper, D. M. L. *et al.* (2011) 'Visualization of 3D osteon morphology by synchrotron radiation micro-CT', *Journal of Anatomy*, 219(4), pp. 481–489. doi: 10.1111/j.1469-7580.2011.01398.x.

Coqueugniot, H. and Weaver, T. D. (2007) 'Brief communication: infracranial maturation in the skeletal collection from Coimbra, Portugal: new aging standards for epiphyseal union', *American Journal of Physical Anthropology*, 134(3), pp. 424–437. doi: 10.1002/ajpa.20683.

Cox, G. and Sealy, J. (1997) 'Investigating identity and life histories: isotopic analysis and historical documentation of slave skeletons found on the Cape Town foreshore, South Africa', *International Journal of Historical Archaeology*, 1(3), pp. 207–224. doi: 10.1023/A:1027349115474.

Crowder, C. M. and Rosella, L. (2007) 'Assessment of intra- and intercostal variation in rib histomorphometry: its impact on evidentiary examination', *Journal of Forensic Sciences*, 52(2), pp. 271–276. doi: 10.1111/j.1556-4029.2007.00388.x.

Cunningham, C., Scheuer, L. and Black, S. (2016) *Developmental juvenile osteology*. Academic Press.

Currey, J. D. (1964) 'Some effects of ageing in human Haversian systems', *Journal of Anatomy*, 98(Pt 1), p. 69.

Currey, J. D. (2013) *Bones: structure and mechanics*. 2nd edn. Princeton University Press.

Dai, J. and Rabie, A. B. M. (2007) 'VEGF: an essential mediator of both angiogenesis and endochondral ossification', *Journal of Dental Research*, 86(10), pp. 937–950. doi: 10.1177/154405910708601006.

Dawson, H. and Brown, K. R. (2013) 'Exploring the relationship between dental wear and status in late medieval subadults from England', *American Journal of Physical Anthropology*, 150(3), pp. 433–441. doi: 10.1002/ajpa.22221.

Dean, M. C. (1987) 'Growth layers and incremental markings in hard tissues; a review of the literature and some preliminary observations about enamel structure in *Paranthropus boisei*', *Journal of Human Evolution*, 16(2), pp. 157–172. doi: 10.1016/0047-2484(87)90074-1.

Dean, M. C. (1989) 'The developing dentition and tooth structure in hominoids', *Folia Primatologica*, 53, pp. 160–176.

Dean, M. C. and Shellis, R. P. (1998) 'Observations on stria morphology in the lateral enamel of Pongo, Hylobates and Proconsul teeth', *Journal of Human Evolution*, 35(4–5), pp. 401–410. doi: 10.1006/jhev.1998.0243.

DelGiudice, M. (2018) 'Middle childhood: an evolutionary-developmental synthesis', in *Handbook of life course health development*. Springer, Cham, pp. 95–107.

Dempster, D. W. *et al.* (2013) 'Standardized nomenclature, symbols, and units for bone histomorphometry: A 2012 update of the report of the ASBMR Histomorphometry Nomenclature Committee', *Journal of Bone and Mineral Research*, 28(1), pp. 2–17. doi: 10.1002/jbmr.1805.

DeWitte, S. and Slavin, P. (2013) 'Between famine and death: England on the eve of the Black Death – Evidence from paleoepidemiology and manorial accounts', *Journal of Interdisciplinary History*, 44(1), pp. 37–60. doi: 10.1162/JINH_a_00500.

Dominguez, V. M. and Agnew, A. M. (2016) 'Examination of factors potentially influencing osteon size in the human rib', *The Anatomical Record*, 299(3), pp. 313–324. doi: 10.1002/ar.23305.

Dominguez, V. M. and Crowder, C. M. (2012) 'The utility of osteon shape and circularity for differentiating human and non-human Haversian bone', *American Journal of Physical Anthropology*, 149(1), pp. 84–91. doi: 10.1002/ajpa.22097.

Dominguez, V. M. and Crowder, C. M. (2015) 'Sex differences in measures of bone remodeling', *Unpublished Podium Presentation, AAFS*.

Du Boulay, F. R. H. (1970) *An age of ambition: English society in the late Middle Ages*. New York: Viking Press.

Dyer, C. (1989) *Standards of living in the later Middle Ages: social change in England c. 1200-1520*. Cambridge University Press.

Dyer, C. (2000) *Everyday life in Medieval England*. A&C Black.

Dyer, C. (2002) *Making a living in the Middle Ages: the people of Britain 850-1520*. Yale University Press.

Dyer, C. (2006a) 'Gardens and garden produce in the later Middle Ages', in Woolgar, C. M., Serjeantson, D., and Waldron, T. (eds) *Food in Medieval England: diet and nutrition*. Oxford: Oxford University Press, pp. 27–40.

Dyer, C. (2006b) 'Seasonal patterns in food consumption in the latter Middle Ages', in Woolgar, C. M., Serjeantson, D., and Waldron, T. (eds) *Food in Medieval England: diet and nutrition*. Oxford: Oxford University Press, pp. 201–214.

van der Eerden, B., Karperien, M. and Wit, J. M. (2003) 'Systemic and local regulation of the growth plate', *Endocrine Reviews*, 24, pp. 782–801.

Eleazer, C. D. and Jankauskas, R. (2016) 'Mechanical and metabolic interactions in cortical bone development', *American Journal of Physical Anthropology*, 160(2), pp. 317–333. doi: 10.1002/ajpa.22967.

Enlow, D. H. (1962) 'A study of the post-natal growth and remodeling of bone', *The American Journal of Anatomy*, 110, pp. 79–101. doi: 10.1002/aja.1001100202.

Epker, B. N. and Frost, H. M. (1965) 'A histological study of remodeling at the periosteal, haversian canal, cortical endosteal, and trabecular endosteal surfaces in human rib', *The Anatomical Record*, 152(2), pp. 129–135. doi: 10.1002/ar.1091520203.

Ericksen, M. F. (1991) 'Histologic estimation of age at death using the anterior cortex of the femur', *American Journal of Physical Anthropology*, 84(2), pp. 171–179. doi: 10.1002/ajpa.1330840207.

Evans, F. G. (1976) ‘Mechanical properties and histology of cortical bone from younger and older men’, *The Anatomical Record*, 185(1), pp. 1–11. doi: 10.1002/ar.1091850102.

Eveleth, P. B. (1975) ‘Differences between ethnic groups in sex dimorphism of adult height’, *Annals of Human Biology*, 2(1), pp. 35–39. doi: 10.1080/03014467500000541.

Everts, V. *et al.* (2002) ‘The bone lining cell: its role in cleaning howship’s lacunae and initiating bone formation’, *Journal of Bone and Mineral Research*, 17(1), pp. 77–90. doi: 10.1359/jbmr.2002.17.1.77.

Fahy, G. E. *et al.* (2017) ‘Bone deep: variation in stable isotope ratios and histomorphometric measurements of bone remodelling within adult humans’, *Journal of Archaeological Science*, 87, pp. 10–16. doi: 10.1016/j.jas.2017.09.009.

Felder, A. A. *et al.* (2017) ‘Secondary osteons scale allometrically in mammalian humerus and femur’, *Royal Society Open Science*, 4(11), p. 170431. doi: 10.1098/rsos.170431.

Ferretti, M. *et al.* (1999) ‘Histomorphometric study on the osteocyte lacuno-canalicular network in animals of different species. II. Parallel-fibered and lamellar bones’, *Italian Journal of Anatomy and Embryology*, 104, pp. 121–131.

Fildes, V. (1986) *Breasts, bottles and babies-a history of infant feeding.* Edinburgh University Press.

FitzGerald, C. M. (1998) ‘Do enamel microstructures have regular time dependency? Conclusions from the literature and a large-scale study’, *Journal of Human Evolution*, 35(4–5), pp. 371–386. doi: 10.1006/jhev.1998.0232.

Fleming, P. (2001) *Family and household in Medieval England*. Palgrave New York.

Frost, H. M. (1969) ‘Tetracycline-based histological analysis of bone remodeling’, *Calcified Tissue International*, 3(1), pp. 211–237. doi: 10.1007/BF02058664.

Frost, H. M. (1997) ‘Why do marathon runners have less bone than weight lifters? A vital-biomechanical view and explanation’, *Bone*, 20(3), pp. 183–189. doi: 10.1016/S8756-3282(96)00311-0.

Frost, H. M. and Wu, K. (1967) ‘Histological measurement of bone formation rates in contemporary, archeological and paleontological compact bone’, in *Miscellaneous papers in paleopathology*. Flagstaff: Museum of Northern Arizona, pp. 2–22.

Fujita, T. (1939) ‘Neue feststellungen uber Retzius’ schen parallelstreifung des zahnschmelzes’, *Anatomischer Anzeiger*, 87, pp. 350–355.

Fukuhara, T. (1959) ‘Comparative anatomical studies of the growth lines in the enamel of mammalian teeth’, *Acta Anatomica Nipponica*, 34, pp. 322–332.

Fuller, B. T., Richards, M. P. and Mays, S. (2003) ‘Stable carbon and nitrogen isotope variations in tooth dentine serial sections from Wharram Percy’, *Journal of Archaeological Science*, 30(12), pp. 1673–1684. doi: 10.1016/S0305-4403(03)00073-6.

Gantt, D. G. (1982) ‘Neogene hominid evolution: a tooth’s inside view’, in Kurten, B. (ed.) *Teeth: form, function, and evolution*. Columbia University Press, pp. 93–108.

Garn, S. M. *et al.* (1958) ‘The sex difference in tooth calcification’, *Journal of Dental Research*, 37(3), pp. 561–567. doi: 10.1177/00220345580370032801.

Garn, S. M. (1970) *The earlier gain and later loss of cortical bone*. Springfield, Illinois: Thomas.

Gasser, T. *et al.* (2000) ‘Sex dimorphism in growth’, *Annals of Human Biology*, 27(2), pp. 187–197. doi: 10.1080/030144600282299.

Gocha, T., Robling, A. G. and Stout, S. D. (2018) ‘Histomorphometry of human cortical bone: applications to age estimation’, in Katzenberg, M. A. and Saunders, S. R. (eds) *Biological anthropology of the human skeleton*. 3rd edn. Hoboken, NJ: John Wiley & Sons, Inc., pp. 149–182. doi: 10.1002/9780470245842.ch5.

Goldberg, P. J. P. (1986) ‘Female labour, service and marriage in the late Medieval urban North’, *Northern History*, 22(1), pp. 18–38. doi: 10.1179/007817286790616552.

Goldberg, P. J. P. (1992) *Women, work, and life cycle in a Medieval economy: women in York and Yorkshire c. 1300-1520*. Oxford: Oxford University Press.

Goldman, H. M. *et al.* (2009) ‘Ontogenetic patterning of cortical bone microstructure and geometry at the human mid-shaft femur’, *The Anatomical Record*, 292(1), pp. 48–64. doi: 10.1002/ar.20778.

Goldman, H. M. *et al.* (2014) ‘Intracortical remodeling parameters are associated with measures of bone robustness’, *The Anatomical Record*, 297(10), pp. 1817–1828. doi: 10.1002/ar.22962.

Goliath, J. R. (2010) *Variation in osteon circularity and its impact on estimating age at death*. PhD Thesis. The Ohio State University.

Goliath, J. R., Stewart, M. C. and Stout, S. D. (2016) 'Variation in osteon histomorphometrics and their impact on age-at-death estimation in older individuals', *Forensic Science International*, 262, pp. 282.e1-282.e6. doi: 10.1016/j.forsciint.2016.02.053.

Goodman, A. H. (1991) 'Health, adaptation, and maladaptation in past societies', in Bush, H. and Zvelebil, M. (eds) *Health in past societies: biocultural interpretations of human skeletal remains in archaeological contexts*. Oxford: Tempus Reparatum (BAR International Series 567), pp. 31–38.

Goodman, A. H. and Armelagos, G. J. (1988) 'Childhood stress and decreased longevity in a prehistoric population', *American Anthropologist*, 90(4), pp. 936–944. doi: 10.1525/aa.1988.90.4.02a00120.

Gosman, J. H. (2012) 'Growth and development: morphology, mechanisms, and abnormalities', in Crowder, C. M. and Stout, S. D. (eds) *Bone histology – An anthropological perspective*. Boca Raton: CRC Press, pp. 23–44.

Gosman, J. H. *et al.* (2013) 'Development of cortical bone geometry in the human femoral and tibial diaphysis', *The Anatomical Record*, 296(5), pp. 774–787. doi: 10.1002/ar.22688.

Griffin, R. C. and Donlon, D. (2009) 'Patterns in dental enamel hypoplasia by sex and age at death in two archaeological populations', *Archives of Oral Biology*, 54, pp. S93–S100. doi: 10.1016/j.archoralbio.2008.09.012.

Grine, F. E. (2005) 'Enamel thickness of deciduous and permanent molars in modern Homo sapiens', *American Journal of Physical Anthropology*, 126(1), pp. 14–31.

Gross, T. S. *et al.* (2002) 'Noninvasive loading of the murine tibia: an in vivo model for the study of mechanotransduction', *Journal of Bone and Mineral Research*, 17(3), pp. 493–501. doi: 10.1359/jbmr.2002.17.3.493.

Guatelli-Steinberg, D. (2001) 'What can developmental defects of enamel reveal about physiological stress in nonhuman primates?', *Evolutionary Anthropology: Issues, News, and Reviews*, 10(4), pp. 138–151. doi: 10.1002/evan.1027.

Gustafson, A. G. (1955) 'The similarity between contralateral pairs of teeth.', *Odontologisk Tidskrift*, 63(3), p. 245.

Gustafson, G. and Gustafson, A. G. (1967) 'Microanatomy and histochemistry of enamel', in Allan, J. H. (ed.) *Structural and chemical organization of teeth*. New York: Academic Press, pp. 75–134.

Gustafson, G. and Koch, G. (1974) 'Age estimation up to 16 years of age based on dental development.', *Odontologisk revy*, 25(3), pp. 297–306.

Gysi, A. (1939) 'Metabolism in adult enamel', *Dental Digest*, 37, pp. 661–668.

Haavikko, K. (1970) 'The formation and the alveolar and clinical eruption of the permanent teeth. An orthopantomographic study.', *Suomen Hammaslaakariseuran Toimituksia = Finska Tandlakarsallskapets Forhandlingar*, 66(3), p. 103.

Hägg, U. and Taranger, J. (1982) 'Maturation indicators and the pubertal growth spurt', *American Journal of Orthodontics*, 82(4), pp. 299–309. doi: 10.1016/0002-9416(82)90464-X.

Halsall, G. (1995) *Early Medieval cemeteries: an introduction to burial archaeology in the post-Roman west*. Skelmorlie: Cruithne Press.

Han, S. H. *et al.* (2009) 'Microscopic age estimation from the anterior cortex of the femur in Korean adults', *Journal of Forensic Sciences*, 54(3), pp. 519–522. doi: 10.1111/j.1556-4029.2009.01003.x.

Hanawalt, B. A. (1977) 'Childrearing among the lower classes of late Medieval England', *The Journal of Interdisciplinary History*, 8(1), pp. 1–22.

Harvey, P. H. and Clutton-Brock, T. H. (1985) 'Life history variation in primates', *Evolution*, 39(3), p. 559. doi: 10.1111/j.1558-5646.1985.tb00395.x.

Hastings, M. (1997) 'The vertebrate clock: localisation, connection and entrainment', *Physiology and Pharmacology of Biological Rhythms*, 125, pp. 1–28. doi: 10.1007/978-3-662-09355-9_1.

Hauspie, R. *et al.* (1985) 'Decomposition of sexual dimorphism in adult size of height, sitting height, shoulder width and hip width in a British and West Bengal sample', in Ghesquire, J., Martin, R. D., and Newcombe, F. (eds) *Human sexual dimorphism*. London: Taylor and Frances, pp. 207–215.

Havill, L. M. *et al.* (2013) 'Intracortical bone remodeling variation shows strong genetic effects', *Calcified Tissue International*, 93(5), pp. 472–480. doi: 10.1007/s00223-013-9775-x.

Haydock, H. *et al.* (2013) 'Weaning at Anglo-Saxon Raunds: implications for changing breastfeeding practice in Britain over two millennia', *American Journal of Physical Anthropology*, 151(4), pp. 604–612. doi: 10.1002/ajpa.22316.

Hedgecock, N. L. *et al.* (2007) 'Quantitative regional associations between remodeling, modeling, and osteocyte apoptosis and density in rabbit tibial midshafts', *Bone*, 40(3), pp. 627–637. doi: 10.1016/j.bone.2006.10.006.

Hennig, C. *et al.* (2015) 'Does 3D orientation account for variation in osteon morphology assessed by 2D histology?', *Journal of Anatomy*, 227(4), pp. 497–505. doi: doi.org/10.1111/joa.12357.

Hicks, M. and Hicks, A. (2001) *St Gregory's Priory, Northgate, Canterbury: excavations 1988-1991*. Canterbury: Canterbury Archaeological Trust Limited.

Hillman, H. (2000) 'Limitations of clinical and biological histology', *Medical Hypotheses*, pp. 553–564. doi: 10.1054/mehy.1999.0894.

Hillson, S. (1992) 'Dental enamel growth, perikymata and hypoplasia in ancient tooth crowns.', *Journal of the Royal Society of Medicine*, 85(8), p. 460.

Hillson, S. (1996) *Dental anthropology*. Cambridge University Press.

Hillson, S. (2014) *Tooth development in human evolution and bioarchaeology*. Cambridge: Cambridge University Press. doi: 10.1017/CBO9780511894916.

Hillson, S. and Bond, S. (1997) 'Relationship of enamel hypoplasia to the pattern of tooth crown growth: a discussion', *American Journal of Physical Anthropology*, 104(1), pp. 89–103. doi: 10.1002/(SICI)1096-8644(199709)104:1<89::AID-AJPA6>3.0.CO;2-8.

Hobdell, M. H. and Howe, C. E. (1971) 'Variation in bone matrix volume associated with osteocyte lucunae in mammalian and reptilian bone', *Israel Journal of Medical Sciences*, 7(3), pp. 492–493.

Hogg, R. T. *et al.* (2015) 'Lemur biorhythms and life history evolution', *PLoS ONE*, 10(8), p. e0134210. doi: 10.1371/journal.pone.0134210.

Holst, M. (2005) 'The human bone', in Spall, C. A. and Toop, N. J. (eds) *Blue Bridge Lane and Fishergate House, York. Report on excavations: July 2000 to July 2002*. York: Archaeological Planning Consultancy, Ltd.

Holt, J. C. (1972) 'Politics and property in early medieval England', *Past & Present*, 57(1), pp. 3–52. doi: 10.1093/past/57.1.3.

Hoppa, R. D. (1992) ‘Evaluating human skeletal growth: an Anglo-Saxon example’, *International Journal of Osteoarchaeology*, 2(4), pp. 275–288. doi: 10.1002/oa.1390020403.

Humphrey, L. T. (2014) ‘Isotopic and trace element evidence of dietary transitions in early life’, *Annals of Human Biology*, 41(4), pp. 348–357. doi: 10.3109/03014460.2014.923939.

Hunter, R. L. and Agnew, A. M. (2016) ‘Intraskeletal variation in human cortical osteocyte lacunar density: implications for bone quality assessment’, *Bone Reports*, 5, pp. 252–261. doi: 10.1016/j.bonr.2016.09.002.

Jepsen, K. J., Bigelow, E. M. R. and Schlecht, S. H. (2015) ‘Women build long bones with less cortical mass relative to body size and bone size compared with men’, *Clinical Orthopaedics and Related Research*, 473(8), pp. 2530–2539. doi: 10.1007/s11999-015-4184-2.

Jernvall, J. and Jung, H. S. (2000) ‘Genotype, phenotype, and developmental biology of molar tooth characters’, *American Journal of Physical Anthropology*, 113, pp. 171–190.

Jernvall, J. and Thesleff, I. (2000) ‘Reiterative signaling and patterning during mammalian tooth morphogenesis’, *Mechanisms of Development*, 92(1), pp. 19–29. doi: 10.1016/S0925-4773(99)00322-6.

Jernvall, J. and Thesleff, I. (2012) ‘Tooth shape formation and tooth renewal: evolving with the same signals’, *Development*, 139(19), pp. 3487–3497. doi: 10.1242/dev.085084.

Jewell, H. M. (1991) ‘North and South: The antiquity of the great divide’, *Northern History*, 27(1), pp. 1–25. doi: 10.1179/007817291790175655.

Jewell, H. M. (1994) *The North-South divide: the origins of northern consciousness in England*. Manchester University Press.

Johnson, K. *et al.* (2003) ‘Linked deficiencies in extracellular PPi and osteopontin mediate pathologic calcification associated with defective PC-1 and ANK expression’, *Journal of Bone and Mineral Research*, 18(6), pp. 994–1004. doi: 10.1359/jbmr.2003.18.6.994.

Johnson, L. C. (1964) ‘Morphologic analysis in pathology: the kinetics of disease and general biology of bone’, *Bone biodynamics*.

Jowsey, J. (1966) ‘Studies of Haversian systems in man and some animals.’, *Journal of Anatomy*, 100(4), pp. 857–864.

Keough, N., L’Abbé, E. N. and Steyn, M. (2009) ‘The evaluation of age-related histomorphometric variables in a cadaver sample of lower socioeconomic status: implications for estimating age at death’, *Forensic Science International*, 191(1–3), pp. 114.e1-114.e6. doi: 10.1016/j.forsciint.2009.07.012.

Kerley, E. R. (1965) ‘The microscopic determination of age in human bone’, *American Journal of Physical Anthropology*, 23(2), pp. 149–163. doi: 10.1002/ajpa.1330230215.

Kerley, E. R. and Ubelaker, D. H. (1978) ‘Revisions in the microscopic method of estimating age at death in human cortical bone’, *American Journal of Physical Anthropology*, 49(4), pp. 545–546. doi: 10.1002/ajpa.1330490414.

Kirsch, T. *et al.* (1997) ‘Regulated production of mineralization-competent matrix vesicles in hypertrophic chondrocytes’, *The Journal of Cell Biology*, 137(5), pp. 1149–1160. doi: 10.1083/jcb.137.5.1149.

Knothe Tate, M. L. *et al.* (2004) ‘The osteocyte’, *The International Journal of Biochemistry and Cell Biology*, 36(1), pp. 1–8. doi: 10.1016/S1357-2725(03)00241-3.

Knowles, D. (1951) *The Episcopal Colleagues of Archbishop Thomas Becket: being the Ford Lectures delivered in the University of Oxford in Hilary Term 1949*. Cambridge: Cambridge University Press.

Kousteni, S. and Bilezikian, J. P. (2008) ‘Cellular actions of parathyroid hormone’, in Bilezikian, J. P., Raisz, L. G., and Martin, T. J. (eds) *Principles of bone biology*. 3rd edn. San Diego: Elsevier Academic Press, pp. 639–656.

LaCroix, P. (1971) ‘The internal remodeling of bones’, in Bourne, G. H. (ed.) *The biochemistry and physiology of bone*. 2nd edn. New York: Academic Press, pp. 119–144.

Lamb, A. L. *et al.* (2014) ‘Multi-isotope analysis demonstrates significant lifestyle changes in King Richard III’, *Journal of Archaeological Science*, 50, pp. 559–565. doi: 10.1016/j.jas.2014.06.021.

Landeros, O. and Frost, H. M. (1966) ‘Comparison of amounts of remodeling activity in opposite cortices of ribs in children and adults’, *Journal of Dental Research*, 45(1), pp. 152–158. doi: 10.1177/00220345660450010701.

Lanyon, L. E. *et al.* (1982) 'Mechanically adaptive bone remodelling', *Journal of Biomechanics*, 15(3), pp. 141–154. doi: 10.1016/0021-9290(82)90246-9.

Lanyon, L. E. and Rubin, C. T. (1984) 'Static vs dynamic loads as an influence on bone remodelling', *Journal of Biomechanics*, 17(12), pp. 897–905. doi: 10.1016/0021-9290(84)90003-4.

Lee, K. C. L., Maxwell, A. and Lanyon, L. E. (2002) 'Validation of a technique for studying functional adaptation of the mouse ulna in response to mechanical loading', *Bone*, 31(3), pp. 407–412. doi: 10.1016/S8756-3282(02)00842-6.

Lewis, A. B. and Garn, S. M. (1960) 'The relationship between tooth formation and other maturational factors', *The Angle Orthodontist*, 30(2), pp. 70–77.

Lewis, M. E. (2002) 'Impact of industrialization: comparative study of child health in four sites from Medieval and post-Medieval England (A.D. 850-1859)', *American Journal of Physical Anthropology*, 119(3), pp. 211–223. doi: 10.1002/ajpa.10126.

Lewis, M. E. (2016) 'Work and the adolescent in Medieval England 900–1550: the osteological evidence', *Medieval Archaeology*, 60(1), pp. 138–171. doi: 10.1080/00766097.2016.1147787.

Lewis, M. E., Shapland, F. and Watts, R. (2016) 'The influence of chronic conditions and the environment on pubertal development. An example from Medieval England', *International Journal of Paleopathology*, 12, pp. 1–10. doi: 10.1016/j.ijpp.2015.10.004.

Li, C. and Risnes, S. (2004) 'A comparison of resins for embedding teeth, with special emphasis on adaptation to enamel surface as evaluated by scanning electron microscopy', *Archives of Oral Biology*, 49(1), pp. 77–83. doi: 10.1016/S0003-9969(03)00194-8.

Li, J., Parada, C. and Chai, Y. (2017) 'Cellular and molecular mechanisms of tooth root development', *Development*, 144(3), pp. 374–384. doi: 10.1242/dev.137216.

Lieberman, D. E. *et al.* (2003) 'Optimization of bone growth and remodeling in response to loading in tapered mammalian limbs', *Journal of Experimental Biology*, 206(18), pp. 3125–3138. doi: 10.1242/jeb.00514.

Lieberman, D. E., Devlin, M. J. and Pearson, O. M. (2001) 'Articular area responses to mechanical loading: effects of exercise, age, and skeletal location', *American Journal of Physical Anthropology*, 116(4), pp. 266–277. doi: 10.1002/ajpa.1123.

Lomas, R. (1996) *County of conflict: Northumberland from Conquest to Civil War*. East Linton: Tuckwell Press.

Louis, G. M. B. *et al.* (2008) 'Environmental Factors and Puberty Timing: expert panel research needs', *Pediatrics*, 121(Supplement 3), pp. S192–S207. doi: 10.1542/peds.1813E.

Lovejoy, C. O. *et al.* (1985) 'Chronological metamorphosis of the auricular surface of the ilium: a new method for the determination of adult skeletal age at death', *American Journal of Physical Anthropology*, 68(1), pp. 15–28. doi: 10.1002/ajpa.1330680103.

Luo, Z. C. *et al.* (2003) 'Growth in early life and its relation to pubertal growth', *Epidemiology*, pp. 65–73.

Lyle, M. (2002) *Canterbury: 2000 years of history*. Stroud: Tempest.

Maat, G. J. R., Van Den Bos, R. P. M. and Aarents, M. J. (2001) 'Manual preparation of ground sections for the microscopy of natural bone tissue: update and modification of Frost's rapid manual method', *International Journal of Osteoarchaeology*, 11(5), pp. 366–374. doi: 10.1002/oa.578.

Mackie, E. J. *et al.* (2008) 'Endochondral ossification: how cartilage is converted into bone in the developing skeleton', *The International Journal of Biochemistry and Cell Biology*, 40(1), pp. 46–62.

Mackie, E. J., Tatarczuch, L. and Mirams, M. (2011) 'The skeleton: a multi-functional complex organ: the growth plate chondrocyte and endochondral ossification.', *Journal of Endocrinology*, 211, pp. 109–121. doi: 10.1530/JOE-11-0048.

Macpherson, P. M. (2005) *Tracing change: an isotopic investigation of Anglo-Saxon childhood diet*. PhD Thesis. University of Sheffield.

Maggiano, C. M. (2012a) *Histomorphometry of humeral primary bone: evaluating the endosteal lamellar pocket as an indicator of modeling drift in archaeological and modern skeletal samples*. PhD Thesis. The Ohio State University.

Maggiano, C. M. (2012b) 'Making the mold', in Crowder, C. M. and Stout, S. D. (eds) *Bone histology – An anthropological perspective*. Boca Raton: CRC Press, pp. 45–90.

Maggiano, C. M. *et al.* (2016) 'Methods and theory in bone modeling drift: comparing spatial analyses of primary bone distributions in the human humerus', *Journal of Anatomy*, 228(1), pp. 190–202. doi: 10.1111/joa.12383.

Maggiano, I. S. *et al.* (2011) 'A distinct region of microarchitectural variation in femoral compact bone: histomorphology of the endosteal lamellar pocket', *International Journal of Osteoarchaeology*, 21(6), pp. 743–750. doi: doi.org/10.1002/oa.1159.

Maggiano, I. S. *et al.* (2015) 'Drifting diaphyses: asymmetry in diametric growth and adaptation along the humeral and femoral length', *The Anatomical Record*, 298(10), pp. 1689–1699. doi: 10.1002/ar.23201.

Maggiano, I. S. *et al.* (2016) 'Three-dimensional reconstruction of Haversian systems in human cortical bone using synchrotron radiation-based micro-CT: morphology and quantification of branching and transverse connections across age', *Journal of Anatomy*, 228(5), pp. 719–732. doi: 10.1111/joa.12430.

Mahoney, P. (2008) 'Intraspecific variation in M1 enamel development in modern humans: implications for human evolution', *Journal of Human Evolution*, 55(1), pp. 131–147. doi: 10.1016/j.jhevol.2008.02.004.

Mahoney, P. (2010) 'Two-dimensional patterns of human enamel thickness on deciduous (dm1, dm2) and permanent first (M1) mandibular molars', *Archives of Oral Biology*, 55(2), pp. 115–126. doi: 10.1016/j.archoralbio.2009.11.014.

Mahoney, P. (2011) 'Human deciduous mandibular molar incremental enamel development', *American Journal of Physical Anthropology*, 144(2), pp. 204–214. doi: 10.1002/ajpa.21386.

Mahoney, P. (2012) 'Incremental enamel development in modern human deciduous anterior teeth', *American Journal of Physical Anthropology*, 147(4), pp. 637–651. doi: 10.1002/ajpa.22029.

Mahoney, P., Miszkiewicz, J. J., *et al.* (2016) 'Biorhythms, deciduous enamel thickness, and primary bone growth: a test of the Havers-Halberg Oscillation hypothesis', *Journal of Anatomy*, 228(6), pp. 919–928. doi: 10.1111/joa.12450.

Mahoney, P., Schmidt, C. W., *et al.* (2016) 'Deciduous enamel 3D microwear texture analysis as an indicator of childhood diet in medieval Canterbury, England', *Journal of Archaeological Science*, 66, pp. 128–136. doi: 10.1016/j.jas.2016.01.007.

Mahoney, P. *et al.* (2017) 'Enamel biorhythms of humans and great apes: the Havers-Halberg Oscillation hypothesis reconsidered', *Journal of Anatomy*, 230(2), pp. 272–281. doi: 10.1111/joa.12551.

Mahoney, P. *et al.* (2018) 'The biorhythm of human skeletal growth', *Journal of Anatomy*, 232(1), pp. 26–38. doi: 10.1111/joa.12709.

Mantzoros, C. S. (1997) 'A longitudinal assessment of hormonal and physical alterations during normal puberty in boys. V. Rising leptin levels may signal the onset of puberty', *Journal of Clinical Endocrinology & Metabolism*, 82(4), pp. 1066–1070. doi: 10.1210/jc.82.4.1066.

Marks, S. C. and Odgren, P. R. (2002) 'Structure and development of the skeleton', in Bilezikian, J. P., Raisz, L. G., and Rodan, G. A. (eds) *Principles of bone biology*. 2nd edn. San Diego: Elsevier Academic Press, pp. 3–15. doi: 10.1016/B978-012098652-1.50103-7.

Marotti, G. *et al.* (1990) 'Structure-function relationships in the osteocyte.', *Italian Journal of Mineral and Electrolyte Metabolism*, 4(2), pp. 93–106.

Marotti, G. and Zallone, A. Z. (1980) 'Changes in the vascular network during the formation of Haversian systems', *Cells Tissues Organs*, 106(1), pp. 84–100. doi: 10.1159/000145171.

Martin, D. L. and Armelagos, G. J. (1979) 'Morphometrics of compact bone: an example from Sudanese Nubia', *American Journal of Physical Anthropology*, 51(4), pp. 571–577. doi: 10.1002/ajpa.1330510409.

Martin, L. B. (1985) 'Significance of enamel thickness in hominoid evolution', *Nature*, 314(6008), pp. 260–263. doi: 10.1038/314260a0.

Martin, L. B. (1986) 'Relationships among great apes and humans', in Wood, B. A., Martin, L. B., and Andrews, P. (eds) *Major topics in primate and human evolution*. Cambridge: Cambridge University Press, pp. 161–187.

Martin, L. B. and Boyde, A. (1984) 'Rates of enamel formation in relation to enamel thickness in hominoid primates', in Fearnhead, R. and Suga, S. (eds) *Tooth enamel*. New York: Elsevier, pp. 447–451.

Martin, L. B., Boyde, A. and Grine, F. E. (1988) 'Enamel structure in primates: a review of scanning electron microscope studies.', *Scanning Microscopy*, 2(3), pp. 1503–1526.

Martin, R. B. *et al.* (1998) *Skeletal tissue mechanics*. New York: Springer.

Martin, R. B. (2003) ‘Fatigue damage, remodeling, and the minimization of skeletal weight’, *Journal of Theoretical Biology*, 220(2), pp. 271–276. doi: 10.1006/jtbi.2003.3148.

Martin, R. B. and Burr, D. B. (1989) *Structure, function, and adaptation of compact bone*. Raven Press.

Massler, M. and Schour, I. (1946) ‘The appositional life span of the enamel and dentin-forming cells: I. Human deciduous teeth and first permanent molars’, *Journal of Dental Research*, 25(3), pp. 145–150. doi: 10.1177/00220345460250030601.

Mauras, N. *et al.* (1996) ‘Sex steroids, growth hormone, insulin-like growth factor-1: neuroendocrine and metabolic regulation in puberty’, *Hormone Research in Paediatrics*, 45(1–2), pp. 74–80. doi: 10.1159/000184763.

May, R. L., Goodman, A. H. and Meindl, R. S. (1993) ‘Response of bone and enamel formation to nutritional supplementation and morbidity among malnourished Guatemalan children’, *American Journal of Physical Anthropology*, 92(1), pp. 37–51. doi: 10.1002/ajpa.1330920104.

Mays, S. *et al.* (2013) *Science and the dead: a guideline for the destructive sampling of archaeological human remains for scientific analysis*. English Heritage Publishing with the Advisory Panel on the Archaeology of Burials in England.

Mays, S. *et al.* (2017) ‘Child bioarchaeology: perspectives on the past 10 years’, *Childhood in the Past*, 10(1), pp. 38–56. doi: 10.1080/17585716.2017.1301066.

Mays, S., Richards, M. P. and Fuller, B. T. (2002) ‘Bone stable isotope evidence for infant feeding in Mediaeval England’, *Antiquity*, 76(293), pp. 654–656. doi: 10.1017/S0003598X00091067.

McFarlane, G., Littleton, J. and Floyd, B. (2014) ‘Estimating striae of Retzius periodicity nondestructively using partial counts of perikymata’, *American Journal of Physical Anthropology*, 154, pp. 251–258.

McIntyre, L. and Bruce, G. (2010) ‘Excavating All Saints: a Medieval church rediscovered’, *Current Archaeology*, pp. 30–37.

Meckel, A. H., Griebstein, W. J. and Neal, R. J. (1965) ‘Structure of mature human dental enamel as observed by electron microscopy’, *Archives of Oral Biology*, 10(5), pp. 775–783. doi: 10.1016/0003-9969(65)90131-7.

Meindl, R. S. *et al.* (1985) 'A revised method of age determination using the os pubis, with a review and tests of accuracy of other current methods of pubic symphyseal aging', *American Journal of Physical Anthropology*, 68(1), pp. 29–45. doi: 10.1002/ajpa.1330680104.

Mimura, F. (1939) 'The periodicity of growth lines seen in enamel', *Kobyo-shi*, 13, pp. 454–455.

Miszkiewicz, J. J. (2015a) 'Histology of a Harris line in a human distal tibia', *Journal of Bone and Mineral Metabolism*, 33(4), pp. 462–466. doi: 10.1007/s00774-014-0644-0.

Miszkiewicz, J. J. (2015b) 'Linear enamel hypoplasia and age-at-death at Medieval (11th–16th Centuries) St. Gregory's Priory and Cemetery, Canterbury, UK', *International Journal of Osteoarchaeology*, 25(1), pp. 79–87. doi: 10.1002/oa.2265.

Miszkiewicz, J. J. (2016) 'Investigating histomorphometric relationships at the human femoral midshaft in a biomechanical context', *Journal of Bone and Mineral Metabolism*, 34(2), pp. 179–192. doi: 10.1007/s00774-015-0652-8.

Miszkiewicz, J. J. and Mahoney, P. (2016) 'Ancient human bone microstructure in Medieval England: comparisons between two socio-economic groups', *The Anatomical Record*, 299(1), pp. 42–59. doi: 10.1002/ar.23285.

Miszkiewicz, J. J. and Mahoney, P. (2018) 'Histomorphometry and cortical robusticity of the adult human femur', *Journal of Bone and Mineral Metabolism*. doi: 10.1007/s00774-017-0899-3.

Moggi-Cecchi, J., Pacciani, E. and Pinto-Cisternas, J. (1994) 'Enamel hypoplasia and age at weaning in 19th-century Florence, Italy', *American Journal of Physical Anthropology*, 93(3), pp. 299–306. doi: 10.1002/ajpa.1330930303.

Moorrees, C. F. A., Fanning, E. A. and Hunt, E. E. (1963a) 'Age variation of formation stages for ten permanent teeth', *Journal of Dental Research*, 42(6), pp. 1490–1502. doi: 10.1177/00220345630420062701.

Moorrees, C. F. A., Fanning, E. A. and Hunt, E. E. (1963b) 'Formation and resorption of three deciduous teeth in children', *American Journal of Physical Anthropology*, 21(2), pp. 205–213.

Mosley, J. R. *et al.* (1997) 'Strain magnitude related changes in whole bone architecture in growing rats', *Bone*, 20(3), pp. 191–198. doi: 10.1016/S8756-3282(96)00385-7.

Mosley, J. R. and Lanyon, L. E. (1998) 'Strain rate as a controlling influence on adaptive modeling in response to dynamic loading of the ulna in growing male rats', *Bone*, 23(4), pp. 313–318. doi: 10.1016/S8756-3282(98)00113-6.

Mosley, J. R. and Lanyon, L. E. (2002) 'Growth rate rather than gender determines the size of the adaptive response of the growing skeleton to mechanical strain', *Bone*, 30(1), pp. 314–319. doi: 10.1016/S8756-3282(01)00626-3.

Mulhern, D. M. (2000) 'Rib remodeling dynamics in a skeletal population from Kulubnarti, Nubia', *American Journal of Physical Anthropology*, 111(4), pp. 519–530. doi: 10.1002/(SICI)1096-8644(200004)111:4<519::AID-AJPA7>3.0.CO;2-7.

Mulhern, D. M. and Van Gerven, D. P. (1997) 'Patterns of femoral bone remodeling dynamics in a medieval Nubian population', *American Journal of Physical Anthropology*, 104(1), pp. 133–146. doi: 10.1002/(SICI)1096-8644(199709)104:1<133::AID-AJPA9>3.0.CO;2-S.

Mullender, M. G. *et al.* (1996) 'Osteocyte density and histomorphometric parameters in cancellous bone of the proximal femur in five mammalian species', *Journal of Orthopaedic Research*, 14(6), pp. 972–979. doi: 10.1002/jor.1100140618.

Murphy, M. (1998) 'Feeding medieval cities: some historical approaches', in Carlin, M. and Rosenthal, J. T. (eds) *Food and eating in Medieval Europe*. Bloomsbury Publishing, pp. 117–131.

Nanci, A. (2017) *Ten Cate's oral histology: development, structure, and function*. 9th edn. Elsevier Health Sciences.

Nanci, A. and Warshawsky, H. (1984) 'Characterization of putative secretory sites on ameloblasts of the rat incisor', *American Journal of Anatomy*, 171(2), pp. 163–189.

Nava, A., Frayer, D. W. and Bondioli, L. (2019) 'Longitudinal analysis of the microscopic dental enamel defects of children in the Imperial Roman community of Portus Romae (necropolis of Isola Sacra, 2nd to 4th century CE, Italy)', *Journal of Archaeological Science Reports*, 23, pp. 406–415.

Newman, H. N. and Poole, D. F. (1974) 'Observations with scanning and transmission electron microscopy on the structure of human surface enamel', *Archives of Oral Biology*, 19, pp. 1135–1143.

Newman, H. N. and Poole, D. F. (1993) 'Dental enamel growth.', *Journal of the Royal Society of Medicine*, 86(1), p. 61.

Nicholas, D. M. (2014) *The growth of the Medieval city: from late antiquity to the early fourteenth Century*. New York: Routledge.

Nicolella, D. P. *et al.* (2006) 'Osteocyte lacunae tissue strain in cortical bone', *Journal of Biomechanics*, 39(9), pp. 1735–1743. doi: 10.1016/j.jbiomech.2005.04.032.

Noback, C. R. and Robertson, G. G. (1951) 'Sequences of appearance of ossification centers in the human skeleton during the first five prenatal months', *American Journal of Anatomy*, 89(1), pp. 1–28. doi: 10.1002/aja.1000890102.

Nolan, J., Harbottle, B. and Vaughan, J. (2010) 'The early medieval cemetery at the Castle, Newcastle upon Tyne', *Archaeologia Aeliana*. (5th), (39), pp. 147–287.

Norman, A. W. and Litwack, G. (2014) *Hormones*. 3rd edn. Academic Press.

van Oers, R. F. M., Ruimerman, R., Tanck, E., *et al.* (2008) 'A unified theory for osteonal and hemi-osteonal remodeling', *Bone*, 42(2), pp. 250–259. doi: 10.1016/j.bone.2007.10.009.

van Oers, R. F. M., Ruimerman, R., van Rietbergen, B., *et al.* (2008) 'Relating osteon diameter to strain', *Bone*, 43(3), pp. 476–482. doi: 10.1016/j.bone.2008.05.015.

Onland-Moret, N. C. *et al.* (2005) 'Age at menarche in relation to adult height: the EPIC study', *American Journal of Epidemiology*, 162(7), pp. 623–632. doi: 10.1093/aje/kwi260.

Orimo, H. (2010) 'The mechanism of mineralization and the role of alkaline phosphatase in health and disease', *Journal of Nippon Medical School*, 77(1), pp. 4–12. doi: 10.1272/jnms.77.4.

Osborn, J. W. (1970) 'The mechanism of ameloblast movement: a hypothesis', *Calcified Tissue Research*, 5(1), pp. 344–359. doi: 10.1007/BF02017564.

Osborn, J. W. (1990) 'A 3-dimensional model to describe the relation between prism directions, parazones and diazones, and the Hunter-Schreger bands in human tooth enamel', *Archives of Oral Biology*, 35(11), pp. 869–878. doi: 10.1016/0003-9969(90)90065-I.

Ott, S. M. (2002) ‘Histomorphometric analysis of bone remodeling’, in Bilezikian, J. P., Raisz, L. G., and Rodan, G. A. (eds) *Principles of bone biology*. 2nd edn. San Diego: Elsevier Academic Press, pp. 303–319.

Paine, R. R. and Brenton, B. P. (2006) ‘Dietary health does affect histological age assessment: an evaluation of the Stout and Paine (1992) age estimation equation using secondary osteons from the rib’, *Journal of Forensic Sciences*, 51(3), pp. 489–492. doi: 10.1111/j.1556-4029.2006.00118.x.

Palliser, D. M. (2014) *Medieval York: 600-1540*. Oxford: Oxford University Press.

Parfitt, A. M. (1983) ‘The physiologic and clinical significance of bone histomorphometric data’, in Recker, R. R. (ed.) *Bone histomorphometry: techniques and interpretation*. Boca Raton: CRC Press, pp. 143–223.

Parfitt, A. M. *et al.* (2000) ‘Structural and cellular changes during bone growth in healthy children’, *Bone*, 27(4), pp. 487–494. doi: 10.1016/S8756-3282(00)00353-7.

Parfitt, A. M. (2002a) ‘Life history of osteocytes: relationship to bone age, bone remodeling, and bone fragility’, *Journal of Musculoskeletal and Neuronal Interactions*, 2(6), pp. 499–500.

Parfitt, A. M. (2002b) ‘Targeted and nontargeted bone remodeling: relationship to basic multicellular unit origination and progression’, *Bone*, 30(1), pp. 5–7. doi: 10.1016/S8756-3282(01)00642-1.

Pazzaglia, U. E. *et al.* (2012) ‘Morphometry and patterns of lamellar bone in human Haversian systems’, *The Anatomical Record*, 295(9), pp. 1421–1429. doi: 10.1002/ar.22535.

Pearson, O. M. and Lieberman, D. E. (2004) ‘The aging of Wolff’s law: ontogeny and responses to mechanical loading in cortical bone’, *American Journal of Physical Anthropology*, 125(S39), pp. 63–99. doi: 10.1002/ajpa.20155.

Pettit, A. R. *et al.* (2008) ‘Osteal macrophages: a new twist on coupling during bone dynamics’, *Bone*, 43(6), pp. 976–982. doi: 10.1016/j.bone.2008.08.128.

Pfeiffer, S. K. (1998) ‘Variability in osteon size in recent human populations’, *American Journal of Physical Anthropology*, 106(2), pp. 219–227. doi: 10.1002/(SICI)1096-8644(199806)106:2<219::AID-AJPA8>3.0.CO;2-K.

Pfeiffer, S. K. *et al.* (2006) 'Secondary osteon and Haversian canal dimensions as behavioral indicators', *American Journal of Physical Anthropology*, 131(4), pp. 460–468. doi: 10.1002/ajpa.20454.

Pfeiffer, S. K. *et al.* (2016) 'Cortical bone histomorphology of known-age skeletons from the Kirsten collection, Stellenbosch University, South Africa', *American Journal of Physical Anthropology*, 160(1), pp. 137–147. doi: 10.1002/ajpa.22951.

Phenice, T. W. (1969) 'A newly developed visual method of sexing the os pubis', *American Journal of Physical Anthropology*, 30(2), pp. 297–301. doi: 10.1002/ajpa.1330300214.

Pinto, D. C. and Pace, E. D. (2015) 'A silver-stain modification of standard histological slide preparation for use in anthropology analyses', *Journal of Forensic Sciences*, 60(2), pp. 391–398. doi: 10.1111/1556-4029.12697.

Pitfield, R., Miszkiewicz, J. J. and Mahoney, P. (2017) 'Cortical histomorphometry of the human humerus during ontogeny', *Calcified Tissue International*, 101(2), pp. 148–158. doi: 10.1007/s00223-017-0268-1.

Plant, T. and Shahab, M. (2002) 'Neuroendocrine mechanisms that delay and initiate puberty in higher primates', *Physiology and Behavior*, 77(4–5), pp. 717–722. doi: 10.1016/S0031-9384(02)00924-1.

Powell, A., Serjeantson, D. and Smith, P. (2001) 'Food consumption and disposal: the animal remains', in Hicks, M. and Hicks, A. (eds) *St Gregory's Priory Northgate Canterbury excavations*. Canterbury: Canterbury Archaeological Trust Limited, pp. 289–333.

Promislow, D. E. L. and Harvey, P. H. (1990) 'Living fast and dying young: a comparative analysis of life-history variation among mammals', *Journal of Zoology*, 220(3), pp. 417–437. doi: 10.1111/j.1469-7998.1990.tb04316.x.

Raab, D. M. *et al.* (1991) 'A histomorphometric study of cortical bone activity during increased weight-bearing exercise', *Journal of Bone and Mineral Research*, 6(7), pp. 741–749. doi: 10.1002/jbmr.5650060712.

Rang, M. (1969) *The growth plate and its disorders*. E. & S. Livingstone Ltd.

Reiche, I., Vignaud, C. and Menu, M. (2002) 'The crystallinity of ancient bone and dentine: new insights by transmission electron microscopy', *Archaeometry*, 44(3), pp. 447–459. doi: 10.1111/1475-4754.00077.

Reid, D. J., Beynon, A. D. and Ramirez Rozzi, F. V. (1998) 'Histological reconstruction of dental development in four individuals from a medieval site in Picardie, France', *Journal of Human Evolution*, 35(4–5), pp. 463–477. doi: 10.1006/jhev.1998.0233.

Reid, D. J. and Dean, M. C. (2000) 'Brief communication: the timing of linear hypoplasias on human anterior teeth', *American Journal of Physical Anthropology*, 113(1), pp. 135–139. doi: 10.1002/1096-8644(200009)113:1<135::AID-AJPA13>3.0.CO;2-A.

Reid, D. J. and Dean, M. C. (2006) 'Variation in modern human enamel formation times', *Journal of Human Evolution*, 50(3), pp. 329–346. doi: 10.1016/j.jhevol.2005.09.003.

Reid, D. J. and Ferrell, R. J. (2006) 'The relationship between number of striae of Retzius and their periodicity in imbricational enamel formation', *Journal of Human Evolution*, 50(2), pp. 195–202. doi: 10.1016/j.jhevol.2005.09.002.

Reid, S. A. (1986) 'A study of lamellar organisation in juvenile and adult human bone', *Anatomy and Embryology*, 174(3), pp. 329–338. doi: 10.1007/BF00698783.

Remaggi, F. *et al.* (1998) 'Histomorphometric study on the osteocyte lacuno-canalicular network in animals of different species. I. Woven-fibered and parallel-fibered bones', *Italian Journal of Anatomy and Embryology*, 103, pp. 145–155.

Retzius, A. (1837) 'Bemerkungen über den inneren bau der zähne. mit besonderer rücksicht auf dem in zahnknochen vorkommenden röhrenbau', *Archives of Anatomy and Physiology*, pp. 486–566.

Richards, M. P., Mays, S. and Fuller, B. T. (2002) 'Stable carbon and nitrogen isotope values of bone and teeth reflect weaning age at the Medieval Wharram Percy site, Yorkshire, UK', *American Journal of Physical Anthropology*, 119(3), pp. 205–210. doi: 10.1002/ajpa.10124.

Richman, E. A., Ortner, D. J. and Schulter-Ellis, F. P. (1979) 'Differences in intracortical bone remodeling in three aboriginal American populations: possible dietary factors', *Calcified Tissue International*, 28(1), pp. 209–214. doi: 10.1007/BF02441238.

Rigby, S. H. (1995) *English society in the later Middle Ages: class, status and gender*. Macmillan International Higher Education.

Risnes, S. (1986) 'Enamel apposition rate and the prism periodicity in human teeth', *European Journal of Oral Sciences*, 94(5), pp. 394–404. doi: 10.1111/j.1600-0722.1986.tb01779.x.

Risnes, S. (1998) 'Growth tracks in dental enamel', *Journal of Human Evolution*, 35(4–5), pp. 331–350. doi: 10.1006/jhev.1998.0229.

Robinson, C. *et al.* (1998) 'The developing enamel matrix: nature and function', *European Journal of Oral Sciences*, 106(S1), pp. 282–291. doi: 10.1111/j.1600-0722.1998.tb02188.x.

Robinson, C., Kirkham, J. and Hallsworth, A. S. (1988) 'Volume distribution and concentration of protein, mineral and water in developing bovine enamel', *Archives of Oral Biology*, 33(3), pp. 159–162.

Robling, A. G. *et al.* (2001) 'Modulation of appositional and longitudinal bone growth in the rat ulna by applied static and dynamic force', *Bone*, 29(2), pp. 105–113. doi: 10.1016/S8756-3282(01)00488-4.

Robling, A. G., Castillo, A. B. and Turner, C. H. (2006) 'Biomechanical and molecular regulation of bone remodeling', *Annual Review of Biomedical Engineering*, 8(1), pp. 455–498. doi: 10.1146/annurev.bioeng.8.061505.095721.

Robling, A. G. and Stout, S. D. (1999) 'Morphology of the drifting osteon', *Cells Tissues Organs*, 164(4), pp. 192–204. doi: 10.1159/000016659.

Robling, A. G. and Stout, S. D. (2003) 'Histomorphology, geometry, and mechanical loading in past populations', in Agarwal, S. C. and Stout, S. D. (eds) *Bone loss and osteoporosis: an anthropological perspective*. Boston, MA: Springer, pp. 189–205.

Rollason, D. (2003) *Northumbria, 500-1100: creation and destruction of a kingdom*. Cambridge: Cambridge University Press.

Roodman, G. D. (1996) 'Advances in bone biology: the osteoclast', *Endocrine Reviews*, 17(4), pp. 308–332. doi: 10.1210/edrv-17-4-308.

Rose, J. C., Armelagos, G. J. and Lallo, J. W. (1978) 'Histological enamel indicator of childhood stress in prehistoric skeletal samples', *American Journal of Physical Anthropology*, 49(4), pp. 511–516. doi: 10.1002/ajpa.1330490411.

Rubin, P. (1964) ‘Dynamic classification of bone dysplasias’, *Academic Medicine*, 39(11), p. 1059.

Ruff, C., Holt, B. and Trinkaus, E. (2006) ‘Who’s afraid of the big bad Wolff?: “Wolff’s law” and bone functional adaptation’, *American Journal of Physical Anthropology*, 129(4), pp. 484–498. doi: 10.1002/ajpa.20371.

Rushton, M. A. (1933) ‘On the fine contour lines of the enamel of milk teeth’, *Dental Record*, 53, pp. 170–171.

Saunders, S. R. and Hoppa, R. D. (1993) ‘Growth deficit in survivors and non-survivors: biological mortality bias in subadult skeletal samples’, *American Journal of Physical Anthropology*, 36(S17), pp. 127–151. doi: 10.1002/ajpa.1330360608.

Savage, V. M. *et al.* (2007) ‘Scaling of number, size, and metabolic rate of cells with body size in mammals’, *Proceedings of the National Academy of Sciences*, 104(11), pp. 4718–4723. doi: 10.1073/pnas.0611235104.

Scheuer, L. and Black, S. (2000) ‘Development and ageing of the juvenile skeleton’, in Cox, M. and Mays, S. (eds) *Human osteology: in archaeology and forensic science*. Cambridge University Press, pp. 9–21.

Schlecht, S. H. *et al.* (2012) ‘Brief communication: the effects of disuse on the mechanical properties of bone: what unloading tells us about the adaptive nature of skeletal tissue’, *American Journal of Physical Anthropology*, 149(4), pp. 599–605. doi: 10.1002/ajpa.22150.

Schnitzler, C. M. and Mesquita, J. M. (2013) ‘Cortical porosity in children is determined by age-dependent osteonal morphology’, *Bone*, 55(2), pp. 476–486. doi: 10.1016/j.bone.2013.03.021.

Schofield, J. and Vince, A. G. (2003) *Medieval towns: the archaeology of British towns in their European setting*. A&C Black.

Schour, I. (1936) ‘The neonatal line in the enamel and dentin of the human deciduous teeth and first permanent molar’, *Journal of the American Dental Association*, 23(10), pp. 1946–1955. doi: 10.14219/jada.archive.1936.0277.

Schour, I. and Hoffman, M. M. (1939) ‘Studies in tooth development: II. the rate of apposition of enamel and dentin in man and other mammals’, *Journal of Dental Research*, 18(2), pp. 161–175. doi: 10.1177/00220345390180020601.

Schour, I. and Poncher, H. G. (1937) 'Rate of apposition of enamel and dentin, measured by the effect of acute fluorosis', *American Journal of Diseases of Children*, 54(4), pp. 757–776.

Schwartz, G. T. *et al.* (2005) 'Dental development in *Megaladapis edwardsi* (Primates, Lemuriformes): implications for understanding life history variation in subfossil lemurs', *Journal of Human Evolution*, 49(6), pp. 702–721.

Schwartz, G. T., Reid, D. J. and Dean, M. C. (2001) 'Developmental aspects of sexual dimorphism in hominoid canines', *International Journal of Primatology*, 22(5), pp. 837–860. doi: 10.1023/A:1012073601808.

Seeman, E. (2002) 'Pathogenesis of bone fragility in women and men', *The Lancet*, 359(9320), pp. 1841–1850. doi: 10.1016/S0140-6736(02)08706-8.

Serjeantson, D. (2006) 'Birds: food and a mark of status', in Woolgar, C. M., Serjeantson, D., and Waldron, T. (eds) *Food in Medieval England: diet and nutrition*. Oxford: Oxford University Press, pp. 131–147.

Serjeantson, D. and Woolgar, C. M. (2006) 'Fish consumption in Medieval England.', in Woolgar, C. M., Serjeantson, D., and Waldron, T. (eds) *Food in Medieval England: diet and nutrition*. Oxford: Oxford University Press, pp. 102–130.

Shapland, F., Lewis, M. E. and Watts, R. (2015) 'The lives and deaths of young Medieval women: the osteological evidence', *Medieval Archaeology*, 59(1), pp. 272–289. doi: 10.1080/00766097.2015.1119392.

Shellis, R. P. (1998) 'Utilization of periodic markings in enamel to obtain information on tooth growth', *Journal of Human Evolution*, 35(4–5), pp. 387–400. doi: 10.1006/jhev.1998.0260.

Shinoda, H. and Okada, M. (1988) 'Diurnal rhythms in the formation of lamellar bone in young growing animals', *Proceedings of the Japan Academy, Series B*, 64(10), pp. 307–310. doi: 10.2183/pjab.64.307.

Shopfner, C. E. (1966) 'Periosteal bone growth in normal infants: a preliminary report', *American Journal of Roentgenology*, 97(1), pp. 154–163.

Sierant, M. L. and Bartlett, J. D. (2012) 'Stress response pathways in ameloblasts: implications for amelogenesis and dental fluorosis', *Cells*, 1(3), pp. 631–645. doi: 10.3390/cells1030631.

Silva, G. A. B., Moreira, A. and Alves, J. B. (2011) 'Histological processing of teeth and periodontal tissues for light microscopy analysis.', in *Light microscopy*. Totowa, NJ: Humana Press, pp. 19–36. doi: 10.1007/978-1-60761-950-5_2.

Skedros, J. G., Hunt, K. J., *et al.* (2003) 'Ontogenetic and regional morphologic variations in the turkey ulna diaphysis: implications for functional adaptation of cortical bone', *The Anatomical Record*, 273A(1), pp. 609–629. doi: 10.1002/ar.a.10073.

Skedros, J. G., Sybrowsky, C. L., *et al.* (2003) 'Regional differences in cortical bone organization and microdamage prevalence in Rocky Mountain mule deer', *The Anatomical Record*, 274A(1), pp. 837–850. doi: 10.1002/ar.a.10102.

Skedros, J. G., Knight, A. N., *et al.* (2013) 'Scaling of Haversian canal surface area to secondary osteon bone volume in ribs and limb bones', *American Journal of Physical Anthropology*, 151(2), pp. 230–244. doi: 10.1002/ajpa.22270.

Skedros, J. G., Keenan, K. E., *et al.* (2013) 'Secondary osteon size and collagen/lamellar organization ("osteon morphotypes") are not coupled, but potentially adapt independently for local strain mode or magnitude', *Journal of Structural Biology*, 181(2), pp. 95–107. doi: 10.1016/j.jsb.2012.10.013.

Skedros, J. G. *et al.* (2018) 'Sealed osteons in animals and humans: low prevalence and lack of relationship with age', *Journal of Anatomy*, 232(5), pp. 824–835.

Skedros, J. G. and Doutré, M. S. (2019) 'Uncertainties regarding the physical basis of lamellar bone periodicity in secondary osteons suggest that surrogates based on infilling/periodicity rates should be considered', in *Program of the 88th Annual Meeting of the American Association of Physical Anthropologists*. Cleveland, OH: Wiley-Liss Inc., pp. 230–231. doi: 10.1002/ajpa.23802.

Skedros, J. G., Hunt, K. J. and Bloebaum, R. D. (2004) 'Relationships of loading history and structural and material characteristics of bone: development of the mule deer calcaneus', *Journal of Morphology*, 259(3), pp. 281–307. doi: 10.1002/jmor.10167.

Skedros, J. G., Mason, M. W. and Bloebaum, R. D. (1994) 'Differences in osteonal micromorphology between tensile and compressive cortices of a bending skeletal system: indications of potential strain-specific differences in bone microstructure', *The Anatomical Record*, 239(4), pp. 405–413. doi: 10.1002/ar.1092390407.

Skedros, J. G., Mason, M. W. and Bloebaum, R. D. (2001) 'Modeling and remodeling in a developing artiodactyl calcaneus: a model for evaluating Frost's Mechanostat

hypothesis and its corollaries', *The Anatomical Record*, 263(2), pp. 167–185. doi: 10.1002/ar.1094.

Skobe, Z. (2006) 'SEM evidence that one ameloblast secretes one keyhole-shaped enamel rod in monkey teeth', *European Journal of Oral Sciences*, 114(s1), pp. 338–342. doi: 10.1111/j.1600-0722.2006.00305.x.

Smit, T. H., Burger, E. H. and Huyghe, J. M. (2002) 'A case for strain-induced fluid flow as a regulator of bmu-coupling and osteonal alignment', *Journal of Bone and Mineral Research*, 17(11), pp. 2021–2029. doi: 10.1359/jbmr.2002.17.11.2021.

Smith, B. H. (1991) 'Standards of human tooth formation and dental age assessment', in Kelley, M. and Larsen, C. S. (eds) *Advances in dental anthropology*. New York: Wiley-Liss Inc., pp. 143–168.

Smith, T. M. *et al.* (2003) 'Molar crown formation in Miocene hominoids: a preliminary synthesis.', in *Program of the 72nd Annual Meeting of the American Association of Physical Anthropologists*. Tempe, AZ: Wiley-Liss Inc., p. 196. doi: 10.1002/ajpa.10252.

Smith, T. M. (2006) 'Experimental determination of the periodicity of incremental features in enamel', *Journal of Anatomy*, 208(1), pp. 99–113. doi: 10.1111/j.1469-7580.2006.00499.x.

Smith, T. M. *et al.* (2007) 'New perspectives on chimpanzee and human molar crown development', in Bailey, S. E. and Hublin, J. J. (eds) *Dental perspectives on human evolution: state of the art research in dental paleoanthropology*. Dordrecht: Springer, pp. 177–192.

Smith, T. M. (2008) 'Incremental dental development: methods and applications in hominoid evolutionary studies', *Journal of Human Evolution*, 54(2), pp. 205–224.

Snape, M. and Bidwell, P. (2002) 'Excavations at Castle Garth, Newcastle upon Tyne, 1976–92 and 1995–6: the excavation of the Roman fort', *Archaeologia Aeliana*. (5th), 31, pp. 1–249.

Spall, C. A. and Toop, N. J. (2005) *Blue Bridge Lane and Fishergate House, York. Report on excavations: July 2000 to July 2002*. York: Archaeological Planning Consultancy, Ltd.

Speakman, J. R. (2005) 'Body size, energy metabolism and lifespan', *Journal of Experimental Biology*, 208(9), pp. 1717–1730. doi: 10.1242/jeb.01556.

Specker, B. and Vukovich, M. (2007) 'Evidence for an Interaction between exercise and nutrition for improved bone health during growth', in Daly, R. M. and Petit, M. A. (eds) *Medicine and sport science*. Basel: Karger, pp. 50–63. doi: 10.1159/000103004.

Srinivasan, S. *et al.* (2002) 'Low-magnitude mechanical loading becomes osteogenic when rest is inserted between each load cycle', *Journal of Bone and Mineral Research*, 17(9), pp. 1613–1620. doi: 10.1359/jbmr.2002.17.9.1613.

Stearns, S. C. (1989) 'Trade-offs in life-history evolution', *Functional Ecology*, 3(3), pp. 259–268.

Stewart, M. C. *et al.* (2015) 'Intraskeletal variability of relative cortical area in humans', *The Anatomical Record*, 298(9), pp. 1635–1643. doi: 10.1002/ar.23181.

Stewart, N. A. *et al.* (2017) 'Sex determination of human remains from peptides in tooth enamel', *Proceedings of the National Academy of Sciences*, 114(52), pp. 13649–13654. doi: 10.1073/pnas.1714926115.

Stone, D. (2006) 'The consumption of field crops in late Medieval England', in Woolgar, C. M., Serjeantson, D., and Waldron, T. (eds) *Food in Medieval England: diet and nutrition*. Oxford: Oxford University Press, pp. 11–26.

Stone, R. J. and Stone, J. A. (2003) *Atlas of skeletal muscles*. McGraw-Hill.

Storm, T. *et al.* (1993) 'Changes in bone histomorphometry after long-term treatment with intermittent, cyclic etidronate for postmenopausal osteoporosis', *Journal of Bone and Mineral Research*, 8(2), pp. 199–208. doi: 10.1002/jbmr.5650080211.

Stout, S. D. and Crowder, C. M. (2012) 'Bone remodeling, histomorphology, and histomorphometry', in Crowder, C. M. and Stout, S. D. (eds) *Bone histology – An anthropological perspective*. Boca Raton: CRC Press, pp. 1–21.

Stout, S. D. and Lueck, R. (1995) 'Bone remodeling rates and skeletal maturation in three archaeoloqical skeletal populations', *American Journal of Physical Anthropology*, 98(2), pp. 161–171. doi: 10.1002/ajpa.1330980206.

Stout, S. D. and Paine, R. R. (1992) 'Histological age estimation using rib and clavicle', *American Journal of Physical Anthropology*, 87(1), pp. 111–115. doi: 10.1002/ajpa.1330870110.

Stout, S. D., Porro, M. A. and Perotti, B. (1996) 'Brief communication: a test and correction of the clavicle method of Stout and Paine for histological age estimation of

skeletal remains', *American Journal of Physical Anthropology*, 100(1), pp. 139–142. doi: 10.1002/(SICI)1096-8644(199605)100:1<139::AID-AJPA12>3.0.CO;2-1.

Streeter, M. (2010) 'A four-stage method of age at death estimation for use in the subadult rib cortex', *Journal of Forensic Sciences*, 55(4), pp. 1019–1024. doi: 10.1111/j.1556-4029.2010.01396.x.

Streeter, M. A. (2005) *Histomorphometric characteristics of the subadult rib cortex: normal patterns of dynamic bone modeling and remodeling during growth and development*. PhD Thesis. University of Missouri-Columbia.

Stroud, G. and Kemp, R. L. (1993) *Cemetery of St. Andrew Fishergate*. London: Current British Archaeology.

Sugawara, Y. *et al.* (2013) 'The early mouse 3D osteocyte network in the presence and absence of mechanical loading', *Bone*, 52(1), pp. 189–196. doi: 10.1016/j.bone.2012.09.033.

Swales, D. L. M. (2013) *Life stress: a bio-cultural investigation into the later Anglo-Saxon population of the Black Gate Cemetery.* PhD Thesis. University of Sheffield.

Sykes, N. (2006) 'From cu and sceap to beffe and motton', in Woolgar, C. M., Serjeantson, D., and Waldron, T. (eds) *Food in Medieval England: diet and nutrition*. Oxford: Oxford University Press, pp. 56–71.

Takahashi, H., Epker, B. and Frost, H. M. (1965) 'Relation between age and size of osteons in man', *Henry Ford Hospital Medical Bulletin*, 13, pp. 25–31.

Takahashi, H. and Frost, H. M. (1966) 'Age and sex related changes in the amount of cortex of normal human ribs', *Acta Orthopaedica Scandinavica*, 37(2), pp. 122–130. doi: 10.3109/17453676608993272.

Tan, S. H. X., Sim, Y. F. and Hsu, C.-Y. S. (2017) 'Difference in striae periodicity of Heilongjiang and Singaporean Chinese teeth', *Frontiers in Physiology*, 8, p. 442. doi: 10.3389/fphys.2017.00442.

Tang, Y. *et al.* (2009) 'TGF-β1–induced migration of bone mesenchymal stem cells couples bone resorption with formation', *Nature Medicine*, 15(7), pp. 757–765. doi: 10.1038/nm.1979.

Tanner, J. M. (1951) 'Some notes on the reporting of growth data', *Human Biology*, 23(2), p. 93.

Tanner, J. M. (1981) *A history of the study of human growth*. Cambridge University Press.

Tanner, J. M. and Cameron, N. (1980) 'Investigation of the mid-growth spurt in height, weight and limb circumferences in single-year velocity data from the London 1966–67 growth survey', *Annals of Human Biology*, 7(6), pp. 565–577. doi: 10.1080/03014468000004681.

Tanner, J. M., Whitehouse, R. H. and Takaishi, M. (1966) 'Standards from birth to maturity for height, weight, height velocity, and weight velocity: British children, 1965. II.', *Archives of Disease in Childhood*, 41(220), pp. 613–635. doi: 10.1136/adc.41.220.613.

Tatton-Brown, T. (1995) 'The beginnings of St. Gregory's Priory and St. John's Hospital in Canterbury', in *Canterbury and the Norman Conquest: churches, saints and scholars, 1066*. Hambledon Continuum.

Tommasini, S. M., Nasser, P. and Jepsen, K. J. (2007) 'Sexual dimorphism affects tibia size and shape but not tissue-level mechanical properties', *Bone*, 40(2), pp. 498–505. doi: 10.1016/j.bone.2006.08.012.

Tommerup, L. J. *et al.* (1993) 'Does weight-bearing exercise affect non-weight-bearing bone?', *Journal of Bone and Mineral Research*, 8(9), pp. 1053–1058. doi: 10.1002/jbmr.5650080905.

Totland, G. K. *et al.* (2011) 'Sustained swimming increases the mineral content and osteocyte density of salmon vertebral bone', *Journal of Anatomy*, 219(4), pp. 490–501. doi: 10.1111/j.1469-7580.2011.01399.x.

Trueta, J. (1963) 'The role of the vessels in osteogenesis', *The Journal of Bone and Joint Surgery. British volume*, 45-B(2), pp. 402–418. doi: 10.1302/0301-620X.45B2.402.

Ural, A. and Vashishth, D. (2006) 'Interactions between microstructural and geometrical adaptation in human cortical bone', *Journal of Orthopaedic Research*, 24(7), pp. 1489–1498. doi: 10.1002/jor.20159.

Vaananen, H. K. *et al.* (2000) 'The cell biology of osteoclast function', *Journal of Cell Science*, 113(3), pp. 377–381.

Vercellotti, G. *et al.* (2011) 'Intrapopulation variation in stature and body proportions: social status and sex differences in an Italian medieval population (Trino Vercellese,

VC)', *American Journal of Physical Anthropology*, 145(2), pp. 203–214. doi: 10.1002/ajpa.21486.

Vicente-Rodríguez, G. *et al.* (2008) 'Independent and combined effect of nutrition and exercise on bone mass development', *Journal of Bone and Mineral Metabolism*, 26(5), pp. 416–424. doi: 10.1007/s00774-007-0846-9.

Villa, C. and Lynnerup, N. (2010) 'Technical note: a stereological analysis of the cross-sectional variability of the femoral osteon population', *American Journal of Physical Anthropology*, 142(3), pp. 491–496. doi: 10.1002/ajpa.21269.

Vrba, E. and Grine, F. (1978) 'Australopithecine enamel prism patterns', *Science*, 202(4370), pp. 890–892. doi: 10.1126/science.102032.

Waldron, T. (2009) *Palaeopathology*. Cambridge University Press.

Wall, C. E. (1991) 'Evidence of weaning stress and catch-up growth in the long bones of a central California Amerindian sample', *Annals of Human Biology*, 18(1), pp. 9–22. doi: 10.1080/03014469100001362.

Wallace, I. J. *et al.* (2012) 'Genetic variations and physical activity as determinants of limb bone morphology: an experimental approach using a mouse model', *American Journal of Physical Anthropology*, 148(1), pp. 24–35. doi: 10.1002/ajpa.22028.

Warshawsky, H. *et al.* (1981) 'The development of enamel structure in rat incisors as compared to the teeth of monkey and man', *The Anatomical Record*, 200(4), pp. 371–399.

Watts, R. (2015) 'The long-term impact of developmental stress. Evidence from later Medieval and post-Medieval London (AD1117-1853)', *American Journal of Physical Anthropology*, 158(4), pp. 569–580. doi: 10.1002/ajpa.22810.

Weber, D. F. and Ashrafi, S. H. (1979) 'Structure of Retzius lines in partially demineralized human enamel', *The Anatomical Record*, 194(4), pp. 563–569. doi: 10.1002/ar.1091940409.

White, T. D., Black, M. T. and Folkens, P. A. (2011) *Human osteology*. 3rd edn. Academic press.

Wighton, A. H. J., Jones, C. G. and Bell, L. S. (2012) 'Plastic embedding and polishing of bone for reflected light and electron microscopy', *Methods in molecular biology*, 915, pp. 21–36. doi: 10.1007/978-1-61779-977-8_2.

Wilson, D. F. and Shroff, F. R. (1970) 'The nature of the striae of Retzius as seen with the optical microscope', *Australian Dental Journal*, 15(3), pp. 162–171.

Witzel, C. *et al.* (2008) 'Insights from the inside: histological analysis of abnormal enamel microstructure associated with hypoplastic enamel defects in human teeth', *American Journal of Physical Anthropology*, 136(4), pp. 400–414. doi: 10.1002/ajpa.20822.

Wojda, S. J. *et al.* (2013) 'Black bears with longer disuse (hibernation) periods have lower femoral osteon population density and greater mineralization and intracortical porosity', *The Anatomical Record*, 296(8), pp. 1148–1153. doi: 10.1002/ar.22720.

Wolff, J. L. (1892) *The law of bone remodelling. Translated by Maquet P, Furlong R, in 1986*. Berlin: Springer-Verlag.

Wood, J. W. *et al.* (1992) 'The osteological paradox: problems of inferring prehistoric health from skeletal samples [and comments and reply]', *Current Anthropology*, 33(4), pp. 343–370. doi: 10.1086/204084.

Woolgar, C. M. (2006) 'Group diets in late Medieval England', in Woolgar, C. M., Serjeantson, D., and Waldron, T. (eds) *Food in Medieval England: diet and nutrition*. Oxford: Oxford University Press, pp. 191–200.

Woolgar, C. M., Serjeantson, D. and Waldron, T. (2006) *Food in Medieval England: diet and nutrition*. Oxford: Oxford University Press.

Wu, K. *et al.* (1970) 'Haversian bone formation rates determined by a new method in a mastodon, and in human diabetes mellitus and osteoporosis', *Calcified Tissue Research*, 6(1), pp. 204–219. doi: 10.1007/BF02196201.

Yamada, S., Tadano, S. and Fujisaki, K. (2011) 'Residual stress distribution in rabbit limb bones', *Journal of Biomechanics*, 44(7), pp. 1285–1290. doi: 10.1016/j.jbiomech.2011.01.038.

Yoshino, M. *et al.* (1994) 'Histological estimation of age at death using microradiographs of humeral compact bone', *Forensic Science International*, 64(2–3), pp. 191–198. doi: 10.1016/0379-0738(94)90231-3.

Young, D. R. *et al.* (1986) 'Immobilization-associated osteoporosis in primates', *Bone*, 7(2), pp. 109–117. doi: 10.1016/8756-3282(86)90682-4.

Zhu, W., Robey, P. G. and Boskey, A. L. (2009) ‘The regulatory role of matrix proteins in mineralization of bone’, in Marcus, R. et al. (eds) *Fundamentals of osteoporosis*. San Diego: Elsevier Academic Press, pp. 153–202.

Zoetis, T. *et al.* (2003) ‘Species comparison of postnatal bone growth and development’, *Birth Defects Research Part B: Developmental and Reproductive Toxicology*, 68(2), pp. 86–110. doi: 10.1002/bdrb.10012.

Appendix A

Table A.A.1 *Sample*

Site	SK number	Age-at-death	Age group	Bone sampled	Tooth sampled
NGB	5	14	Adolescent (13-18)	Humerus	Maxillary 1st Molar
NGB	15	18	Adolescent (13-18)	Rib	Maxillary 1st Molar
NGB	17	5	Young child (3-7)	Humerus	Maxillary 1st Molar
NGB	21	6	Old child (8-12)	Humerus	Maxillary 1st Incisor
NGB	25	3	Young child (3-7)	Humerus	Maxillary 1st Molar
NGB	26	4	Young child (3-7)	Humerus	Maxillary 1st Molar
NGB	29	4	Young child (3-7)	Rib	Maxillary 1st Molar
NGB	30	18	Adolescent (13-18)	Rib	Maxillary 1st Molar
NGB	32	3	Young child (3-7)	Rib	Mandibular 1st Molar
NGB	40	5	Young child (3-7)	Humerus	Mandibular 1st Molar
NGB	41	17	Adolescent (13-18)	Rib	Maxillary 1st Incisor
NGB	42	11	Old child (8-12)	Humerus	Maxillary 1st Molar
NGB	44	8	Old child (8-12)	Humerus	Mandibular 1st Molar
NGB	52	18	Adolescent (13-18)	Rib	Mandibular 2nd Molar
NGB	57	3	Young child (3-7)	Humerus	Maxillary 1st Molar
NGB	78	9	Old child (8-12)	Humerus	Mandibular 1st Molar
NGB	83	4	Young child (3-7)	Humerus	Mandibular 1st Molar
NGB	88	8	Old child (8-12)	Rib	Mandibular 1st Molar
NGB	90	14	Adolescent (13-18)	Humerus	Maxillary 2nd Molar
NGA	10	14	Adolescent (13-18)	Humerus	Mandibular 1st Molar
NGA	17	10	Old child (8-12)	Humerus	Maxillary 1st Molar
NGA	27	11	Old child (8-12)	Humerus	Mandibular 1st Molar
NGA	31	3	Young child (3-7)	Rib	Maxillary 1st Molar
NGA	34	15	Adolescent (13-18)	Rib	Maxillary 1st Molar
NGA	40	3	Young child (3-7)	Rib	Mandibular 1st Molar
NGA	46	4	Young child (3-7)	Humerus	Mandibular 1st Molar
NGA	47	18	Adolescent (13-18)	Rib	Mandibular 2nd Molar
NGA	49	9	Old child (8-12)	Humerus	Mandibular 1st Molar
NGA	59	4	Young child (3-7)	Rib	Maxillary 1st Incisor
NGA	73	3	Young child (3-7)	Rib	Maxillary 1st Molar
NGA	82	9	Old child (8-12)	Humerus	Mandibular 1st Molar
NGA	84	14	Adolescent (13-18)	Humerus	Mandibular 1st Molar
NGA	97	12	Old child (8-12)	Humerus	Maxillary 2nd Molar
NGA	102	3	Young child (3-7)	Humerus	Maxillary 1st Molar
NGA	107	5	Young child (3-7)	Humerus	Maxillary 1st Molar

Site	SK number	Age-at-death	Age group	Bone sampled	Tooth sampled
NGA	117	3	Young child (3-7)	Humerus	Maxillary 1st Molar
NGA	121	5	Young child (3-7)	Humerus	Mandibular 1st Molar
NGA	123	14	Adolescent (13-18)	Humerus	Mandibular 1st Molar
NGA	127	11	Old child (8-12)	Rib	Mandibular 1st Molar
NGA	130	17	Adolescent (13-18)	Rib	Mandibular 1st Molar
NGA	142	13	Adolescent (13-18)	Humerus	Mandibular 1st Molar
NGA	145	13	Adolescent (13-18)	Rib	Maxillary 1st Molar
NGA	150	4	Young child (3-7)	Humerus	Maxillary 1st Molar
NGA	154	4	Young child (3-7)	Rib	Mandibular 1st Molar
NGA	168	15	Adolescent (13-18)	Rib	Mandibular 1st Molar
NGA	174	3	Young child (3-7)	Rib	Maxillary 1st Molar
NGA	176	13	Adolescent (13-18)	Rib	Maxillary 2nd Molar
NGA	178	3	Young child (3-7)	Humerus	Maxillary 1st Molar
NGA	206	3	Young child (3-7)	Humerus	Mandibular 1st Molar
NGA	214	11	Old child (8-12)	Humerus	Maxillary 1st Molar
NGA	219	13	Adolescent (13-18)	Rib	Maxillary 1st Molar
NGA	230	9	Old child (8-12)	Humerus	Maxillary 1st Molar
NGA	232	6	Young child (3-7)	Humerus	Mandibular 1st Molar
NGA	233	16	Adolescent (13-18)	Humerus	Maxillary 1st Molar
NGA	235	5	Young child (3-7)	Humerus	Maxillary 1st Molar
NGA	240	10	Old child (8-12)	Rib	Maxillary 1st Molar
NGA	253	10	Old child (8-12)	Humerus	Mandibular 1st Molar
NGA	257	9	Old child (8-12)	Rib	Mandibular 1st Molar
NGA	260	6	Young child (3-7)	Rib	Maxillary 1st Molar
NGA	261	6	Young child (3-7)	Humerus	Mandibular 1st Molar
NGA	269	8	Old child (8-12)	Humerus	Mandibular 1st Molar
NGA	282	5	Young child (3-7)	Humerus	Maxillary 1st Molar
NGA	286	8	Old child (8-12)	Humerus	Mandibular 1st Molar
NGA	319	17	Adolescent (13-18)	Humerus	Mandibular 1st Molar
NGA	339	11	Old child (8-12)	Humerus	Maxillary 2nd Molar
NGA	360	8	Old child (8-12)	Humerus	Mandibular 1st Molar
NGA	363	4	Young child (3-7)	Humerus	Mandibular 1st Molar
NGA	364	10	Old child (8-12)	Rib	Maxillary 1st Molar
NGA	373	3	Young child (3-7)	Humerus	Maxillary 1st Molar
NGA	374	5	Young child (3-7)	Rib	Maxillary 1st Molar
NGA	376	17	Adolescent (13-18)	Humerus	Mandibular 1st Molar
NGA	389	10	Old child (8-12)	Humerus	Mandibular 1st Molar
NGA	417	6	Young child (3-7)	Rib	Mandibular 1st Molar
NGA	447	11	Old child (8-12)	Rib	Mandibular 1st Molar

Site	SK number	Age-at-death	Age group	Bone sampled	Tooth sampled
NGA	462	17	Adolescent (13-18)	Humerus	Maxillary 1st Molar
NGA	492	4	Young child (3-7)	Humerus	Mandibular 1st Molar
NGA	494	19	Adolescent (13-18)	Rib	Mandibular 2nd Molar
NGA	495	4	Young child (3-7)	Rib	Maxillary 1st Molar
NGA	515		Young adult	Multiple	Maxillary 1st Molar
NGA	516	3	Young child (3-7)	Humerus	Maxillary 1st Molar
NGA	585	19	Adolescent (13-18)	Rib	Maxillary 1st Molar
NGA	607	9	Old child (8-12)	Rib	Maxillary 1st Molar
NGA	620	12	Old child (8-12)	Humerus	Mandibular 2nd Molar
NGA	631	4	Young child (3-7)	Humerus	Maxillary 1st Molar
NGA	655	18	Adolescent (13-18)	Rib	Maxillary 1st Molar
NGA	665	3	Young child (3-7)	Humerus	Mandibular 1st Molar
NGA	666	14	Adolescent (13-18)	Rib	Maxillary 1st Molar
NGA	671	7	Young child (3-7)	Rib	Maxillary 1st Molar
NGA	703		Young adult	Multiple	Mandibular 2nd Molar
NGA	707	16	Adolescent (13-18)	Humerus	Mandibular 1st Molar
NGA	708	13	Adolescent (13-18)	Rib	Mandibular 2nd Molar
NGA	716	7	Young child (3-7)	Humerus	Maxillary 1st Molar
NGA	727		Young adult	Multiple	Maxillary 2nd Molar
NGA	730	5	Young child (3-7)	Humerus	Maxillary 1st Molar
NGA	736	7	Young child (3-7)	Humerus	Mandibular 1st Molar
NGA	739	9	Old child (8-12)	Humerus	Mandibular 1st Molar
NGA	747		Young adult	Multiple	Maxillary 2nd Molar
NGA	753	4	Young child (3-7)	Humerus	Maxillary 1st Molar
NGA	760	14	Adolescent (13-18)	Humerus	Mandibular 1st Molar
NGA	762	15	Adolescent (13-18)	Rib	Maxillary 1st Molar
NGA	778	17	Adolescent (13-18)	Rib	Maxillary 1st Molar
NGA	779	8	Old child (8-12)	Rib	Maxillary 1st Molar
NGA	781	4	Young child (3-7)	Humerus	Maxillary 1st Molar
NGA	782	7	Young child (3-7)	Humerus	Mandibular 1st Molar
NGA	789	13	Adolescent (13-18)	Rib	Maxillary 3rd Molar
NGA	796	13	Adolescent (13-18)	Humerus	Mandibular 2nd Molar
NGA	799	7	Young child (3-7)	Rib	Maxillary 1st Molar
NGA	800	8	Old child (8-12)	Rib	Maxillary 1st Molar
NGA	801	7	Young child (3-7)	Humerus	Maxillary 1st Molar
NGA	802	4	Young child (3-7)	Humerus	Mandibular 1st Molar
NGA	812	5	Young child (3-7)	Rib	Maxillary 1st Molar
NGA	819	10	Old child (8-12)	Rib	Maxillary 1st Molar
NGA	823	5	Young child (3-7)	Rib	Mandibular 1st Molar

Site	SK number	Age-at-death	Age group	Bone sampled	Tooth sampled
NGA	859	8	Old child (8-12)	Humerus	Maxillary 1st Molar
NGA	860	14	Adolescent (13-18)	Humerus	Maxillary 1st Molar
NGA	863		Young adult	Multiple	Mandibular 2nd Molar
NGA	885	4	Young child (3-7)	Rib	Maxillary 1st Molar
NGA	889	13	Adolescent (13-18)	Rib	Maxillary 2nd Molar
NGA	901		Young adult	Multiple	Mandibular 2nd Molar
NGA	917		Young adult	Multiple	Maxillary 2nd Molar
NGA	960	4	Young child (3-7)	Humerus	Mandibular 1st Molar
NGA	962	18	Adolescent (13-18)	Rib	Maxillary 1st Molar
NGA	1029	7	Young child (3-7)	Humerus	Mandibular 1st Molar
NGA	1030	17	Adolescent (13-18)	Humerus	Mandibular 1st Molar
NGA	1061	5	Young child (3-7)	Humerus	Maxillary 1st Molar
NGA	1095	8	Old child (8-12)	Rib	Maxillary 1st Molar
NGA	1119	17	Adolescent (13-18)	Humerus	Mandibular 2nd Molar
NGA	1122		Young adult	Multiple	Mandibular 2nd Molar
NGA	1139	10	Old child (8-12)	Humerus	Mandibular 1st Molar
NGA	1165		Young adult	Multiple	Maxillary 2nd Molar
NGA	1196	5	Young child (3-7)	Rib	Mandibular 1st Incisor
NGA	1216		Young adult	Multiple	Mandibular 2nd Molar
NGA	1241	6	Young child (3-7)	Rib	Mandibular 1st Molar
NGA	1242	8	Old child (8-12)	Rib	Mandibular 1st Molar
NGA	1244	5	Young child (3-7)	Rib	Mandibular 1st Molar
YFH	7	8	Old child (8-12)	Rib	Mandibular 1st Molar
YFH	12	5	Young child (3-7)	Rib	Mandibular 1st Molar
YFH	16	5	Young child (3-7)	Rib	Mandibular 1st Molar
YFH	36	17	Adolescent (13-18)	Rib	Maxillary 1st Molar
YFH	46	12	Old child (8-12)	Rib	Mandibular 1st Molar
YFH	56	11	Old child (8-12)	Rib	Mandibular 2nd Molar
YFH	65	3	Young child (3-7)	Rib	Maxillary 1st Molar
YFH	85	9	Old child (8-12)	Rib	Mandibular 1st Molar
YFH	93	7	Young child (3-7)	Rib	Maxillary 1st Molar
YFH	95	4	Young child (3-7)	Rib	Maxillary 1st Molar
YFH	97	11	Old child (8-12)	Rib	Maxillary 1st Molar
YFH	117	12	Old child (8-12)	Rib	Maxillary 1st Molar
YFH	122	5	Young child (3-7)	Rib	Maxillary 1st Molar
YFH	128	6	Young child (3-7)	Rib	Maxillary 1st Molar
YFH	137	10	Old child (8-12)	Rib	Maxillary 1st Molar
YFH	142	16	Adolescent (13-18)	Rib	Maxillary 2nd Molar
YFH	153	10	Old child (8-12)	Rib	Mandibular 1st Molar

Site	SK number	Age-at-death	Age group	Bone sampled	Tooth sampled
YFH	174	15	Adolescent (13-18)	Rib	Mandibular 1st Molar
YFH	250	16	Adolescent (13-18)	Rib	Maxillary 1st Molar
YFH	307	14	Adolescent (13-18)	Rib	Maxillary 1st Molar
YFB	2057	14	Adolescent (13-18)	Humerus	Maxillary 1st Molar
YFB	2283	17	Adolescent (13-18)	Humerus	Mandibular 1st Molar
YFB	2329	4	Young child (3-7)	Humerus	Maxillary 1st Molar
YFB	2765	9	Old child (8-12)	Humerus	Maxillary 1st Molar
YFB	2775	11	Old child (8-12)	Humerus	Maxillary 1st Molar
YFB	2824	7	Young child (3-7)	Humerus	Mandibular 1st Molar
YFB	3296	15	Adolescent (13-18)	Humerus	Maxillary 1st Molar
YFB	3413	9	Old child (8-12)	Humerus	Maxillary 1st Molar
YFB	3580	11	Old child (8-12)	Humerus	Mandibular 1st Molar
YFB	3664	13	Adolescent (13-18)	Humerus	Mandibular 1st Molar
YFB	3689	15	Adolescent (13-18)	Humerus	Mandibular 1st Molar
YFB	3807	12	Old child (8-12)	Humerus	Maxillary 1st Molar
YFB	4067	12	Old child (8-12)	Humerus	Maxillary 1st Molar
BGN	26	17	Adolescent (13-18)	Humerus	Maxillary 1st Molar
BGN	48	7	Young child (3-7)	Humerus	Maxillary 1st Molar
BGN	96	14	Adolescent (13-18)	Humerus	Mandibular 1st Molar
BGN	103	4	Young child (3-7)	Humerus	Maxillary 1st Molar
BGN	132	17	Adolescent (13-18)	Humerus	Maxillary 1st Molar
BGN	138	5	Young child (3-7)	Humerus	Maxillary 1st Molar
BGN	187	12	Old child (8-12)	Humerus	Mandibular 1st Molar
BGN	231	5	Young child (3-7)	Humerus	Maxillary 1st Molar
BGN	248	7	Young child (3-7)	Humerus	Maxillary 1st Molar
BGN	274	9	Old child (8-12)	Humerus	Maxillary 1st Molar
BGN	365	6	Young child (3-7)	Humerus	Mandibular 1st Molar
BGN	412	6	Young child (3-7)	Humerus	Maxillary 1st Molar
BGN	570	15	Adolescent (13-18)	Humerus	Maxillary 1st Molar
BGN	575	11	Old child (8-12)	Humerus	Maxillary 2nd Molar
BGN	576	15	Adolescent (13-18)	Humerus	Maxillary 1st Molar
BGN	601	9	Old child (8-12)	Humerus	Maxillary 1st Molar
BGN	624	11	Old child (8-12)	Humerus	Maxillary 1st Molar

Appendix B

Table A.B.1 *Paired correlations with paired samples t-test for intra-observer error testing*

	N	r^2	*p*	t	df	*p*
OPD	19	0.749	<0.01**	-0.077	18	0.94
N.On	19	0.645	<0.01**	-0.995	18	0.33
N.On.Fg	19	0.921	<0.01**	1.912	18	0.07
On.Ar	19	0.633	<0.01**	-0.691	18	0.50
On.Dm	19	0.507	0.03*	0.131	18	0.90
On.Cr	19	0.125	0.61	-0.091	18	0.93
H.Ca.Ar	19	0.766	<0.01**	0.105	18	0.92
H.Ca.Dm	19	0.535	0.02*	1.230	18	0.24
Re.On.Ar	19	0.566	0.01**	-0.708	18	0.49
P.On.Dn	19	0.577	0.01**	-0.295	18	0.77

† Statistical significance value: *p<0.05, **p<0.01.

Table A.B.2 *Paired correlations with paired samples t-test for inter-observer error testing*

	N	r^2	*p*	t	df	*p*
RP	10	0.881	0.01**	0.361	9	0.73
OPD	10	0.652	0.04*	1.225	9	0.25
N.On	10	0.477	0.16	0.513	9	0.62
N.On.Fg	10	0.365	0.30	1.644	9	0.14
On.Ar	10	-0.038	0.92	0.242	9	0.81
On.Dm	10	-0.044	0.91	0.523	9	0.61
On.Cr	10	0.175	0.63	0.968	9	0.36
H.Ca.Ar	10	0.343	0.33	0.647	9	0.53
H.Ca.Dm	10	0.032	0.93	0.206	9	0.84
Re.On.Ar	10	-0.165	0.65	-0.404	9	0.70
P.On.Dn	10	0.322	0.36	0.127	9	0.90

† Statistical significance value: *p<0.05, **p<0.01.

Appendix C

PRELIMINARY STUDY: DOES LINEAR ENAMEL HYPOPLASIA AFFECT THE APPEARANCE OF INCREMENTAL MARKINGS?

A.C.1 | Introduction

Childhood physiological stress can cause hypoplastic defects in enamel formation that appear macroscopically on the tooth surface (Hillson, 1992; Reid and Dean, 2000; Guatelli-Steinberg, 2001). They can be divided into three classes according to their morphology; furrow-form, pit-form, and plane-form (Hillson, 2014). Furrow-form defects, also known as linear enamel hypoplasia (LEH), are the most commonly reported type of hypoplastic defect (Hillson and Bond, 1997; Griffin and Donlon, 2009). The LEH defects are caused by a systemic pause in the enamel secretion of all active ameloblasts so that the defect will be seen in all concurrently forming enamel along the tooth row (Hillson, 2014). Other types of hypoplastic defects and isolated furrow-form defects are formed by local pauses in ameloblast activity (Hillson, 2014). Hypoplastic defects can only form during the juvenile period while the enamel is still forming, but they are retained permanently on the enamel surface and are usually most evident on the labial sides of the incisors and canines.

Attempts have been made to link LEH to a range of specific causes including juvenile malnutrition and disease (Goodman and Armelagos, 1988), weaning (Blakey, Leslie and Reidy, 1994; Moggi-Cecchi, Pacciani and Pinto-Cisternas, 1994), and socio-economic status (May, Goodman and Meindl, 1993; Miszkiewicz, 2015b). These aetiologies lead to non-specific LEH development by causing a general disruption to the cells that are responsible for growth, which include secretory ameloblasts. Linear enamel hypoplastic defects are often considered as non-specific indicators of stress due to the

difficulty of determining a specific cause for hypoplasia formation in archaeological examples (Rose, Armelagos and Lallo, 1978; Goodman, 1991).

The presence of LEH may complicate histological studies of enamel growth. During normal growth ameloblasts secrete enamel in cyclical rhythms, resulting in the formation of microscopic incremental lines within the enamel. A circadian rhythm of 24 hours produces short-period lines known as cross striations (Risnes, 1986; Bromage, 1991). A circa-septan rhythm of between six and 12 days, with a mode of eight days (Reid and Dean, 2006; Smith *et al.*, 2007), produces long-period lines that are known as Retzius lines (Retzius, 1837). Cross striations and Retzius lines are both used to measure enamel formation and tooth growth in histological studies and both types of incremental lines are formed by cyclical changes to ameloblast activity. It is possible that these incremental lines may be affected by the systemic disruption of ameloblast activity in LEH formation. Thus, it is necessary to clarify whether the formation of LEH can cause a change in the incremental markings within tooth enamel.

A.C.2 | Materials and Methods

Three erupted unworn permanent teeth were selected from archaeological human remains from the St Gregory's Priory, Canterbury, assemblage. Two were isolated mandibular canines that exhibited furrow-form defects (IT1 and IT2). It is unknown whether these defects were localised or systemic as there was no antimere available for comparison. The third tooth selected was a mandibular second incisor of an eight-year-old juvenile (SK82). This tooth had a furrow-form defect that was judged to be a systemic defect by the presence of corresponding defects on the other anterior teeth in the same mandible.

Histological slides were produced using standard methods (Mahoney, 2008). These methods are described above in section 2.6.2 and are briefly summarised here. The

teeth were embedded in resin (Buehler EpoxiCure®) and sectioned through the tip of the cusp and the dentine horn using a Buehler Isomet 1000 precision saw. The sections were fixed to glass microscope slides (Evo Stick® resin), ground with a series of grinding pads (P400, P600, P1200) (Buehler® EcoMet 300) to a final thickness of 50-100 μm, and polished with a 0.3 μm aluminium oxide powder (Buehler® Micro-Polish II). Each section was cleaned in an ultrasonic bath, dehydrated in 95-100% ethanol, cleared (Histoclear®), and mounted with a coverslip using a xylene-based mounting medium (DPX®).

The teeth were examined at 20x and 40x magnification with a 10x oculus using a high-powered microscope (Olympus® BX51) with a mounted camera (Olympus® DP25). Images of the teeth were obtained and examined in CELL® Live Biology imaging software. Each tooth was divided into thirds; cuspal – the upper third extending from the cusp tip, lateral – the central third, and cervical – the lower third extending to the cervix. In each third, the Retzius periodicity (RP) was calculated by counting the number of cross striations along an enamel prism between two adjacent Retzius lines that clearly emerged at the outer enamel surface. Local daily secretion rates (DSR) were also calculated in each third. The DSR is calculated by measuring between six cross striations and dividing the measurement by five to get a daily mean secretion rate. This process was repeated six times in each third so that a grand mean local DSR could be calculated (Mahoney, 2008). RP and DSR were calculated a further three times for each tooth, immediately before the LEH, during the defect, and immediately after the defect.

A.C.3 | Results

All three teeth display an overall reduction in DSR from the cuspal enamel to the cervical enamel (**Table A.C.1**). Additionally, the DSR showed changes associated with the LEH

in all the teeth. The DSR is reduced in the enamel of the defect as compared to the enamel immediately preceding the defect. The DSR increases immediately after the defect. In one tooth (IT1 PC_1) the DSR increases to a rate that is higher than the DSR before the defect. However, in SK82 PI_2 and IT2 PC_1, although the DSR increases from the mid-defect rate, it does not reach the pre-defect rate.

Table A.C.1 *Retzius periodicity and enamel daily secretion rate variation throughout the crowns of three permanent anterior mandibular teeth*

		SK82 (PI_2)	IT1 (PC_1)	IT2 (PC_1)
Cuspal Enamel	RP		6	11
	DSR		3.77	4.45
Lateral Enamel	RP	8	6	11
	DSR	4.56	3.75	4.41
Cervical Enamel	RP	8	6	11
	DSR	4.10	3.69	3.85
Enamel Before Defect	RP	8	6	11
	DSR	4.54	3.57	4.26
Enamel During Defect	RP	8	6	11
	DSR	3.51	3.36	3.57
Enamel After Defect	RP	10	8	11
	DSR	3.83	4.00	4.02

Retzius periodicity did not change for one tooth (IT2 PC_1). However, the RP did change across the LEH in the other two teeth (IT1 PC_1 and SK82 PI_2). In SK82 PI_2 the RP rose from 8 in the enamel before and during the defect to 10 in the enamel immediately after the defect. Similarly, In IT1 PC_1 the RP rose from 6 in the enamel before and during the defect to 8 in the enamel immediately after the defect.

A.C.4 | Discussion

The DSRs measured here suggests that enamel secretion rates slow during the formation of the defect and then rebound after the defect. Daily secretion rate decreases during hypoplastic defects because systemic stress alters the activity of the enamel-secreting

ameloblasts. Witzel *et al.* (2008) described a furrow-form defect in the enamel of a permanent mandibular first molar that showed a reduction in DSR within the defect. Although other teeth that were examined showed no change in DSR, indicating that there is some variation in how LEH are formed. The DSRs here show that enamel secretion increases after the defect, although the magnitude of this increase did vary. This finding could indicate that ameloblast activity rebounds after LEH, but the extent of the rebound varies.

Little is known about the underlying cause of Retzius line formation, but it is generally accepted that Retzius periodicity varies between individuals but remains constant along the tooth row within an individual (Mahoney, 2011, 2012; Hillson, 2014). Additional analysis showed that RP remained constant between a deciduous second molar and a permanent first molar from the same individual (Mahoney, 2012). However, there is growing evidence that RP can differ between deciduous and permanent dentition within individuals. Mahoney *et al.* (2017) found that RP changed between the deciduous maxillary second molar and the permanent maxillary first molar in four individuals. This study found that RP can vary across enamel defects within a tooth, but it does not always vary. These studies suggest that RP is more variable than previously thought.

The increase in RP seen in two of the teeth could indicate that RP is linked to enamel growth and under the control of a biorhythm. It is possible that the combined increase in DSR and RP after the LEH could indicate that ameloblasts deposit more enamel between each 'beat' of the biorhythm (Mahoney *et al.*, 2017). This could be considered as a period of 'catch-up' growth following the disturbance of ameloblast activity. Catch-up growth has previously been demonstrated in bones but not teeth (Tanner, 1981; Wall, 1991). Further investigation of the possible link between RP, enamel growth, and a biorhythm is needed.

A.C.5 | Conclusion and Implications for the Main Methodology

Evidence from this study indicates that the presence of LEH can affect the morphology of incremental lines in the enamel. The manifestation of cross striations is altered around the LEH because of a reduction in DSR during the defect and a subsequent increase in DSR after the defect. Additionally, the RP within a tooth can increase immediately after a LEH, but it does not always show a change. Consequently, skeletons with evidence of linear enamel hypoplasia on the teeth will not be selected for the following chapters.

Appendix D

Table A.D.1 *Mann-Whitney U test of side differences for the histological variables from the humerus with all ages pooled*

Variable	N	Right	Left	U	*p*
Ct.Wi (mm)	102	49.16	56.63	956.00	0.24
OPD	102	51.34	51.84	1109.00	0.94
N.On	102	34.71	40.30	476.00	0.29
N.On.Fg	102	35.93	37.72	535.50	0.72
On.Ar (μm^2)	93	49.56	41.89	802.50	0.20
On.Cr	93	48.52	43.97	867.00	0.44
On.Dm (μm)	93	46.60	46.31	939.50	0.96
H.Ca.Ar (μm^2)	93	45.12	50.76	844.50	0.34
H.Ca.Dm (μm)	93	46.02	47.44	916.50	0.81

† Statistical significance value: *$p < 0.05$, **$p < 0.01$.

Table A.D.2 *Kolmogorov-Smirnov tests of normality of the histological variables from the humerus and rib with all ages pooled*

	Humerus			Rib		
Variable	N	Z	*p*	N	Z	*p*
Ct.Wi (mm)	102	0.072	0.20			
Ct.Ar (mm^2)				73	0.105	0.20
OPD	102	0.113	<0.01**	73	0.064	0.20
N.On	102	0.166	<0.01**	73	0.094	0.20
N.On.Fg	102	0.282	<0.01**	73	0.154	<0.01**
On.Ar (μm^2)	93	0.060	0.20	70	0.078	0.20
Re.On.Ar (%)	93	0.208	<0.01**	70	0.126	<0.01**
On.Cr	93	0.101	0.02*	70	0.072	0.20
On.Dm (μm)	93	0.128	0.01**	70	0.112	0.03*
H.Ca.Ar (μm^2)	93	0.153	<0.01**	70	0.126	<0.01**
H.Ca.Dm (μm)	93	0.125	<0.01**	70	0.073	0.20

† Statistical significance value: *$p < 0.05$, **$p < 0.01$.

Table A.D.3 *Descriptive statistics (non-transformed) of the rib histological variables from high-status and low-status children from Canterbury, with Mann-Whitney U results comparing humerus histological variables from high-status and low-status children (3-12 yrs), younger children (3-7 yrs) and older children (8-12 yrs) from Canterbury*

		High-status			Low-status			
Age group	Variable	N	Mean	SD	N	Mean	SD	*p*
3-12 yrs	Ct.Ar (mm^2)	3	17.95	5.37	22	15.31	4.62	0.24
	Pr.Ca.Dn	3	5.47	2.37	28	4.77	3.68	0.29
	OPD	3	3.67	3.25	28	4.50	2.78	0.68
	N.On	3	2.97	2.10	28	2.84	2.30	0.91
	N.On.Fg	3	0.70	1.21	28	1.28	1.54	0.65
	On.Ar (μm^2)	3	31796.73	3158.91	25	38216.62	9744.50	0.17
	On.Cr	3	0.842	0.027	25	0.869	0.030	0.19
	On.Dm (μm)	3	163.57	14.90	25	184.35	29.94	0.17
	H.Ca.Ar (μm^2)	3	1469.49	376.20	25	1673.38	633.32	0.52
	H.Ca.Dm (μm)	3	33.79	6.04	25	36.66	6.12	0.67
3-7 yrs	Ct.Ar (mm^2)	2	16.03	5.96	14	13.50	3.89	0.42
	Pr.Ca.Dn	2	6.11	2.95	18	5.82	4.14	0.67
	OPD	2	1.85	1.10	18	3.82	2.93	0.44
	N.On	2	1.85	1.10	18	1.81	1.95	0.90
	N.On.Fg	2	0.00	0.00	18	1.10	1.94	0.58
	On.Ar (μm^2)	2	31610.20	4443.94	15	37058.34	8405.99	0.37
	On.Cr	2	0.840	0.038	15	0.866	0.025	0.37
	On.Dm (μm)	2	165.40	20.59	15	181.53	27.18	0.53
	H.Ca.Ar (μm^2)	2	1643.81	317.38	15	1583.93	376.72	0.82
	H.Ca.Dm (μm)	2	37.24	1.26	15	36.04	5.61	0.44
8-12 yrs	Ct.Ar (mm^2)	1	21.79		8	18.47	4.24	0.44
	Pr.Ca.Dn	1	4.18		10	2.89	1.50	0.55
	OPD	1	7.31		10	5.73	2.06	0.55
	N.On	1	5.22		10	4.38	1.99	0.86
	N.On.Fg	1	2.09		10	1.54	0.67	0.57
	On.Ar (μm^2)	1	32169.80		10	39954.03	11734.89	0.55
	On.Cr	1	0.846		10	0.874	0.038	0.36
	On.Dm (μm)	1	159.91		10	188.57	34.76	0.55
	H.Ca.Ar (μm^2)	1	1120.86		10	1807.55	903.05	0.36
	H.Ca.Dm (μm)	1	26.90		10	37.595	7.02	0.36

† Statistical significance value: $*p < 0.05$, $**p < 0.01$.

Appendix E

Table A.E.1 *Mann Whitney U of sex differences in the histological variables from the tibia, femora, metacarpals, radii, humeri, ribs, clavicles, and occipitals*

Variable	N	*U*	*p*	Variable	N	*U*	*p*
Tibia				**Humerus**			
N.On	10	9.000	0.47	N.On	10	9.500	0.53
N.On.Fg	10	11.000	0.75	N.On.Fg	10	11.000	0.75
OPD	10	10.000	0.60	OPD	10	9.500	0.53
On.Ar (μm^2)	10	9.000	0.47	On.Ar (μm^2)	10	12.000	0.92
Re.On.Ar (%)	10	7.000	0.25	Re.On.Ar (%)	10	5.500	0.12
H.Ca.Ar (μm^2)	10	7.000	0.25	H.Ca.Ar (μm^2)	10	8.000	0.35
Ot.Dn	10	4.000	0.08	Ot.Dn	10	9.000	0.47
Femur				**Rib**			
N.On	10	10.000	0.60	N.On	10	11.000	0.75
N.On.Fg	10	5.500	0.12	N.On.Fg	10	4.000	0.08
OPD	10	1.000	<0.02*	OPD	10	4.000	0.08
On.Ar (μm^2)	10	7.000	0.25	On.Ar (μm^2)	10	11.000	0.75
Re.On.Ar (%)	10	10.000	0.60	Re.On.Ar (%)	10	9.000	0.47
H.Ca.Ar (μm^2)	10	10.000	0.60	H.Ca.Ar (μm^2)	10	8.000	0.35
Ot.Dn	10	9.000	0.47	Ot.Dn	9	4.000	0.14
Metacarpal				**Clavicle**			
N.On	10	9.000	0.47	N.On	10	7.000	0.25
N.On.Fg	10	5.500	0.12	N.On.Fg	10	11.000	0.75
OPD	10	5.000	0.12	OPD	10	7.000	0.25
On.Ar (μm^2)	10	5.000	0.15	On.Ar (μm^2)	10	10.000	0.60
Re.On.Ar (%)	10	7.000	0.25	Re.On.Ar (%)	10	12.000	0.92
H.Ca.Ar (μm^2)	10	12.000	0.92	H.Ca.Ar (μm^2)	10	9.000	0.47
Ot.Dn	9	6.000	0.33	Ot.Dn	10	10.000	0.60
Radius				**Occipital**			
N.On	10	5.500	0.15	N.On	10	12.000	0.92
N.On.Fg	10	2.000	<0.03*	N.On.Fg	10	0.000	<0.01**
OPD	10	0.500	0.01*	OPD	10	3.000	0.06
On.Ar (μm^2)	10	11.000	0.75	On.Ar (μm^2)	10	5.000	0.12
Re.On.Ar (%)	10	11.000	0.75	Re.On.Ar (%)	10	3.000	0.06
H.Ca.Ar (μm^2)	10	11.000	0.75	H.Ca.Ar (μm^2)	10	9.000	0.47
Ot.Dn	10	8.000	0.35	Ot.Dn	8	5.000	0.38

† Statistical significance value: *$p < 0.05$, **$p < 0.01$.

Table A.E.2 *Bonferroni post-hoc tests for GLM of the histological variables compared between the tibia, femora, metacarpals, radii, humeri, ribs, clavicles, and occipitals*

		N.On			N.On.Fg			OPD		
Bone 1	Bone 2	Mean dif.	Std. Err.	*p*	Mean dif.	Std. Err.	*p*	Mean dif.	Std. Err.	*p*
Tib	Fem	-0.588	0.666	1.00	-0.342	1.025	1.00	-0.930	1.12	1.00
	Met	-0.475	0.497	1.00	-1.042	1.120	1.00	-1.517	1.05	1.00
	Rad	0.310	0.588	1.00	0.002	1.055	1.00	0.312	1.05	1.00
	Hum	-1.310	0.680	1.00	-1.250	0.892	1.00	-2.232	1.07	1.00
	Rib	-1.659	0.999	1.00	0.299	1.438	1.00	-1.360	1.02	1.00
	Cla	0.896	0.467	1.00	-0.181	1.469	1.00	0.715	1.29	1.00
	Occ	3.196	0.781	0.08	5.116	1.178	0.05*	8.313	0.90	<0.01**
Fem	Tibia	0.588	0.666	1.00	0.342	1.025	1.00	0.930	1.12	1.00
	Met	0.112	0.628	1.00	-0.700	0.879	1.00	-0.587	0.71	1.00
	Rad	0.898	0.790	1.00	0.344	0.875	1.00	1.242	0.52	1.00
	Hum	-0.722	0.209	0.20	-0.908	0.764	1.00	-1.302	0.74	1.00
	Rib	-1.071	0.985	1.00	0.641	1.048	1.00	-0.430	0.92	1.00
	Cla	1.484	0.666	1.00	0.161	1.033	1.00	1.645	0.68	1.00
	Occ	3.784	1.130	0.24	5.459	1.203	0.04*	9.243	1.15	<0.01**
Met	Tib	0.475	0.497	1.00	1.042	1.120	1.00	1.517	1.05	1.00
	Fem	-0.112	0.628	1.00	0.700	0.879	1.00	0.587	0.71	1.00
	Rad	0.786	0.677	1.00	1.044	1.053	1.00	1.829	0.95	1.00
	Hum	-0.834	0.712	1.00	-0.208	1.178	1.00	-0.715	1.12	1.00
	Rib	-1.184	0.934	1.00	1.341	1.512	1.00	0.157	1.00	1.00
	Cla	1.371	0.428	0.30	0.861	0.836	1.00	2.232	0.99	1.00
	Occ	3.672	0.850	0.05*	6.159	1.218	0.02*	9.830	1.41	<0.01**
Rad	Tib	-0.310	0.588	1.00	-0.002	1.055	1.00	-0.312	1.05	1.00
	Fem	-0.898	0.790	1.00	-0.344	0.875	1.00	-1.242	0.52	1.00
	Met	-0.786	0.677	1.00	-1.044	1.053	1.00	-1.829	0.95	1.00
	Hum	-1.620	0.767	1.00	-1.252	0.630	1.00	-2.544	0.77	0.25
	Rib	-1.969	0.908	1.00	0.297	1.044	1.00	-1.672	0.81	1.00
	Cla	0.586	0.478	1.00	-0.183	1.168	1.00	0.403	0.94	1.00
	Occ	2.886	0.709	0.08	5.115	0.795	<0.01**	8.001	1.07	<0.01**
Hum	Tib	1.310	0.680	1.00	1.250	0.892	1.00	2.232	1.07	1.00
	Fem	0.722	0.209	0.20	0.908	0.764	1.00	1.302	0.74	1.00
	Met	0.834	0.712	1.00	0.208	1.178	1.00	0.715	1.12	1.00
	Rad	1.620	0.767	1.00	1.252	0.630	1.00	2.544	0.77	0.25
	Rib	-0.349	0.951	1.00	1.549	1.081	1.00	0.872	1.05	1.00
	Cla	2.205	0.692	0.31	1.069	1.176	1.00	2.947	0.92	0.31
	Occ	4.506	1.144	0.10	6.366	0.645	<0.01**	10.545	0.76	<0.01**
Rib	Tib	1.659	0.999	1.00	-0.299	1.438	1.00	1.360	1.02	1.00
	Fem	1.071	0.985	1.00	-0.641	1.048	1.00	0.430	0.92	1.00
	Met	1.184	0.934	1.00	-1.341	1.512	1.00	-0.157	0.10	1.00
	Rad	1.969	0.908	1.00	-0.297	1.044	1.00	1.672	0.81	1.00
	Hum	0.349	0.951	1.00	-1.549	1.081	1.00	-0.872	1.05	1.00
	Cla	2.555	0.798	0.30	-0.480	1.767	1.00	2.075	1.44	1.00
	Occ	4.855	0.910	0.01**	4.818	1.342	0.16	9.673	1.42	<0.01**
Cla	Tib	-0.896	0.467	1.00	0.181	1.469	1.00	-0.715	1.29	1.00
	Fem	-1.484	0.666	1.00	-0.161	1.033	1.00	-1.645	0.68	1.00
	Met	-1.371	0.428	0.30	-0.861	0.836	1.00	-2.232	0.99	1.00
	Rad	-0.586	0.478	1.00	0.183	1.168	1.00	-0.403	0.94	1.00
	Hum	-2.205	0.692	0.31	-1.069	1.176	1.00	-2.947	0.92	0.31
	Rib	-2.555	0.798	0.30	0.480	1.767	1.00	-2.075	1.44	1.00
	Occ	2.301	0.617	0.13	5.297	1.156	0.04*	7.598	1.04	<0.01**
Occ	Tib	-3.196	0.781	0.08	-5.116	1.178	0.052	-8.31	0.89	<0.01**
	Fem	-3.784	1.130	0.24	-5.459	1.203	0.04*	-9.24	1.15	<0.01**
	Met	-3.672	0.850	0.05*	-6.159	1.218	0.02*	-9.83	1.41	<0.01**
	Rad	-2.886	0.709	0.08	-5.115	0.795	<0.01**	-8.00	1.07	<0.01**
	Hum	-4.506	1.144	0.10	-6.366	0.645	<0.01**	-10.55	0.76	<0.01**
	Rib	-4.855	0.910	0.01**	-4.818	1.342	0.16	-9.673	1.42	<0.01**
	Cla	-2.301	0.617	0.13	-5.297	1.156	0.04*	-7.598	1.04	<0.01**

		On.Ar (μm²)			Re.On.Ar (%)		
Bone 1	Bone 2	Mean dif.	Std. Err.	*p*	Mean dif.	Std. Err.	*p*
Tib	Fem	-3566.695	3453.35	1.00	0.004	0.003	1.00
	Met	3376.387	887.61	0.12	0.002	0.003	1.00
	Rad	-3029.965	1895.94	1.00	0.005	0.003	1.00
	Hum	1191.698	2057.19	1.00	-0.001	0.001	1.00
	Rib	9113.528	2098.14	0.05*	0.003	0.003	1.00
	Cla	-7831.534	2848.43	0.63	-0.008	0.003	0.38
	Occ	2903.359	3706.77	1.00	0.010	0.004	0.73
Fem	Tibia	3566.695	3453.35	1.00	-0.004	0.003	1.00
	Met	6943.082	3339.42	1.00	-0.002	0.003	1.00
	Rad	536.731	3649.50	1.00	0.001	0.005	1.00
	Hum	4758.393	2661.22	1.00	-0.005	0.003	1.00
	Rib	12680.22	3344.46	0.12	-0.001	0.004	1.00
	Cla	-4264.839	4098.86	1.00	-0.013	0.004	0.47
	Occ	6470.055	2411.59	0.70	0.006	0.006	1.00
Met	Tib	-3376.387	887.61	0.12	-0.002	0.003	1.00
	Fem	-6943.082	3339.42	1.00	0.002	0.003	1.00
	Rad	-6406.352	1781.76	0.16	0.003	0.004	1.00
	Hum	-2184.689	1748.39	1.00	-0.003	0.003	1.00
	Rib	5737.141	1498.83	0.11	0.001	0.002	1.00
	Cla	-11207.92	2393.71	0.03*	-0.010	0.003	0.10
	Occ	-473.028	3792.48	1.00	0.008	0.006	1.00
Rad	Tib	3029.965	1895.94	1.00	-0.005	0.003	1.00
	Fem	-536.731	3649.50	1.00	-0.001	0.005	1.00
	Met	6406.352	1781.76	0.16	-0.003	0.004	1.00
	Hum	4221.662	2428.19	1.00	-0.006	0.004	1.00
	Rib	12143.49	2165.61	<0.01**	-0.002	0.004	1.00
	Cla	-4801.570	2813.79	1.00	-0.013	0.003	0.09
	Occ	5933.324	3904.72	1.00	0.005	0.005	1.00
Hum	Tib	-1191.698	2057.19	1.00	0.001	0.001	1.00
	Fem	-4758.393	2661.22	1.00	0.005	0.003	1.00
	Met	2184.689	1748.39	1.00	0.003	0.003	1.00
	Rad	-4221.662	2428.19	1.00	0.006	0.004	1.00
	Rib	7921.831	1583.47	0.02*	0.004	0.003	1.00
	Cla	-9023.232	2421.32	0.13	-0.008	0.003	0.98
	Occ	1711.662	3342.88	1.00	0.011	0.004	1.00
Rib	Tib	-9113.528	2098.14	0.05*	-0.003	0.003	1.00
	Fem	-12680.22	3344.46	0.12	0.001	0.004	1.00
	Met	-5737.141	1498.83	0.11	-0.001	0.002	1.00
	Rad	-12143.49	2165.61	<0.01**	0.002	0.004	1.00
	Hum	-7921.831	1583.47	0.02*	-0.004	0.003	1.00
	Cla	-16945.06	2322.38	<0.01**	-0.012	0.002	0.02*
	Occ	-6210.169	4008.51	1.00	0.007	0.006	1.00
Cla	Tib	7831.534	2848.43	0.63	0.008	0.003	0.38
	Fem	4264.839	4098.86	1.00	0.013	0.004	0.47
	Met	11207.92	2393.71	0.03*	0.010	0.003	0.10
	Rad	4801.570	2813.79	1.00	0.013	0.003	0.09
	Hum	9023.232	2421.32	0.13	0.008	0.003	0.98
	Rib	16945.06	2322.38	<0.01**	0.012	0.002	0.02*
	Occ	10734.89	3689.36	0.49	0.019	0.004	0.07
Occ	Tib	-2903.359	3706.77	1.00	-0.010	0.004	0.73
	Fem	-6470.055	2411.59	0.70	-0.006	0.006	1.00
	Met	473.028	3792.48	1.00	-0.008	0.006	1.00
	Rad	-5933.324	3904.72	1.00	-0.005	0.005	1.00
	Hum	-1711.662	3342.88	1.00	-0.011	0.004	1.00
	Rib	6210.169	4008.51	1.00	-0.007	0.006	1.00
	Cla	-10734.89	3689.36	0.49	-0.019	0.004	0.07

		H.Ca.Ar (μm^2)			Ot.Dn		
Bone 1	Bone 2	Mean dif.	Std. Err.	*p*	Mean dif.	Std. Err.	*p*
Tib	Fem	27.839	53.26	1.00	27.839	53.26	1.00
	Met	-53.114	60.92	1.00	-53.114	60.92	1.00
	Rad	54.945	39.09	1.00	54.945	39.09	1.00
	Hum	47.619	35.59	1.00	47.619	35.59	1.00
	Rib	3.480	49.68	1.00	3.480	49.68	1.00
	Cla	33.516	49.88	1.00	33.516	49.88	1.00
	Occ	234.615	31.55	<0.01**	234.615	31.55	<0.01**
Fem	Tibia	-27.839	53.26	1.00	-27.839	53.26	1.00
	Met	-80.952	62.79	1.00	-80.952	62.79	1.00
	Rad	27.106	37.12	1.00	27.106	37.12	1.00
	Hum	19.780	41.09	1.00	19.780	41.09	1.00
	Rib	-24.359	44.84	1.00	-24.359	44.84	1.00
	Cla	5.678	40.12	1.00	5.678	40.12	1.00
	Occ	206.777	55.44	0.27	206.777	55.44	0.27
Met	Tib	53.114	60.92	1.00	53.114	60.92	1.00
	Fem	80.952	62.79	1.00	80.952	62.79	1.00
	Rad	108.059	71.75	1.00	108.059	71.75	1.00
	Hum	100.733	41.01	1.00	100.733	41.01	1.00
	Rib	56.593	53.13	1.00	56.593	53.13	1.00
	Cla	86.630	41.27	1.00	86.630	41.27	1.00
	Occ	287.729	45.26	0.02*	287.729	45.26	0.02*
Rad	Tib	-54.945	39.09	1.00	-54.945	39.09	1.00
	Fem	-27.106	37.12	1.00	-27.106	37.12	1.00
	Met	-108.06	71.75	1.00	-108.06	71.75	1.00
	Hum	-7.326	39.75	1.00	-7.326	39.75	1.00
	Rib	-51.465	52.03	1.00	-51.465	52.03	1.00
	Cla	-21.429	47.69	1.00	-21.429	47.69	1.00
	Occ	179.670	52.07	0.38	179.670	52.07	0.38
Hum	Tib	-89.296	119.34	1.00	-47.619	35.59	1.00
	Fem	-377.41	179.13	1.00	-19.780	41.09	1.00
	Met	20.204	97.08	1.00	-100.73	41.01	1.00
	Rad	-383.48	156.51	1.00	7.326	39.75	1.00
	Rib	213.403	111.06	1.00	-44.139	42.28	1.00
	Cla	5.245	149.49	1.00	-14.103	36.29	1.00
	Occ	-276.28	259.43	1.00	186.996	24.76	<0.01**
Rib	Tib	-302.70	169.01	1.00	-3.480	49.68	1.00
	Fem	-590.81	114.45	<0.02*	24.359	44.84	1.00
	Met	-193.20	50.06	0.11	-56.593	53.13	1.00
	Rad	-596.88	191.74	0.35	51.465	52.03	1.00
	Hum	-213.40	111.06	1.00	44.139	42.28	1.00
	Cla	-208.16	105.34	1.00	30.037	39.49	1.00
	Occ	-489.69	248.27	1.00	231.14	38.19	<0.03*
Cla	Tib	-94.541	196.56	1.00	-33.516	49.88	1.00
	Fem	-382.66	157.51	1.00	-5.678	40.12	1.00
	Met	14.959	109.41	1.00	-86.630	41.27	1.00
	Rad	-388.73	201.51	1.00	21.429	47.69	1.00
	Hum	-5.245	149.49	1.00	14.103	36.29	1.00
	Rib	208.158	105.34	1.00	-30.037	39.49	1.00
	Occ	-281.53	198.81	1.00	201.099	40.50	0.07
Occ	Tib	186.987	267.75	1.00	-234.62	31.55	<0.01**
	Fem	-101.13	275.63	1.00	-206.78	55.44	0.27
	Met	296.487	245.08	1.00	-287.73	45.26	0.02*
	Rad	-107.20	270.79	1.00	-179.67	52.07	0.38
	Hum	276.283	259.43	1.00	-187.00	24.76	<0.01**
	Rib	489.686	248.27	1.00	-231.14	38.19	<0.03*
	Cla	281.528	198.81	1.00	-201.10	40.50	0.07

† Statistical significance value: *$p < 0.05$, **$p < 0.01$.

Appendix F

Table A.F.1 *Kolmogorov-Smirnov tests of normality for untransformed histological variables from the rib*

Variable	N	Z	*p*
Tt.Ar (mm^2)	50	0.100	0.20
Ct.Ar (mm^2)	50	0.087	0.20
Re.Ct.Ar (%)	50	0.116	0.19
OPD	50	0.104	0.20
On.Ar (μm^2)	47	0.089	0.20
Re.On.Ar (%)	47	0.139	0.02*
On.Dm (μm)	47	0.130	0.05*
H.Ca.Ar (μm^2)	47	0.133	0.04*
H.Ca.Dm (μm)	47	0.085	0.20

† Statistical significance value: *$p < 0.05$, **$p < 0.01$.

Table A.F.2 *Kolmogorov-Smirnov tests of normality for transformed histological variables from the rib*

Variable	N	Z	*p*
lgTt.Ar (mm^2)	50	0.128	0.08
lgCt.Ar (mm^2)	50	0.093	0.20
lgRe.Ct.Ar (%)	50	0.083	0.20
sqrtOPD	50	0.137	0.20
lgOn.Ar (μm^2)	47	0.058	0.20
lgRe.On.Ar (%)	47	0.142	0.19
lgOn.Dm (μm)	47	0.112	0.18
lgH.Ca.Ar (μm^2)	47	0.107	0.20
lgH.Ca.Dm (μm^2)	47	0.091	0.20

† Statistical significance value: *$p < 0.05$, **$p < 0.01$.

Table A.F.3 *Descriptive (transformed) statistics for the rib microstructure for the younger children (3-7 yrs) and the older children (8-12 yrs)*

Age group	Variable	N	Mean	SD
3-7 yrs	lgTt.Ar (mm^2)	24	1.41	0.12
	lgCt.Ar (mm^2)	24	1.14	0.12
	lgRe.Ct.Ar (%)	24	1.72	0.08
	sqrtOPD	29	1.64	0.83
	lgOn.Ar (μm^2)	26	4.54	0.10
	lgRe.On.Ar (%)	26	-0.02	0.01
	lgOn.Dm (μm)	26	2.25	0.06
	lgH.Ca.Ar (μm^2)	26	3.19	0.14
	lgH.Ca.Dm (μm^2)	26	1.55	0.07
8-12 yrs	lgTt.Ar (mm^2)	18	1.57	0.08
	lgCt.Ar (mm^2)	18	1.27	0.09
	lgRe.Ct.Ar	18	1.71	0.08
	sqrtOPD	21	2.43	0.42
	lgOn.Ar (μm^2)	21	4.60	0.11
	lgRe.On.Ar (%)	21	-0.02	0.01
	lgOn.Dm (μm)	21	2.28	0.06
	lgH.Ca.Ar (μm^2)	21	3.18	0.15
	lgH.Ca.Dm (μm^2)	21	1.55	0.07